



HAL
open science

**Varved lake sediments as archives for high-resolution
millennial-long climate reconstructions: from
sedimentation processes to paleoclimatology - Two case
studies from the Northern Swiss Alps and North-eastern
Poland**

Benjamin Amann

► **To cite this version:**

Benjamin Amann. Varved lake sediments as archives for high-resolution millennial-long climate reconstructions: from sedimentation processes to paleoclimatology - Two case studies from the Northern Swiss Alps and North-eastern Poland. Global Changes. University of Bern, 2014. English. NNT: . tel-02409926

HAL Id: tel-02409926

<https://hal.science/tel-02409926>

Submitted on 20 Dec 2019

HAL is a multi-disciplinary open access archive for the deposit and dissemination of scientific research documents, whether they are published or not. The documents may come from teaching and research institutions in France or abroad, or from public or private research centers.

L'archive ouverte pluridisciplinaire **HAL**, est destinée au dépôt et à la diffusion de documents scientifiques de niveau recherche, publiés ou non, émanant des établissements d'enseignement et de recherche français ou étrangers, des laboratoires publics ou privés.

Varved lake sediments as archives for high-resolution millennial-long climate reconstructions: from sedimentation processes to paleoclimatology

-

Two case studies from the Northern Swiss Alps and North-eastern Poland

Inauguraldissertation
der Philosophisch-naturwissenschaftlichen Fakultät
der Universität Bern

vorgelegt von
Benjamin Amann
von Arpenans, France

Leiter der Arbeit:
Prof. Dr. M. Grosjean
Universität Bern

Varved lake sediments as archives for high-resolution millennial-long climate reconstructions: from sedimentation processes to paleoclimatology

-

Two case studies from the Northern Swiss Alps and North-eastern Poland

Inauguraldissertation
der Philosophisch-naturwissenschaftlichen Fakultät
der Universität Bern

vorgelegt von
Benjamin Amann
von Arpenans, France

Leiter der Arbeit:
Prof. Dr. M. Grosjean
Universität Bern

Von der Philosophisch-naturwissenschaftlichen Fakultät angenommen

Bern, 19.12.2014 (defence)

Der Dekan
Prof. Dr. G. Colangelo

Table of Contents

Abstract	V
Résumé	VI
1. Introduction and outline	7
1.1. Motivation	
1.2. Concerns about climatic change	
1.3. Varved lake sediments as paleoclimate archives: potential and limitations	
1.4. Research questions, objectives and aims of the thesis	
1.5. Outline of the thesis	
2. Material and methods	19
2.1. Sedimentation process understanding	
2.2. Coring and data processing	
2.3. Sediment dating	
2.4. Proxy-climate calibration and reconstruction	
3. Reflectance spectroscopy in the visible range (VIS-RS)	29
3.1. Introduction	
3.2. Methodology: principle and use	
3.3. Spectral indices for the biochemical varves of Lake Żabińskie	
3.4. Spectral indices for the clastic varves of Lake Oeschinen	
4. Lake Oeschinen: clastic varves	41
4.1. Site description	
4.2. Climate	
4.3. Sedimentation processes, varve formation and event layers	
4.4. Quantitative high-resolution warm season rainfall recorded in varved sediments of Lake Oeschinen, northern Swiss Alps: calibration and validation AD 1901-2008 Published in <i>Journal of Paleolimnology</i>	
4.5. A millennial-long record of warm season precipitation and flood frequency for the North-western Alps inferred from varved lake sediments: implications for the future Submitted to <i>Quaternary Science Reviews</i>	
5. Lake Żabińskie: biochemical varves	103
5.1. Site selection and description	
5.2. Climate	
5.3. Sedimentation processes and varve formation	
5.4. Spring temperature variability and eutrophication history inferred from sedimentary pigments in the varved sediments of Lake Żabińskie, NE Poland AD 1907-2008 Accepted in <i>Global and Planetary Change</i>	
6. Summary and conclusions	137
Appendix A1.1 – A.3	145

Abstract

The recent warming of the global climate is well recognized. Many of the observed changes are unprecedented over decades to millennia. This conclusion could be drawn because an increasing number of paleoclimate time series with the detail needed, have and are being developed.

At the same time, it is also recognized that further advances in this field of research are still limited by the scarcity of well calibrated and quantified time series of reconstructed variables from natural paleoclimate archives that cover the last Millennium. For instance, the interaction between temperature and precipitation, and its influence on the flood properties remain an open question.

For this thesis, two lakes were investigated for their potential as paleoclimate archives:

- Proglacial **Lake Oeschinen** in the Bernese Alps that contains clastic varves
- Glacial **Lake Żabińskie** in northeast Poland that contains biochemical varves

The following three research questions were addressed: (i) Can we use information from rapid surface scanning reflectance spectroscopy in the visible light range (VIS-RS) as a quantitative proxy for the composition of lake sediments? (ii) Can we calibrate sediment proxy data and VIS-RS data with climate variables in the instrumental period? (iii) Can we produce a 1000-year long quantitative climate reconstruction from sediment proxy data and VIS-RS data?

Scanning VIS-RS methodology was explored on the biochemical varves of Lake Żabińskie and the clastic varves of Lake Oeschinen. In Lake Żabińskie, the absorption trough centred at 660-670nm ($RABD_{660;670}$) could be calibrated to the total concentration of chlorins (chlorophyll-*a* degradation products = {Pheophytin-*a* + Pyropheophytin-*a*}; $r = 0.75$, $p < 0.01$) as measured by High Performance Liquid Chromatography (HPLC). In Lake Oeschinen, mean 1st derivative VIS-RS spectra were calibrated to the proportions of calcite/siliciclastics ($r = 0.96$, $p < 0.01$) as measured by loss on ignition.

The study from Lake Oeschinen revealed that varve thickness could be used as a quantitative predictor for cumulative alpine warm-season precipitation ($r_{MJ} = 0.71$, $r_{MJJA} = 0.60$, $p_c < 0.01$; AD 1901-2008). This calibration model was used to produce a record of precipitation and flood frequency back to AD 884. Beyond answering research question (ii) and (iii), this millennial-long record enabled assessing the relationship between temperature, precipitation and floods over the past 1000 years.

In the study of Lake Żabińskie, multivariate statistics were performed on a multi-proxy data set of sedimentary pigments and other biochemical proxies. Results showed the recent lake eutrophication could be quantitatively discriminated from climate-driven changes for the period AD 1907-2008. Sedimentary pigments related to chlorophyll-*a* (Chl-*a* and degradation products) were not affected by the eutrophication-based processes, but responded to spring March-to-May temperature ($r = 0.63$, $p_c < 0.05$). This suggested that sediment photopigments from Lake Żabińskie can be used for a climate reconstruction.

Résumé

Le réchauffement global de la planète est aujourd'hui reconnu et sans précédent sur une échelle de temps décennale à millénaire. Cette conclusion a pu être formulée grâce notamment au recours à des données climatiques sur le passé de très bonne qualité, qui ont été et sont encore produites. Dans le même temps, il est de plus en plus admis que de nouvelles avancées dans ce domaine de la Recherche restent restreintes par la rareté des variables climatiques couvrant les 1000 dernières années et produites de manière quantitative à partir d'archives naturelles du paléoclimat. Pour exemple, l'interaction entre les températures et précipitations, ainsi que leur influence mutuelle sur les propriétés et le contrôle des crues restent à examiner.

À travers ce projet de doctorat, deux lacs ont été sélectionnés pour l'étude du paléoclimat:

- **Lac d'Oeschinen**, un lac d'altitude des Alpes Suisses qui présente des varves de type clastique
- **Lac Żabińskie**, au Nord-est de la Pologne qui présente des varves de type biogéochimique

Nous avons adressé les trois questions de recherche suivantes: (i) est-il possible d'utiliser la spectroscopie à lecture optique (VIS-RS; 380-730nm) afin de déterminer de manière quantitative la composition des sédiments lacustres? (ii) Peut-on calibrer les données proxy et VIS-RS de ces sédiments avec les données climatiques pour la période instrumentale, et cibler le proxy à utiliser pour reconstruire le climat passé? (iii) Peut-on produire un jeu de données climatiques, à partir des informations proxy et VIS-RS, qui soit quantitatif et couvrant les 1000 dernières années?

Les résultats obtenus à partir de la spectroscopie à lecture optique sur les varves ont révélé que cette technique est un outil solide à la caractérisation d'éléments spécifiques (quantité et composition). Pour le lac Żabińskie, la bande d'absorption VIS-RS à 660-670 nm a pu être étalonnée aux concentrations en Chlorins (produits de dégradation de la chlorophylle-*a* = {Phéophytine-*a* + Pyropheophytine-*a*}; $r = 0.75$, $p < 0.01$) mesurées par Chromatographie en phase Liquide à Haute Performance (CLHP). Pour le Lac d'Oeschinen, la dérivée première du spectre VIS-RS a pu être étalonnée aux proportions en calcite/siliciclastics ($r = 0.96$, $p < 0.01$) mesurées par perte au feu.

L'enregistrement varvé du Lac d'Oeschinen a été utilisé pour reconstruire les précipitations d'été (Mai à Août) et reconstituer l'évolution de la fréquence des crues pour le Nord-ouest des Alpes jusqu'en 884 ($r_{\text{varve thickness;MJJJA}} = 0.60$, $p < 0.01$; AD 1901-2008). Au-delà d'avoir répondu aux questions de recherche (ii) et (iii), cet enregistrement nous a également permis d'étudier les relations qui lient température, précipitation et fréquence de crue à travers ce millénaire.

Nous avons réalisé une étude statistique multi-variée à partir de pigments et autres proxy biochimiques des sédiments du lac Żabińskie afin de séparer quantitativement le signal climatique du signal d'eutrophisation pour la période 1907-2008. Plus particulièrement, les données pigmentaires relatives à la chlorophylle-*a* (matière première et produits de dégradation) ont montré une corrélation significative avec les températures printanières (Mars à Mai, $r = 0.63$, $p < 0.05$). À des fins de perspectives, ces résultats peuvent servir à reconstruire le climat en Pologne.

Chapter 1



1. Introduction and outline

1.1. Motivation

“The recent warming of our global climate is unequivocal and many of the observed changes are unprecedented over decades to millennia”. This is one of the key messages provided by the last comprehensive scientific assessments of climate change (IPCC 2013).

This statement has been made possible because quantitative and spatially explicit global and regional climate reconstructions over the past millennium have been made available. This research topic has received a lot of scientific and public attention (MILLENNIUM 2011; PAGES 2k Consortium 2013; IPCC 2013).

Sound knowledge of past climate and its variability is required to improve our understanding of the operational mode of the Earth system. This is essential to assess the sensitivity of the Earth’s climate to natural and anthropogenic forcings and, ultimately, to reduce uncertainty in future climate projections (Jansen et al. 2007; Hegerl et al. 2006; Mann et al. 2008; Villalba et al. 2009; Masson-Delmotte et al. 2013).

In this context, the last 1000 years are of particular interest as most of that time was in a period when natural climate fluctuations were the dominant causes of the changes that can be measured (e.g. volcanic and solar forcings). Moreover, this period encompasses a broad range of climate variability, which includes the relatively warm Medieval Climate Anomaly (MCA, AD 900-1300) and the relatively cool Little Ice Age (LIA, AD 1400-1900).

Nevertheless, it has been recognized that an important obstacle for further advances in this field of research is the scarcity of well calibrated and quantified, annually resolved time series of reconstructed variables, such as precipitation and temperature, from natural paleoclimate archives.

1.2. Concerns about climatic change

With regard to temperature variability, substantial advances have been made for the Northern Hemisphere, for which an increasing number of paleoclimate time series with the detail needed, have and are being produced. This has enabled improving comprehensive assessments of long-term regional changes in temperature conditions (Fig. 1.1). However, most of the insights into past temperature variability from reconstructions and model simulations are for annual means (PAGES 2k Consortium 2013; Masson-Delmotte et al. 2013). At the same time, it is increasingly recognized that the temporal structure of climate variability differs substantially among the four seasons of the year, which may lead to diverse trends and uncertainties (Luterbacher et al. 2004; Xoplaki et al. 2005; de Jong et al. 2013). In this context, seasonally-resolved climate reconstructions provide insight into the mechanisms or forcings underlying observed climate variability, and enable investigations of the seasonal dependency of past and future climate changes. To date, such information remains limited.

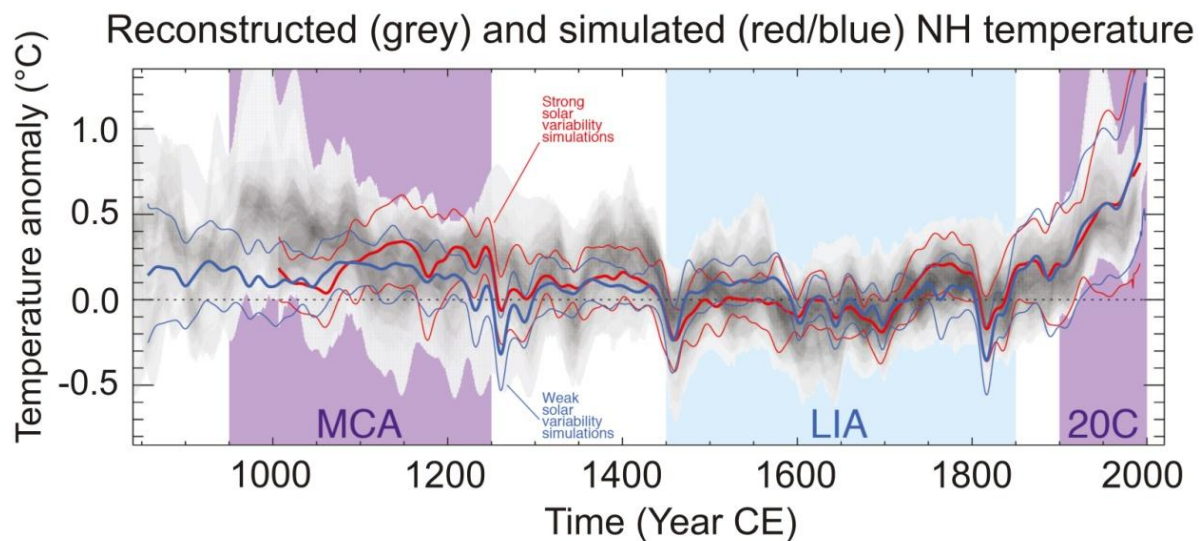


Fig. 1.1 Northern Hemisphere temperature for the last millennium reconstructed from proxy data and model simulations (Masson-Delmotte et al. 2013 in IPCC 2013)

Information about precipitation and past hydroclimatic conditions remains poor. This can be attributed to the paucity of precipitation-sensitive proxies and a lack of data. This has made comprehensive assessments of long-term regional changes in precipitation very difficult (Büntgen et al. 2010; Wilson et al. 2013; Masson-Delmotte et al. 2013). Long precipitation time series are required to evaluate the long-term relationship between temperature and precipitation, and to

assess whether a future warmer climate would lead to a drier or moister climate. A first theoretical approach is to consider that the interaction between temperature and precipitation follows the Clausius-Clapeyron relation. Work by Held and Soden (2006) and O’Gorman and Muller (2010) showed that a pattern of ‘dry gets drier and wet gets wetter’ is rather expected. In a most recent study, Greve et al. (2014) demonstrated that only 10.8% of the global land area shows a clear ‘dry gets drier, wet gets wetter’ pattern (DDWW paradigm), while 9.5% show the opposite (i.e. ‘dry gets wetter and wet gets drier’; Fig. 1.2). Therefore, to date, knowledge about the interaction between temperature and precipitation and how it will evolve with climate change remains an open question.

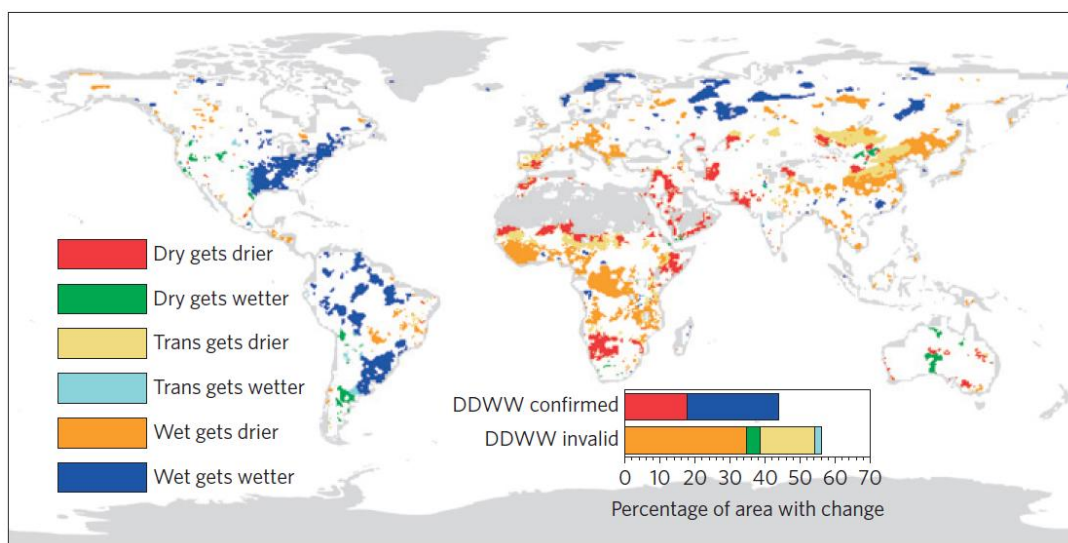


Fig. 1.2 ‘Wet gets wetter, dry gets drier’ WWDD paradigm world map (Greve et al. 2014)

Changes in the hydroclimate are most relevant as they may also lead to changes in the frequency and intensity of floods in the near future (Köplin et al. 2014). Changes in the properties of such extreme events are of particular concern for society, especially in vulnerable mountainous areas such as the European Alps (IPCC 2012; Christensen et al. 2013; Smith et al. 2013). However, it remains poorly understood how changes in temperature, precipitation and regional synoptic-scale weather patterns interact and influence the properties and statistics of flood events. To date, in Europe it is not possible to obtain a consistent climate change signal from high-resolution regional climate models for future projections of strong rainfall events (Fig. 1.3; Frei et al. 2006; CH2011, 2011).

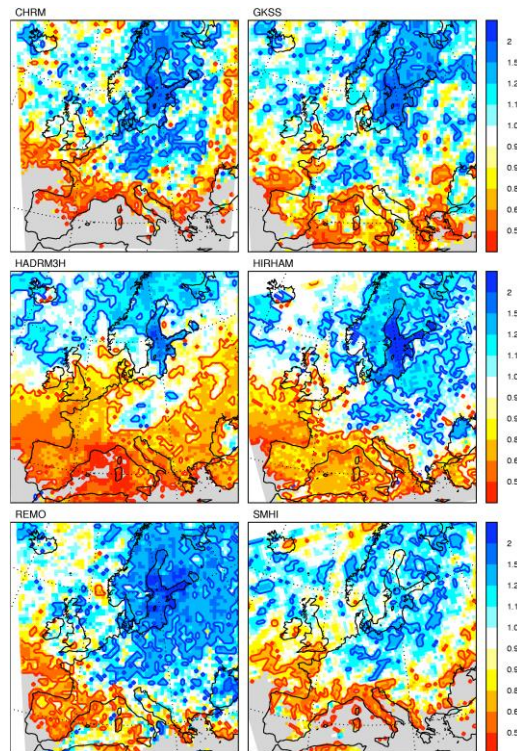


Fig. 1.3 Ratio $[(2071-2100)/(1961-1990)]$ of the 5-yr return value for 1-day precipitation total ($\times 1d.5$) in summer (June-August). Results are given for six regional climate models under the A2 emission scenario. Blue (red) colours correspond to an increase (decrease) of flood frequency in the near future (Frei et al. 2006)

1.3. Varved lake sediments as paleoclimate archives: potential and limitations

Among natural paleoclimate archives, varved lake sediments contain records of climate and environmental change at very high resolution and chronological accuracy (Zolitschka et al. 2007; Pienitz and Lotter 2009). Numerous studies have shown that lake sediments may provide records of temperature variability (Hughen et al. 2000; Moore et al. 2001; Kalugin et al. 2007; von Gunten et al. 2009; Larocque-Tobler et al. 2012; Saunders et al. 2013), precipitation variability (Wohlfart et al. 1998; Cockburn and Lamoureux 2007; Elbert et al. 2012; Saunders et al. 2012), and flood events (Lamoureux et al. 2000; Chapron et al. 2002; Bussmann and Anselmetti 2010; Gilli et al. 2013; Wilhelm et al. 2013). This is a very active field of research.

However, the study of lake sediments for paleoclimatology may be limited by two obstacles. The first is that most of the analytical techniques for the acquisition of proxy data are time consuming and often expensive. This may restrict the temporal resolution and the length of the paleoclimate records. This is the reason why rapid reflectance scanning spectroscopy in the visible range (VIS-RS) was explored as an alternative of time-demanding analytical techniques. The second obstacle applies to lakes that are surrounded by human presence (e.g. settlements, cultivation field, and forest clearance). Anthropogenic activities in the lake surroundings may significantly influence the structure and composition of the varves and mask the climate information preserved in the sediments. Therefore, the influence of human activities on lake sedimentation processes needs to be quantified prior to using varved lake sediments as a paleoclimatic archive.

1.4. Research questions, objectives and aims of the thesis

The following three research questions are addressed through this PhD thesis:

- (i) Can we use rapid scanning reflectance spectroscopy in the visible range (VIS-RS) as a quantitative proxy for the composition of lake sediments?
- (ii) Can we calibrate sediment proxy data and VIS-RS data with climate variables during the instrumental period?
- (iii) Can we produce a 1000-year long quantitative climate reconstruction from sedimentological proxies and VIS-RS data?

To answer these research questions, our objectives are to test and apply scanning VIS-RS on sediments from two lakes in Europe, and to explore the potential of these two lakes as paleoclimatic archives:

- Proglacial **Lake Oeschinen** in the northern Swiss Alps, which contains clastic varves
- Glacial **Lake Żabińskie** in northeast Poland, which contains biochemical varves

Therefore the specific aims of this thesis are to:

- Lake Oeschinen {
 - (i) Calibrate and validate VIS-RS data with the mineralogical composition of sediments from Lake Oeschinen using 'synthetic sediments' and sediment cores
 - (ii) Calibrate sediment proxy data from the minerogenic varves of Lake Oeschinen with climate data during the instrumental period
 - (iii) Produce a millennial-long reconstruction of a climate variable (summer precipitation) using sedimentological and mineralogical proxies, and VIS-RS data
- Lake Żabińskie {
 - (iv) Explore scanning VIS-RS methodology on biochemical varves of Lake Żabińskie and calibrate VIS-RS with quantitative specific sedimentary pigments (determined by high performance liquid chromatography)
 - (vi) Test whether biochemical proxies, pigment data and VIS-RS data can be calibrated to climate data and whether they can be used for climate reconstructions

1.5. Outline of the thesis

After the motivation, research questions and aims of the thesis were introduced, the methods applied on the varved sediments of the two lakes are described in Chapter 2. In this chapter, we present the methodologies associated with sediment process understanding, sediment coring, and sampling. How the sediments were dated and which statistical methods were used to calibrate sediment proxy data with climate variables are also shown in this chapter.

In Chapter 3, visible reflectance spectroscopy is explored as a novel, non-destructive tool for rapid acquisition of proxy data from clastic and biochemical varves. The aim of the chapter is to answer the first research question addressed in the previous section.

The study about the clastic varves of Alpine Lake Oeschinen is presented in Chapter 4. In this chapter, we describe the study site, its climate and how the varves are formed. We also demonstrate that the sediment proxy data are correlated to warm-season precipitation. This enables reconstructing past precipitation variability and to produce a record of flood frequency spanning the last Millennium.

In Chapter 5, the study about the biochemical varves of Polish Lake Żabińskie is introduced. The lake catchment and the climate of the study area are described in this chapter. After presenting results from monitoring of the lake water and the sediment fluxes, we show that the biogeochemical data from Lake Żabińskie sediments can be used to infer a spring temperature signal and a history of human eutrophication.

Finally, in Chapter 9, the main achievements and challenges are summarized and general conclusions are drawn.

References (Chapter 1)

- Bussmann, F., Anselmetti, F.S., 2010. Rossberg landslide history and flood chronology as recorded in Lake Lauerz sediments (Central Switzerland). *Swiss Journal of Geosciences* 103, 43-59
- Büntgen, U., Franke, J., Frank, D., Wilson, R., González-Rouco, F., Esper, J., 2010. Assessing the spatial signature of European climate reconstructions. *Climate Research* 41, 125-130
- CH2011, 2011. Swiss Climate Change Scenarios CH2011, published by C2SM, MeteoSwiss, ETH, NCCR Climate, and OcCC, Zurich, Switzerland, 88 pp
- Chapron, E., Desmet, M., De Putter, T., Loutre, M.F., Beck, C., deconinck, J.F., 2002. Climatic variability in the northwestern Alps, France, as evidenced by 600 years of terrigenous sedimentation in Lake Le Bourget. *The Holocene* 12, 177-185
- Christensen, J.H., Krishna Kumar, K., Aldrian, E., An, S.-I., Cavalcanti, I.F.A., de Castro, M., Dong, W., Goswami, P., Hall, A., Kanyanga, J.K., Kitoh, A., Kossin, J., Lau, N.-C., Renwick, J., Stephenson, D.B., Xie, S.-P., Zhou, T., 2013. Climate Phenomena and their Relevance for Future Regional Climate Change. In: *Climate Change 2013: The Physical Science Basis. Contribution of Working Group I to the Fifth Assessment Report of the Intergovernmental Panel on Climate Change* [Stocker, T.F., Qin, D., Plattner, G.-K., Tignor, M., Allen, S.K., Boschung, J., Nauels, A., Xia, Y., Bex, V., Midgley, P.M. (eds.)]. Cambridge University Press, Cambridge, United Kingdom and New York, NY, USA, 91 pp
- Cockburn, J.M.H., Lamoureux, S.F., 2007. Century-scale variability in late-summer rainfall events recorded over seven centuries in sub annually laminated lacustrine sediments, White Pass, British Columbia. *Quaternary Research* 67, 193-203
- de Jong, R., Kamenik, C., Grosjean, M., 2013. Cold-season temperatures in the European Alps during the past millennium: variability, seasonality and recent trends. *Quaternary Science Reviews* 82: 1-12
- Elbert, J., Grosjean, M., von Gunten, L., Urrutia, R., Fischer, D., Wartenburger, R., Ariztegui, D., Fujak, M., Hamann, Y., 2012. Quantitative high-resolution winter (JJA) precipitation reconstruction from varved sediments of Lago Plomo 47°S, Patagonian Andes, AD 1530–2002. *The Holocene* 22, 465-474
- Frei, C., Schöll, R., Fukutome, S., Schmidli, J., Vidale, P.L., 2006. Future change of precipitation extremes in Europe: Intercomparison of scenarios from regional climate models. *Journal of Geophysical Research* 111, D06105
- Gilli, A., Anselmetti, F.S., Glur, L., Wirth, S.B., 2013. Lake sediments as archives of recurrence rates and intensities of past flood events. In: Schneuwly- Bollschweiler, M., Stoffel, M., Rudolf-Miklau, F. (Eds.), *Dating Torrential Processes on Fans and Cones – Methods and Their Application for Hazard and Risk Assessment. Advances in Global Change Research*, 47. Springer Netherlands, pp 225-242
- Greve, P., Orłowsky, B., Mueller, B., Sheffield, J., Reichstein, M., Seneviratne, S.I., 2014. Global assessment of trends in wetting and drying over land. *Nature Geoscience*, Advance Online Publication (14 September 2014)
- Hegerl, G.C., Crowley, T.J., Hydem W.T., Frame, D.J., 2006. Climate sensitivity constrained by temperature reconstructions over the past seven centuries. *Nature* 440, 1029-1032
- Held, I.M., Soden, B.J., 2006. Robust Responses of the Hydrological Cycle to Global Warming. *Journal of Climate* 19, 5686-5699

Hughen, K.A., Overpeck, J.T., Anderson, R.F., 2000. Recent warming in a 500-year palaeotemperature record from varved sediments, Upper Soper Lake, Baffin Island, Canada. *Holocene* 10, 9-19

IPCC, 2012. Managing the Risks of Extreme Events and Disasters to Advance Climate Change Adaptation. A Special Report of Working Groups I and II of the Intergovernmental Panel on Climate Change [Field, C.B., Barros, V., Stocker, T.F., Qin, D., Dokken, D.J., Ebi, K.L., Mastrandrea, M.D., Mach, K.J., Plattner, G.-K., Allen, S.K., Tignor, M., Midgley, P.M. (eds.)]. Cambridge University Press, Cambridge, UK, and New York, NY, USA, 582 pp

IPCC, 2013. Summary for Policymakers. In: *Climate Change 2013: The Physical Science Basis. Contribution of Working Group I to the Fifth Assessment Report of the Intergovernmental Panel on Climate Change* [Stocker, T.F., Qin, D., Plattner, G.-K., Tignor, M., Allen, S.K., Boschung, J., Nauels, A., Xia, Y., Bex, V., Midgley, P.M. (eds.)]. Cambridge University Press, Cambridge, United Kingdom and New York, NY, USA, 29 pp

Jansen, E., Overpeck, K.R., Briffa, J.-C., Duplessy, F., Joos, V., Masson-Delmotte, D., Olago, B., Otto-Bliesner, W.R., Peltier, S., Rahmstorf, R., Ramesh, D., Raynaud, D., Rind, O., Solomina, R., Villalba, and D. Zhang, 2007: Palaeoclimate. In *Climate Change 2007: The Physical Science Basis. Contribution of Working Group I to the Fourth Assessment Report of the Intergovernmental Panel on Climate Change*. S. Solomon, D. Qin, M. Manning, Z. Chen, M. Marquis, K.B. Averyt, M. Tignor, and H.L. Miller, Eds. Cambridge University Press, 433-497

Kalugin, I., Daryin, A., Smolyaninova, L., Andreev, A., Diekmann, B., Khlystov, O., 2007. 800-year-long records of annual air temperature and precipitation over southern Siberia inferred from Teletskoye Lake sediments. *Quaternary Research* 67, 400-410

Köplin, N., Schädler, B., Viviroli, D., Weingartner, R., 2014. Seasonality and magnitude of floods in Switzerland under future climate change. *Hydrological Processes* 28, 2567-2578

Lamoureux, S.F., 2000. Five centuries of interannual sediment yield and rainfall-induced erosion in the Canadian High Arctic recorded in lacustrine varves. *Water Resource Research* 36, 309-318

Larocque-Tobler, I., Stewart, M.M., Quinlan, R., Trachsel, M., Kamenik, C., Grosjean, M., 2012. A last millennium temperature reconstruction using chironomids preserved in sediments of anoxic Seebergsee (Switzerland): consensus at local, regional and Central European scales. *Quaternary Science Reviews* 41, 49-56

Luterbacher, J., Dietrich, D., Xoplaki, E., Grosjean, M., Wanner, H., 2004. European Seasonal and Annual Temperature Variability, Trends, and Extremes since 1500. *Science* 303: 1499-1503

Mann, M.E., Zhang, Z., Hughes, M.K., Bradley, R.S., Miller S.K., Rutherford, S., Ni, F., 2008. Proxy-based reconstructions of hemispheric and global surface temperature variations over the past two millennia. *Proceedings of the National Academy of Sciences* 105, 13252-13257

Masson-Delmotte, V., Schulz, M., Abe-Ouchi, A., Beer, J., Ganopolski, A., González Rouco, J.F., Jansen, E., Lambeck, K., Luterbacher, J., Naish, T., Osborn, T., Otto-Bliesner, B., Quinn, T., Ramesh, R., Rojas, M., Shao, X., Timmermann, A., 2013. Information from Paleoclimate Archives. In: *Climate Change 2013: The Physical Science Basis. Contribution of Working Group I to the Fifth Assessment Report of the Intergovernmental Panel on Climate Change* [Stocker, T.F., Qin, D., Plattner, G.-K., Tignor, M., Allen, S.K., Boschung, J., Nauels, A., Xia, Y., Bex, V., Midgley, P.M. (eds.)]. Cambridge University Press, Cambridge, United Kingdom and New York, NY, USA

MILLENNIUM 2011. EU FP6 IP_ <http://www.ncdc.noaa.gov/paleo/pubs/millennium/millennium.html>

Moore, J.J., Huguen, K.A., Miller, G.H., Overpeck, J.T., 2001. Little Ice Age recorded in summer temperature reconstruction from varved sediments of Donard Lake, Baffin Island, Canada *Journal of Paleolimnology* 25, 503-517

O’Gorman, P.A., Muller, C.J., 2010. How closely do changes in surface and column water vapor follow Clausius-Clapeyron scaling in climate-change simulations? *Environmental Research Letters* 5, 025207

PAGES 2k Consortium, 2013. Continental-scale temperature variability during the last two millennia. *Nature Geoscience* 6, 339-346

Pienitz, R., Lotter, A., 2009. Editorial: advances in paleolimnology. In: Pienitz R, Lotter A, Newman L, Kiefer T (eds) *Advances in paleolimnology*. PAGES News 17, 89-136

Saunders, K.M., Grosjean, M., Hodgson, D.A., 2013. A 950 year temperature reconstruction from Duckhole Lake, southern Tasmania, Australia. *The Holocene* 23, 771-783

Saunders, K.M, Kamenik, C., Hodgson, D.A., Hunziker, S., Siffert, L., Fischer, D., Fujak, M., Gibson, J.A.E., Grosjean, M., 2012. Late Holocene changes in precipitation in northwest Tasmania and their potential links to shifts in the Southern Hemisphere westerly winds. *Global and planetary change* 92-93, 82-91

Smith, K., 2013. *Environmental hazards: Assessing risk and reducing disaster*. Routledge, Taylor and Francis Group (eds.). New York, NY, USA, 478 pp

Villalba, R., Grosjean, M., Kiefer, T., 2009. Long-term multi-proxy climate reconstructions and dynamics in South America (LOTRED-SA): state of the art and perspectives. *Palaeogeography Palaeoclimatology Palaeoecology* 281, 175-179

von Gunten, L., Grosjean, M., Rein, B., Urrutia, R., Appleby, P., 2009. A quantitative high-resolution summer temperature reconstruction based on sedimentary pigments from Laguna Aculeo, central Chile, back to AD 850. *The Holocene* 19, 873-881

Wilhelm, B., Arnaud, F., Sabatier, P., Magand, O., Chapron, E., Courp, T., Tachikawa, K., Fanget, B., Malet, E., Pignol, C., Bard, E., Delannoy, J.J., 2013. Palaeoflood activity and climate change over the last 1400 years recorded by lake sediments in the north-west European Alps. *Journal of Quaternary Science* 28, 189-199

Wilson, R., Miles, D., Loader, N.J., Melvin, T., Cunningham, L., Cooper, R., Briffa, K., 2013. A millennial long March–July precipitation reconstruction for southern-central England. *Climate Dynamics* 40, 997-1017

Wohlfarth, B., Holmquist B., Cato I., Linderson, H., 1998. The climatic significance of clastic varves in the Ångermanälven Estuary, northern Sweden, AD 1860 to 1950. *The Holocene* 8, 521-534

Xoplaki, E., Luterbacher, J., Paeth, H., Dietrich, D., Steiner, N., Grosjean, M., Wanner, H., 2005. European spring and autumn temperature variability and change of extremes over the last half millennium. *Geophysical Research Letters* 32, 1-4

Zolitschka, B., 2007. Varved lake sediments. In: Elias SA (ed) *Encyclopedia of quaternary science*. Elsevier, Amsterdam, pp 3105-3114

Chapter 2



2. Material and methods**2.1. Sedimentation process understanding**

A first methodological step consisted in understanding sedimentation processes that led to varve formation in the two lakes under investigation. This work consisted of lake-catchment descriptions, water-column measurements, sediment trapping and contemporary sediment analyses.

In both lakes, logging thermistors were placed at different water depth for more than two years, which included two ice-cover periods in the thermal profiles. Oxygen and chlorophyll-*a* were also monitored in the water of Lake Żabińskie using a YSI 6820 meter (Yellow Spring Instrument, USA) and a Minitracka II C fluorometer (Chelsea Instruments, UK) respectively. Conductivity and pH were measured through the water column with a Hydrolab Water Sonde (Minisonde 4a).

Sediment traps were deployed near the lake bottom and collected every month in Lake Żabińskie, and every two to five months in Lake Oeschinen. Mass accumulation rate (MAR, in $\text{g cm}^{-2} \text{d}^{-1}$) was calculated, and the mineralogical and biogeochemical composition of the sediments were determined (more details are presented in the 'Methods' sections of Chapters 4 and 5).

2.2. Coring and data processing

Sediment cores with overlapping segments were retrieved with (i) an UWITEC gravity corer for surface sediments and (ii) an UWITEC piston corer for deeper sections. The cores with biochemical sediments from Lake Żabińskie were kept dark after collection to prevent sedimentary pigment degradation from exposure to light and oxygen. Back in the laboratory, the core segments were split lengthwise and photographed digitally. One core-half was used to develop the chronology (varve counting, ^{210}Pb and ^{14}C dates). The other core-half was used to establish the multi-proxy data set (non-destructive scans and sub-sampling).

Water content and dry bulk density (DBD) were calculated after the samples had been freeze dried. The relative proportions of organic matter and calcite content were derived from loss on ignition (LOI) at 550°C and 950°C, respectively (Dean 1974; Heiri et al. 2001). X-ray diffraction (XRD) was measured on Lake Oeschinen samples using a Philips PW 3710 (Institute of Geology, University of Bern) to characterize the mineralogical fraction after LOI₉₅₀ (Mauchle, 2010). Particle size analysis was performed on homogenized samples devoid of organic matter (H_2O_2 digestion) using laser diffraction (Malvern Mastersizer 2000, University of Bern). Total organic carbon, total nitrogen and total sulphur were measured using a CNS Vario El cube (Elemental Analyser, University of Bern) on about 15 mg homogenized and freeze-dried samples devoid of inorganic carbon (10% HCl digestion). Samples for biogenic Silica (BSi), a proxy for diatom abundance and productivity (Conley, 1988;

Conley and Schelske 2001), were prepared using the alkaline leaching method (30% H₂O₂ + 1M NaOH at 90°C for 3h). BSi concentrations were measured by ICP-OES (inductively coupled plasma optical emission spectrometry) at the Paul-Scherrer Institute (PSI), Villigen, Switzerland. Silica concentrations were corrected for inorganic silica (Ohlendorf and Sturm, 2008).

Sedimentary pigments from biochemical sediments were measured with high performance liquid chromatography (HPLC) using a Beckmann Coulter HPLC system equipped with Waters Spherisorb ODS2 5 µm column (250 mm x 4.6 mm) at the Institute of Plant Sciences, University of Bern. Sedimentary pigment preparation (sample sectioning, extraction in acetone, elution) and measurements followed standard procedures (Airs et al. 2001; Reuss et al. 2005; Reuss et al. 2010). The interpretation of pigment properties was based on standard literature (Swain 1985; Lami et al. 2000; Leavitt and Hodgson 2001; Reuss et al. 2010). More technical details related to pigment extraction, identification and quantification are provided in Appendix A.3.

2.3. Sediment dating

The varve chronology was inferred from high-resolution digital images of the fresh core surface and resin-embedded sediment slabs for Lake Żabińskie (Fig. 2.1), and from thin sections for Lake Oeschinen (Fig. 2.2). Preparation of sediment slabs followed standard protocols using the freeze drying technique, followed by embedding in epoxy resin (Lamoureux 1994; Lotter and Lemke 1999; Lamoureux 2001). Varves thickness was semi-automatically measured using the software package WinGeol Lamination Tool (0.01-mm resolution; Meyer et al. 2006).

Independent dating methods (¹³⁷Cs, ²¹⁰Pb, ¹⁴C) were used most recently by Bonk et al. (in progress) on the sediments of Lake Żabińskie, and confirmed that the laminae are annual. We applied the same criteria for varve distinction and counting, which is shown in the Appendix (Fig. A2).

The annual nature of the varves in Lake Oeschinen was first shown for the upper 25-cm sediments by Leemann and Niessen (1994). Most recently, this was corroborated for the first 50 cm by Mauchle (2010) from a CRS ²¹⁰Pb model (constant rate of supply; Appleby 2001) constrained by the AD 1963 ¹³⁷Cs peak. We sampled six terrestrial plant macrofossils for ¹⁴C dating to validate the varve chronology in the rest of the sediment sequence. ¹⁴C dates were obtained from Accelerator Mass Spectrometry (AMS) at the LARA lab of the University of Bern (Szidat et al. 2014) and calibrated online using the Oxcal program and the Intcal13 calibration curve (Reimer et al. 2013). Varve chronology used for the final reconstruction is shown in the Appendix (Fig. A1.1 - A1.8 and Table A1).

2.4. Proxy-climate calibration and reconstruction

The different proxy data were first regularized to annual values according to the varve chronology (linear interpolation) in order to be compared against climate time series. Then, both the proxy time series and the climate time series were smoothed with a triangular filter (3-yr, 5-yr and 7-yr filter). This procedure accounts for dating uncertainty and for errors induced by core sampling and data regularization.

Each proxy time series was correlated in a matrix with individual monthly and lagged 2-12 months means of temperature and precipitation at annual resolution and for the different filters. Results with the best correlation and consistency with the sedimentation processes were selected for the 'proxy-climate' calibrations (Żabińskie and Oeschinen) and reconstruction (Oeschinen).

Climate variables were inferred from proxy data using ordinary least squares regression (inverse regression). Probability values were corrected for serial autocorrelation induced by filtering (Bayley and Hammersley 1946; de Jong and Kamenik 2011). The quality of the proxy-climate calibrations was assessed using the split-period approach (cross-validation with calibration and verification periods). Objective criteria such as reduction of error (RE), coefficient of efficiency (CE) and root mean square error of prediction (RMSEP) were calculated following standard procedures (Cook et al. 1994; von Gunten et al. 2012a).

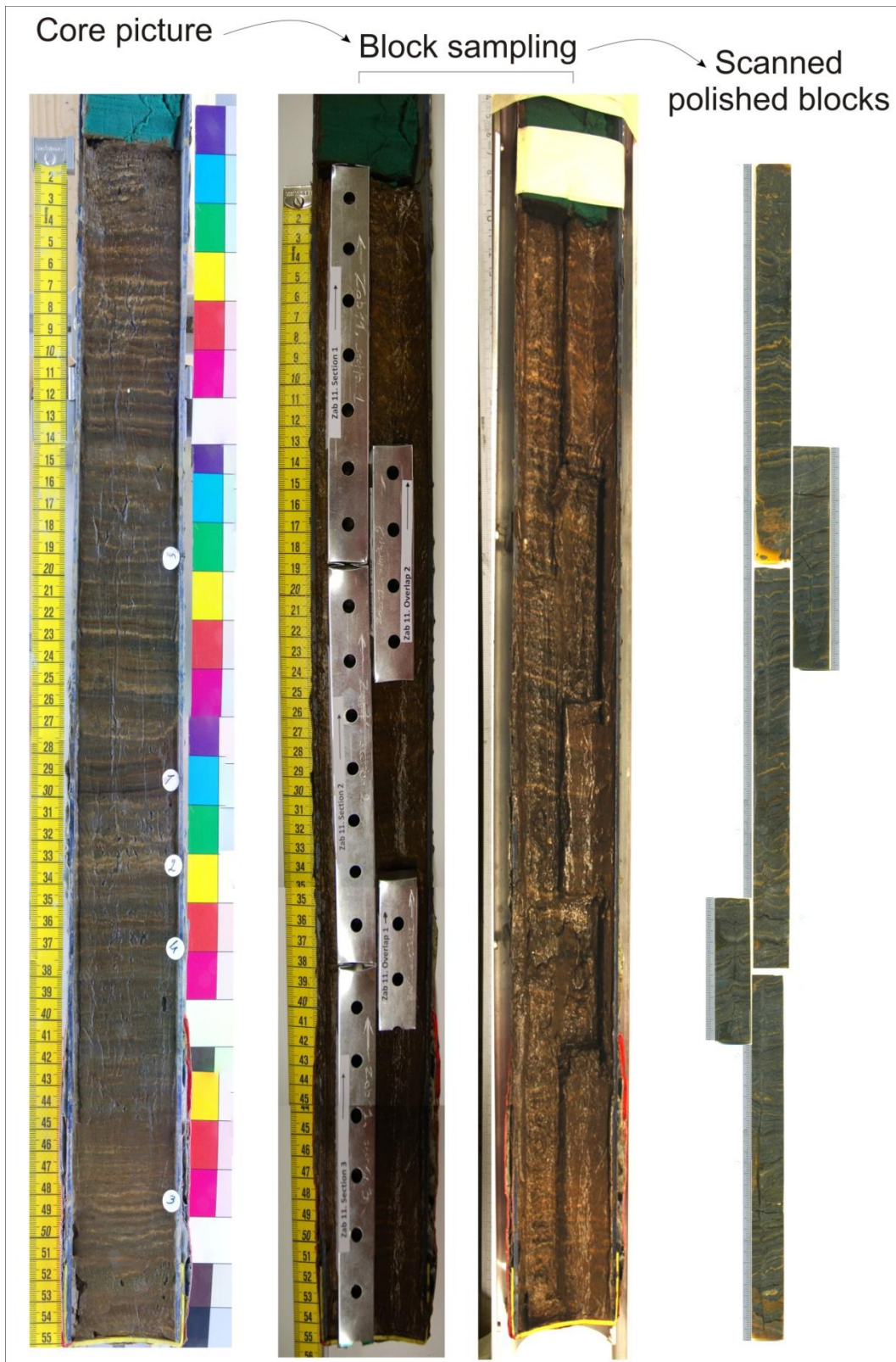


Fig. 2.1 Core picture and resin-embedded blocks sampling for the varve chronology from Lake Żabińskie

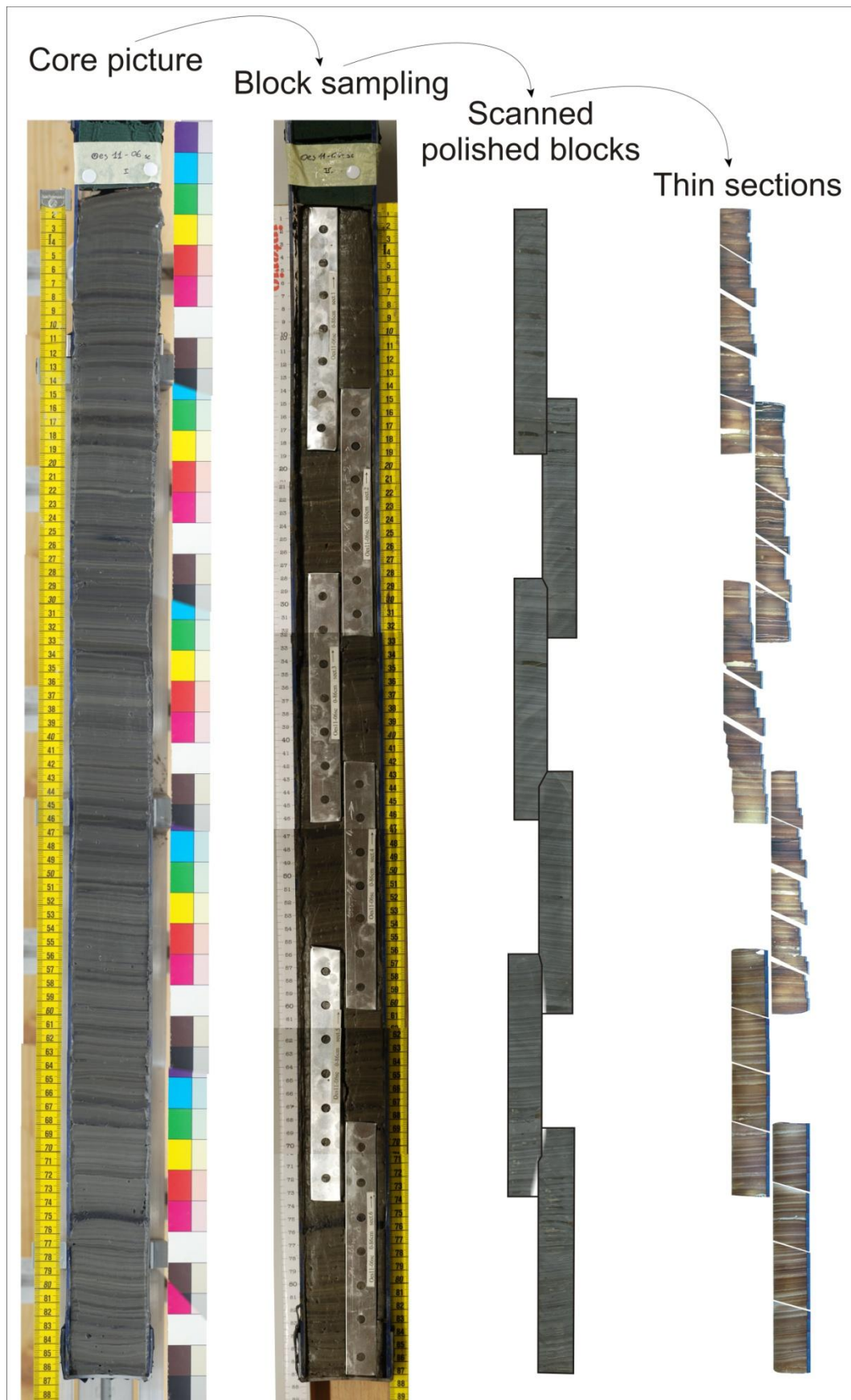


Fig. 2.2 Methodology for resin-embedded blocks sampling and thin sections preparation required to develop the varve chronology from Lake Oeschinen

References (Chapter 2)

- Airs, R.L., Atkinson, J.A., Keely, B.J., 2001. Development and application of a high resolution liquid chromatographic method for the analysis of complex pigment distributions. *Journal of Chromatography* 917, 167-177
- Appleby, P.G., 2001. Chronostratigraphic techniques in recent sediments. In: Last WM, Smol JP (eds) *Tracking environmental change using lake sediments: basin analysis, coring, and chronological techniques*. Kluwer, Dordrecht, pp 171-201
- Bayley, G.V., Hammersley, J.M., 1946. The “effective” number of independent observations in an autocorrelated time series. *Supplement to the Journal of the Royal Statistical Society* 8, 184-197
- Bonk, A., Goslar, T., Tylmann, W., Wacnik, A., Grosjean, M., in progress. Multiple dating of varved sediment cores from Lake Żabińskie
- Conley, D.J., 1988. Biogenic Silica as an Estimate of Siliceous Microfossil Abundance in Great-Lakes Sediments. *Biogeochemistry* 6, 161-179
- Conley, D.J., Schelske, C.L., 2001. Biogenic silica. In: Smol JP, Birks HJB, Last WM (eds) *Tracking environmental change using lake sediments. Vol 3: terrestrial, algal and siliceous indicators*. Kluwer, Dordrecht, pp 281-293
- Cook, E.R., Briffa, K.R., Jones, P.D. 1994. Spatial regression methods in dendroclimatology – a review and comparison of 2 techniques. *International Journal of Climatology* 14, 379-402
- de Jong, R., Kamenik, C., 2011. Validation of a chrysophyte stomatocyst-based cold-season climate reconstruction from high Alpine Lake Silvaplana, Switzerland. *Journal of Quaternary Science* 26, 268-275
- Dean, W.E., 1974. Determination of carbonate and organic matter in calcareous sediments and sedimentary rocks by loss on ignition: comparison with other methods. *Journal of Sedimentary Petrology* 44, 242-248
- Heiri, O., Lotter, A.F., Lemcke, G., 2001. Loss on ignition as a method for estimating organic and carbonate content in sediments: reproducibility and comparability of results. *Journal of Paleolimnology* 25, 101-110
- Lami, A., Guilizzoni, P., Marchetto, A., 2000. High resolution analysis of fossil pigments, carbon, nitrogen and sulphur in the sediment of eight European Alpine lakes: the MOLAR project. *Journal of Limnology* 59, 15-28
- Lamoureux, S.F., 1994. Embedding unfrozen lake sediments for thin section preparation. *Journal of Paleolimnology* 10, 141-146
- Lamoureux, S.F., 2001. Varve chronology techniques. In: Last WM, Smol JP (eds) *Tracking environmental change using lake sediments: basin analysis, coring, and chronological techniques*. Kluwer, Dordrecht, pp 247-260
- Leavitt, P.R., Hodgson, D.A., 2001. Sedimentary pigments. In: Smol JP, Birks HJB, Last WM (eds) *Tracking environmental change using lake sediments. Vol 3: terrestrial, algal and siliceous indicators*. Kluwer, Dordrecht, pp 295-325

Leemann, A., Niessen, F., 1994. Varve formation and the climatic record in an Alpine proglacial lake: calibrating annually laminated sediments against hydrological and meteorological data. *The Holocene* 4, 1-8

Lotter, A.F., Lemcke, G., 1999. Methods for preparing and counting biochemical varves. *Boreas* 28, 243-252

Mauchle, F., 2010. The modern sediments of Lake Oeschinen (Swiss Alps) as an archive for climatic and meteorological events. MSc dissertation, Institute of Geography and OCCR, University of Bern, Switzerland

Meyer, M.C., Faber, R., Spotl, C., 2006. The wingeol lamination tool: new software for rapid, semi-automated analysis of laminated climate archives. *The Holocene* 16, 753-761

Ohlendorf, C., Sturm, M., 2008. A modified method for biogenic silica determination. *Journal of Paleolimnology* 39, 137-142

Reimer, P., Bard, E., Bayliss, A., Beck, J., Blackwell, P., Bronk Ramsey, C., Buck, C., Cheng, H., Edwards, R., Friedrich, M., Grootes, P., Guilderson, T., Haflidason, H., Hajdas, I., Hatté, C., Heaton, T., Hoffmann, D., Hogg, A., Hughen, K., Kaiser, K., Kromer, B., Manning, S., Niu, M., Reimer, R., Richards, D., Scott, E., Southon, J., Staff, R., Turney, C., van der Plicht, J., 2013. Intcal13 and Marine13 radiocarbon age calibration curves 0–50,000 years cal BP. **Radiocarbon** 55, 1869-1887.

Reuss, N., Conley, D.J., Bianchi, T.S., 2005. Preservation conditions and the use of sediment pigments as a tool for recent ecological reconstruction in four Northern European estuaries. *Marine Chemistry* 95, 283-302

Reuss, N., Leavitt, P.R., Hall, R.I., Bigler, C., Hammarlund, D., 2010. Development and application of sedimentary pigments for assessing effects of climatic and environmental changes on subarctic lakes in northern Sweden. *Journal of Paleolimnology* 43, 149-169

Swain, E.B., 1985. Measurement and interpretation of sedimentary pigments. *Freshwater Biology* 15, 53-75

Szidat, S., Salazar, G.A., Vogel, E., Battaglia, M., Wacker, L., Synal, H.-A., Türlér, A., 2014. ¹⁴C analysis and sample preparation at the new Bern Laboratory for the Analysis of Radiocarbon with AMS (LARA). *Radiocarbon* 56, 561-566.

von Gunten, L., Grosjean, M., Kamenik, C., Fujak, M., Urrutia, R., 2012. Calibrating biogeochemical and physical climate proxies from non-varved lake sediments with meteorological data: methods and case studies. *Journal of Paleolimnology* 47, 583-600

Chapter 3



3. Reflectance spectroscopy in the visible range (VIS-RS)

3.1. Introduction

Varved lake sediments are a well-known natural paleoclimatic archive that provides high-resolution records. They have been investigated using a wide range of biological, sedimentological, geophysical, mineralogical and biogeochemical proxies to infer past climatic changes (Pienitz et al. 2009). However, producing such high-quality datasets from varved lake sediments is very difficult, which explains why lake sediment data are still poorly represented in comprehensive multi-proxy reconstructions (e.g. Mann et al. 2008).

One fundamental methodological obstacle in the study of lake sediments for paleoclimatology is that most of the analytical techniques are destructive, time consuming and often expensive. Naturally, this limits the number of data points that can be generated and, in turn, restricts the temporal resolution and the length of the paleoclimate records.

In recent years, major developments have been made in the field of rapid, scanning, non-destructive techniques with direct measurements on sediment cores to address and reduce these limitations. These techniques include X-Ray Fluorescence scans (Zolitschka et al. 2001; Brauer et al. 2009; among others) and reflectance spectroscopy in the visible (VIS-RS, 380-730 nm) spectral range (Rein and Sirocko 2002; Rein et al. 2005).

In this chapter, we present a methodological study about the use of rapid scanning VIS-RS on biochemical varves and clastic varves.

3.2. Methodology: principle and use

Fig. 3.1 shows the portable device used for VIS-RS scans on fresh sediment core surfaces (GretagMcBeth Spectrolino, Switzerland), and the typical spectra obtained from the biochemical varves of Lake Żabińskie (Poland) and the clastic varves of Lake Oeschinen (Swiss Alps). This technique provides calibrated reflectance spectra in the visible range with a spectral resolution of 10 nm and a spatial resolution of 0.2 cm. The advantages of this technique is that it is rapid (> 1000 data points can be generated per day), inexpensive and non-destructive (Trachsel et al. 2010).

3. Reflectance spectroscopy in the visible range (VIS-RS)

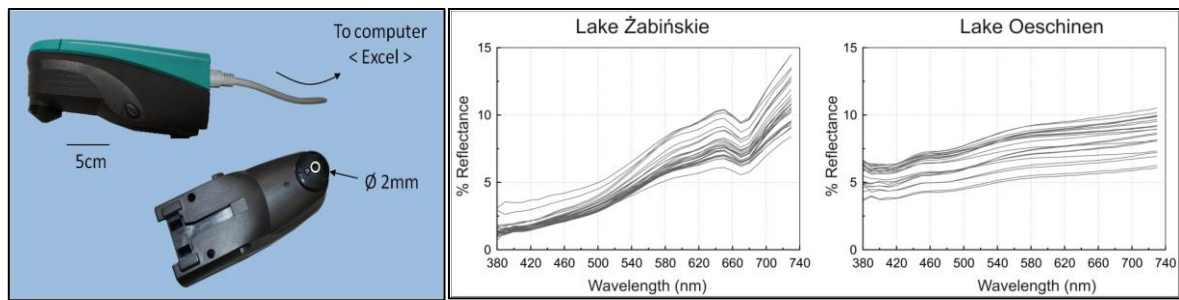


Fig. 3.1 a) Picture of the portable Spectrolino device used for VIS-RS scanning and, b) raw visible reflectance spectra obtained from the biochemical varves of Lake Żabińskie and the clastic varves from Lake Oeschinen

The challenge for VIS-RS is how to interpret and transform raw reflectance spectroscopy data into information about specific and well-defined organic or inorganic sediment compounds as determined by analytical techniques (referred to as a ‘proxy-proxy’ calibration). In a pioneering study, Rein and Sirocko (2002) derived spectral indices indicative of specific sediment compounds. For instance, they calculated the ratio between the reflectance values at 570 and 630 nm (index R_{570}/R_{630}) to estimate the contribution of terrigenous sediments (mainly illite, chlorite, biotite) in mineroclastic sediments. They also defined an index in organic-rich sediments referred to as the Relative Absorption Band Depth ($RABD_{660;670}$), which is an estimate of the amplitude of the absorption trough centred at 660 to 670 nm (max. Chlorophyll-*a* absorption). They could relate this index to the content of sedimentary chlorophyll-*a* compounds, with the formula:

$$RABD_{660;670} = \frac{(6 \cdot R_{590} + 7 \cdot R_{730}) / 13}{R_{\min(660;670)}}$$

Whereby R_i is the reflectance value (in %) at the *i* wavelength (see next section for the graphical representation of $RABD_{660;670}$ on biochemical sediments).

A few studies on lake sediments have shown that these indices derived from scanning VIS-RS can be calibrated directly to meteorological data and used for high-resolution quantitative climate reconstructions. Among the best examples, von Gunten et al. (2009) found a positive correlation between the index $RABD_{660;670}$ and Austral summer temperature in a lake study from Central Chile, which enabled them to reconstruct temperature back to AD 850 (Fig. 3.2a). Increasing $RABD_{660;670}$ was interpreted as an increase in primary productivity (Chlorophyll-*a*), favoured by warmer summer temperature. Also, Trachsel et al. (2010) found a positive correlation between a multivariate VIS-RS dataset related to clay minerals (R_{590}/R_{630} among others) and summer temperature in a lake study from the northeast Alps (Fig. 3.2b). This enabled them to extend the temperature time-series back to AD 1177. In this case, increased R_{590}/R_{630} was interpreted as an increase in minerogenic-sediment

3. Reflectance spectroscopy in the visible range (VIS-RS)

transport (clay), which was enhanced by the effect of summer temperature on glacier melt-water. In another study, Saunders et al. (2012) found an inverse correlation between R_{660}/R_{670} (indicator of pigment diagenesis) and annual rainfall from northwest Tasmania, extending the rainfall record back to 1150 BC (Fig. 3.2c). Increased R_{660}/R_{670} was interpreted as an increase in pigment diagenesis (decrease in pigment preservation). This was attributed to more light penetration under reduced rainfall conditions and shallower lake level. Finally, de Jong et al. (2013) reconstructed summer temperature in the high Andes back to 1000 BC from the calibration between R_{570}/R_{630} and temperature (Fig. 3.2d). Increased R_{570}/R_{630} was interpreted as a higher content in fine lithogenic sediments (clay minerals), due to a longer ice-cover period governed by cooler summer temperature.

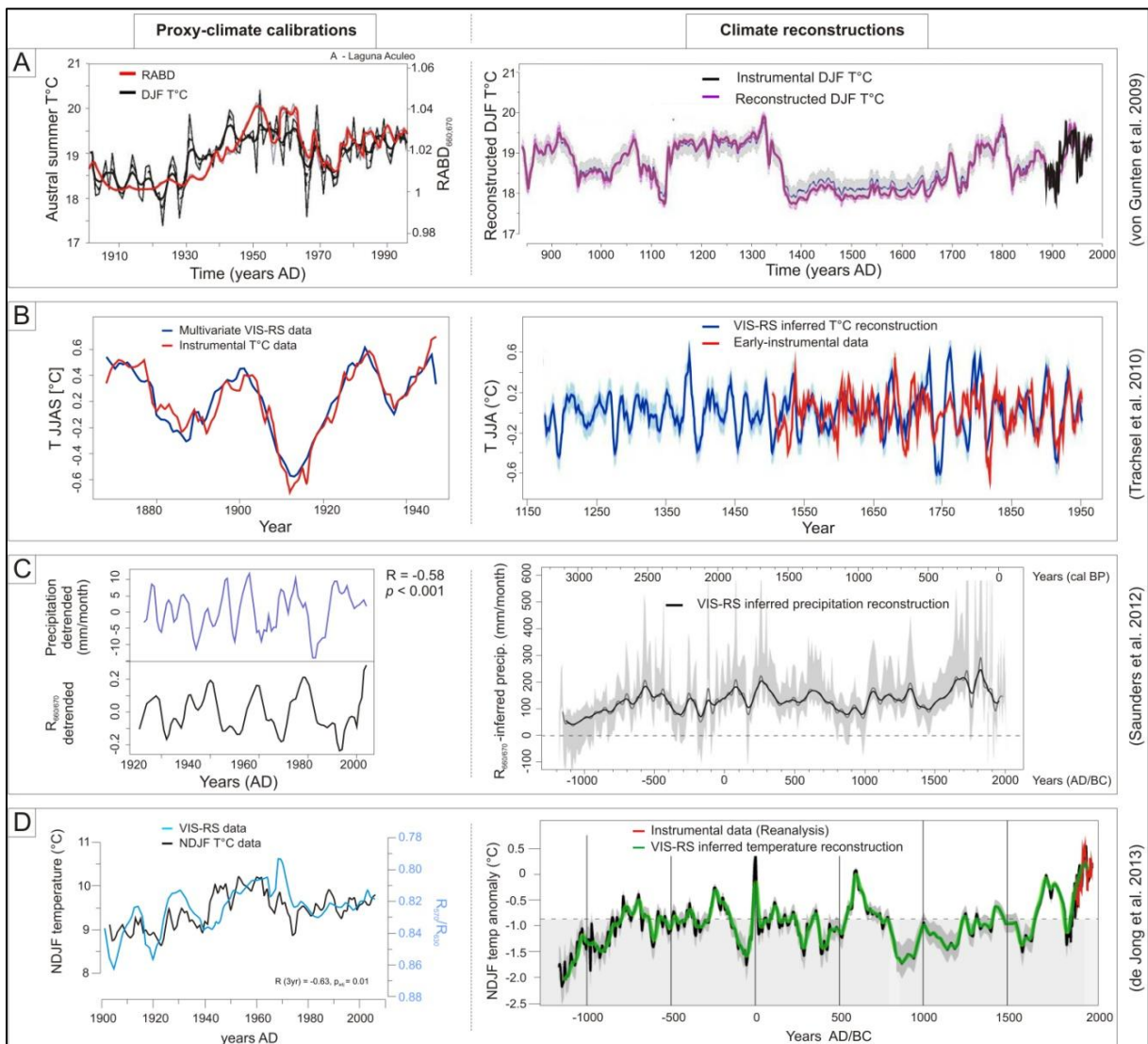


Fig. 3.2 Four examples of lake sediment studies that used scanning VIS-RS data directly for high-resolution quantitative climate calibrations (left panel) and reconstructions (right panel): a) in Central Chile (von Gunten et al. 2009); b) in the NE Alps (Trachsel et al. 2010); c) in NW Tasmania (Saunders et al. 2012); and d) in the High Central Andes (de Jong et al. 2013)

3. Reflectance spectroscopy in the visible range (VIS-RS)

These reconstructions (Fig. 3.2) are all based on direct statistical relationships between VIS-RS data (i.e. established indices) and climate data. However, the proxy-climate relationship is specific to each individual lake system, which sets limits on the interpretation of VIS-RS data in relation to the sediment compounds. Consequently, this makes it difficult to search for the biogeochemical processes that might explain the relationship between VIS-RS and changes in climate variability. Therefore, calibration and validation of VIS-RS data with specific, well-defined sediment compounds as determined by established analytical techniques, remains a basis for any sound paleoenvironmental interpretation.

Better known are the detection and calibration of organic compounds by reflectance spectroscopy in the visible (and near-infrared) range on sub-samples under controlled conditions (Rosen et al. 2000; Das et al. 2005; Wolfe et al. 2006; Michelutti et al. 2010). However, VIS-RS on subsamples is methodologically very different from VIS-RS logging performed directly on the fresh sediment cores (method explored here).

Thus, the aim of this chapter is to develop calibration and validation 'proxy-proxy' models between scanning VIS-RS data and specific well-defined sediment compounds from analytical techniques for the two lakes studied in this thesis.

3.3. Spectral indices for the biochemical varves of Lake Żabińskie

Biochemical sediments from Lake Żabińskie are of particular interest in the context of VIS-RS as they contain high concentrations of sedimentary pigments related to Chl-*a*. These compounds have relatively strong and specific absorption bands in the visible spectral range centred between 660 and 670 nm (Fig. 3.3, *upper panel*). This enables applying the index $RABD_{660;670}$ established by Rein and Sirocko (2002) on reflectance spectra measured on the sediments of Lake Żabińskie. To test whether the calibration with sedimentary pigments related to Chl-*a* can be improved, we additionally applied some other indices. These indices consisted in the ratio R_{660}/R_{670} , the Relative Absorption Band Area between 590 and 730 nm ($RABA_{590;730}$; Fig. 3.3, area in blue) and the Relative Absorption Band Area between 650 and 730 nm ($RABA_{650;730}$). The calculation of these indices follows Trachsel et al. (2010). Two additional indices were also derived from the first-derivative spectra (Fig. 3.3, *lower panel*) such as the ratio R'_{690}/R'_{660} , and the minimum value of the first-derivative spectra between 650 and 680 nm ($\min(R'_{650;680})$).

3. Reflectance spectroscopy in the visible range (VIS-RS)

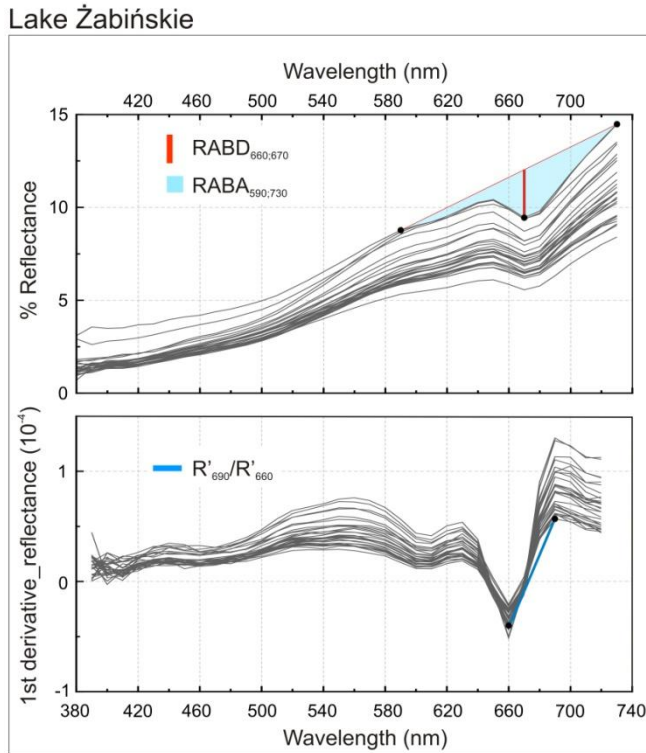


Fig. 3.3
Examples of raw reflectance spectra and associated first-derivative spectra from the biochemical varves of Lake Żabińskie

These VIS-RS indices were then compared with specific sedimentary pigment compounds as measured by High Performance Liquid Chromatography (HPLC). The pigments considered for calibration were the chlorophyll-*a*, and its degradation products (chlorins) pheophytin-*a* and pyro-pheophytin-*a* (Fig. 3.4). More details about pigment extraction, identification and quantification can be found in Appendix A.3 and the corresponding Fig. A.3.

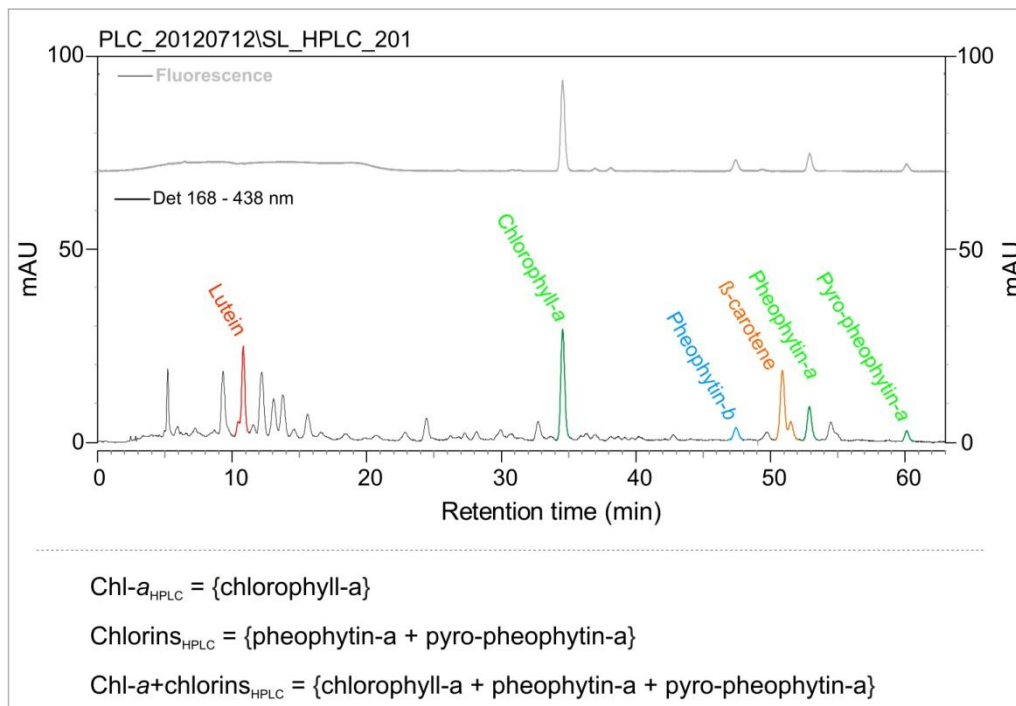


Fig. 3.4 HPLC chromatogram of a biochemical sample from the sediments of Lake Żabińskie

3. Reflectance spectroscopy in the visible range (VIS-RS)

Correlation tests (Table 3.1) showed that $RABD_{660;670}$ is mostly highly correlated ($r = 0.75$, $p < 0.01$) to the content of chlorins (Chl-*a* degradation products = {pheophytin-*a* + pyropheophytin-*a*}). Surprisingly, correlation coefficients between each of the six VIS-RS indices and HPLC data decrease when primary Chl-*a* is included (Table 3.1).

Table 3.1 Correlation coefficient between the VIS-RS index $RABD_{660;670}$ and compound-specific HPLC measurements

	Chl- <i>a</i> HPLC	Chl- <i>a</i> + chlorins HPLC	Chlorins HPLC
$RABD_{660;670}$	0.36	0.58 *	0.75 *
R_{660}/R_{670}	0.36	0.57 *	0.73 *
$RAB_{590;730}$	0.26	0.47 *	0.65 *
$RAB_{650;730}$	0.21	0.43 *	0.62 *
R'_{690}/R'_{660}	0.35	0.53 *	0.67 *
$\min(R'_{650;680})$	0.34	0.54 *	0.69 *

* $p < 0.01$

To assess the causes that led to different correlation coefficients, we presented in Fig. 3.5 the calibration models from (i) $RABD_{660;670}$ and {Chl-*a* + chlorins} ($r = 0.58$), and (ii) $RABD_{660;670}$ and Chlorins only ($r = 0.75$). The first plot on Fig. 3.5a shows that the weaker correlation between $RABD_{660;670}$ and the overall sum of {Chl-*a* + chlorins} seems to be driven by six points that exceed the 2*standard deviation in the linear model (Fig. 3.5a, red points). The second plot on Fig. 3.5a shows that these six points correspond to samples that have the highest proportions of primary Chl-*a* as compared to its degradation products (ratio Chl-*a*/chlorins > 0.8). Furthermore, a clear trend can be observed in the plot between the residuals of the linear model ($RABD_{660;670}$ vs. {Chl-*a* + chlorins}) and proportions of Chl-*a*/chlorins. This trend is highly dependent on the six points with the highest proportions of primary Chl-*a*. This suggests that VIS-RS data cannot be used for Chl-*a*/chlorins ratios that exceed a value of 0.8.

Interestingly, these findings are in line with work performed by Das et al. (2005), who similarly defined threshold in primary Chl-*a* for which reflectance spectroscopy cannot be applied. This can be explained by the fact that primary Chl-*a* has an absorption maximum at around 663 nm (Frigaard et al. 1996), while VIS-RS data from our study provide insight into the spectral properties at 660 and 670 nm (10 nm spectral resolution).

The 'proxy-proxy' calibration and validation model between $RABD_{660;670}$ and chlorins is shown in Fig. 3.5b. The split period approach ($n_{\text{calibration}} = 26$, $n_{\text{validation}} = 25$) suggests that the model performs well (RE = 0.62, CE = 0.61) with highly significant statistical skills (von Gunten et al. 2012).

3. Reflectance spectroscopy in the visible range (VIS-RS)

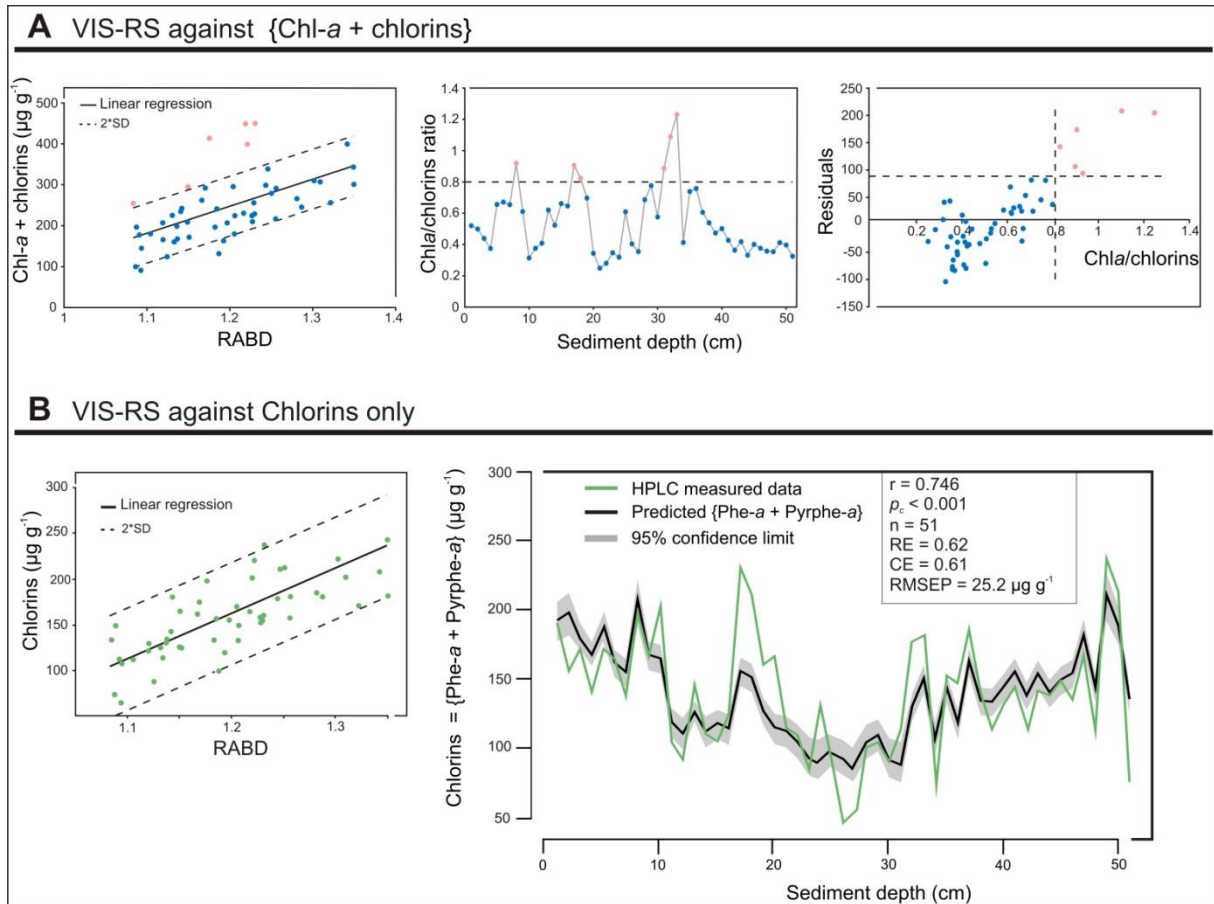


Fig. 3.5 Comparison between VIS-RS logging and compound-specific HPLC data: a) for the overall sum {Chl-a + chlorins} and b) uniquely for chlorins {Pheophytin-a + Pyropheophytin-a}. The final 'proxy-proxy model' and its performance are shown on the lower right panel

On the basis of our results, we concluded that scanning VIS-RS provides a valuable, fast, non-destructive and highly-resolved technique to infer chlorin concentrations from the biochemical sediments of Lake Żabińskie. In Chapter 5, it will be demonstrated that chlorin content (inferred from VIS-RS) is correlated with spring temperature variability (March to May; highest chlorophyll-a concentrations recorded in limnological monitoring). This will offer the possibility for a high-resolution spring temperature reconstruction back in time.

3.4. Spectral indices for the clastic varves of Lake Oeschinen

VIS-RS spectra from the sediments of Lake Oeschinen show that a different methodology needs to be applied to clastic varves (Fig. 3.6; *upper panel*). Based on the hypothesis that proportions of calcite (bright) might be distinguished from proportions of siliciclastic material (dark) using VIS-RS data, a specific methodology was applied to these varves.

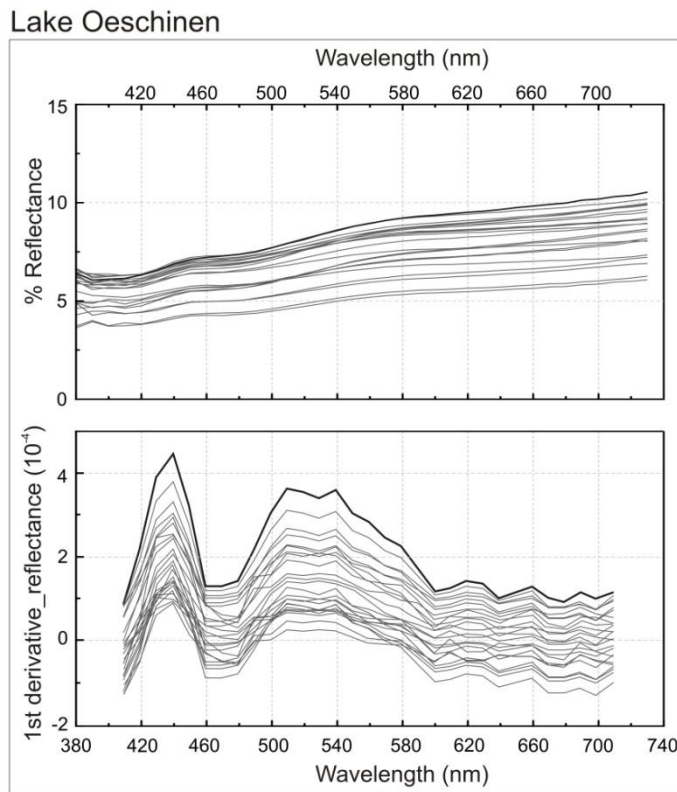


Fig. 3.6
Examples of raw reflectance spectra and associated first-derivative spectra from the clastic varves of Lake Oeschinen

Here, we developed an algorithm from VIS-RS to infer mixing ratios of the principal mineral groups (calcite versus siliciclastics). A series of ‘synthetic sediments’ with known mixing ratios ranging from a maximum content of calcite (100% in theory, end-member 1) to a maximum content of siliciclastics (100% in theory, end-member 2) were prepared. In order to keep comparable grain size, the ‘synthetic sediments’ were prepared directly from the sediment core by mineral separation (enrichment versus depletion) and remixing (Table 3.2). This methodology was designed in a way that the composition of the ‘synthetic sediments’ encompassed the full range of content in calcite and siliciclastics measured by LOI₉₅₀ (loss on ignition at 950°C) through the entire sediment sequence of Lake Oeschinen.

3. Reflectance spectroscopy in the visible range (VIS-RS)

Table 3.2 Methodology for the sample preparation of ‘synthetic sediment’ samples

	Carbonates	Siliciclastics
Enrich	Remove organic matter [H ₂ O ₂]	Remove organic matter [H ₂ O ₂] and Remove carbonates [10% HCl]
Deplete	Remove carbonates [10% HCl]	-

These ‘synthetic sediments’ were then analysed with VIS-RS scans (~50 replicates/remixing), starting from the end-members to gain information about the spectral properties of the different mixed phases. To account for the different water content between ‘synthetic sediments’ and the sediment core, the first derivative spectrum was calculated (Fig. 3.6, *lower panel*; Debret et al. 2011).

Figs. 3.7a and 3.7b show the comparison between the mean first-derivative VIS-RS from 44 remixing samples and the content of calcite and siliciclastics as derived from LOI₉₅₀. Results reveal that the relationship between VIS-RS data and content of calcite (or siliciclastics) is not linear but seems to follow an exponential function. However, Fig. 3.7c shows that the mean first-derivative VIS-RS can be used to infer the ratio calcite/siliciclastics following a linear relation with a highly significant correlation ($r = 0.965$, $p < 0.01$). On the basis of these results, we concluded that scanning VIS-RS provides a valuable technique to infer calcite/siliciclastics proportions in the mineroclastic sediments of Lake Oeschinen.

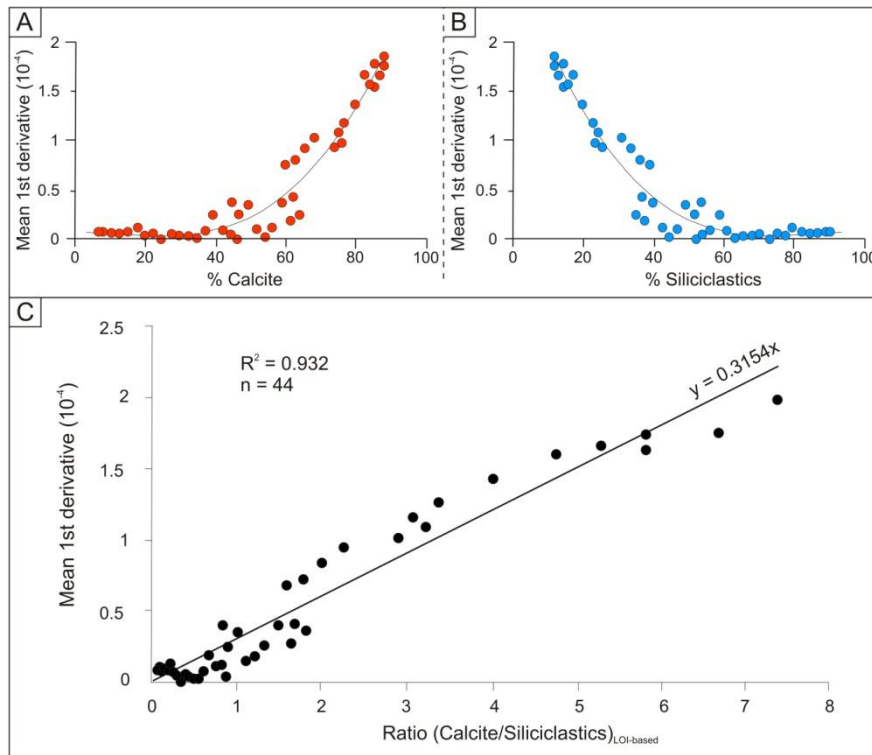


Fig. 3.7 Comparison between the mean 1st derivative of VIS-RS spectra in Lake Oeschinen and a) calcite content as derived from LOI₉₅₀, b) siliciclastic content as derived from LOI₉₅₀, and c) the ratio calcite/siliciclastics

References (Chapter 3)

- Brauer, A., Dulski, P., Mangili, C., Mingram, J., Liu, J., 2009. The potential of varves in high-resolution paleolimnological studies. *PAGES news* 17, 3
- Das, B., Vinebrooke, R.D., Sanchez-Azofeifa, A., Rivard, B., Wolfe, A.P., 2005. Inferring sedimentary chlorophyll concentrations with reflectance spectroscopy: a novel approach to reconstructing historical changes in the trophic status of mountain lakes. *Canadian Journal of Fisheries and Aquatic Sciences* 62, 1067-1078
- De Jong, R., Kamenik, C., Grosjean, M., 2013. Cold-season temperatures in the European Alps during the past millennium: variability, seasonality and recent trends. *Quaternary Science Reviews* 82, 1-12
- Debret, M., Sebag, D., Desmet, M., Balsam, W., Copard, Y., Mourier, B., Susperrigui, A.-S., Arnaud, F., Bentaleb, I., Chapron, E., Lallier-Vergès, E., Winiarski, T., 2011. Spectrocolorimetric interpretation of sedimentary dynamics: The new "Q7/4 diagram". *Earth-Science Reviews* 109, 1-19.
- Mann, M.E., Zhang, Z., Hughes, M.K., Bradley, R.S., Miller S.K., Rutherford, S., Ni, F., 2008. Proxy-based reconstructions of hemispheric and global surface temperature variations over the past two millennia. *Proceedings of the National Academy of Sciences* 105, 13252-13257
- Michelutti, N., Blais, J. M., Cumming, B.F., Paterson, A.M., Rühland, K., Wolfe, A.P., Smol, J.P., 2010. Do spectrally inferred determinations of chlorophyll a reflect trends in lake trophic status? *Journal of Paleolimnology* 43, 205-217
- Pienitz, R., Lotter, A., 2009. Editorial: advances in paleolimnology. In: Pienitz R, Lotter A, Newman L, Kiefer T (eds) *Advances in paleolimnology*. *PAGES News* 17, 89-136
- Rein, B., Sirocko, F., 2002. In-situ reflectance spectroscopy – analysing techniques for high-resolution pigment logging in sediment cores. *International Journal of Earth Sciences* 91, 950-954
- Rein, B., Lückge, A., Reinhardt, L., Sirocko, F., Wolf, A., Dullo, W.-C., 2005. El Niño variability off Peru during the last 20,000 years. *Paleoceanography* 20, 1-17
- Rosen, P., Dabakk, E., Renberg, I., Nilsson, M., Hall, R., 2000. Near-infrared spectrometry (NIRS): a new tool for inferring past climatic changes from lake sediments. *The Holocene* 10, 161-166
- Saunders, K.M., Kamenik, C., Hodgson, D.A., Hunziker, S., Siffert, L., Fischer, D., Fujak, M., Gibson, J.A.E., Grosjean, M., 2012. Late Holocene changes in precipitation in northwest Tasmania and their potential links to shifts in the Southern Hemisphere westerly winds. *Global and Planetary Change* 92-93, 82-91
- Trachsel, M., Grosjean, M., Schnyder, D., Kamenik, C., Rein, B., 2010. Scanning reflectance spectroscopy (380–730 nm): a novel method for quantitative high-resolution climate reconstructions from minerogenic lake sediments. *Journal of Paleolimnology* 44, 979-994
- von Gunten, L., Grosjean, M., Rein, B., Urrutia, R., Appleby, P., 2009. A quantitative high-resolution summer temperature reconstruction based on sedimentary pigments from Laguna Aculeo, central Chile, back to AD 850. *The Holocene* 19, 873-881
- Von Gunten, L., D'Andrea, W.J., Bradley, R., Huang, Y., 2012. Proxy-to-proxy calibration: Increasing the temporal resolution of quantitative climate reconstructions. *Scientific Reports* 2, 609
- Wolfe, A.P., Vinebrooke, R.D., Michelutti, N., Rivard, B., Das, B., 2006. Experimental calibration of lake-sediment spectral reflectance to chlorophyll a concentrations: methodology and paleolimnological validation. *Journal of Paleolimnology* 36, 91-100
- Zolitschka, B., Mingram, J., van der Gaast, S., Jansen, F., Naumann, R., 2001. Sediment logging techniques. *DPER1*. Kluwer Academic Press. Chapter 7, 137-154

Chapter 4



4. Lake Oeschinen: clastic varves

4.1. Site description

Lake Oeschinen (43°30'N, 7°44'E) is a high elevation (1580 m a.s.l.) proglacial lake located in the northern Swiss Alps, 55 km south of Bern (Fig. 4.1a). It is part of the first UNESCO World Natural Heritage site of the European Alps. It has been protected since 1933 and was inscribed in the UNESCO list in 2001. The lake basin has a maximum depth of 56 m (Fig. 4.1b).

Bedrock in the catchment is mostly composed of Mesozoic limestone of Jurassic and Cretaceous age (Fig. 4.1c in blue and green, respectively). However, the northern part of the catchment comprises two sizable belts of Tertiary Flysch deposits (Fig. 4.1c in yellow), which consist of easily erodible sandstones with abundant siliclastic minerals (mainly quartz, illite and chlorite; Suchy et al. 1997; Mauchle 2010).

The relatively small (22 km²) but steep catchment is characterized by high summits that reach up to 3660 m a.s.l. Glacier cover accounts for about 30% of the watershed, whereby all glaciers are located in the limestone part of the catchment.

The entire catchment area is drained by watercourses in the north and north-east (Tertiary Flysch + limestone) that account together for about 60% of the catchment, and by watercourses in the south (only limestone) that account for 40% of the catchment (Fig. 4.1c).

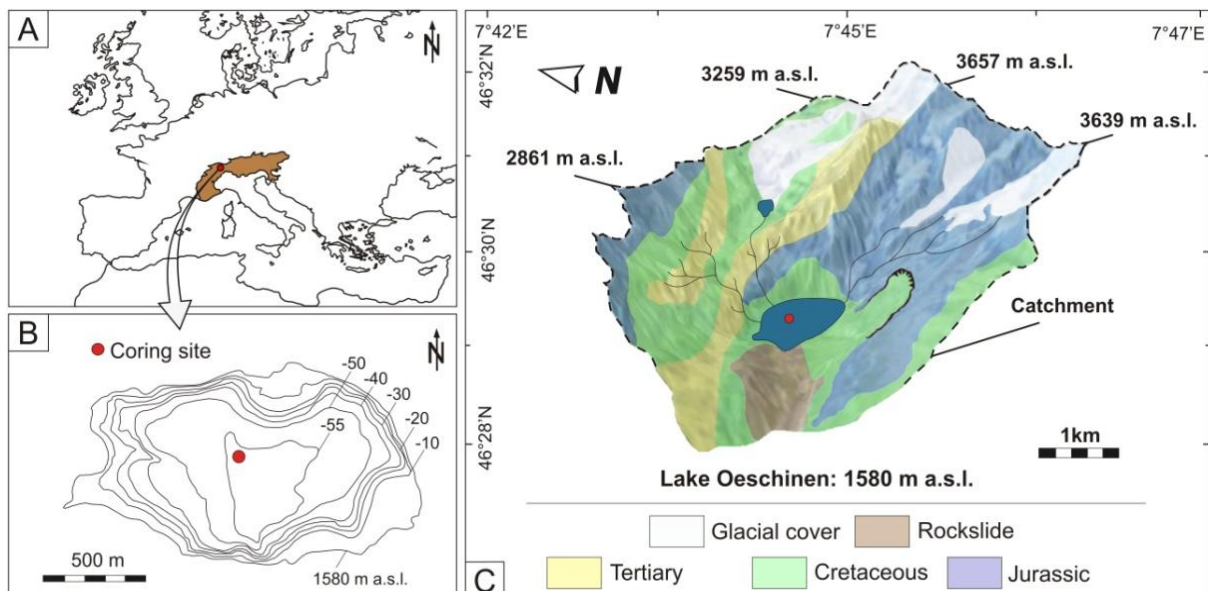


Fig. 4.1 Situation and characteristics of Lake Oeschinen with a) location in the European Alps, b) bathymetric map of the lake basin with the coring location (courtesy: A. Gilli ETH Zurich), and c) geological settings of the catchment area

Lake Oeschinen has received considerable scientific attention since the mid 20th century (Fig. 4.2), with studies completed by Niklaus (1967) and Leemann (1993). Later, Leemann and Niessen (1994) discovered the presence of clastic varves of simple ‘bimodal’ composition (principally calcite and siliciclastics). This enabled the construction of a high-precision chronology. Most recently, a study by Mauchle (2010) reviewed previous work and demonstrated that the varves of Lake Oeschinen preserve a warm season precipitation signal.

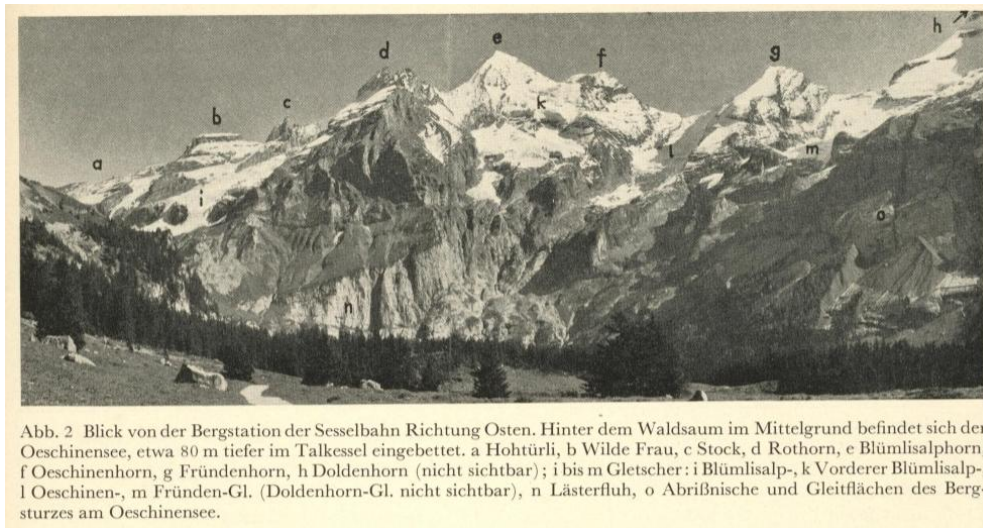


Fig. 4.2 Picture from Lake Oeschinen by Niklaus (1967)

4.2. Climate

Climate of the European Alps

Climate variability is the main factor that controls the natural environment of mountains, and influences properties of the biological, physical and chemical processes (Beniston 2005). Furthermore, climate variability and trends are recognized to be more pronounced in mountainous areas, as they are susceptible to the effects of rapidly changing climates (Giorgi et al. 1997; Wanner et al. 1997; Beniston 2000; Beniston 2005).

The European Alps are arguably one of the best mountainous regions to study climate and environmental changes due to the richness in available data. Alpine weather and climate research has a very long tradition, which has led to a dense instrumental network of long meteorological data.

The European Alps have undergone a temperature increase of about + 2°C between the late 19th and early 21st centuries, which corresponds to more than twice the rate of average warming of the Northern Hemisphere (Auer et al. 2007; Böhm et al. 2008). Changes in precipitation are moderate in terms of the yearly total, but show significant changes between the seasons.

Particularly, a decrease in summer precipitation and, in most regions, an increase in spring and winter precipitation has been observed throughout the last 150 years (EEA 2007).

Climatologically, the European Alps are of particular interest as they constitute a boundary between mediterranean, North Atlantic and continental climates (Wanner et al. 1997). This leads to a relatively complex climate system in the Alps that is influenced by global seasonal, inter-annual and decadal-scale climate change and variability (Sodemann and Zubler 2010). This complexity places the Alps into an interesting position for testing whether climate in this specific region responded to the Clausius-Clapeyron relation and to the ‘dry gets drier, wet gets wetter’ scheme over the past millennium (see Chapter 1). Another interesting point is to assess how representative the reconstructions from the study area (Lake Oeschinen) are for the North-western Alps and other parts of Europe.

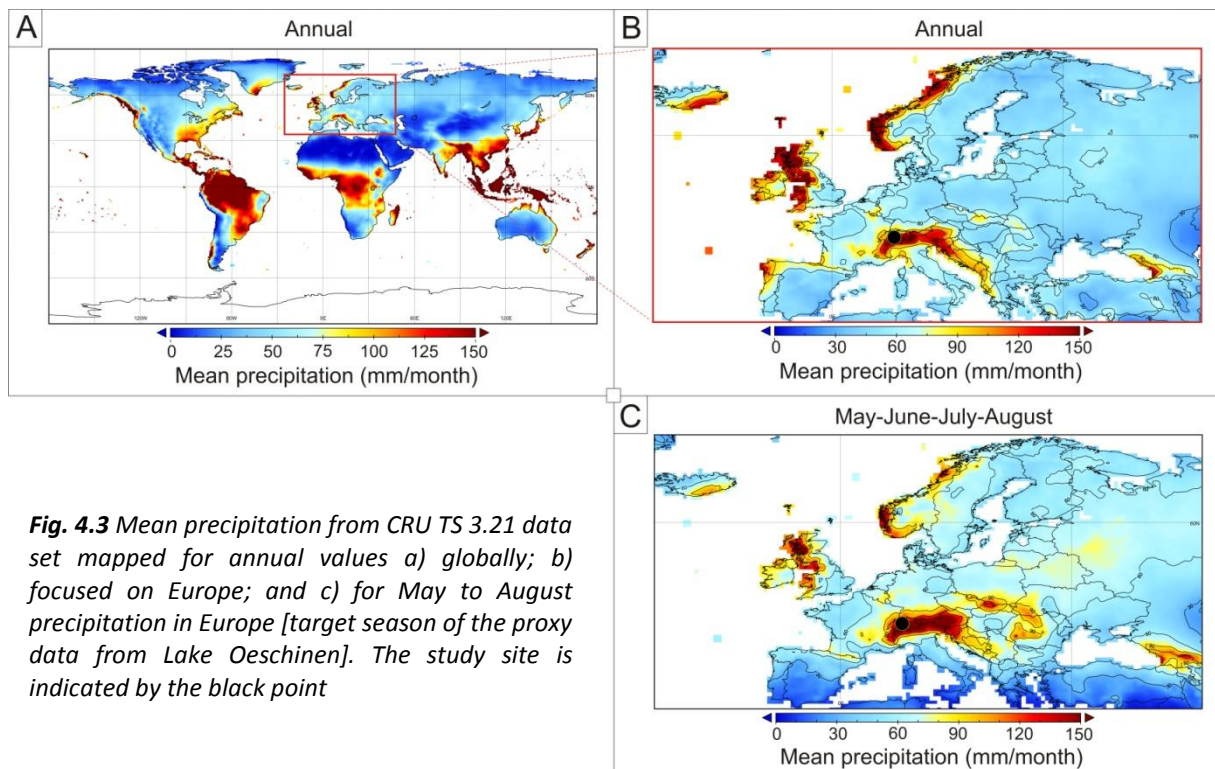


Fig. 4.3 Mean precipitation from CRU TS 3.21 data set mapped for annual values a) globally; b) focused on Europe; and c) for May to August precipitation in Europe [target season of the proxy data from Lake Oeschinen]. The study site is indicated by the black point

Fig. 4.3 shows the particular importance of precipitation in the Alps, which is considered as a relatively humid region of the world (Figs. 4.3a) with up to 150 mm/month (12-month mean; CRU TS 3.21 data set). Figs. 4.3b and 4.3c show the contribution of mean precipitation in Europe for annual mean and warm season from May to August (target of the study on Lake Oeschinen). Similarities between the two maps suggest that the warm season precipitation contributes significantly to the annual mean values.

Fig. 4.4 shows the correlation field analysis for our study site and Europe (CRU TS 3.21, 0.5°x0.5°; Jones and Harris 2013). This analysis indicates that the warm season precipitation from our study sites is representative for most of the western Alps. This includes Switzerland, large parts of France and Germany (Figs. 4.4a, b).

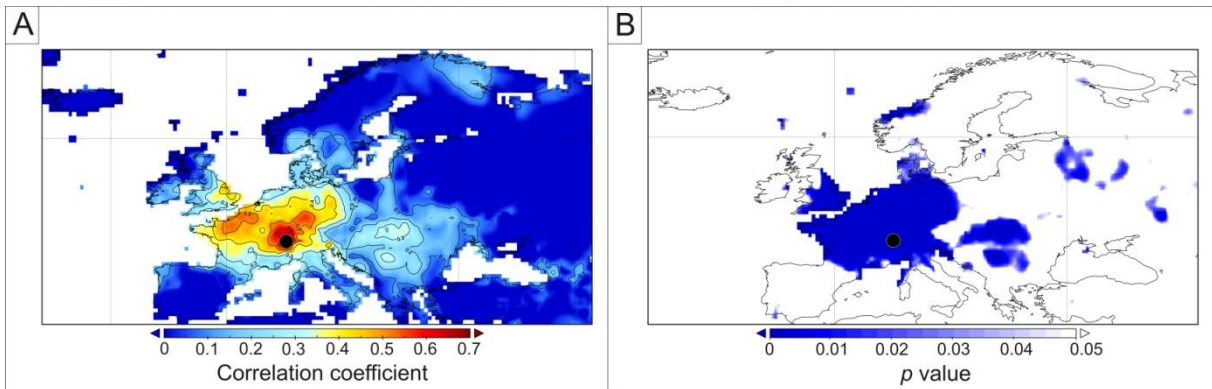


Fig. 4.4 a) Correlation map between May to August precipitation for our study site (Kandersteg – Lake Oeschinen) and CRU TS 3.21 data over Europe and b) corresponding *p* values where the blue zone delimitates highly significant correlations. The study site is indicated by the black point

Instrumental data for Lake Oeschinen

Climate data considered for the study of Lake Oeschinen were taken from nearby meteorological stations (MeteoSwiss network; <https://gate.meteoswiss.ch/idaweb/>). Monthly precipitation data are available for the period AD 1900-2009 from the meteorological station of Kandersteg (1176 m a.s.l.), located 3 km in the valley downhill of the lake. Temperature data over the same period are available from the meteorological station of Adelboden (1320 m a.s.l.), located 13 km west Lake Oeschinen.

For the study related to flood history, monthly averages and monthly maxima river discharge data were obtained from the gauging station of Kander-Hondrich located about 20 km downstream of the lake outflow. Continuous data covered the period AD 1917-2009.

4.3. Sedimentation processes, varve formation and event layers

Reconstructions of past climate and other environmental changes from lake sediments require that the conditions affecting sedimentation processes in lakes are understood (Ojala et al. 2013). Indeed, assessing how the environmental information is incorporated into the sediment record is fundamental when aiming at reconstructing past climate. The so-called ‘process studies’ that chronicle present-day conditions of lake sedimentation processes are a prerequisite for palaeolimnological studies (Flower et al. 1990; Leemann and Niessen 1994; Bluszcz et al. 2008; Tylmann et al. 2012). Furthermore, these ‘process studies’ are important as the atmosphere-catchment-lake system is unique to each lake (Lamoureux 1999).

In this context, we combined information from lake-catchment descriptions, water-column measurements, sediment trapping and sediment analyses. The aims are to (i) understand sedimentation processes that lead to varve formation and event-layer deposition, and (ii) support the choice of the sediment proxy for climate reconstruction.

Water column analysis

Lake Oeschinen is oligotrophic and aquatic macrophytes are absent. A pH of 7.9 ± 0.3 and a conductivity of $148 \pm 15 \mu\text{S}\cdot\text{cm}^{-1}$ were recorded in August 2013.

The thermal profile shows that Lake Oeschinen is dimictic (Fig. 4.5). The lake is stratified in summer for five months (early May to the end of September) and inversely stratified during the winter months when ice-cover develops. A first mixing occurs with cold temperatures in November, while the second mixing occurs with warmer spring temperatures, usually in early May. Maximum near-surface water temperature is recorded in August, with a maximum of ca. 16.8°C in 2012.

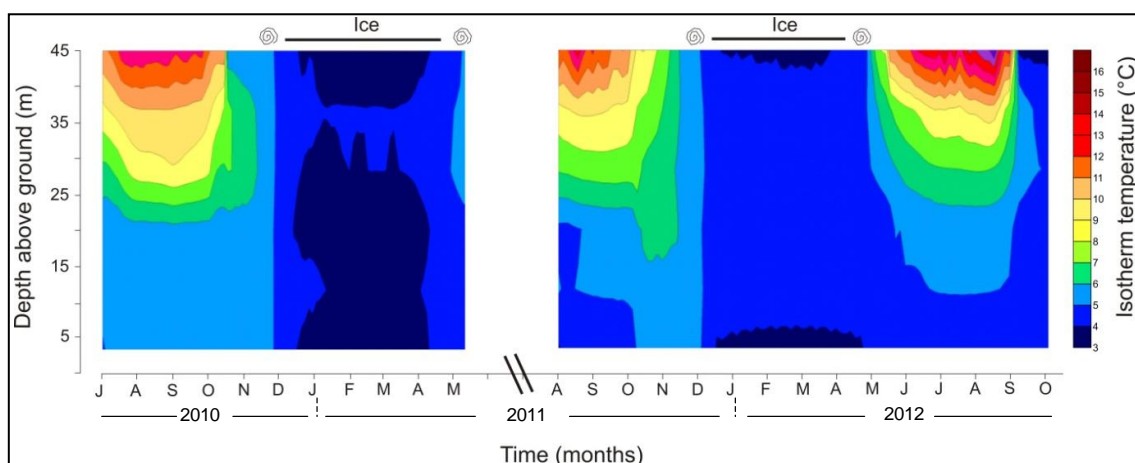


Fig. 4.5 Thermal profile of Lake Oeschinen between July 2010 and October 2012

Sediment trap analysis

To study recent sedimentation processes, sediment traps were deployed near the bottom of the lake from May 2007 to October 2010 (Fig. 4.6). Sediment trap data show two interesting results: (i) Mass Accumulation Rate (MAR) seems to mirror the patterns in precipitation integrated over the same period of investigation, (ii) MAR data reflect flood-induced accumulation (heavy rainfall events), such as for the flood that occurred on 10th October 2011. This extreme event led to important road and railway damages in the vicinity of the Kander River, which is drained by Lake Oeschinen water. This event caused higher erosion in the catchment of the Lake ($MAR = 25 \text{ g cm}^{-2} \text{ d}^{-1}$), which can clearly be distinguished from the 'background' sedimentation.

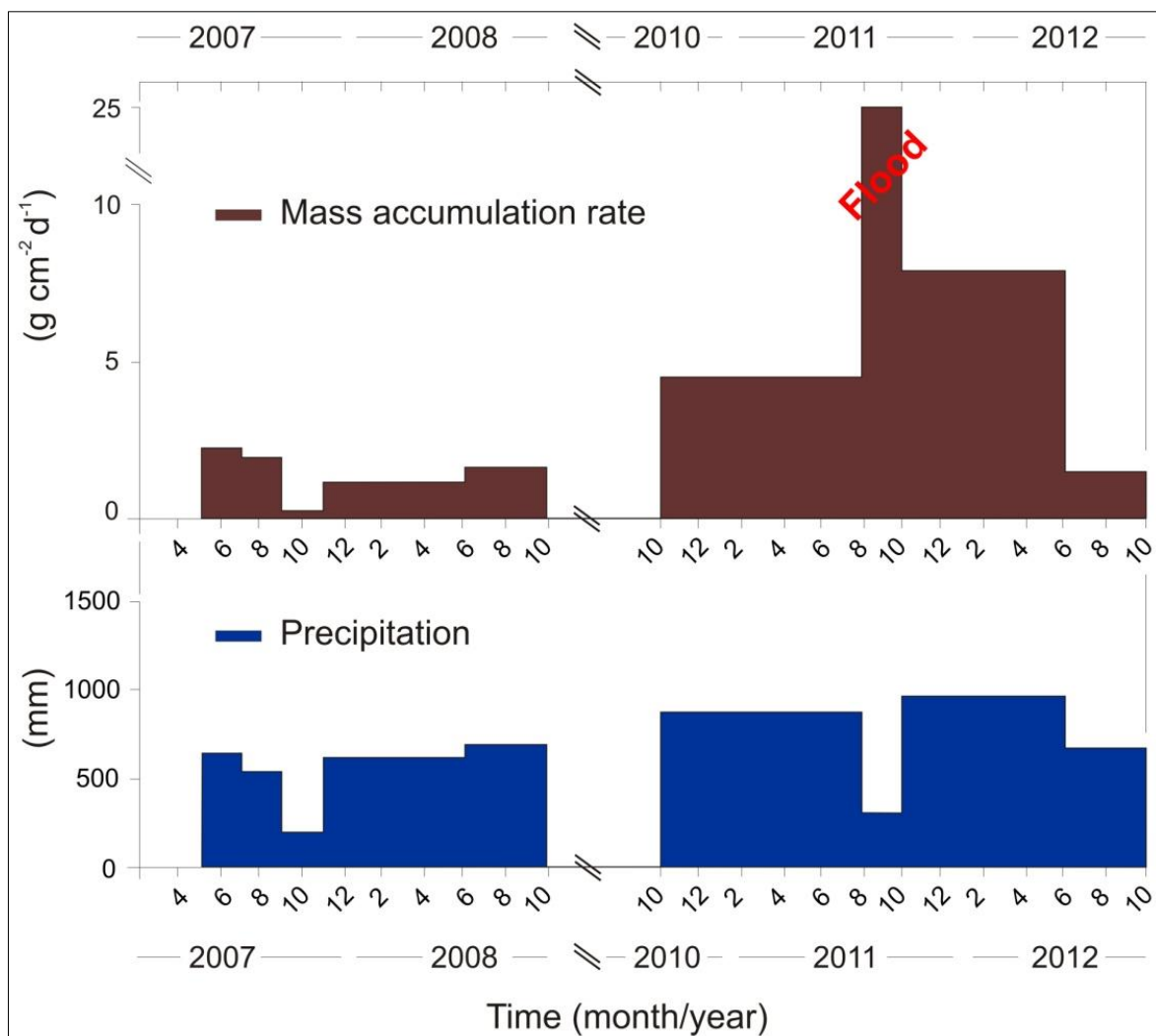


Fig. 4.6 Comparison of sediment mass accumulation rate from sediment traps with precipitation integrated over the period 2007-2012

Sediment analysis

A combination of the thin sections, particle size analysis and X-ray diffraction (XRD) was used to characterize typical varve deposition (Fig. 4.7; following Mauchle 2010). Results show that the mineral composition and distribution of the catchment bedrock (limestone in the high-elevation glaciated areas, siliciclastics in the lower elevation Flysch areas) are the basis for the formation and properties of the varves. During spring snowmelt and summer rainfall, a dark and coarse ($> 15 \mu\text{m}$ mean size) basal layer is deposited. This layer is rich in quartz and phyllosilicates (illite and chlorite), with a third from calcite. This suggests that the material is eroded mainly from the northern Flysch siliciclastic-rich catchment during spring and summer. Field observations support this finding. During winter, clay-size particles ($2 \mu\text{m}$ mean size) settle through the water column under calm conditions when the lake is ice-covered. These particles are composed of calcite grains (85 %; XRD) produced mainly by glacier abrasion in the limestone part of the catchment.

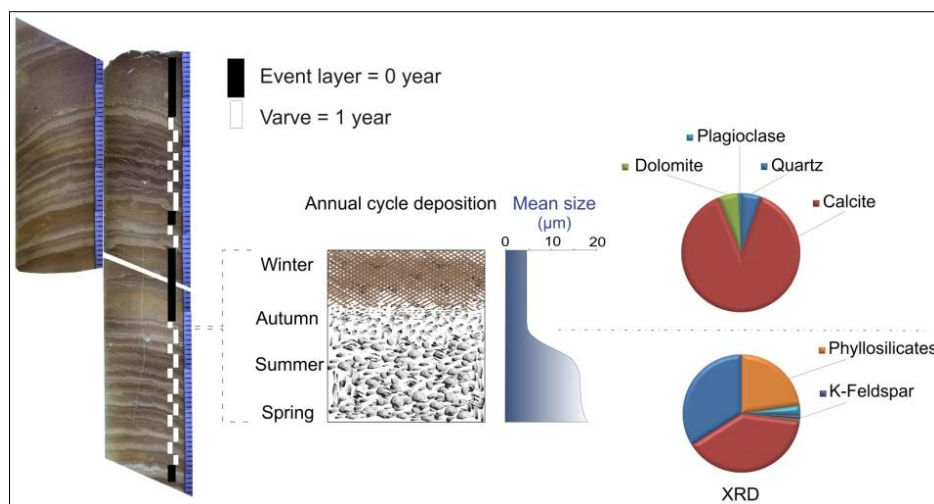


Fig. 4.7 Sediment properties: thin sections showing a typical sequence of varves intercalated by flood layers (turbidites), a sketch of an annual deposition, mean particle size and XRD measurements of a typical varve

More detailed analysis of the thin sections revealed three subtypes of varves that differ in their internal structure and particle size distribution (Fig. 4.8). Type I consists of very thin (1-1.5 mm) fining upward sequences with a typical Gaussian distribution of silt-size particles (red curve, Fig. 4.8). Type II is thicker (~ 3 mm) and presents coarser particles with a larger amount of sand-size grains (yellow curve, Fig. 4.8). Type III shows internal micro-laminations, most probably produced by punctual and small thunderstorms that occurred within a year of sediment deposition. This leads to a 'bimodal distribution' of particle sizes (blue curve, Fig. 4.8). In contrast, flood layers are marked by a much higher sedimentation (> 5 to 7 mm) with particles mostly composed of sand (90% of the total volume $> 100 \mu\text{m}$, black curve, Fig. 4.8). These layers also consist of a systematic grading of the particle sizes and are often associated with an erosive base.

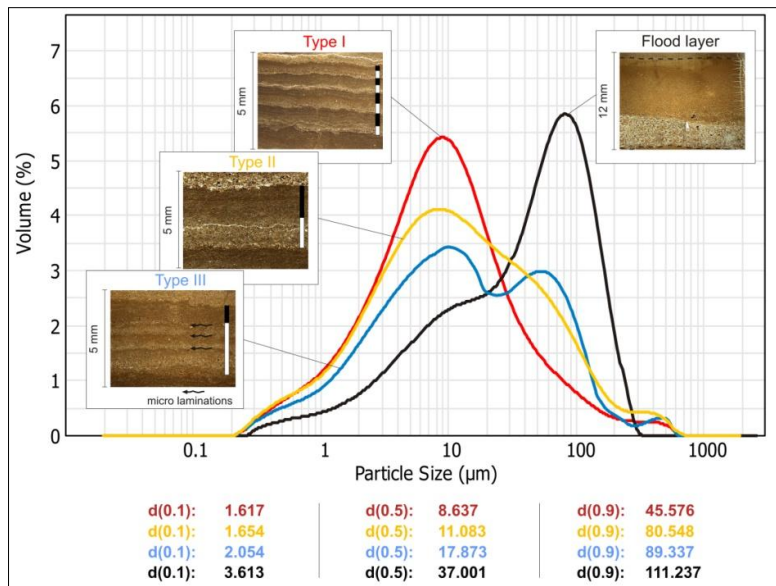


Fig. 4.8 Photomicrographs and particle size distributions for typical varve sub-types (I to III) and for a flood layer. The lower panel shows the particle sizes representing 10%, 50% and 90% of the sample volume

On the basis of these three facies types of varves in Lake Oeschinen, it was hypothesised that properties of the hydrograph could reflect the different types of varves (Fig. 4.9). For instance, we tested whether the number of internal laminations in a varve of Type III could be associated with a similar number of peaks in daily discharge from the corresponding year. On the one hand, this would have been a strong argument to validate and/or constrain the varve chronology within the instrumental period. On the other hand, the different subtypes of varves could have been used to reconstruct hydrograph properties beyond the instrumental period. Unfortunately, no consistent picture could be drawn from this comparison (Fig. 4.9), neither by defining threshold criteria in discharge data, nor by tuning the varve chronology within the counting uncertainty (Typically ± 3 varve years).

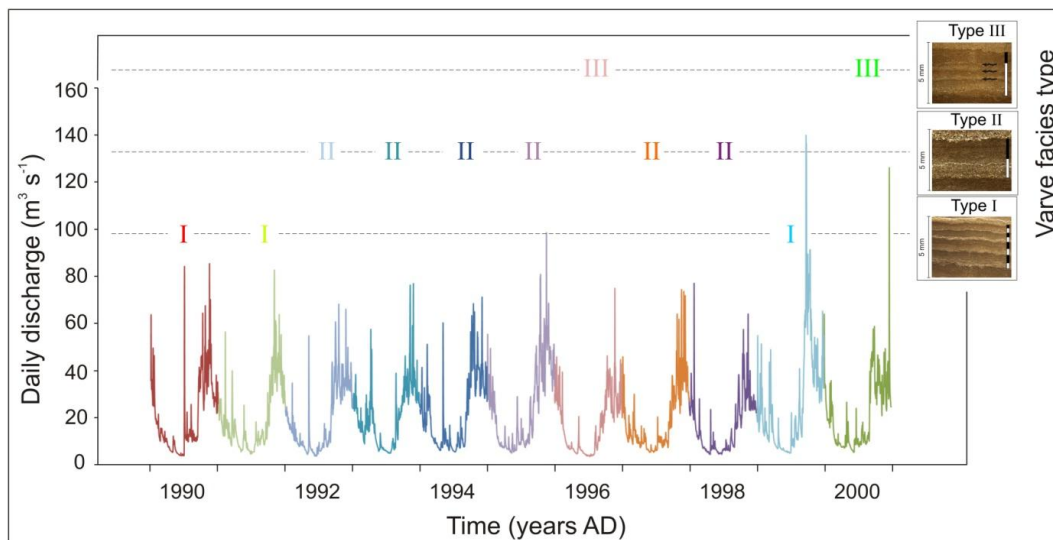


Fig. 4.9 Comparison between daily discharge data and the facies type of the varves for Lake Oeschinen. The sample period AD 1990-2000 is presented here as an example

Event layers and flood history

Event layers contrast significantly from the background sedimentation consisting of the clastic varves. These event layers are characterized by a different sedimentology with a high modal grain size, low clay content and high sand content, and higher rates of sediment accumulation. These characteristics and separation from the varves can clearly be seen in the adapted triangular plot in Fig. 4.10.

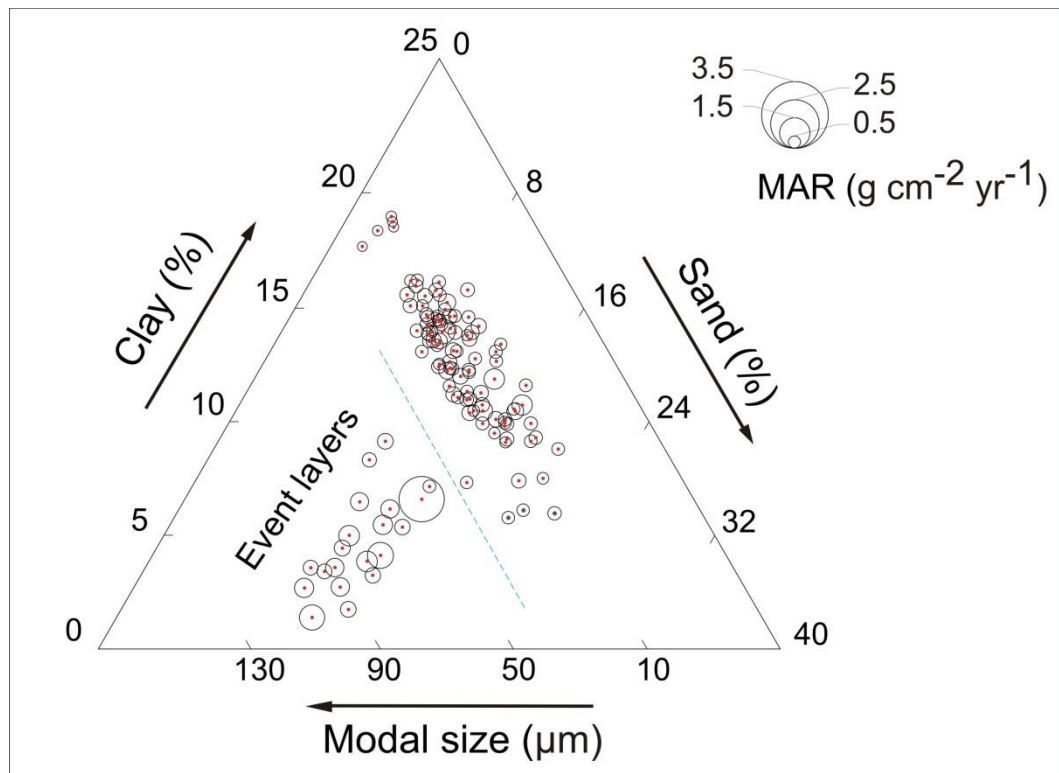


Fig. 4.10 Triangular plot of the particle size distribution for the varves and event layers (140 data points). Event layers and varves are separated based on clay %, sand % and modal grain size. The different sizes of the circle points represent different values of mass accumulation rates (MAR)

It has been previously shown from sediment trap data that the sediments from Lake Oeschinen could be used to reflect a flood event through the occurrence of an event layer (Fig. 4.6). To extend this finding on a longer time scale, we compared the occurrence of several event layers in the surface core of Lake Oeschinen with discharge data back to AD 1917 (Fig. 4.11).

It is not known whether event layers can be related to maxima in monthly mean and/or monthly discharge maxima; therefore, both data sets are shown for the comparison in Fig. 4.11. Floods can result in the succession of short rainfall events of high intensities and yield, leading to high discharge, or to intensive and/or long snowmelt conditions that can also be associated with intense rainfall. Results show that event layers with a high sedimentation (> 5 to 7 mm) from Lake Oeschinen

sediment cores can generally be associated with high maximum discharge data, sometimes with a time difference of ± 2 years (Fig. 4.11). This remains well within the varve counting uncertainty (± 3 years until AD 1920). Therefore, these event layers can be used to record flood events (flood frequency record). However, no significant correlation could be found between the thicknesses of these event layers and flood discharge intensities during the instrumental period. Thus, event layer thickness cannot be used as a proxy for flood intensity.

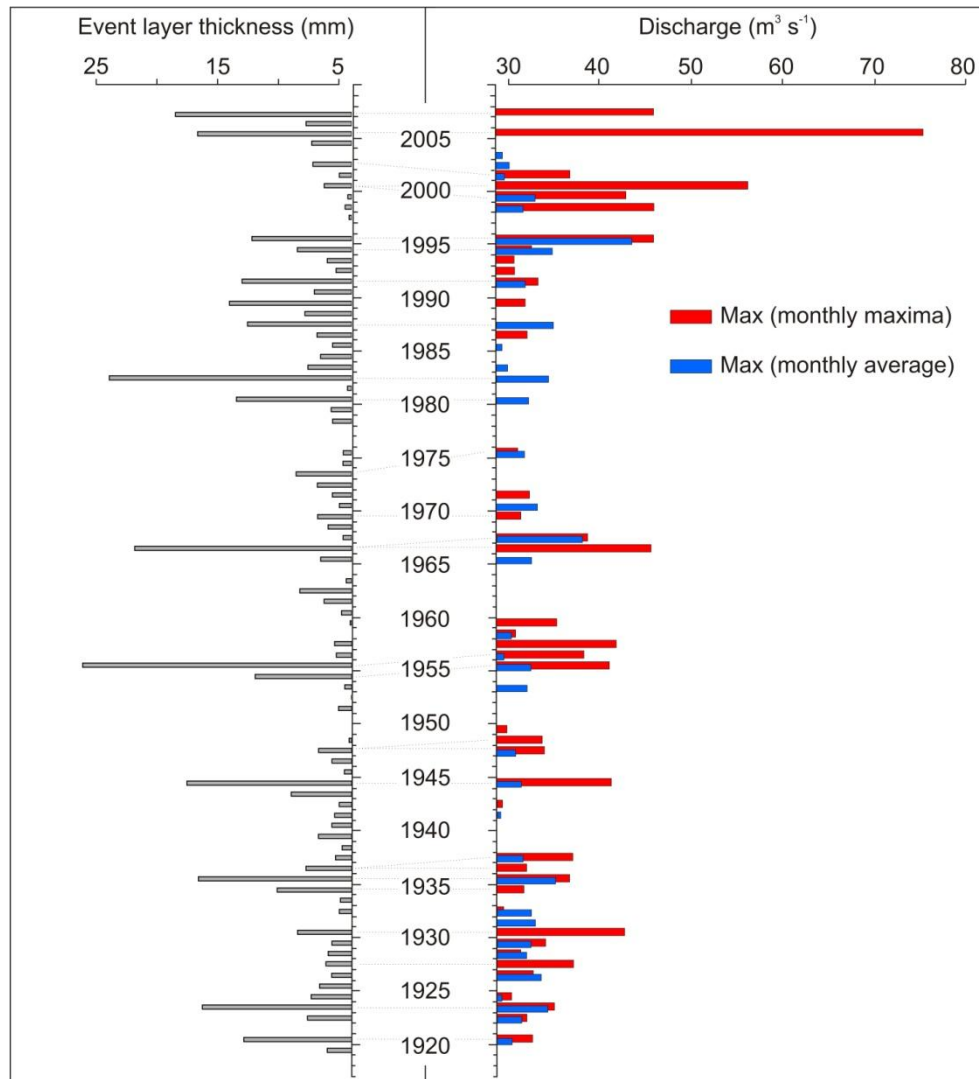


Fig. 4.11 Comparison between the thicknesses of event layers found in the sediments of Lake Oeschinen and discharge data recorded about 20 km downstream of the lake outflow for the period AD 1917-2009

References (Chapter 4.1 – 4.3)

- Auer, I., Böhm, R., Jurkovic, A. et al., 2007. 'HISTALP — Historical instrumental climatological surface time series of the Greater Alpine Region 1760–2003'. *International Journal of Climatology* 27, pp. 17–46
- Beniston, M., 2000. Environmental change in mountains and uplands. In Arnold and Hodder Publishers, London, UK, and Oxford University Press, NY, USA, 172 pp
- Beniston, M., 2005. Mountain climates and climatic change: an overview of processes focusing on the European Alps. *Pure and Applied Geophysics* 162, 1587-1606
- Bluszcz, P., Kirilova, E., Lotter, A.F., Ohlendorf, C., Zolitschka, B., 2008. Global Radiation and Onset of Stratification as Forcing Factors of Seasonal Carbonate and Organic Matter Flux Dynamics in Hypertrophic Hardwater Lake (Sacrower See, Northeastern Germany). *Aquatic Geochemistry* 14, 73-98.
- Böhm, R., Jones, P.D., Hiebl, J., Hiebl, J., Frank, D., Brunetti, M., Maugeri, M., 2008. The early instrumental warm-bias: A solution for long central European temperature series 1760–2007. *Climatic Change* 101, 41-67
- EEA — European Environment Agency, 2007. Regional climate change and adaptation – The Alps facing the challenge of changing water resources. EEA Technical report No 8/2009
- Flower, R.F., 1990. Seasonal changes in sedimenting material collected by high aspect ratio sediment traps operated in a holomictic eutrophic lake. *Hydrobiologia* 214, 311-316
- Giorgi, F., Mearns, L.O., 1999. Approaches to the simulation of regional climate change: A review. *Reviews of Geophysics* 29, 191-216
- Jones, P., Harris, I., 2013. CRU TS3.21: Climatic Research Unit (CRU) Time-Series (TS) Version 3.21 of High Resolution Gridded Data of Month-by-month Variation in Climate (Jan.1901 - Dec.2012), [Internet]. University of East Anglia Climatic Research Unit (CRU). NCAS British Atmospheric Data Centre.
- Lamoureux, S.F., 1999. Catchment and lake controls over the formation of varves in monomictic Nicolay Lake, Cornwall Island, Nunavut. *Canadian Journal of Earth Sciences* 36, 1533-1546
- Leemann, A., 1993. Rhythmite in alpinen Vorgletscherseen: Warvenstratigraphie und Aufzeichnung von Klimaveränderungen. PhD dissertation ETH 10386, Zürich, Switzerland
- Leemann, A., Niessen, F., 1994. Varve formation and the climatic record in an Alpine proglacial lake: calibrating annually laminated sediments against hydrological and meteorological data. *The Holocene* 4, 1-8
- Mauchle, F., 2010. The modern sediments of Lake Oeschinen (Swiss Alps) as an archive for climatic and meteorological events. MSc dissertation, Institute of Geography and OCCR, University of Bern, Switzerland
- Niklaus, M., 1967. Geomorphologische und limnologische Untersuchungen am Öschinensee. PhD dissertation. Kümmerly und Frey, Bern

Ojala, A.E.K., Kosonen, E., Weckström, J., Korkkonen, S., Korhola, A., 2013. Seasonal formation of clastic-biogenic varves: the potential for palaeoenvironmental interpretations. *GFF* 135, 237-247

Sodemann, H., Zubler, E., 2010. Seasonal and inter-annual variability of the moisture sources for Alpine precipitation during 1995–2002. *International Journal of Climatology* 30, 947-961.

Suchy, V., Frey, M., Wolf, M., 1997. Vitrinite reflectance and shear-induced graphitization in orogenic belts: a case study from the Kandersteg area, Helvetic Alps, Switzerland. *International Journal of Coal Geology* 34, 1-20

Tylmann, W., Szpakowska, K., Ohlendorf, C., Woszczyk, M., Zolitschka, B., 2012. Conditions for deposition of annually laminated sediments in small meromictic lakes: a case study of Lake Suminko (northern Poland). *Journal of Paleolimnology* 47, 55-70

Wanner, H., Rickli, R., Salvisberg, E., Schmutz, C., Schüepp, M., 1997. Global climate change and variability and its influence on Alpine climate—concepts and observations. *Theoretical and Applied Climatology* 58, 221-243

4.4. Quantitative high-resolution warm season rainfall recorded in varved sediments of Lake Oeschinen, northern Swiss Alps: calibration and validation AD 1901-2008

Study published in *Journal of Paleolimnology*

Quantitative high-resolution warm season rainfall recorded in varved sediments of Lake Oeschinen, northern Swiss Alps: calibration and validation AD 1901–2008

Benjamin Amann · Fabian Mauchle ·
Martin Grosjean

Received: 7 May 2013 / Accepted: 18 December 2013 / Published online: 24 January 2014
© Springer Science+Business Media Dordrecht 2014

Abstract High-resolution, well-calibrated records of lake sediments are critically important for quantitative climate reconstructions, but they remain a methodological and analytical challenge. While several comprehensive paleotemperature reconstructions have been developed across Europe, only a few quantitative high-resolution studies exist for precipitation. Here we present a calibration and verification study of lithoclastic sediment proxies from proglacial Lake Oeschinen (46°30'N, 7°44'E, 1,580 m a.s.l., north–west Swiss Alps) that are sensitive to rainfall for the period AD 1901–2008. We collected two sediment cores, one in 2007 and another in 2011. The sediments are characterized by two facies: (A) mm-laminated clastic varves and (B) turbidites. The annual character of the laminae couplets was confirmed by radiometric dating (^{210}Pb ,

^{137}Cs) and independent flood-layer chronomarkers. Individual varves consist of a dark sand-size spring–summer layer enriched in siliciclastic minerals and a lighter clay-size calcite-rich winter layer. Three subtypes of varves are distinguished: Type I with a 1–1.5 mm fining upward sequence; Type II with a distinct fine-sand base up to 3 mm thick; and Type III containing multiple internal microlaminae caused by individual summer rainstorm deposits. Delta-fan surface samples and sediment trap data fingerprint different sediment source areas and transport processes from the watershed and confirm the instant response of sediment flux to rainfall and erosion. Based on a highly accurate, precise and reproducible chronology, we demonstrate that sediment accumulation (varve thickness) is a quantitative predictor for cumulative boreal alpine spring (May–June) and spring/summer (May–August) rainfall ($r_{\text{MJ}} = 0.71$, $r_{\text{MJJ A}} = 0.60$, $p < 0.01$). Bootstrap-based verification of the calibration model reveals a root mean squared error of prediction ($\text{RMSEP}_{\text{MJ}} = 32.7$ mm, $\text{RMSEP}_{\text{MJJ A}} = 57.8$ mm) which is on the order of 10–13 % of mean MJ and MJJA cumulative precipitation, respectively. These results highlight the potential of the Lake Oeschinen sediments for high-resolution reconstructions of past rainfall conditions in the northern Swiss Alps, central and eastern France and south-west Germany.

B. Amann · M. Grosjean
Oeschger Center for Climate Change Research,
University of Bern, Bern, Switzerland
e-mail: martin.grosjean@oeschger.unibe.ch

B. Amann (✉)
Institute of Geography, University of Bern, Erlachstrasse
9a T3, 3012 Bern, Switzerland
e-mail: benjamin.amann@giub.unibe.ch

F. Mauchle
MeteoSwiss, Krähbühlstrasse 58, Zurich, Switzerland
e-mail: fabian.mauchle@meteoswiss.ch

Keywords Lake sediments · Clastic varves ·
Sedimentology · Limnogeology · Climate
change · Paleoclimatology

Introduction

High-resolution quantitative reconstructions of climate variables are crucial for understanding Earth system variability, assessing the sensitivity of the climate to natural and anthropogenic forcing, and thus reducing uncertainty in future climate projections (Hegerl et al. 2006; Mann et al. 2008; Villalba et al. 2009; PAGES 2 k Consortium 2013). Data from natural paleoclimatic archives are one of the few means, together with documentary data, to obtain this information beyond the instrumental period.

In this context, lake sediments are valuable natural paleoclimatic archives due to their potential to preserve climate variability through very long times and at a high temporal resolution (Zolitschka 1996; Pienitz and Lotter 2009). This is particularly true for varved lake sediments that contain records of past climate at annual resolution and with high chronological precision for millennial to Holocene scales (Zolitschka 2007). Although the scientific community has greatly extended worldwide knowledge about lake sediments and varve records (Ojala et al. 2012), very few have actually generated quantitative very high-resolution multi-century to millennial long climate reconstructions (Hughen et al. 2000; Moore et al. 2001; Kalugin et al. 2007; McKay et al. 2008; Trachsel et al. 2008, 2010; von Gunten et al. 2009; Larocque-Tobler et al. 2010; Larocque-Tobler et al. 2011; Stewart et al. 2011; Elbert et al. 2012; Saunders et al. 2013; PAGES 2 K Consortium 2013).

Moreover, while considerable advances have been made in developing temperature reconstructions in Europe and the Alps for the last 1,000 years (Trachsel et al. 2012; PAGES 2 k Consortium 2013), very little is known about past precipitation (Casty et al. 2005; Pauling et al. 2006; Trachsel et al. 2008; Büntgen et al. 2011). However, precipitation regimes are fundamental for understanding the variability of the water cycle, which is arguably as important as fluctuations in temperature. In many ways the water cycle is even and often more relevant for society, especially in sensitive Alpine areas, notably with regard to flood extremes (Pfister 1999).

This data scarcity is mainly due to the difficulties in obtaining robust, well calibrated and quantified long time series, preferably annually resolved, of reconstructed climate variables from different archives, including lake sediments.

This paper reports the varve thickness-warm season precipitation calibration and validation (AD 1901–2008) of a varve record from proglacial Lake Oeschinen in the northern Swiss Alps. Leemann and Niessen (1994) previously reported a mixed temperature and precipitation signal recorded in the sediments of this lake. In their study they found a correlation of $r = 0.45$ between varve thickness and mean summer air temperature for observations between AD 1962–1982 ($n = 21$), and a strong covariance with summer precipitation. Here, we show on a longer record ($n = 108$) that Lake Oeschinen's sediments record a warm season precipitation signal and how temperature modulates the sediment-precipitation relationship, in particular for very cold years (AD 1900–1915) and the period in the 1960–1970s investigated by Leemann and Niessen (1994).

To achieve this aim, we first interpret the hydroclimatic varve formation process by comparing sediment thin sections with delta fan surface samples, sediment trap and meteorological data. We then provide a set of high-resolution sediment proxy data (facies, mineralogical and geochemical sediment properties) with a robust chronology for the calibration period AD 1901–2008. Finally we test the statistical relationship between the precipitation regime and the varve properties, and its potential for the extension of the varve record beyond the instrumental period.

Study site

Lake Oeschinen (46°30'N, 7°44'E) is a proglacial lake (1.18 km²) located in the northern Swiss Alps, 55 km south of Bern at an altitude of 1,580 m (Fig. 1a). The lake is oligotrophic, dimictic, thermally stratified in summer, and ice-covered from December through early May. The lake basin, formed by a Holocene rockslide (9.5 cal kyrs BP), is topographically closed and has an underground outflow through the rockslide body (Niklaus 1967; Leemann and Niessen 1994). Annual lake level fluctuations average 12 m from a minimum of a 44-m water depth measured in late winter to a maximum depth of 56 m in summer.

Bedrock in the catchment is mostly composed of Mesozoic limestone of Jurassic and Cretaceous age (Fig. 1a, in blue and green). The northern part of the catchment however, includes two important belts of Tertiary Flysch deposits (Fig. 1a, in yellow), which

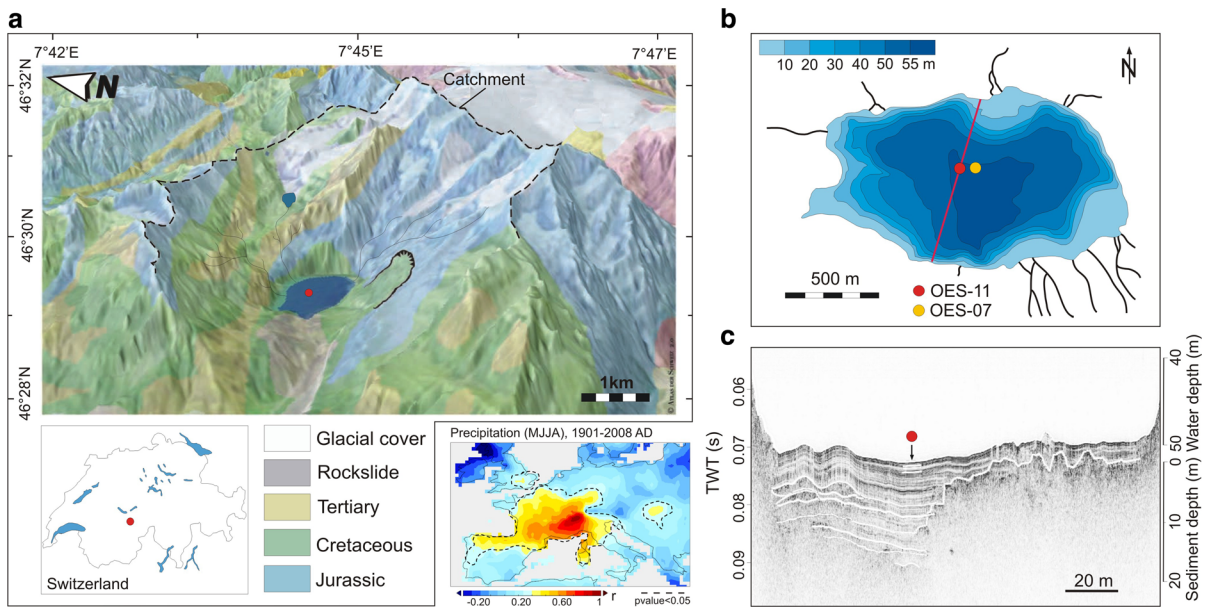


Fig. 1 Characteristics of Lake Oeschinen: **a** location in the Bernese Swiss Alps, topographical and geological settings of the catchment area, spatial correlation maps for warm season precipitation; **b** bathymetric map of the lake basin adapted from

Leemann and Niessen (1994) showing the two coring sites; **c** details of the south–north seismic profile with the location of core OES-11 (courtesy: A. Gilli ETH Zurich)

consist of erodible sandstones with abundant siliciclastic minerals (Suchy et al. 1997). Mountains in the catchment area (22 km²) reach 3,660 m and glacier cover accounts for about 30 % of the watershed (reference year 1993). Hydro-geologically, the catchment can be subdivided into three watershed systems separating the creeks of the north from creeks of the south and those from the north–east. Geological properties of these watersheds are reported in Table 1. A small moraine-dammed proglacial lake was formed in the late 1950s (2,148 m a.s.l., Fig. 1a) after the Blüemlisalp Glacier retreated. It now acts as a hydrological intermediate between the largest glacier of the catchment and Lake Oeschinen.

Climate variability in the Bernese northern Swiss Alps is influenced by both Atlantic and continental regimes. The North Atlantic Oscillation (NAO) is the dominant climate mode driving these influences, where the Azores High and surface heat lows over the Eurasian land mass alternately influence the variability of the summer system (Wanner et al. 1997; Casty et al. 2005).

Monthly mean temperature data are available from the meteorological station of Adelboden (1,320 m

a.s.l., 13 km west of Lake Oeschinen) and range from −2.9 °C in January to 15.0 °C in July (AD 1900–2009; MeteoSwiss). Precipitation data over the same period are available from the meteorological station of Kandersteg (1,176 m a.s.l.), located 3 km west and downhill of the lake. They display unimodal summer–winter cycles typical of the northern Alps (Brunetti et al. 2006) with a total annual precipitation of 1,173 mm. Monthly mean precipitation ranges from 69 mm in February to a peak of 142 mm in July. Local thunderstorms are relatively frequent and critical because they occasionally cause numerous and severe damage, notably in the vicinity of the Kander River that flows downstream Lake Oeschinen (Schmocker-Fackel and Naef 2010).

The CRU TS 3.0 precipitation data (Mitchell and Jones 2005; grid cell 46.5–47°N and 7.5–8°E) are significantly correlated with the meteorological station of Kandersteg ($r_{\text{MJJA}} = 0.55$, $p < 0.05$, 1901–2008). Spatial correlation maps with the CRU TS gridded data show that warm season precipitation in the area of Lake Oeschinen is representative for the western Alps including Switzerland, middle and eastern France and southern Germany (Fig. 1a).

Table 1 Subdivision of the lake catchment according to hydro-geological properties and XRD mineralogy of their respective delta sediment samples

Draining area	% Catchment	Glaciers	Geology	XRD (powder)					
				Calcite	Clays	Quartz	Dolomite	K-feldspar	Plagioclase
North	20	–	Jurassic and cretaceous + tertiary	39.0 (±5.7)	22.7 (±6.8)	33.9 (±2.3)	0.51 (±0.12)	1.09 (±0.30)	2.79 (±0.59)
South	40	3 glaciers	Jurassic and cretaceous limestone	88.2 (±3.9)	0	5.56 (±2.30)	5.63 (±1.90)	0.04 (±0.08)	0.59 (±0.22)
North-East	40	1 glacier (Bluemlisalp)	Cretaceous and tertiary	75.1 (±5.0)	88.2 (±3.9)	9.79 (±1.48)	1.93 (±0.38)	0.52 (±0.22)	0.26 (±0.13)

Materials and methods

Sedimentation process study

Delta fan sediment samples were collected around the shoreline of Lake Oeschinen, homogeneously powdered and analysed by X-ray diffraction (XRD, Philips PW 3710, 0.02°2θ resolution) for quantitative determination of mineral compositions. Results are expressed as weight percent and grouped according to the hydro-geological sub-division of the lake catchment.

Two sediment traps (cylindrical, $\phi = 9$ cm) were deployed at 4 m above the lake floor from May 2007 to October 2008 to monitor seasonal sediment supply into the lake at the coring site. Trapped material was freeze-dried and weighed to calculate dry mass accumulation rates (MAR) over the seasonal intervals of sampling. The lithogenic fractions of the samples were also analysed for particle size distribution using laser diffraction (Malvern Mastersizer 2000S) after removal of organic matter (with H₂O₂) and biogenic opal (with NaOH).

Sediment coring and processing

Two short sediment cores were recovered in October 2007 (UWITEC freezing corer, 1 m long; core OES-07) and in August 2011 (UWITEC gravity corer, 87 cm long; core OES-11) from Lake Oeschinen. The choice of the coring sites was based on bathymetric and seismic surveys (Fig. 1b, c). In the laboratory, cores were split lengthwise, described and photographed. Both cores were stratigraphically correlated with turbidite layers and laminae couplets. While thin sections and laminae counts were made on both cores, OES-07 was used for radiometric chronology measurements, and OES-11 was sampled to develop the multi-proxy data set with destructive analytical techniques.

Thin sections were taken from overlapping sediment slabs (7 × 1.5 × 0.5 cm) using freeze-drying and resin-epoxy embedding techniques (Lamoureux 2001). Laminae identification and a master chronology were generated by collating and merging optical-microscopy pictures (magnification × 10) of the thin sections. The thickness of lamina couplets was semi-automatically measured using the software package WinGeol Lamination Tool (0.01-mm resolution;

Meyer et al. 2006). Varves were counted three times independently by two analysts. Varve counting errors were assessed from the standard deviation of the different chronologies.

To corroborate the annual nature of laminae couplets, core OES-07 was stratigraphically sampled with spacing from 0.2 to 1.9 cm (2–3 years intervals) according to homogeneous sedimentary facies (Arnaud et al. 2002). Samples were analysed for ^{226}Ra , ^{210}Pb and ^{137}Cs by Gamma-ray spectrometry (EAWAG, Duebendorf). Unsupported ^{210}Pb was calculated by the level-by-level method and turbidites were removed from the $^{210}\text{Pb}_{\text{unsupported}}$ profile (Arnaud et al. 2002). We used the Constant Rate of Supply model (CRS; Appleby 2001), unconstrained and constrained by the AD 1963 ^{137}Cs peak, to convert ^{210}Pb activities into numerical sediment ages.

The varve chronology inferred from core OES-11 was validated by the comparison between turbidite layers and HQ >10 flood events (discharges larger than high-probability flood events of a 10-year return period) documented in the Kander River in AD 1930, 1944, 1955, 1968, 1987 and 1999 (Schmocker-Fackel and Naef 2010). The consistency of the two chronologies from OES-07 to OES-11 was assessed by comparing the cumulative sedimentation rates from the two cores.

To produce the multi-proxy data set, individual laminae were carefully scraped from the fresh core OES-11. Subsamples were analysed for water content, organic carbon (OC), calcite content and particle size distribution. OC and calcite contents were derived from loss on ignition at 550 °C (LOI₅₅₀) and 950 °C (LOI₉₅₀) respectively. Temperature and time of sample exposure were set following Heiri et al. (2001). The residual after LOI₉₅₀ is summarized as the siliciclastic fraction (mainly quartz, feldspars and clay minerals).

Varve thicknesses were then converted into annual mass accumulation rate (MAR) after Niessen et al. (1992):

$$\text{MAR} = s * \rho_s * (1 - \phi) \tag{1}$$

$$\phi = w * \rho_s / (w * \rho_s + (1 - w) * \rho_w) = \text{porosity} \tag{2}$$

$$\begin{aligned} \rho_s &= W_D / (\Pi * r^2 * S) \\ &= \text{dry bulk density of sediments (g cm}^{-3}\text{)} \end{aligned} \tag{3}$$

where *s* is the thickness of the laminae (cm), ρ_w is the pore-water density (1.0 g cm⁻³), *w* is the water

content (%), W_D is the dry sample mass, *S* is the sample width and *r* is the radius of the coring tube (2.9 cm). Fluxes (g cm⁻² year⁻¹) of OC, calcite and siliciclastics were calculated by multiplying the component concentrations with MAR.

Statistics

Annual lake sediment data were also 3-year triangular filtered prior to calibration with meteorological data. This accounts for errors in the sampling of individual varves and for dating uncertainties while still allowing a high number of independent observations (degrees of freedom; Kamenik et al. 2009; von Gunten et al. 2012). Pearson correlations were developed between all analysed proxies and meteorological data, and statistical calibrations were performed using Ordinary Least-Squares (OLS) regression model (inverse regression). Each proxy was correlated in a matrix with individual monthly and 2–12 months means of temperature (monthly mean, max and min) and precipitation (mean and cumulative) at both annual and 3-year filtered resolutions. The probability values (*p*) were corrected for serial autocorrelation and multiple testing (de Jong and Kamenik 2011). As shown in the section below, varve thickness was used as the best predictor for warm season precipitation. Since both time series showed a significant increase in the variance after AD 1950 we did not use the split period approach (von Gunten et al. 2012) to validate the calibration model. Instead, the root mean squared error of prediction (RMSEP) was calculated using the bootstrap cross-validation method (Birks 2005).

Results

Hydrological and geological influences on sediment supply

The hydro-geological properties of the three watersheds around Lake Oeschinen are clearly reflected in the mineralogy of the creek deltas (Table 1). Fractured and loose sediments eroded from the northern Flysch catchment are characterized by a high proportion of quartz (34 %) and clay minerals (23 %, mainly illite and chlorite), while calcite composes 39 % of the sample mass. In contrast, delta fan sediments related to the southern glaciated catchment (compact limestone)

are mainly composed of calcite (88 %) without any clay minerals and only 6 % of quartz. The third group of delta fan sediments characterizes particles eroded from the north–eastern drainage area. This zone is influenced by both the Blüemlisalp glacier (Cretaceous) and runoff from the north (Tertiary and Cretaceous). Accordingly, the mineralogy shows a mixed signal, with 75 % of calcite, 10 % of quartz and 12 % of clay minerals. Small proportions of dolomite (<5 %), K-feldspar (<2 %) and plagioclase (<3 %) typify the entire catchment.

Figure 2a depicts the sequential fluxes of total dry mass and mean grain size of particles trapped 4 m above lake floor between May 2007 and October 2008. The flux of particles varied from $0.1 \text{ mg cm}^{-2} \text{ day}^{-1}$ of very fine particles (4 μm) recorded in autumn (Sept–Nov 2007) to a maximum of $2.1 \text{ mg cm}^{-2} \text{ day}^{-1}$ with grains of 8 μm recorded in spring/early summer (May–July 2007). The flux of particles stays high in summer (July–September 2007) with $1.9 \text{ mg cm}^{-2} \text{ day}^{-1}$ and mean grain size is 11 μm . A pure winter signal could not be recorded because sampling was possible only after the onset of snow melt and ice out in June 2008. Thus the relatively high winter sedimentation rate ($1.1 \text{ mg cm}^{-2} \text{ day}^{-1}$) is most likely influenced by early spring snowmelt. Similarly, the last sampling interval (July–October 2008) integrated both summer and early autumn, with a particle flux of $1.5 \text{ mg cm}^{-2} \text{ day}^{-1}$.

The distribution of sediment particle flux over the period of investigation (2007–2008) reveals fairly close patterns with monthly averaged precipitation (Fig. 2a). Maximum rainfall is observed from May to July (215 mm) and slightly decreases in summer (180 mm), while autumn records a minimum of 68 mm. Averaged precipitation also mirrors the flux distribution for the last two sampling periods, with 78 and 138 mm obtained in June and October 2008, respectively. Such patterns cannot clearly be detected when comparing with monthly averaged temperature.

A similar methodology was applied to the sediment trap data recorded in 1991 by Leemann and Niessen (1994). Results in sedimentation rates during the period of investigation also show good agreements with monthly-averaged precipitation measured in Kandersteg rather than with temperature (Fig. 2b).

Qualitative seasonal differences are also observed in the mineralogy of trapped particles (Fig. 2c). Increased proportions of both quartz and clay minerals

(illite and chlorite, indicative of the northern Flysch catchment) are found during the progression of summer (from blue to green curve; Fig. 2c). In contrast, particles trapped in autumn (orange curve) and winter (red curve) are characterized by higher proportions of calcite (+40 %) and low amounts of clay minerals.

Sediment analysis

Sediments recovered from both cores of Lake Oeschinen consist mainly of light- to dark-grey (Munsell colour: 2.5Y-6/1 to 2.5Y-4/1, respectively) rhythmically laminated mineroclastic material with low OC (mean 1.98 %).

The thin sections revealed that the cores are composed of two sediment facies (Fig. 3): lamina couplets (Facies A), intercalated by several graded units interpreted as turbidite layers (Facies B). Facies A alternately comprises sandy and clay-rich laminae with a systematic fining upwards and an average thickness of 3.22 mm. Facies A exhibits three sub-types differing in their internal structure: Type I is characterized by very thin (1–1.5 mm) fining upward sequences and accounts for 31 % of the core. Type II is thicker (>3 mm), comprises coarser particles and is the most abundant type found through the whole section (48 %, Fig. 6c). Type III is composed of multiple internal microlaminations and accounts for 21 %. Conversely, Facies B shows high sedimentation (>7 mm), with often coarse (sand) basal layers and modal grain sizes ranging from coarse silt to sand (20–105 μm , respectively).

Chronology

Unsupported ^{210}Pb activity exponentially decreased from the top of core OES-07 downwards (Fig. 4a). ^{137}Cs first appeared at 32 cm (start of ^{137}Cs fallout, AD 1954) with a maximum peak measured at 28 cm (^{137}Cs peak AD 1963). The minor ^{137}Cs peak at 13 cm is attributed to the AD 1986 Chernobyl fallout.

The overall chronology inferred from laminae counts on core OES-07 is consistent with the radiometric chronology (^{210}Pb -CRS model constrained with the AD 1963 ^{137}Cs peak), with the ^{137}Cs markers and AD 1987 historical flood (Fig. 4a). The unconstrained CRS model reveals an age difference of 2 years for AD 1963 ($<\pm 1\sigma$) as compared with the constrained CRS model. Hence, laminae couplets

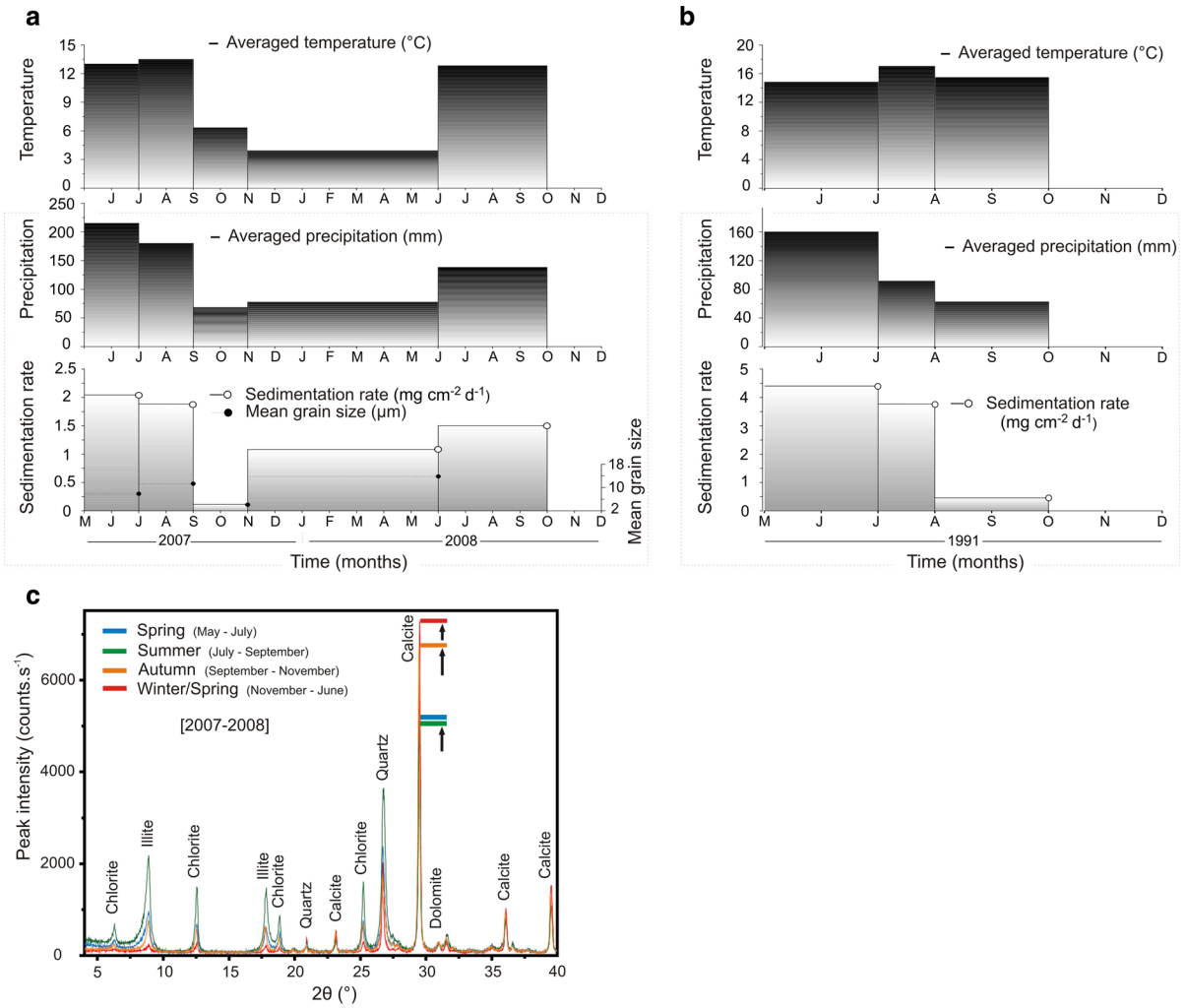


Fig. 2 Sediment trap properties: **a** comparison of sediment mass accumulation rate and mean grain size with precipitation and temperature through the period 2007–2008; **b** comparison between reported sediment accumulation rate measured in 1991

by Leemann and Niessen (1994) and monthly-averaged precipitation and temperature; **c** qualitative X-ray diffractogram showing the seasonally-distinct mineralogy of the trapped particles

(Facies A) are considered as annual varves. Note that the varves in the uppermost part of core OES-07 are poorly preserved and could not be reliably counted (Fig. 4a).

The independent varve counting on the top 50 cm of core OES-11 (Fig. 4b) indicates an age of 111 years (AD 1900–2011). This age-depth model is verified by six turbidite layers corresponding to high-flood events (HQ >10) in the region of the Kander River in AD 1930, 1944, 1955, 1968, 1987 and 1999. The cumulative counting error stays below ± 3 years from the top of the core to AD 1920, but reaches a maximum of ± 5.2 years around AD 1900.

Figure 4c shows the relationship between the sedimentation rates of the two cores. This relationship exhibits almost no deviation from the 1:1 line and indicates a high reproducibility of the chronology and the varve thickness in both cores ($r^2 = 0.99$).

Lithology and physical sediment parameters

Figure 5 summarizes the time series of the proxy data from core OES-11 after removal of the turbidite layers (Facies B). These sediment parameters comprise the water content, the analysis of the grain size, the sedimentary rock type, MAR and the varve thickness.

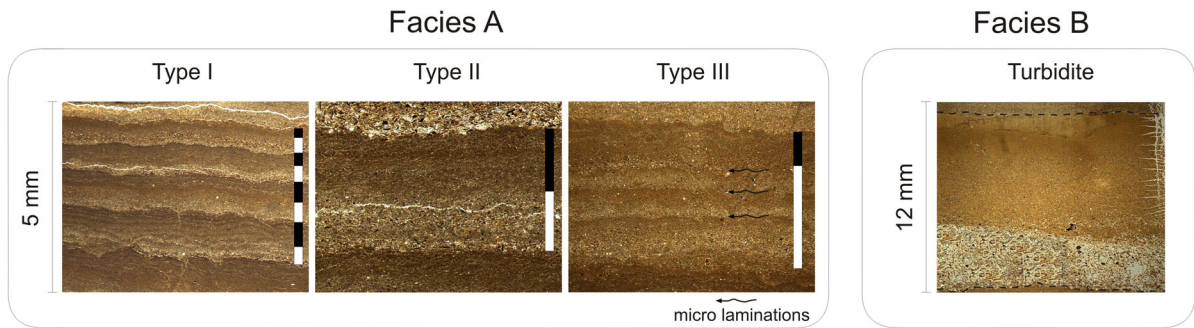


Fig. 3 Photomicrographs of the different sediment facies types. *Facies A*: the laminae couplets present three different sub-type internal structures. The white and black boxes represent spring–

summer (silt to sand) and winter (clay-size particles) accumulation respectively. *Facies B*: a typical high-sedimentation turbidite layer

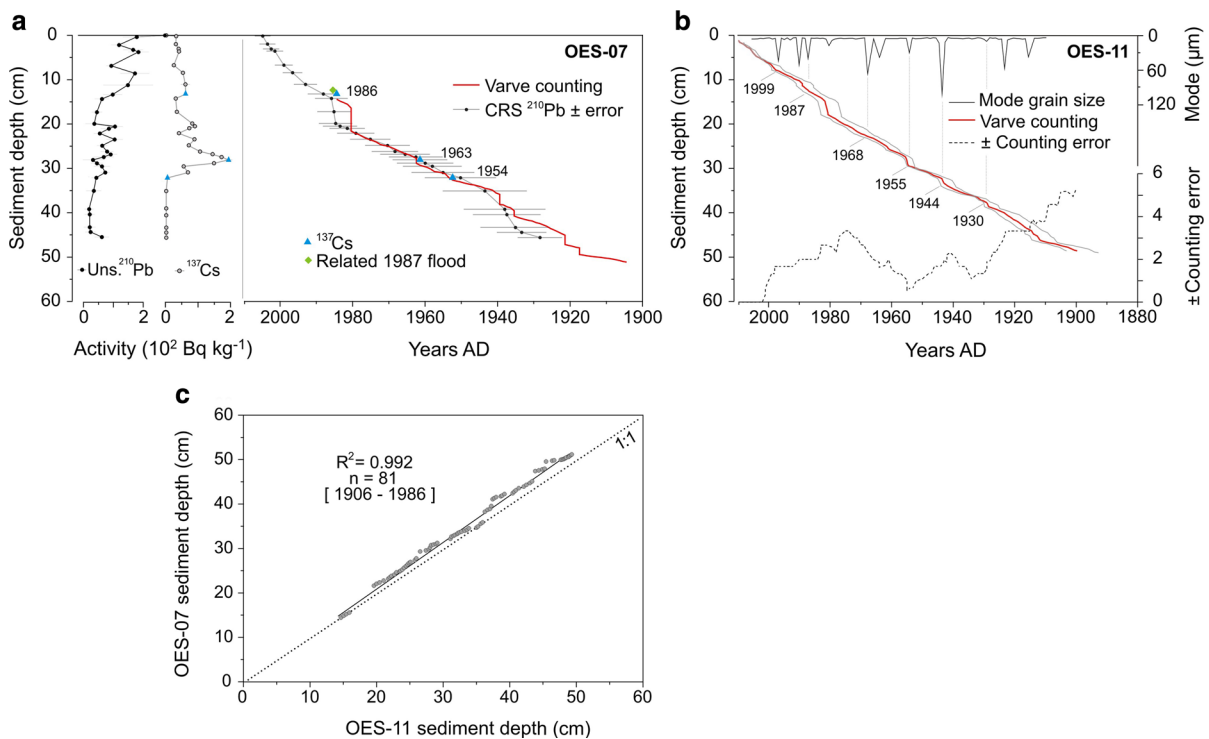


Fig. 4 Sediment chronologies: **a** downcore activities of unsupported ^{210}Pb and ^{137}Cs for OES-07, and comparison between the ^{210}Pb -CRS model constrained with the AD 1963-radiocesium peak and varve counting; **b** varve ages with counting errors for

OES-11. The dates report the consistency between turbidites, high modal grain size and documented floods in 1930, 1944, 1955, 1968, 1987, 1999 (Schmocker-Fackel and Naef 2010); **c** correlation of the sedimentation rates from the two cores

The water-content profile presents values between 28.6 and 35 % with minor fluctuations. Mean grain size values are around 25 μm and fluctuate considerably. A minimum of 9.5 μm is found in AD 1910, while a maximum of 44.4 μm is observed for the year AD 1983. The $\text{wt}^{\text{clay}}/\text{wt}^{\text{sand}}$ proportion stays fairly stable from AD 1915 onwards with a mean ratio of 1.8. In contrast, a

sharp and obvious increase of this ratio occurs between AD 1906 and AD 1914 with the extreme value of 71.8 recorded in AD 1912, indicating a virtual absence of sand-sized particles during this time. Component flux profiles display a high variability with no apparent trends; mean values of 4.47 $\text{mg cm}^{-2} \text{year}^{-1}$ for OC, 143 $\text{mg cm}^{-2} \text{year}^{-1}$ for calcite, and 79.1 $\text{mg cm}^{-2} \text{year}^{-1}$

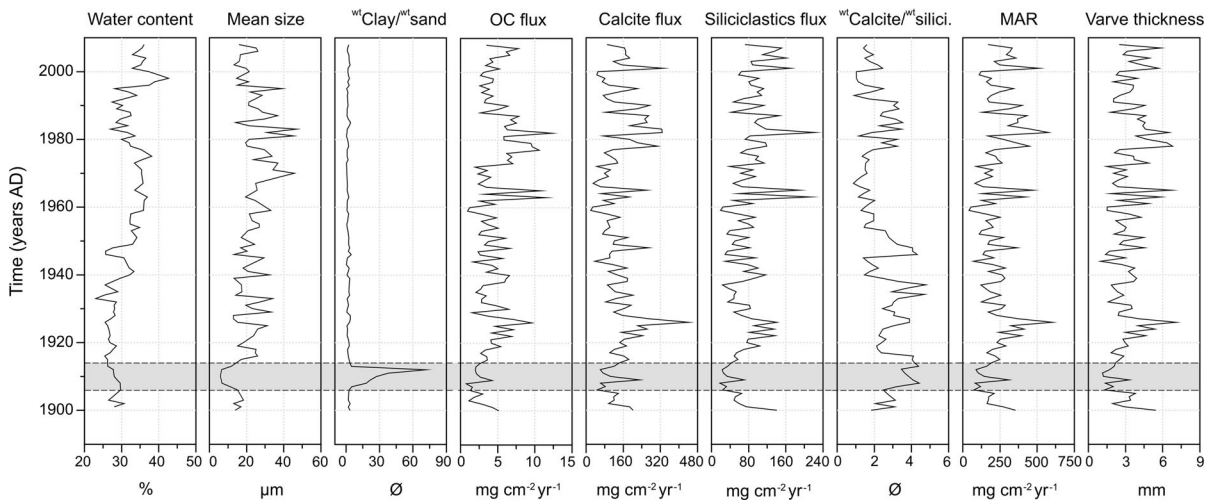


Fig. 5 Time series of proxy data of Lake Oeschinen (core OES-11). The horizontal shaded grey area highlights the zone with anomalous sediment properties

for siliciclastics can be noted. Although OC, calcite and siliciclastic particle fluxes differ in quantity, their curves show almost identical shapes and are strongly correlated with MAR ($r = 0.83$, $r = 0.96$ and $r = 0.87$, respectively $p < 0.01$). Averaged MAR amounts to $232 \text{ mg cm}^{-2} \text{ year}^{-1}$. Similarly, the MAR profile, derived from varve thickness, is highly correlated with this latter ($r = 0.89$, $p < 0.01$).

The shaded grey area in Fig. 5 (AD 1907–1913) highlights a part of the sediment core that is characterized by anomalies in the profiles, most clearly in the ratio of clay-sized particles to sand (values $\gg 10$). Additionally, the absolute lowest values in mean grain size are observed in this section ($< 10 \mu\text{m}$). This time interval is also marked by an increase in the ratio of $\text{wt}^{\text{t}}\text{calcite}/\text{wt}^{\text{t}}\text{siliciclastics}$ (maximum 3.5) and by low varve thicknesses (mean of 2.10 mm) and MAR ($158.2 \text{ mg cm}^{-2} \text{ year}^{-1}$).

Calibration and validation

Pearson correlation matrices reveal the best proxy-climate relationship for varve thickness as a significant ($p < 0.05$) predictor for cumulative warm season precipitation (Table 2, left panel). To explore the response sensitivity of varve thickness to seasonal precipitation, the two highest correlations are considered (MJJA and MJ). These relationships are significant for values at annual resolution ($r = 0.53$ and $r = 0.51$ respectively) and 3-year filtered resolution ($r = 0.56$ and $r = 0.61$ respectively).

In contrast, no significant temperature signal is found in the varve thickness or any of the other proxies of Lake Oeschinen, except a weak signal for SON temperature and varve thickness ($r = 0.38$ at $p < 0.05$) for 3-year triangular filtered data.

Figure 6a shows the calibration of 3-year filtered varve thickness data to MJJA and MJ cumulative precipitation. The calibration statistics yield $\text{RMSEP}_{\text{bootstrap}} = 57.8 \text{ mm}$ for cumulative MJJA precipitation (32.7 mm for cumulative MJ precipitation). The $\text{RMSEP}_{\text{bootstrap}}$ values account for 16 % of their respective peak-to-peak amplitudes and for 10–13 % of the mean cumulative precipitation.

The 21-year moving correlation between rainfall and varve thickness shows two distinct time-related patterns (Fig. 6b): positive correlations from AD 1916 onwards and negative correlations until AD 1915. Before AD 1915, the correlation between varve thickness and summer temperature appears to be positive and significant (up to $r = 0.5$, $p < 0.05$; vertical shading in Fig. 6), and the proxy data show anomalies (horizontal shading in Fig. 5).

Discussion

Sedimentation processes

We combine surface and sediment trap samples to interpret the varve formation processes. We use the following principles: (1) the mineralogical composition

Table 2 *Left panel:* Pearson correlation coefficients between seasonal climate variables and varve thickness for raw data (1900–2009; $n = 110$) and 3-year filtered data (1901–2008; $n = 108$), as well as for MAR at 3-year filtered data ($*p < 0.05$). *Right panel:* correlation coefficients reported from the study of Leemann and Niessen (1994) and varve thickness record from our study compared with annual precipitation and summer (JJAS) temperature recorded in Adelboden (11 km western Lake Oeschinen)

Precipitation	Varve thickness		MAR 3-year filter	Precipitation	1962–1982 Annual Adelboden
	Raw data	3-year filter			
SON	0.04	0.26	0.13	Leemann and Niessen (1994)	0.07
DJF	0.13	0.27	0.22		
MAM	0.34	0.51*	0.51*		
JJA	0.46*	0.45*	0.37*	This study	0.34
MJJA	0.53*	0.56*	0.49*		
MJ	0.51*	0.62*	0.58*		
Temperature			Temperature		1962–1982 JJAS Adelboden
SON	0.19	0.38*	0.40*	Leemann and Niessen (1994)	0.45*
DJF	0.15	0.26	0.25		
MAM	0.01	0.05	0.03	This study	0.11
JJA	−0.03	0.17	0.17		

is diagnostic of the source areas and, in consequence of the erosion process (snowmelt and glacial abrasion in the glaciated southern limestone watershed; snowmelt and water erosion in the non-glaciated northern Flysch watershed); (2) the sediment grain size is diagnostic for the kinetic energy in the lake and thus for the season of deposition (large grains settle during summer when undercurrents are active and wind mixing strong; small particles settle during winter under ice-covered calm conditions); (3) the sediment mass accumulation is indicative of the intensity of the transport and settling processes. Accordingly, varve formation can be generalized in three phases.

The highest sedimentation rates observed in alpine spring (May–June; Fig. 2a, b) are likely due to a combination of snowmelt and rainfall in the catchment. This forms a basal sand layer. The mineralogical composition of these sediments suggests that particles are transported from all three parts of the catchment (Fig. 2c; Table 1). Particularly substantial is the influence of the northern Flysch catchment which is enriched in dark phyllosilicates (illite, chlorite).

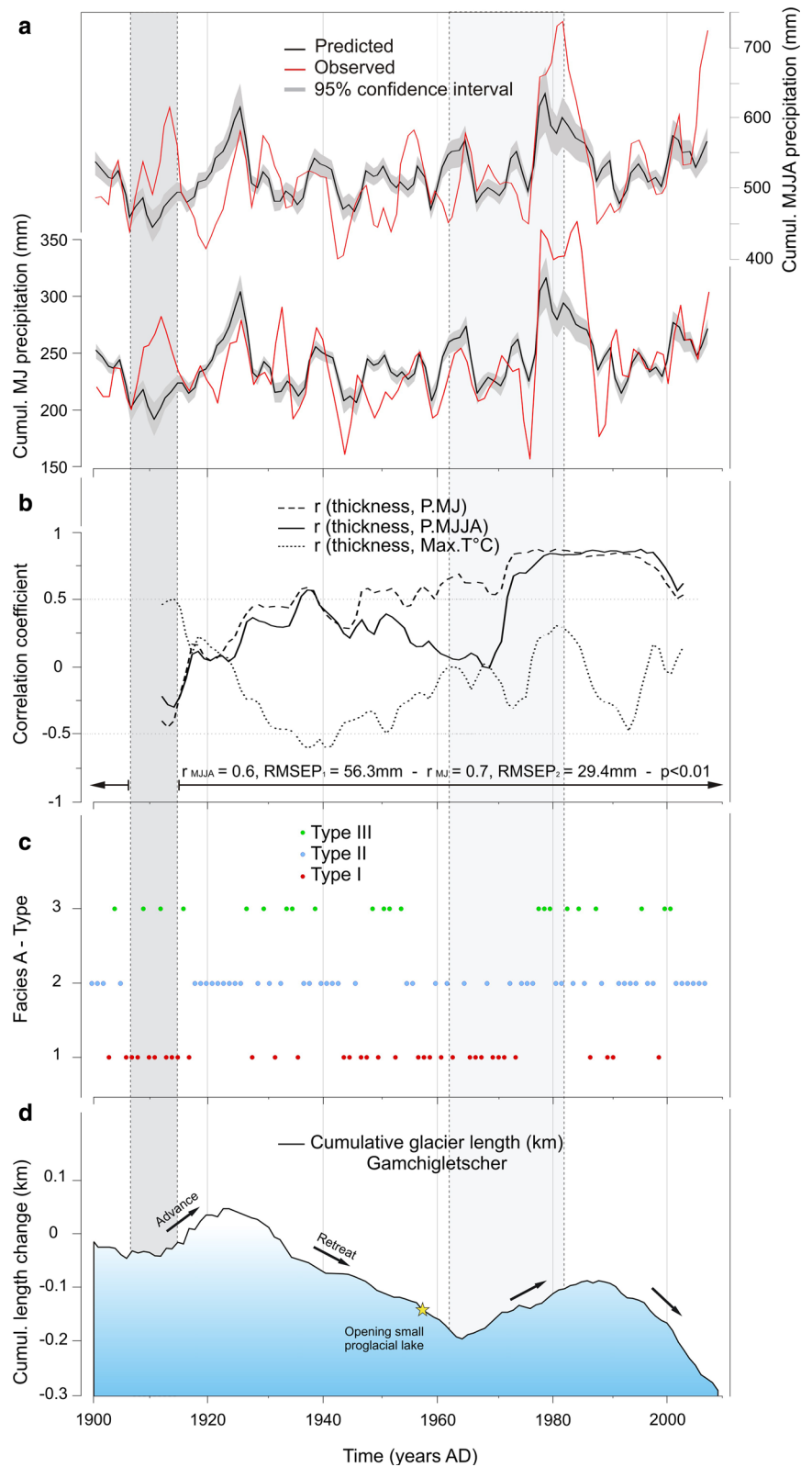
In summer, the high erosivity of rainstorms and active undercurrents related to creek discharge play a major role. They transport large proportions of sand directly to the coring site close to the centre of the lake. These individual rainstorms are also suggested to form

the micro-laminations found in the varves of Type III (Fig. 3). Abundant dark phyllosilicate minerals indicate that particles are mainly eroded from the northern Flysch units. The importance of undercurrents in summer has also been reported for Lake Oeschinen by Leemann and Niessen (1994).

In winter, clay-size light calcite particles settle through the water column under very calm conditions, when the lake is frozen. These fine particles are produced by glacier abrasion on the calcareous bedrock and transported by meltwater into the lake during the entire ice-free season. In summer, however, these fine particles remain in suspension. Leemann and Niessen (1994) measured average concentrations of 5.0 mg L^{-1} suspended sediments in the water column in summer 1991.

In summary, an individual varve comprises one dark spring/summer layer, sometimes multiple dark summer event layers (varves Type III) and one light winter lamina. It is mainly the summer layer that differs in the three varve types of the core. It was not possible to identify significant hydrometeorological controls over interannual accumulation variability of these three varve types (Lamoureux 2000). This is mainly due to the non presence of a hydrometric station directly at the outflow of the lake catchment and to varve counting uncertainties through the cores.

Fig. 6 a Comparison between MJJA, MJ instrumental rainfall data (red lines) and predicted rainfall from varve thickness (black line represents the mean; grey area represents the 95 % confidence envelope); **b** running correlations (21-year moving windows) of MJJA, MJ rainfall and maximum temperature with varve thickness; **c** distribution of Type I–III varves; **d** cumulative length changes of Glacier Gamchi (km). The vertical dark grey area refers to the period with cold summers and anomalous varves (enhanced temperature signal), the light grey vertical area shows the calibration period (AD 1962–1982) used by Leemann and Niessen (1994)



It is well established that rainfall can exert a discernible influence on annual MAR through erosion (Ohlendorf et al. 1997). Although deposition rates can vary substantially, both spatially and temporally (Schiefer and Gilbert 2008), all trends and conclusions concerning the formation of the varves in Lake Oeschinen closely agree. Leemann and Niessen (1994) similarly suggested that varve formation is directly controlled by sediment inputs from catchment inflows, which increase in quantity and grain size during the early season.

However, a disagreement remains between Leemann and Niessen (1994) and this study concerning the nature of the climate variable that influences the varve formation in Lake Oeschinen. Because no hydrometric station was present at the lake, Leemann and Niessen (1994) used the relationship between summer temperature and suspension load of river Lonza (Lötschen valley, 11 km southeast of Lake Oeschinen) to explain, by analogy, the sedimentation principle in Lake Oeschinen. Supported by the results shown in Figs. 2a, b (precipitation-driven system), we rejected this hypothesis. We attributed several reasons for this rejection: (1) Lötschental is an inner-Alpine valley with a markedly different hydroclimatic regime to Lake Oeschinen; (2) the catchment area of the Lonza river is approximately three times more vast than the one of Oeschinen; (3) geological settings differ remarkably where no easily erodible Tertiary Flysch are found in the Lötschen valley; (4) the glacier cover is much more extended and therefore not comparable. Nevertheless, the control of inter-annual variations of sedimentation by rainfall needs to be validated by the calibration-in-time approach.

Chronology

In quantitative paleoclimate research, it is crucial to establish a reliable chronology when aiming for high-resolution reconstructions. This is provided in Lake Oeschinen by two cores which were dated with multiple independent varve counts (two analysts). From core OES-07, thirty ^{210}Pb dates were obtained which are consistent with the ^{137}Cs peaks. Core OES-11 presents relatively low varve counting errors (6–10 %) as compared to other varve sediment studies (Ojala et al. 2012) and the chronology was verified by six flood layers of known age. Moreover, the comparison of the different dating methods in these two cores

shows a high degree of reproducibility, which strengthens both chronologies and increases their robustness. For obvious reasons, reproduction of chronologies is not often found in lake sediment research while it remains a standard practice in other disciplines (tree ring research, Hughes 2002).

Varve thickness as a proxy for spring and spring–summer rainfall

Proxy selection

The proxy-climate correlation matrix reveals the strongest climate signal for varve thickness as a predictor for warm season rainfall. The mechanistic relation between rainfall, erosion, sediment transport, and mass accumulation is widely recognized and well understood (Tiljander et al. 2003). Moreover, our sediment trap data (Fig. 2a) show that the response of sediment accumulation to weather (snowmelt and precipitation) is immediate and thus suitable to address variability at interseasonal and annual resolution. This is in line with previous studies in Lake Oeschinen (Leemann and Niessen 1994) and sediment trap data from Lake Silvaplana, eastern Swiss Alps (Blass et al. 2007a).

The sediment water content may substantially affect the annual sediment accumulation measured as varve thickness, which means MAR should be used in preference (Elbert et al. 2012). In Lake Oeschinen, water content varies only within a small range to the extent that varve thickness and MAR are highly correlated ($r = 0.89$; Fig. 5). Moreover varve thickness can be measured from thin sections directly and much more precisely (at annual resolution and with multiple measurements) than MAR which requires sediment subsampling. Since the varves cannot be precisely cut year by year (near-annual at best) for the analysis of MAR, sampling errors are introduced to the MAR data. In our data, the MAR-climate correlation tests present systematically a weaker signal (e.g. $r_{(\text{MAR}, \text{P.MJ})} = 0.58$, $p < 0.05$; Table 2) than for varve thickness. For these reasons varve thickness was used in the analyses.

Proxy-climate relationship

Figures 5, 6 indicate the proxy-climate relationship may be time-dependent and different for the time before and after 1915.

For the period 1916–2008, the moving correlations (Fig. 6b) and the calibration statistics strongly suggest that varve thickness in Lake Oeschinen is primarily and significantly driven by cumulative summer rainfall. Further testing revealed that neither residuals from the varve thickness–rainfall relationship nor any of the other proxies indicate a temperature signal during this period. This, at the first glance, contrasts Leemann and Niessen (1994) who concluded that varve thickness from AD 1962–1982 in Lake Oeschinen (light shaded area in Fig. 6) primarily contains a summer temperature signal. This different interpretation can be attributed to three reasons: (1) Leemann and Niessen (1994) used annual precipitation data from Adelboden (1,320 m a.s.l., 13 km western Lake Oeschinen), while we used summer precipitation data from nearby Kandersteg; (2) Leemann and Niessen (1994) noted a strong covariance between precipitation and rainfall in their data; and (3) the period of their investigation (AD 1962–1982) was rather short and appears in the running correlations of Fig. 6b as a phase with a relatively increasing temperature signal and a weaker precipitation signal. To test the influence of this last point, our varve record was compared to the 1962–1982 meteorological data from Adelboden (JJAS temperature and annual precipitation; Leemann and Niessen 1994). Our varve record performs barely with both variables (Table 2, right panel) implying that other issues have to be considered for the differed interpretations: (1) the critical point of the site specificity (Schiefer and Gilbert 2008); Leemann and Niessen (1994) found that varve thickness in different parts of Lake Oeschinen varied between 0.2 and 1 cm, (2) the uncertainties in the varve counting may significantly affect the calibration models, especially at the annual resolution (maximum counting error ± 3 years in the period 1962–1982, Fig. 4b). This could question the reliability and reproducibility of the varve–meteorology sedimentary records.

Indeed, sedimentation rates in many proglacial lakes are known to be controlled by temperature (Trachsel et al. 2012), but this does not seem to be the case in Lake Oeschinen. The mineralogical composition of the sediments at the coring sites (OES-07 and OES-11) suggest that sediment transport from the glaciated areas is limited and subordinate in comparison to easily erodible material from the Flysch areas, which is sensitive to precipitation.

Interestingly in the period 1901–1915, the correlation between varve thickness and precipitation

disappears and a positive correlation with maximum temperature is established (Fig. 6b). This part of the core is characterized by extremely high proportions of clay-sized particles compared to sand ($^{wt}clay/^{wt}sand > 10$), an increase in the ratio between calcite and siliciclastic material, small grain sizes ($< 10 \mu m$) and low varve thickness (Fig. 5). Ohlendorf et al. (1997) and Blass et al. (2007a) similarly recorded an abnormal decrease in the MAR in the sediment of proglacial Lake Silvaplana (Engadine region, eastern Swiss Alps) at this time which coincides with a cold anomaly during the summer months (AD 1906–1925, MeteoSwiss). This cold anomaly resulted in considerable expansions of most glaciers in the Alps (Glaciological reports 1881–2009; Fig. 6d).

In Lake Oeschinen, the lack of a strong precipitation signal in the varve thickness during very cold periods may be explained by its altitude. Since the catchment of the lake is situated 500–1,500 m above the altitude of the meteorological station, precipitation recorded as rainfall in Kandersteg might have fallen as snow in the high alpine catchment. While snowfall is much less erosive, the length of the period with erosion from rainfall in summer is also reduced during cold periods (Menounos and Clague 2008). This rain/snow threshold in turn leads to very small sedimentation rates, small mean grain size, and reduces flux of siliciclastic material from the Flysch watershed while glacial abrasion from the limestone watershed continues. This leads to varves that are relatively enriched in calcite. Fig. 5 shows high values of the $^{wt}calcite/^{wt}siliciclastic$ ratio (> 3) during this cold phase AD 1907–1913. From these varves (Fig. 5), we can derive two objective criteria ($^{wt}clay/^{wt}sand$ ratios > 10 , mean grain size $< 10 \mu m$; additionally high $^{wt}calcite/^{wt}siliciclastic$ ratios and thin varves) for periods when varve thickness does not contain a summer rainfall signal and for which the calibration is not valid. If these years (or varves) are removed from the calibration period, MJJA precipitation from varve thickness improves by about 8 % ($r = 0.60$, $RMSEP_{bootstrap} = 56.3$ mm) and MJ precipitation by 13 % ($r = 0.71$, $RMSEP_{bootstrap} = 29.4$ mm). Both are highly significant ($p < 0.01$).

Several studies have demonstrated the complex responses of lacustrine sedimentation to a range of climate variables and other factors (Cockburn and Lamoureux 2007; Hodder et al. 2007; Kaufman et al. 2011). In most cases proxies are more likely

influenced by a combination of several variables (temperature, precipitation, glacier melting, non-climatic and stochastic effects) rather than a single climate variable. In our case summer precipitation explains about 40 % of the variance but not more. Moreover the moving proxy-climate correlations in Lake Oeschinen (Fig. 6b) show that the relative influence of precipitation and temperature changes through time, which poses a serious problem for single-variable climate reconstructions. However, the challenge is that many applications in climate research such as data–data comparisons (Trachsel et al. 2012), data-model comparisons or proxy-data assimilation in climate model simulations (Goosse et al. 2012) require time series for a single variable and a specific season of the year.

In the case of Lake Oeschinen, this problem may be addressed using additional independent sediment proxies. It appears from Figs. 5 and 6 that mean grain size is very small ($<10 \mu\text{m}$) and $w^{\text{t}}\text{clay}/w^{\text{t}}\text{sand}$ ratios very high (>10) for the times when the relationship between the varve thickness and precipitation is weak and the influence of temperature becomes important (shaded area Fig. 6). Such objective criteria may help assessing the quality and reliability of climate reconstructions and underpin the value of multi-proxy data sets.

Influence of glacial fluctuations on sedimentation

Glacier fluctuations are known to influence sediment supply into proglacial lakes (Leonard 1997; Jansson et al. 2005, Nussbaumer et al. 2011) and thus modify MAR, varve thickness and structure (Blass et al. 2003). This is the reason why many climate reconstructions from proglacial sediments need to be detrended to account for the effect of glacier length variations (Blass et al. 2007b; Elbert et al. 2012; Trachsel et al. 2012). Blass et al. (2007a) further demonstrated that the 20th century can substantially differ from previous centuries, which questions the extension of the statistical relationships beyond the calibration period.

Accordingly, the 30 % glacier cover in the catchment of Lake Oeschinen might set similar limitations. This does not seem to be the case because (1) the calibration model with the original (not detrended) varve thickness data shows robust results despite large changes in glacier length variations during the 20th

century (Gamchi Glacier; Fig. 6d; note: precipitation does not show a trend in the same period); (2) the mineral mixing ratios in the sediments suggest that sediment flux and varve thickness is dominated by sediments from the non-glaciated Flysch watershed and thus largely independent of glacial erosion, and (iii) the formation of the small lake (Fig. 1a) acting as a sediment trap in front of the Bluemlisalp Glacier from ca. 1950 onwards did not lead to a systematic shift of the varve thickness in Lake Oeschinen. Thus the varve thickness-precipitation calibration in this case seems to be robust and not influenced by glaciers in the catchment. This finding is important with regard to the precipitation reconstruction pre-1901 glacier fluctuations.

Conclusions

We investigated delta-fan surface samples, sediment trap data, two well-dated short sediment cores and hydro-geological catchment properties of proglacial Lake Oeschinen (Swiss Alps) with the aim (1) to understand varve formation processes and (2) to explore the potential of the varved sediments for quantitative high-resolution climate reconstructions. For the proxy-climate calibration we used sediments and local meteorological data for the period AD 1901–2008.

We conclude on the varve formation process from the mineralogical composition and grain size distribution of the individual sediment laminae. A coarse-grained dark basal layer enriched in siliciclastic minerals is formed during spring snowmelt and summer rainfall whereas the bright, fine-grained thin calcite layer is formed during winter under calm conditions when the lake is frozen. Radiometric dating and flood chronomarkers of known age support the annual nature of the laminae couplets (clastic varves). This forms the basis for a highly accurate and precise chronology for the proxy-climate calibration AD 1901–2008.

We conclude from the proxy-climate correlation matrix that varve thickness best contains the climate signal and explains 40–50 % of the variance of summer precipitation ($r_{\text{MJJJA}} = 0.6$, $r_{\text{MJ}} = 0.7$, $p < 0.01$). Varves in rainy summers show higher sediment fluxes, greater thickness and are enriched with siliciclastic minerals from the sub-watershed

characterized by Flysch bedrock and easily erodible material. Varve thickness does not seem to be influenced by length variations of glaciers in the catchment.

We find that the relationship between varve thickness and summer precipitation is not stable for periods with very cold summers as observed between AD 1901 and 1915. Thus we develop objective criteria ($^{wt}clay/^{wt}sand$ ratios >10 , mean grain size $<10\ \mu m$) to identify sediment sections where the proxy-climate calibration model should not be applied.

According to our results, the varved sediments of Lake Oeschinen hold great potential for investigating past precipitation variations and changes in the coupled lake-catchment system beyond the instrumental period.

Acknowledgments We thank Mr Hirschi for granting access to Lake Oeschinen, Richard Niederreiter for help with the freeze coring, and Urs Eggenberger (Institute of Geological Sciences, University of Bern) for assistance with XRD. The help and expertise of Samuel Hagnauer and Daniela Fischer was particularly essential from the field to the lab. Thanks to Mathias Trachsel and Christian Kamenik for statistical discussions, and Krystyna Saunders for comments on this manuscript. This work is funded through the Swiss National Science Foundation 200020-134945.

References

- Appleby PG (2001) Chronostratigraphic techniques in recent sediments. In: Last WM, Smol JP (eds) Tracking environmental change using lake sediments: basin analysis, coring, and chronological techniques. Kluwer, Dordrecht, pp 171–201
- Arnaud F, Lignier V, Revel M, Desmet M, Beck C, Pourchet M, Charlet F, Trente-Saux A, Tribouvillard N (2002) Flood and earthquake disturbance of ^{210}Pb geochronology (Lake Anterne, NW Alps). *Terra Nova* 14:225–232
- Birks HJB (2005) Overview of numerical methods in palaeolimnology. In: Birks HJB, Lotter AF, Juggins S (eds) Tracking environmental change using lake sediments: data handling and numerical techniques. Kluwer, Dordrecht, pp 19–92
- Blass A, Anselmetti FS, Ariztegui D (2003) 60 years of glaciolacustrine sedimentation in Steinsee (Sustenpass, Switzerland) compared with historic events and instrumental meteorological data. *Eclogae Geol Helv* 96(1):59–71
- Blass A, Grosjean M, Troxler A, Sturm M (2007a) How stable are twentieth-century calibration models? A high-resolution summer temperature reconstruction for the eastern Swiss Alps back to AD 1580 derived from proglacial varved sediments. *Holocene* 17:51–63
- Blass A, Bigler C, Grosjean M, Sturm M (2007b) Decadal-scale autumn temperature reconstruction back to AD 1580 inferred from the varved sediments of Lake Silvaplana (south-eastern Swiss Alps). *Quat Res* 68:184–195
- Brunetti M, Maugeri M, Nanni T, Auer I, Böhm R, Schöner W (2006) Precipitation variability and changes in the greater Alpine region over the 1800–2003 period. *J Geophys Res* 111:1–29
- Büntgen U, Tegel W, Nicolussi K, McCormick M, Frank D, Trouet V, Kaplan JO, Herzig F, Heussner KU, Wanner H, Luterbacher J, Esper J (2011) 2500 years of European climate variability and human susceptibility. *Science* 331:578–582
- Casty C, Wanner H, Luterbacher J, Esper J, Böhm R (2005) Temperature and precipitation variability in the European Alps since 1500. *Int J Clim* 25:1855–1880
- Cockburn JMH, Lamoureux SF (2007) Century-scale variability in late-summer rainfall events recorded over seven centuries in sub annually laminated lacustrine sediments, White Pass, British Columbia. *Quat Res* 67:193–203
- de Jong R, Kamenik C (2011) Validation of a chrysophyte stomatocyst-based cold-season climate reconstruction from high Alpine Lake Silvaplana, Switzerland. *J Quat Sci* 26:268–275
- Elbert J, Grosjean M, von Gunten L, Urrutia R, Fischer D, Wartenburger R, Ariztegui D, Fujak M, Hamann Y (2012) Quantitative high-resolution winter (JJA) precipitation reconstruction from varved sediments of Lago Plomo 47°S, Patagonian Andes, AD 1530–2002. *Holocene* 22:465–474
- Glaciological reports, 1881–2009. The Swiss glaciers, year-books of the cryospheric Commission of the Swiss Academy of Sciences (SCNAT) published since 1964 by the Laboratory of Hydraulics, Hydrology and Glaciology (VAW) of ETH Zurich. No. 1–126, (<http://glaciology.ethz.ch/swiss-glaciers/>)
- Goosse H, Guiot J, Mann ME, Dubinkina S, Sallaz-Damaz Y (2012) The medieval climate anomaly in Europe: comparison of the summer and annual mean signals in two reconstructions and in simulations with data assimilation. *Glob Planet Ch* 84–85:35–47
- Hegerl GC, Crowley TJ, Hyde WT, Frame DJ (2006) Climate sensitivity constrained by temperature reconstructions over the past seven centuries. *Nature* 440:1029–1032
- Heiri O, Lotter AF, Lemcke G (2001) Loss on ignition as a method for estimating organic and carbonate content in sediments: reproducibility and comparability of results. *J Paleolimnol* 25:101–110
- Hodder KR, Gilbert R, Desloges JR (2007) Glaciolacustrine varved sediment as an alpine hydroclimatic proxy. *J Paleolimnol* 38:365–394
- Hughen KA, Overpeck JT, Anderson RF (2000) Recent warming in a 500-year palaeotemperature record from varved sediments, Upper Soper Lake, Baffin Island, Canada. *Holocene* 10:9–19
- Hughes MK (2002) Dendrochronology in climatology—the state of the art. *Dendrochronologia* 20:95–116
- Jansson P, Rosqvist G, Schneider T (2005) Glacier fluctuations, suspended sediment flux and glacio-lacustrine sediments. *Geogr Ann A* 87:37–50
- Kalugin I, Daryin A, Smolyaninova L, Andreev A, Diekmann B, Khlystov O (2007) 800-year-long records of annual air temperature and precipitation over southern Siberia inferred from Teletskoye Lake sediments. *Quat Res* 67:400–410

- Kamenik C, van der Knaap WO, van Leeuwen JFN, Goslar T (2009) Pollen/climate calibration based on a near-annual peat sequence from the Swiss Alps. *J Quat Sci* 24:529–546
- Kaufman CA, Lamoureux SF, Kaufman DS (2011) Long-term river discharge and multidecadal climate variability inferred from varved sediments, southwest Alaska. *Quat Res* 76:1–9
- Lamoureux SF (2000) Five centuries of interannual sediment yield and rainfall-induced erosion in the Canadian High Arctic recorded in lacustrine varves. *Water Resour Res* 36:309–318
- Lamoureux SF (2001) Varve chronology techniques. In: Last WM, Smol JP (eds) *Tracking environmental change using lake sediments: basin analysis, coring, and chronological techniques*. Kluwer, Dordrecht, pp 247–260
- Larocque-Tobler I, Grosjean M, Heiri O, Trachsel M, Kamenik C (2010) Thousand years of climate change reconstructed from chironomid subfossils preserved in varved lake Silvaplana, Engadine, Switzerland. *Quat Sci Rev* 29:1940–1949
- Larocque-Tobler I, Quinlan R, Stewart MM, Grosjean M (2011) Chironomid-inferred temperature changes of the last century in anoxic Seebbergsee, Switzerland: assessment of two calibration methods. *Quat Sci Rev* 30:1770–1779
- Leemann A, Niessen F (1994) Varve formation and the climatic record in an Alpine proglacial lake: calibrating annually laminated sediments against hydrological and meteorological data. *Holocene* 4:1–8
- Leonard EM (1997) The relationship between glacial activity and sediment production: evidence from a 4450-year varve record of neoglacial sedimentation in Hector Lake, Alberta, Canada. *J Paleolimnol* 17:319–330
- Mann ME, Zhang Z, Hughes MK, Bradley RS, Miller SK, Rutherford S, Ni F (2008) Proxy-based reconstructions of hemispheric and global surface temperature variations over the past two millennia. *Proc Natl Acad Sci USA* 105:13252–13257
- McKay NP, Kaufman DS, Michelutti N (2008) Biogenic silica concentration as a high-resolution, quantitative temperature proxy at Hallet Lake, south-central Alaska. *Geophys Res Lett* 35:L05709
- Menounos B, Clague JJ (2008) Reconstructing hydro-climatic events and glacier fluctuations over the past millennium from annually laminated sediments of Cheakamus Lake, southern Coast Mountains, British Columbia, Canada. *Quat Sci Rev* 27:701–713
- Meyer MC, Faber R, Spotl C (2006) The wingeol lamination tool: new software for rapid, semi-automated analysis of laminated climate archives. *Holocene* 16:753–761
- Mitchell TD, Jones PD (2005) An improved method of constructing a database of monthly climate observations and associated high-resolution grids. *Int J Climatol* 25:693–712
- Moore JJ, Hughen KA, Miller GH, Overpeck JT (2001) Little Ice Age recorded in summer temperature reconstruction from varved sediments of Donard Lake, Baffin Island, Canada. *J Paleolimnol* 25:503–517
- Niessen F, Wick L, Bonani G, Chondrogianni C, Siegenthaler C (1992) Aquatic system response to climatic and human changes: productivity, bottom water oxygen status, and sapropel formation in Lake Lugano over the last 10,000 years. *Aqua Sci* 54:257–276
- Niklaus M (1967) *Geomorphologische und limnologische Untersuchungen am Öschinensee*. PhD thesis. Kümmerly und Frey, Bern
- Nussbaumer SU, Steinhilber F, Trachsel M, Breitenmoser P, Beer J, Blass A, Grosjean M, Hafner A, Holzhauser H, Wanner H, Zumbühl HJ (2011) Alpine climate during the Holocene: a comparison between records of glaciers, lake sediments and solar activity. *J Quat Sci* 26:703–713
- Ohlendorf C, Niessen F, Weissert H (1997) Glacial varve thickness and 127 years of instrumental climate data: a comparison. *Clim Change* 36:391–411
- Ojala AEK, Francus P, Zolitschka B, Besonen M, Lamoureux SF (2012) Characteristics of sedimentary varve chronologies—a review. *Quat Sci Rev* 43:45–60
- PAGES 2 k Consortium (2013) Continental-scale temperature variability during the last two millennia. *Nat Geosci* 6:339–346
- Pauling A, Luterbacher J, Casty C, Wanner H (2006) Five hundred years of gridded high-resolution precipitation reconstructions over Europe and the connection to large-scale circulation. *Clim Dynamic* 26:387–405
- Pfister C (1999) *Wetternachhersage: 500 Jahre Klimavariationen und Naturkatastrophen (1496–1995)*. Verlag Paul Haupt, Bern
- Pienitz R, Lotter A (2009) Editorial: advances in paleolimnology. In: Pienitz R, Lotter A, Newman L, Kiefer T (eds) *Advances in paleolimnology*. PAGES News 17 (3): 89–136
- Saunders KM, Grosjean M, Hodgson DA (2013) A 950 year temperature reconstruction from Duckhole Lake, southern Tasmania, Australia. *Holocene* 23:771–783
- Schiefer E, Gilbert R (2008) Proglacial sediment trapping in recently formed Silt Lake, Upper Lillooet Valley, Coast Mountains, British Columbia. *Earth Surf Proc Land* 33:1542–1556
- Schmocker-Fackel P, Naef F (2010) More frequent flooding? Changes in flood frequency in Switzerland since 1850. *J Hydrol* 381:1–8
- Stewart M, Larocque-Tobler I, Grosjean M (2011) Quantitative inter-annual and decadal June–July–August temperature variability ca. 570 BC to AD 120 (Iron Age–Roman Period) reconstructed from the varved sediments of Lake Silvaplana. *Switz J Quat Sci* 26:491–501
- Suchy V, Frey M, Wolf M (1997) Vitrinite reflectance and shear-induced graphitization in orogenic belts: a case study from the Kandersteg area, Helvetic Alps, Switzerland. *Int J Coal Geol* 34:1–20
- Tiljander M, Saarnisto M, Ojala AEK, Saarinen T (2003) A 3,000-year palaeoenvironmental record from annually laminated sediment of Lake Korttajärvi, central Finland. *Boreas* 26:566–577
- Trachsel M, Eggenberger U, Grosjean M, Blass A, Sturm M (2008) Mineralogy-based quantitative precipitation and temperature reconstructions from annually laminated lake sediments (Swiss Alps) since AD 1580. *Geophys Res Lett* 35:L13707
- Trachsel M, Grosjean M, Schnyder D, Kamenik C, Rein B (2010) Scanning reflectance spectroscopy (380–730 nm): a novel method for quantitative high-resolution climate reconstructions from minerogenic lake sediments. *J Paleolimnol* 44:979–994

- Trachsel M, Kamenik C, Grosjean M, McCarroll D, Moberg A, Brázdil R, Büntgen U, Dobrovolný P, Esper J, Frank DC, Friedrich M, Glaser R, Larocque-Tobler I, Nicolussi K, Riemann D (2012) Multi-archive summer temperature reconstruction for the European Alps, AD 1053–1996. *Quat Sci Rev* 46:66–79
- Villalba R, Grosjean M, Kiefer T (2009) Long-term multi-proxy climate reconstructions and dynamics in South America (LOTRED-SA): state of the art and perspectives. *Palaeogeogr Palaeoclimatol Palaeoecol* 281:175–179
- von Gunten L, Grosjean M, Rein B, Urrutia R, Appleby P (2009) A quantitative high-resolution summer temperature reconstruction based on sedimentary pigments from Laguna Aculeo, central Chile, back to AD 850. *Holocene* 19:873–881
- von Gunten L, Grosjean M, Kamenik C, Fajak M, Urrutia R (2012) Calibrating biogeochemical and physical climate proxies from non-varved lake sediments with meteorological data: methods and case studies. *J Paleolimnol* 47:583–600
- Wanner H, Rickli R, Salvisberg E, Schmutz C, Schüepp M (1997) Global climate change and variability and its influence on Alpine climate—concepts and observations. *Theor Appl Clim* 58:221–243
- Zolitschka B (1996) High resolution lacustrine sediments and their potential for palaeoclimatic reconstruction. In: Jones PD, Bradley RS, Jouzel J (eds) *Climatic variations and forcing mechanisms of the last 2000 years*. Springer-Verlag, Berlin, pp 453–478
- Zolitschka B (2007) Varved lake sediments. In: Elias SA (ed) *Encyclopedia of quaternary science*. Elsevier, Amsterdam, pp 3105–3114

4.5. A millennial-long record of warm season precipitation and flood frequency for the North-western Alps inferred from varved lake sediments: implications for the future

Submitted to the journal *Quaternary Science Reviews*

A millennial-long record of warm season precipitation and flood frequency for the North-western Alps inferred from varved lake sediments: implications for the future

Amann Benjamin¹, Szidat Sönke² and Grosjean Martin¹

¹Oeschger Centre for Climate Change Research & Institute of Geography – University of Bern

Erlachstrasse 9a T3, CH-3012 Bern, Switzerland

benjamin.amann@giub.unibe.ch

martin.grosjean@oeschger.unibe.ch

² Oeschger Centre for Climate Change Research & Department of Chemistry and Biochemistry – Bern University

Freiestrasse 3, CH-3012 Bern, Switzerland

szidat@dcb.unibe.ch

Submitted: October 07, 2014

Abstract

The recent warming of the global climate is well recognized. However, does a warmer climate also mean a moister climate? Does dry get drier and wet get wetter? This is an important question as it relates to changes in the water cycle and impacts the water resources as well as the frequency and intensity of storms and floods in the near future. In Europe, regional climate models do not show consistent and robust results for future hydroclimatic changes and how extreme events will evolve in response to future climate change.

Paleo-hydroclimatic data from natural archives are one of the few means to assess such changes in the longer context. Here, we present an annually-resolved record of warm season (MJJ) precipitation and summer flood frequency from the varved (annually laminated) sediments of proglacial Lake Oeschinen (46°30'N - 7°44'E, 1580 m, NW Swiss Alps) back to AD 884. These records are inferred from the thickness of annual sediment deposits and the occurrence of flood event layers in the sediments. The chronology of the sediment record is based on multiple varve counts and validated with historical floods chronicled in written documents (back to the 14th century) and ¹⁴C AMS dates.

The precipitation record shows pronounced interannual to centennial variability with humid phases between AD 920 – 950, AD 1100 – 1180, AD 1300 – 1400, AD 1590 – 1650, AD 1700 – 1790, AD 1820 – 1880, and AD 1960 – 2008. Driest conditions are reconstructed for AD 960 – 1080, AD 1250 – 1300 and for AD 1880 – 1900. Our precipitation record is consistent with the few multi-centennial warm-season precipitation records available for Europe.

We did not find a persistent relationship between warm-season precipitation and temperature. In contrast,

results show that the relation between precipitation and temperature has oscillated between positive correlations (warmer gets wetter, cooler gets drier) and negative correlations (warmer gets drier, cooler gets wetter) with a highly significant ($\chi^2 = 99\%$) multidecadal (60 – 70 yrs) periodicity over the last millennium. Possible explanations for this phenomenon are changes in the weather type statistics or the within-weather-type variability, which influence the combinations between precipitation and temperature over Europe and operate at multidecadal scales. Such multidecadal effects might also be important for precipitation scenarios in the Alpine area under future warming.

Our record of flood frequency suggests more frequent floods under cool and humid climates. This picture is consistent with other studies from small and medium size catchments at mid- and high elevations in the Alpine area. However, the 13th century reveals a period with high flood frequency during warm and moderately dry (average precipitation) conditions. This anomalous situation is currently not understood; nonetheless, this is also one out of several possible scenarios for the future. From the different combinations found in our record, we conclude that the relation between floods, precipitation and temperature and, in consequence, future projections remain poorly constrained.

Keywords proglacial Lake - varve chronology - sedimentology - climate change - paleoclimatology - paleofloods

1. Introduction

Our climate is warming. The recent warming is unequivocal and many of the observed changes are unprecedented over decades to millennia. This is one of the key findings of the latest comprehensive scientific assessments of climate change (IPCC 2013) and based on observations and multiple lines of other independent evidence.

However, does a warmer climate also mean a moister climate? A theoretical response to the warming is an increase in evaporation and precipitation following the Clausius-Clapeyron relation. Although at slower rates, Held and Soden (2006) showed that 'moistening' is the case at global and hemispheric scales. Yet, this thermodynamic relationship between temperature, moisture and precipitation can be complicated at regional scales and a pattern "dry gets dryer and wet gets wetter" is rather expected (Held and Soden 2006; O'Gorman and Muller 2010). However, in a most recent study Greve et al. (2014) found that only 10.8% of the global land area show a robust 'dry gets drier, wet gets wetter' pattern (DDWW paradigm); 9.5% of global land area show robust opposite patterns ('dry gets wetter and wet gets drier'), and for most of the land areas the relationship is not conclusive. Thus, large uncertainties still remain due to differences in hydroclimatic conditions among regions and among seasons, and due to spatial and temporal data scarcity (Trenberth and Shea 2005; Huntington 2006).

Changes in the hydroclimate are most relevant since they relate to changes in regional water resources directly. Moreover, changes in the hydroclimate may also lead to changes in the frequency and intensity of storms and floods in the near future (Köplin et al. 2014). Changes in the properties of such extreme events are of particular concern to society, especially in vulnerable Alpine areas (IPCC 2012; Christensen et al. 2013; Smith

2013). However, it remains poorly understood how changes in temperature, precipitation and regional synoptic-scale weather patterns interact and how properties and statistics of extreme events (floods but also droughts) might eventually change. In Europe for instance, future projections of strong 72 h rainfall events from high-resolution regional climate models do not show a consistent and robust climate change signal (CH2011, 2011).

This leads to the following questions we want to address in the present study:

- Has the climate in the region of the NW Swiss Alps responded according to the Clausius-Clapeyron relation (positive correlation between temperature and precipitation) and to the 'wet gets wetter' scheme over the past millennium? Or is the climatological relation between temperature and precipitation not stationary over time and modulated by other effects?
- Was there a relationship between flood frequency, air temperature and precipitation in the past? For instance, were floods more frequent in warmer, colder, wetter or drier climates?

Over the past few decades, the study of past precipitation variability has received relatively little attention, while considerable efforts have been devoted to investigate past temperature changes at regional scales (PAGES 2k, 2013). This can be attributed to the paucity of precipitation-sensitive proxies and a lack of data. This makes comprehensive assessments of long-term regional changes in precipitation conditions difficult. This data situation has been described as "low confidence", "geographical inconsistency", "difficult spatial interpretations", "syntheses too limited to support regional assessment", or "substantial uncertainty due to large regional differences"

(Büntgen et al. 2010; Wilson 2013; Masson-Delmotte et al. 2013; PAGES 2k 2013).

Scarcity of data is also the case in Europe where only a few multi-centennial- to millennial-long precipitation reconstructions exist. These were produced from documentary data and moisture-sensitive tree rings mainly (Brázdil et al. 2002; Linderholm and Chen 2005; Wilson et al. 2005, 2013; Jönsson and Nilsson 2009; Büntgen et al. 2011; Dobrovlný et al. 2014), and from a few lake sediment records (Trachsel et al. 2008; Romero-Viana et al. 2011).

Besides, growing attention has been paid to the reconstruction of floods and flood frequency in Europe, notably using lake sediments. Lakes are excellent natural archives that offer the great opportunity to study past flood events (Glur et al. 2013). Detrital flood layers found in the sediment cores can be linked directly to flood events recorded in instrumental or documentary sources (Debret et al. 2010; Giguet-Covex et al. 2012; Wilhelm et al. 2012a, 2013; Gilli et al. 2013; Wirth et al. 2013b). Further, particularly valuable records have been uncovered from varved (annually laminated) lake sediments. These varves provide up-to-seasonal resolutions and may reduce chronological uncertainties significantly (Zolitschka 2007; Czymzik et al. 2010, 2013; Stewart et al. 2011; Swierczynski 2012, 2013; Wirth et al. 2013a; Corella et al. 2014).

Recently, Lake Oeschinen, a high elevation (1580 m a.s.l.) proglacial varved lake in the North-western Swiss Alps has shown to be an excellent archive to record past warm-season precipitation and flood frequency variability with a reliable and precise varve chronology (Amann et al. 2014). For the calibration period 1901 – 2008, varve thickness was found to be a quantitative predictor for warm season (MJJ and MJ) precipitation ($r_{\text{MJJ}} = 0.6$; $r_{\text{MJ}} = 0.7$, $p < 0.01$, $n = 108$).

This calibration model ‘varve thickness – precipitation’ is the basis for the precipitation

reconstruction back to AD 884 presented in this study. The aims are to investigate the relationship between warm season precipitation, temperature and flood frequency over the past millennium. For this purpose, we will first extend the varve thickness record from Lake Oeschinen to reconstruct past spring/summer precipitation conditions in the North-western Swiss Alps. Then, we will compare this record with temperature variability reconstructed from tree ring data for the same region. Finally, we will use the occurrence of flood layers in the sediment of Lake Oeschinen to investigate, for the first time, the long-term relationship between flood frequency and the amount of precipitation from the same location and the same natural archive.

2. Study site and sediment formation

Lake Oeschinen (46°30'N, 7°44'E) is a proglacial lake situated at 1580 m a.s.l. in the North-western Alps, 55 km south of Bern, Switzerland (Fig. 1a). A Holocene rockslide formed the lake basin (Niklaus 1967). The 56-m deep lake has a sub-surface outflow through the rockslide and drains into the Kander River (Figs. 1b and d). In winter, ice cover develops from December to late April generally.

Mesozoic limestone predominates in the catchment; however, it is interrupted by two sizable belts of Tertiary Flysch deposits (Fig. 1d) that consist of easily erodible siliciclastic-rich sandstones (Suchy et al. 1997). Glacier cover accounts for 30% of the entire lake catchment.

The mineralogical composition and distribution of the bedrock (limestone in the high-elevation glaciated areas, siliciclastics in the lower elevation Flysch areas) is important for the varve formation (Amann et al. 2014). During spring snowmelt and summer rainfall, a coarse-grained dark basal layer is formed. This layer is enriched in siliciclastics eroded from

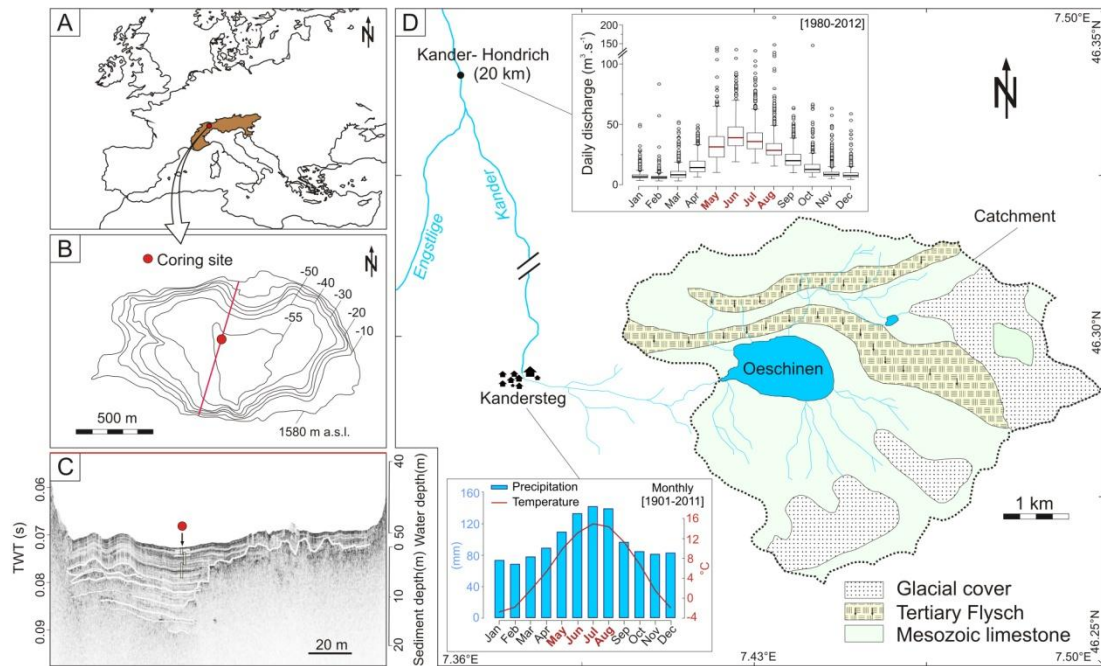


Fig. 1 Situation and characteristics of Lake Oeschinen with a) location in the European Alps, b) bathymetric map of the lake basin with the coring location, c) south-north seismic profile (courtesy: A. Gilli ETH Zurich) and d) geological settings of the catchment area, climate charts from Kandersteg and daily discharge [boxplot] from Kander-Hondrich

the northern Flysch catchment. During winter, clay-size bright calcite particles settle through the water column under very calm conditions when the lake is frozen. These fine particles are produced by glacier abrasion in the limestone part of the catchment. The winter layer has very little influence on the varve thickness (Amann et al. 2014).

Climate variability in the North-western Alps is influenced by both Atlantic and continental regimes with the North Atlantic Oscillation (NAO) as the dominant climate mode (Wanner et al. 1997; Sodemann and Zubler 2010). Highest amounts of precipitation are recorded between May and August (nearby station at Kandersteg; Fig. 1d) with 1173 mm of total annual precipitation. Monthly mean temperatures range from -2.9°C in January to 15°C in July (AD 1900 – 2009; MeteoSwiss). Local thunderstorms associated with heavy rainfall are relatively frequent in the region (Schmocker-Fackel and Naef 2010). These heavy rainfall events occur within a few hours and predominate from May to August (MJJA),

which is the season of interest for our study. Summer rainstorms induce high daily river discharge which is chronicled by the gauging station Kander-Hondrich (Fig. 1d).

3. Material and methods

3.1. Sediment core collection and sampling

Sediment cores with overlapping segments were retrieved with an UWITEC piston corer from the deepest point of Lake Oeschinen in August 2011. The coring site was chosen based on bathymetric and seismic surveys (Fig. 1b, c). The core segments were split lengthwise. A master composite core of 580 cm length was generated by stratigraphic correlation of key sediment strata from visual core inspection and high resolution pictures. One core-half was used to develop the chronology (varve counting and ^{14}C AMS dates). The other core-half was used to establish the multi-proxy data set.

The core was sliced at 1-cm resolution for geochemical data. Water content was calculated after freeze-drying for 24 h. Particle-size distributions of homogenized samples were derived from laser diffraction (Malvern Mastersizer 2000) after removal of organic matter by H₂O₂. Organic carbon and calcite contents were obtained from loss on ignition (LOI) at 550°C and 950°C respectively, following Heiri et al. (2001). The residual after LOI₉₅₀ is summarized as the siliciclastic fraction (mainly quartz, feldspar and clay minerals).

The relative proportions of the two main sediment fractions (calcite and siliciclastics) was also measured by Visible Reflectance Spectroscopy scans (VIS-RS, 380 – 730 nm) using a portable Gretag-Spectrolino (GretagMcBeth, Switzerland). We used the mean 1st-derivative of each VIS-RS spectrum (overall spectral slope) and calibrated these to the LOI₉₅₀-based calcite/siliciclastics ratios (Debret et al. 2011). This allows us to rapidly infer proportions of calcite_(bright)/siliciclastics_(dark) from the entire sediment sequence at a very high (2 mm) resolution (see supplementary material S1 for more details).

3.2. Sediment dating

Thin sections were taken from overlapping sediment slabs (7 x 1.5 x 0.5 cm) using freeze-drying and resin-epoxy embedding techniques (Lamoureux 2001). Laminae identification and turbidite distinction followed Amann et al. (2014). The master chronology was generated by collating and merging optical microscopy pictures (magnification x10) of the thin sections. The thickness of the varves (laminae couplets) was semi-automatically measured using the software package WinGeol Lamination Tool (0.01-mm resolution; Meyer et al. 2006). Varve counting uncertainties were assessed from three independent counts.

The sediment chronology for the upper

50 cm of the core had already been established using a ²¹⁰Pb-CRS model constrained with the AD 1963 ¹³⁷Cs peak, which was consistent with varve counting (Amann et al. 2014). To validate the varve counting in the rest of the sequence, we used six terrestrial plant macrofossils for ¹⁴C dating using Accelerator Mass Spectrometry at the LARA Laboratory of the University of Bern (Szidat et al. 2014). Macrofossils consisted of 4- to 10-mm leaf fragments, fragments of deciduous periderm and other wooden remains (Table 1). Two samples were replicated. ¹⁴C ages were calibrated using the Intcal13 calibration curve (Reimer et al. 2013). In addition, the varve chronology was validated by prominent flood layers in the sediments which were compared with spring-summer flood disasters documented in written archives of the Kander region back to AD 1480 (Pfister 1999; Bütschi 2008).

3.3. Statistics and mapping

With a reliable and precise chronology, we applied the calibration model ‘varve thickness – precipitation’ developed by Amann et al. (2014) to the 580-cm sediment profile. We used inverse linear regression (OLS) from the varve thickness record to reconstruct warm season (MJ and MJJA) precipitation conditions back in time.

In addition to the annual resolution, a triangular filter of 31 years was also applied to emphasise decadal-multidecadal variability (climatology). Significance tests (p-values) were corrected for serial autocorrelation (p_c ; Bayley and Hammersley 1946).

We compared our reconstruction with other multi-centennial European precipitation records to assess the regional coherency. However, the various precipitation records differed in the seasons reconstructed and represent different areas across Europe. Because it is unclear how the different records are expected to relate to each other, we

produced spatial correlation maps for the proxy sites and the respective seasons targeted. For instance, how May-to-August precipitation from Kandersteg (our study) correlates to April-to-June precipitation reconstructed for Central Europe (Büntgen et al 2011). For this purpose, we used the dataset CRU TS 3.21 (Jones and Harris 2013) and mapped the correlations at 0.5° x 0.5° spatial resolution.

To investigate the synoptic weather patterns that may trigger floods in Lake Oeschinen and the North-western Swiss Alps, we produced European-scale composites of wind vector fields, precipitation rates and sea level pressure conditions from nine well-documented flood days between 1981 and 2007. To explore to which extent the composites of the daily heavy rainfall events can be scaled-up to very wet seasons, we also produced these composites for the mean May-to-August conditions of the corresponding years for comparison. Here, we used the 20th Century Reanalysis dataset.

4. Results

4.1. Lithological description and multi-proxy data set

Mineroclastic sediments recovered from Lake Oeschinen generally consist of rhythmically laminated silty loam, intercalated by several dark and thick (up to 46 mm) sandy layers (Fig. 2a). The sediment composition (proportion of ^{wt}calcite/^{wt}siliciclastics) stays fairly stable throughout the entire section with a mean ratio of 3.1 (Fig. 2b). Mean water contents amount to 29.2 % with minor fluctuations (3.4 % standard deviation). The ^{wt}clay/^{wt}sand proportion fluctuates slightly around the mean value of 2.5 from the top of the core to approx. 300 cm sediment depth, and drops to 0.5 in the bottom section that is dominated by sands. This leads to a mean grain

size that ranges between 32.9 µm for the core section 0 – 300 cm and 80.6 µm for the bottom section 300 – 580 cm.

The thin sections and layer counting (validated by ¹⁴C dates; see section 4.2) revealed that the record is continuously varved. These varves consist of layer couplets, whereby the layers of graded sand-to-silt deposits are systematically capped by a layer with clay-size particles. An average thickness of 2.7 mm with a standard deviation of 1.1 mm can be reported. Three sub-types of varves were found that differ in their internal structure (Fig. 2a). Type I is characterized by very thin (1-1.5 mm) fining upward sequences; Type II is thicker (>3 mm) and comprises coarser particles; while multiple internal microlaminations compose varve Type III.

Flood layers are distinguished from the varves in the thin sections (Fig. 2a). These special layers show a high sedimentation with systematic grading of the particle sizes from sand to clay and they often show an erosive base. Fig. 2b shows that flood layers are also marked by a darker colour (core stratigraphy), low ^{wt}calcite/^{wt}siliciclastics proportions (<2.5), low water content and high proportions of sand-size material. Comprehensively, these criteria allows us to distinguish a flood layer (Facies B; Fig. 2a) from a thick varve of type II (Facies A; Fig. 2a). This is of prime importance for the construction of the chronology.

4.2. Sediment chronology

Fig. 3 shows the age-depth model from varve counting placing the base of the core to AD 884 ± 22. The varve counting uncertainty amounts to 9 years from the top of the core to the year AD 1450 (300-cm depth); it reaches a maximum of 30 varve years (c. 2.5%) in the lowest core section where the varves are less well preserved. The robustness of the varve chronology of the top section can be validated by documentary data on floods starting from

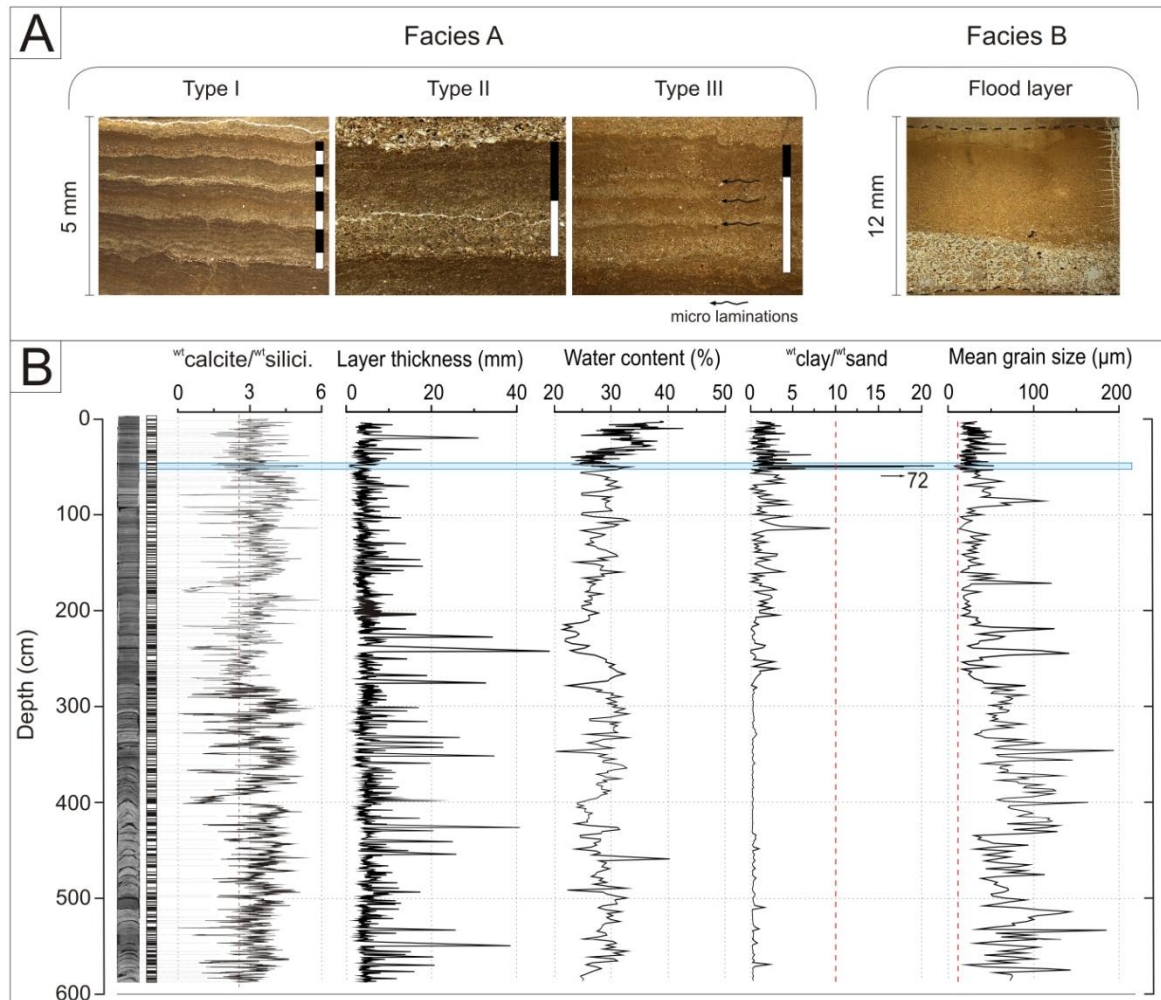


Fig. 2 a) Photomicrographs of Facies A: the varve types with white and black bars representing spring-summer and winter depositions respectively, and Facies B: a typical flood layer; b) multi-proxy dataset with inferred $w^t \text{calcite}/w^t \text{silici}$ from VIS-RS scans, layer thickness (varves and flood layers), and water content and particle size properties. The horizontal blue area highlights the zone where the thresholds (validity) of the calibration model are exceeded; the two thresholds (clay/sand ratio and the mean grain size) are shown by the vertical dashed red lines

AD 1480 onwards (Fig. 3). The comparison shows consistency between the varve-ages of the flood layers found in Lake Oeschinen sediments and the ages of the flood disasters documented in written sources from the Kander River.

The overall chronology inferred from varve counts is consistent with the independent radiometric chronology; i.e., thirty points for ^{210}Pb , five out of six ^{14}C dates and two ^{14}C replicates. The replication of the first two radiocarbon samples ($^{14}\text{C}_1$ and $^{14}\text{C}_2$) shows slightly different probability structures (uncertainty) of the calibrated ages. One ^{14}C

date ($^{14}\text{C}_5$) was excluded from the record because it conferred a too old and inconsistent date, suggesting reworked material. The varve chronology, validated by ^{14}C dates, indicates stable sedimentation rates throughout the entire sediment record.

4.3. Millennial warm season (MJ – MJJA) precipitation reconstruction

Fig. 4a shows the reconstruction of warm season (MJ – MJJA; sum) precipitation at annual and 31-year filtered resolutions from Lake Oeschinen sediments back to AD 884. This

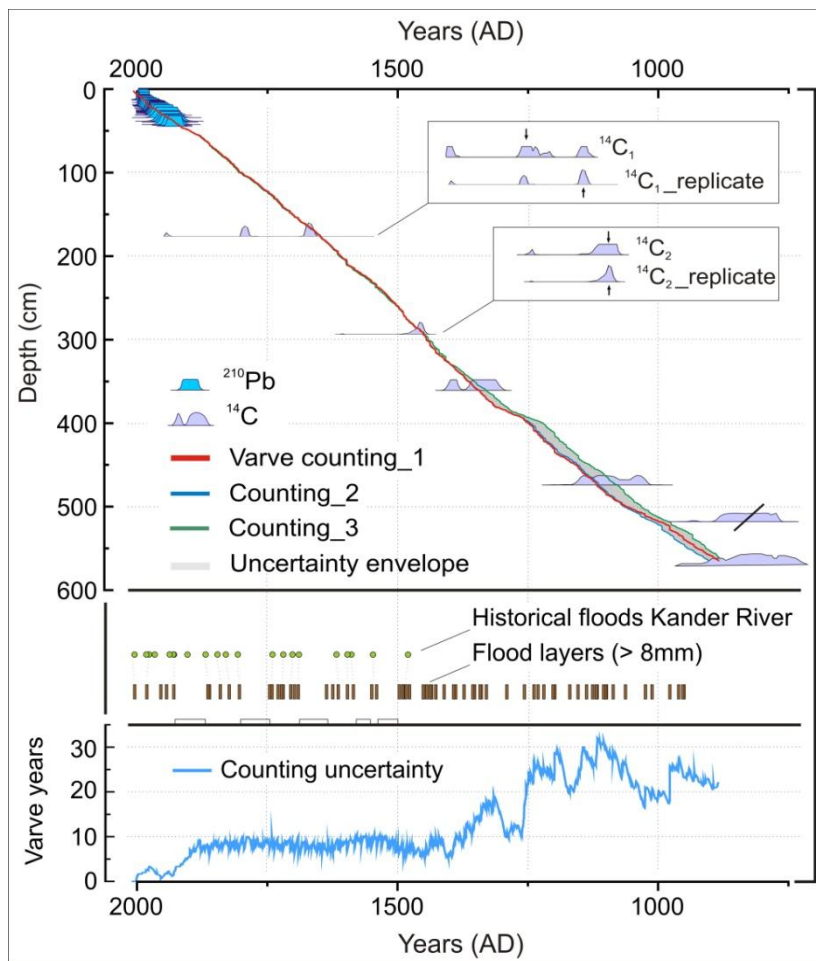


Fig. 3 Sediment chronology derived from varve counting, ^{210}Pb and ^{14}C dates. Middle panel: comparison between the occurrence of prominent turbidite layers and the presence of historical disasters in the Kander area. Lower panel: time series of the varve counting uncertainty

millennial record indicates substantial centennial-scale variability but also decadal-scale fluctuations. Periods with apparent increased wetness (labelled from I to VII) can be noticed in the following time intervals: AD 920 – 950 (I), AD 1100 – 1180 (II), AD 1300 – 1400 (III), AD 1590 – 1650 (IV), AD 1700 – 1790 (V), AD 1820 – 1880 (VI), and AD 1960 – 2008 (VII). Driest conditions are reconstructed for AD 960 – 1080, AD 1250 – 1300 and for AD 1880 – 1900.

The amplitude of reconstructed precipitation remains in the range observed for the calibration period (AD 1901 – 2008, calibration range) except for the two very dry periods AD 960 – 1080 and AD 1250 – 1300.

The comparisons between the precipitation record from Lake Oeschinen and a set of precipitation reconstructions for slightly different seasons and different areas across Europe is shown in Figs. 4b-e and Table 2.

Significant positive correlations ($p_c < 0.01$) were found between lake Oeschinen (this study) and the Greater Alpine Area precipitation (data from Casty et al. 2005), Central Europe (data from Büntgen et al. 2011) and S England/N France (data from Wilson et al. 2013). However, correlation tests did not show significant correlations between Lake Oeschinen precipitation and precipitation in SE Germany (data from Wilson et al. 2005), and with the Czech Lands particularly (data from Dobrovolný et al. 2014). The correlation patterns from the reconstructions are consistent with the spatial correlation maps derived from 20th Century Reanalysis data (maps in Fig. 4).

Fig. 5a shows the comparison between the warm season precipitation reconstruction from Lake Oeschinen and Greater Alpine summer temperature (31-year filtered data). Over the entire last millennium, there is no

Table 1 Details for radiocarbon dating. ^{14}C ages were calibrated online from OxCal. Calibrated ages are given in year AD at 2σ range with cumulative probability in %

Label	BE nr.	Core depth (cm)	Fraction type	Radiocarbon age (^{14}C yr BP $\pm 2\sigma$)	Calibrated age (yr AD with 95.4% prob.)
$^{14}\text{C}_1$	1860.1.1	177 - 178	Twig (Conifer)	199 \pm 19	... (22.2 %) 1935 1805 (50.2%) 1736 1684(23.0 %) 1654
$^{14}\text{C}_{1_Replicate}$	1860.2.1	177 - 178	-	231 \pm 18	1950 (55.6 %) 1944 1800 (38.0%) 1780 1670 (68.2 %) 1645
$^{14}\text{C}_2$	1861.1.1	294 - 296	Twigs (Conifer)	410 \pm 19	1610 (2.8 %) 1602 1491 (92.6 %) 1438
$^{14}\text{C}_{2_Replicate}$	1861.2.1	294 - 296	-	425 \pm 18	1480 (95.4 %) 1435
$^{14}\text{C}_3$	1862.1.1	361 - 362	Twig (Conifer)	595 \pm 19	1406 (23.1 %) 1383 1365 (72.3 %) 1304
$^{14}\text{C}_4$	1863.1.1	474 - 476	Leafs + deciduous periderm	948 \pm 31	1156 (95.4 %) 1024
$^{14}\text{C}_5$	1864.1.1	518 - 522	Wood pieces	1200 \pm 27	894 (91.0 %) 766 741 (4.4 %) 720
$^{14}\text{C}_6$	-	564 - 566	Wooden remain	1210 \pm 80	978 (95.4 %) 666

relationship between the two time-series ($r = -0.09$). However, on shorter (multidecadal) time scales, phases with strong positive correlations ('warmer gets wetter – colder gets drier') alternate with phases of strong negative correlations ('warmer gets drier and colder gets wetter'). 31-yr running correlations between warm-season precipitation and temperature oscillate between negative values (up to $r = -0.6$) and positive values (up to $r = 0.5$) with a highly significant (Chi^2 99%) periodicity between 58 – 73 years throughout the last millennium (Fig. S2, supplementary material). Furthermore, periods with cool and wet conditions coincide with advances of glaciers in the region (around AD 1100, AD 1220, AD 1600, the 17th century, and the 1st half of the 19th century), while warm and dry conditions lead to glacier retreats (Fig. 5a).

4.4. Paleoflood record

Fig. 5b shows the frequency of flood layers (>5 mm) in the sediments of Lake Oeschinen and how this compares with the flood frequency in the Northern Alpine area

(composite of ten sites; data from Glur et al. 2013) and with local paleoclimate variability (Alpine warm-season precipitation from this study, and temperature; Fig. 5a).

Eight periods with higher flood frequency characterize the sediment record, each about 60 years long (labelled as P1 to P8). These periods are dated to AD 1090 – 1140 (P1), AD 1190 – 1240 (P2), AD 1300 – 1380 (P3), AD 1430 – 1510 (P4), AD 1590 – 1650 (P5), AD 1690 – 1750 (P6), AD 1800 – 1870 (P7) and, more recently, starting at AD 1950 (P8).

Seven of these eight flood periods coincide with wetter and cooler conditions in the Alps, while only the period P2 (AD 1190-1240) exhibits high flood frequencies during generally very warm conditions (among the warmest during the last millennium). No significant correlations ($p > 0.05$) were found between the thickness of flood layers (often interpreted as flood intensity) and precipitation ($r = -0.053$) or temperature ($r = -0.083$).

5. Discussion

5.1. Sediment properties – Is the calibration model applicable?

An important issue in paleoclimate studies is the assumption of stationarity; i.e. the question whether or not the proxy-climate calibration model established and validated in the calibration period can be extended back in time. Moreover, the question arises whether or not a calibration of a single proxy (here varve thickness) to a single climate variable (here precipitation) for a particular season (here warm season) is appropriate or might mask the ‘true geo-ecological complexity’ of varve formation. The dilemma is that a common denominator (climate variable for a given season) must be determined for validation purposes, for comprehensive multi-site and multi-proxy regional climate reconstructions (e.g. PAGES 2k, 2013) or for data-model comparisons.

Several studies have demonstrated the complexity of lacustrine systems and how sediment formation is influenced by a combination of several variables (temperature, precipitation, periods of snow accumulation, glacial melt, among others) rather than a single one (Cockburn and Lamoureux, 2007; Hodder et al. 2007; Kaufman et al. 2011). This may also apply to the varves of Lake Oeschinen, notably for specific climate periods such as the Medieval Climate Anomaly (MCA) or the Little Ice Age (LIA).

Amann et al. (2014) have shown that the calibration model ‘varve thickness – precipitation’ is valid if precipitation in the ice-free season falls mainly as rain (not as snow). In consequence, the model is valid if the sediments of the summer layer are mainly composed of silty sand with limited proportions of clay. Therefore, threshold levels for the calibration model were established as $\frac{\text{wt\%clay}}{\text{wt\%sand}} < 10$ and mean grain size > 10

μm (Amann et al. 2014). These conditions are fulfilled for most of the sediment sections considered here (thresholds shown as red vertical dashed lines in Fig. 2b). The horizontal blue line in Fig. 2b highlights the 7-year period (AD 1907-1913) where the sediment data exceed these thresholds and the calibration model does not apply (Amann et al. 2014). Moreover, the calibration period spans a very broad hydroclimatic range from very dry to very humid conditions. This range covers most of the conditions reconstructed for the past millennium except the very dry phases around AD 1000, AD 1300 and AD 1890. These droughts are outside the calibration range and, thus, their amplitudes remain uncertain.

5.2. Sediment chronology

The good preservation of varves in Lake Oeschinen allows for a precise and reliable chronology which is crucial when aiming at high-resolution reconstructions (Fig. 3). The maximum varve counting uncertainty is rather small (c. 2.5 %) and on the order of other high-quality varve chronologies (Ojala et al. 2012).

Of particular interest is the comparison between the varve counts and ^{14}C dates. As it is expected for young ^{14}C dates, $^{14}\text{C}_1$ and $^{14}\text{C}_2$ show a very large range of possible calibrated ages (Fig. 3). More precisely, they show complex structures of probability with two to three relatively narrow discrete possible time-windows, while the age mid-point (50% summed probability) is highly unlikely (Fig. 3). In this case, neither the mid-point nor the time window with the highest probability allows for an unambiguous determination of the correct calendar age from the complex probability density functions. To test different possibilities, we replicated the two first ^{14}C dates. Although the replicate $^{14}\text{C}_1$ confirms the three narrow discrete possible ages, the highest probability (arrows in Fig. 3) moves from the middle

cluster to the oldest cluster of possible ages and matches with the varve chronology. A similar effect is observed in replicate $^{14}\text{C}_2$: one of the two possible time-windows disappeared in the replicate and was transformed into a unique well-confined age cluster with 95.4 % probability. This is a very good tie point for the ^{14}C chronology (Table 1), which suggests that the varve chronology and varve counting uncertainty are very robust.

In addition, the reliability of the varve chronology is confirmed by the consistency between flood layers and documentary data. More than 90 % of the thick flood layers found in the sediments of Lake Oeschinen can be related to flood disasters documented in written archives from the Kander River (Fig. 1d). The difference between the ‘best varve age’ and the ‘real age’ (documentary) of these marker floods is typically smaller than ± 5 to 6 years, which remains well within the varve counting uncertainty (± 9 years until AD 1480).

5.3. Precipitation reconstruction – Reliability and regionalisation

Here we provide the first millennial annually resolved quantitative warm-season precipitation reconstruction for the North-western Alps. The spatial correlation map of May-to-August precipitation shows that the reconstruction from Lake Oeschinen is representative for most of continental Western Europe except for the Mediterranean (Fig. 4a).

Our reconstruction is consistent with independent precipitation data produced from long instrumental data and documentary proxies for the same area back to AD 1659 (Casty et al. 2005, grid cell: 46.25N/6.75E; Fig. 4a and Table 2).

Figs. 4b to 4e show the comparisons of our record with (i) Central European April to June (AMJ) precipitation reconstructed using fir trees (Büntgen et al. 2011), (ii) Southern England/Northern France March to July

(MAMJJ) precipitation reconstructed from oak trees (Wilson et al. 2013), (iii) Southern Bavaria March to August (MAMJJA) precipitation reconstructed from oak trees (Wilson et al. 2005), and (iv) Czech Lands June to August (JJA) precipitation reconstructed from documentary indices and long homogenized instrumental series (Dobrovolný et al. 2014).

The maps in Fig. 4 show the 20th century spatial correlations between warm season May to August precipitation at Lake Oeschinen (black arrows; our study) and precipitation for the respective seasons reconstructed at the sites used for comparison (black boxes). These correlation maps help assess to which degree one would expect consistency between the record of Lake Oeschinen (this study) and the records used for comparison (Fig. 4 and Table 2).

The best correlation and regional consistency with our reconstruction is found for AMJ precipitation reconstructed for Central Europe (Büntgen et al. 2011). Similarities between the two records are found for the wetter periods I, III, V, VI (Fig. 4a, 4b). The wet periods in the 12th century (period II) and around 1600 AD (period IV) are not present in the Büntgen et al. (2011) record but documented in the record of Northern France (Wilson et al. 2013). Our reconstruction compares also well with hydroclimatic conditions in Southern England/Northern France, especially for the wet periods II, IV, V, VI (Table 2; Fig. 2c). Similarly, this reconstruction shows a wetting trend after AD 1950. Finally, precipitation reconstructed in the North-western Alps (this study) does not correlate with the two more continental records from Bavaria and the Czech Lands (Table 2; Fig. 2d and 2e). This is coherent with results from the 20th century correlation maps and particularly true for the Czech Lands. This supports the idea that the West-East moisture gradients over Europe and also the different sources of moisture (Wanner et al. 1997;

4. Lake Oeschinen: clastic varves

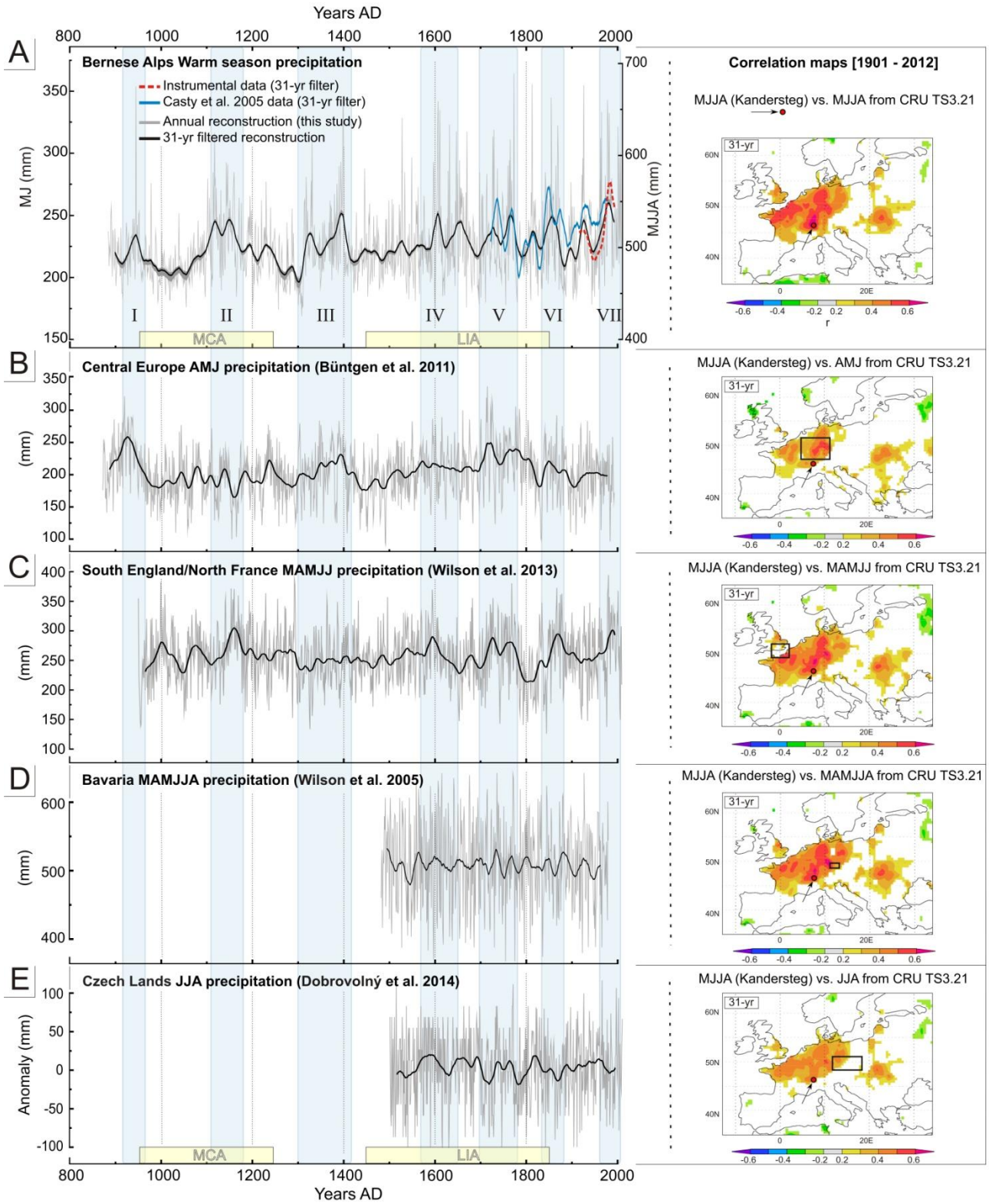


Fig. 4 Comparison and correlation maps between a) Lake Oeschinen warm season precipitation reconstruction with MJJA early-instrumental and documentary data for the North-western Alps (Casty et al. 2005) and with b) Central Europe (Büntgen et al. 2011), c) Southern England and Northern France (Wilson et al. 2013), d) South-East Germany (Wilson et al. 2005) and e) Czech Lands (Dobrovolný et al. 2014)

	MJJJ precipitation (this study)	
	Annual	31 years
MJJJ precipitation [1659 - 2000] Gridded data (Casty et al. 2005)	$r_1 = 0.15$ **	$r_{31} = 0.38$ **
AMJ precipitation [884 - 2005] Central Europe (Büntgen et al. 2011)	$r_1 = 0.10$ **	$r_{31} = 0.31$ **
MAMJJ precipitation [950 - 2009] S England/N France (Wilson et al. 2013)	$r_1 = 0.08$ *	$r_{31} = 0.21$ **
MAMJJJ precipitation [1480 - 1978] Bavaria (Wilson et al. 2005)	$r_1 = 0.06$	$r_{31} = 0.15$ *
JJA precipitation [1501 - 2010] Czech Lands (Dobrovolný et al. 2014)	$r_1 = 0.06$	$r_{31} = 0.09$

** $p_c < 0.01$ * $p_c < 0.05$

Table 2 Correlation coefficients between Lake Oeschinen MJJJ precipitation reconstruction and the different precipitation records of Europe, at annual resolution and for 31 years filtered data

Sodemann and Zubler 2010) operated in a similar way during the past 500 years.

The warm season precipitation reconstruction from Lake Oeschinen does not show any relationship with summer temperature reconstructed from the European Alps (Büntgen et al. 2006) over the past millennium (Fig. 5a). This suggests that neither the Clausius-Clapeyron relation nor a ‘dry gets dryer – wet gets wetter’ scheme does apply in its pure form (Held and Soden 2006), and that the relation between precipitation and temperature (PP-TT) might be more complicated at regional scales (Greve et al. 2014). Our data suggest that the PP-TT relation in the NW Alps was persistently cyclic (multi-decadal ca. 60 – 70 years) throughout the past millennium (Fig. S2, supplementary material). This observation is in line with the finding by Knudsen et al. (2014), who have reported increasing evidence for multidecadal oscillations in paleoclimate archives in the Atlantic realm, and assigned this feature to the Atlantic Multidecadal Oscillation (AMO). At the current state of research, it is premature to speculate about possible mechanisms how AMO would modulate the PP-TT relation in the NW Alps. One possible explanation is a change in the frequency of weather types, another possible explanation might be found in a large

within-weather-type variability (Jacobeit et al. 2003; Küttel et al. 2011). Küttel et al. (2011) reported that “[...] large parts of the changes in European temperatures and precipitation are likely due to within-type variations [...]”. These authors also found that the within-type variability operates at multidecadal scales and they emphasized the role of North Atlantic sea surface temperatures, which are known to influence European climate strongly. Our data also show that multi-decadal cyclicity persisted in pre-industrial time, which would argue against an anthropogenic source for this kind of variability and agree with the conclusions from Küttel et al. (2011) and Knudsen et al (2014).

Furthermore, the ‘precipitation – temperature’ relationship for the past millennium provides novel insight into the climatic conditions that governed glacier length variations of two well documented glaciers in that region: the Great Aletsch Glacier (Holzhauser et al. 2005) and the Lower Grindelwald Glacier (Nussbaumer et al. 2011; Fig. 5a). Our data suggest that substantial glacier advances in the 12th century, in the 14th century, in the 17th and 19th centuries coincided with cool and wet periods. This is in great detail consistent with the findings by Steiner et al. (2008), who analysed the

4. Lake Oeschinen: clastic varves

sensitivity of the Lower Grindelwald Glacier to seasonal precipitation and temperature since the 16th century. In the context of the Maunder Minimum (AD 1645 – 1715; Luterbacher et al. 2001), it is interesting to note that the extremely cold conditions around AD 1690 did not lead to a massive advance due to very dry conditions during that period.

5.4 Climatic control on flood frequency

The millennial-long flood frequency record from Lake Oeschinen reveals that, in the North-western Alps, intense rainfall events were generally more frequent during wet and cool summers. This is true for seven of the eight periods with enhanced flood frequencies

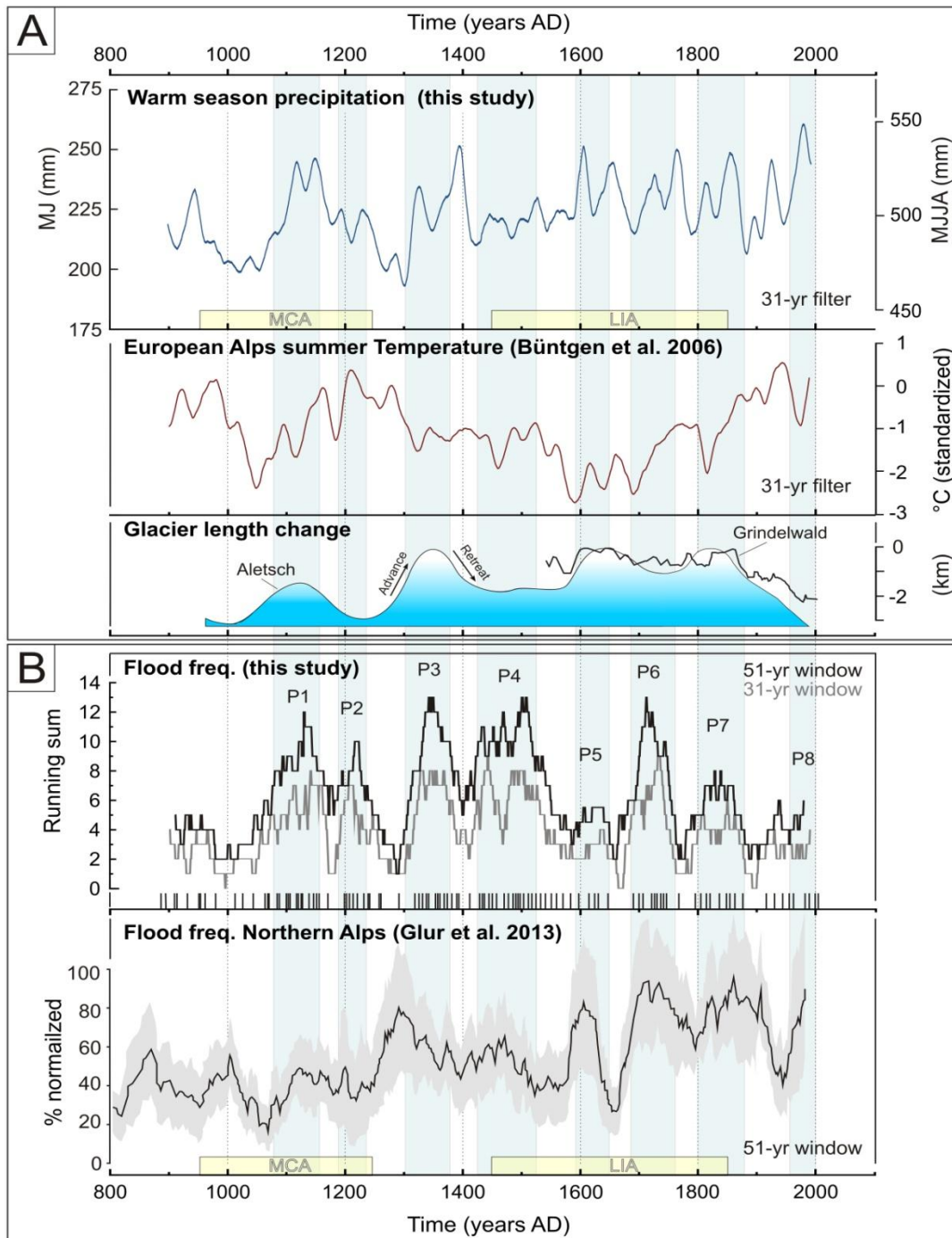


Fig. 5 Comparison of a) local warm season precipitation and temperature of the Greater Alpine Region, as well as fluctuations of local glaciers (Great Aletsch, Lower Grindelwald; Nussbaumer et al. 2011), and b) frequency of flood layers from Lake Oeschinen and flood frequency from the Northern Alps (compilation of ten lakes; Glur et al. 2013)

since AD 884. A positive relation between flood frequency and wet periods is plausible since saturated soils during long rainy seasons lead to enhanced surface runoff and erosion. Moreover, frequent cyclonic weather with moisture-bearing westerly and north-westerly flow to the Alps lead to cooler summers.

Our results support recent findings from an increasing number of studies in the Swiss, German, French and Austrian Alps showing that floods were consistently more frequent during cool periods (Smocker-Fackel and Naef 2010; Stewart et al. 2011; Giguet-Covex et al. 2012; Swierczynski et al. 2012; Wilhelm et al. 2012a; Glur et al. 2013; Wirth et al. 2013b). However, due to the lack of robust regional precipitation reconstructions, the relation between flood frequency and moist climate has remained speculative or information was inferred from low-resolution lake level changes. For the first time, our precipitation reconstruction allows for a direct comparison. Our results show that flood frequency increased during wetter conditions for most of the time during the last millennium. The period around AD 1200 (P2 in Fig. 5a) is enigmatic in the sense that phases with high flood frequency coincided with very warm summer temperatures and relatively dry conditions.

Although this flood peak is missing in the Central and eastern Swiss compilation (Glur et al. 2013), it is present in the French Alps (Wilhelm et al. 2012b, 2013) and seems to be a regional phenomenon. It is also suggested that different synoptic-scale weather patterns with rather convective rain might have triggered flood layers during this warm and relatively dry period in the Medieval Climate Anomaly (MCA). In contrast to all the other lakes studied in the Alps, Lac Blanc-Chamonix in the NW French Alps is the only lake that recorded more frequent floods during generally warm periods (MCA and 20th century; Wilhelm et al. 2013).

In contrast to Wilhelm et al. (2012a), we could not find a statistical relationship between flood layer thickness (in the sediments) and flood/discharge intensity during the instrumental period (Kander river data through the 20th century, Fig. 1). In addition, no significant correlation could be found between flood layer thickness and summer precipitation ($r = -0.05$) or temperature ($r = -0.08$) during the past millennium. However, according to Jenny et al. (2014), one might argue that, due to inhomogeneities of the flood deposit geometry in Alpine lakes, our results based on one sediment core might not be conclusive for this specific purpose.

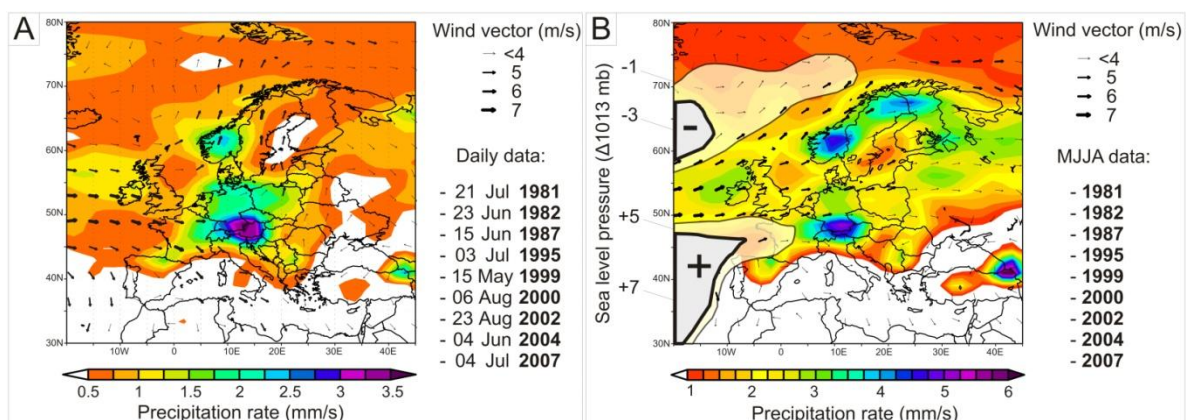


Fig. 6 Composite maps of synoptic scale weather systems (wind vector, sea level pressure and precipitation) for a) nine well-referenced floods days in the vicinity of Kandersteg between 1981 and 2007 and for b) the summer month MJA of the same years

To better understand what triggers flood events at Lake Oeschinen, we explored synoptic-scale weather-types using composites of wind vectors, sea level pressure fields and precipitation rates for nine well documented flood days between 1981 and 2007 (Fig. 6a). The composites for the respective seasons with the flood events are shown in Fig. 6b. The daily and seasonal composites show enhanced zonal flow and the maximum precipitation is found in the E/NE of the Alps, which is typical for cyclonic weather types, and weather type Vb in particular (Nissen et al. 2014). These situations seem to be typical for heavy precipitation and floods in the northern Alps (Sodemann and Zubler 2010) and have been identified as important triggers for flood deposits (Stewart et al. 2011; Glur et al. 2013).

6. Conclusions and implications for future climate change

We have investigated the varve thickness and flood layer properties in a 580-cm long sediment sequence from Lake Oeschinen, NW Swiss Alps, (i) to reconstruct annually-resolved warm season precipitation, and (ii) to assess the flood history back to AD 884. The underlying research questions are:

1. What is the relationship between climatological precipitation and temperature?
2. Is there a relationship between flood frequency, precipitation and temperature variability?

From our analysis we conclude:

- The varve record from Lake Oeschinen provides a robust well-calibrated quantitative record of warm season precipitation back to AD 884. The varve chronology is validated by independent ¹⁴C AMS dates and documentary sources of historical floods. The chronological uncertainty is between 5 and 10 years

back to ca. AD 1400, and between max. 20 to 30 years prior to AD 1250.

- The warm season precipitation record shows interannual to centennial scale variability with particularly humid periods in the 12th and 14th century, repeated humid peaks during the Little Ice Age and in the 20th century. The precipitation record is validated with independent precipitation reconstructions for the same area. Correlation maps from the different seasons of European precipitation records show the spatial and seasonal pattern expected from 20th century Reanalysis data.
- Over the entire past millennium, there is no positive correlation between precipitation and temperature (climatology), contrary to what would be expected from the Clausius-Clapeyron relation or from the 'dry gets dryer – wet gets wetter' scheme. In contrast, the relation between precipitation and temperature has persistently oscillated with a highly significant multidecadal periodicity (60 – 70 yrs) over the last millennium. Although the relation with the Atlantic Multidecadal Oscillation (AMO) remains not clear at the current state of research, changes in the statistics of weather patterns or within-weather-type variability might offer possible explanations. The within-type variability has been documented to operate at multidecadal scales and to influence precipitation and temperature significantly over Europe. Such multidecadal effects in the relation between precipitation and temperature might also operate and be important for precipitation scenarios in the Alpine area under future warming.
- There is an increasingly consistent picture from smaller and medium size catchments in mid- and high elevations

in the Alpine area that warm season floods were generally more frequent during cool and moist periods. However, the 13th century has also documented a period with high flood frequency during warm and moderately dry (average precipitation) conditions. Currently, it is not understood why the 13th century showed a different behaviour with regard to floods than the rest of the past millennium and how the relation floods-precipitation-temperature can be explained in a consistent framework. This would be the cornerstone to assess whether floods in the Alpine area would likely be more or less frequent in a future warmer climate.

Acknowledgements

This research was carried out within the Swiss National Science Foundation grant 200020-134945/1. We thank the Hirschi Family for granting access to Lake Oeschinen, Fabian Mauchle and Bruno Wilhelm especially for discussions on lake sedimentation processes and flood history. Particular thanks go to Daniela Fischer for essential support in the field and the lab. We would also like to thank Mathias Trachsel (University of Bergen) for statistical discussions, and Krystyna Saunders, Rixt de Jong and Iván Hernandez-Almeida (University of Bern) for comments on this manuscript.

References

- Amann, B., Mauchle, F., Grosjean, M., 2014. Quantitative high-resolution warm season rainfall recorded in varved sediments of Lake Oeschinen, northern Swiss Alps: calibration and validation AD 1901–2008. *Journal of Paleolimnology* 51, 375-391.
- Bayley, G.V., Hammersley, J.M., 1946. The “effective” number of independent observations in an autocorrelated time series. *Supplement to the Journal of the Royal Statistical Society* 8, 184-197.
- Brázdil, R., Štěpánková, P., Kyncl, T., Kyncl, J., 2002. Fir tree-ring reconstruction of March – July precipitation in southern Moravia (Czech Republic), 1376 – 1996. *Climate Research* 20, 223-239.
- Büntgen, U., Tegel, W., Nicolussi, K., McCormick, M., Frank, D., Trouet, V., Kaplan, J., Herzig, F., Heussner, U., Wanner, H., Luterbacher, J., Esper, J., 2011. 2500 years of European climate variability and human susceptibility. *Science* 331, 578-582.
- Büntgen, U., Franke, J., Frank, D., Wilson, R., González-Rouco, F., Esper, J., 2010. Assessing the spatial signature of European climate reconstructions. *Climate Research* 41, 125-130.
- Büntgen, U., Frank, D.C., Nievergelt, D., Esper, J., 2006. Summer Temperature Variations in the European Alps, A.D. 755–2004. *Journal of Climate* 19, 5606-5623.
- Bütschi, D., 2008. Gefürchtet, gebändigt und neu gedacht – die Kander. Die Geschichte eines Flusses und «seiner» Menschen (1800-1950). Diplomarbeit am Historischen Institut der Universität Bern, Bern.
- Casty, C., Wanner, H., Luterbacher, J., Esper, J., Böhm, R., 2005. Temperature and precipitation variability in the European Alps since 1500. *International Journal of Climatology* 25, 1855-1880.
- CH2011, 2011. Swiss Climate Change Scenarios CH2011, published by C2SM, MeteoSwiss, ETH, NCCR Climate, and OcCC, Zurich, Switzerland, 88 pp.
- Christensen, J.H., Krishna Kumar, K., Aldrian, E., An, S.-I., Cavalcanti, I.F.A., de Castro, M., Dong, W., Goswami, P., Hall, A., Kanyanga, J.K., Kitoh, A., Kossin, J., Lau, N.-C., Renwick, J., Stephenson, D.B., Xie, S.-P., Zhou, T., 2013. Climate Phenomena and their Relevance for Future Regional Climate Change. In: *Climate Change 2013: The Physical Science Basis. Contribution of Working Group I to the Fifth Assessment Report of the Intergovernmental Panel on Climate Change* [Stocker, T.F., Qin, D., Plattner, G.-K., Tignor, M., Allen, S.K., Boschung, J., Nauels, A., Xia, Y., Bex, V., Midgley, P.M. (eds.)]. Cambridge University Press, Cambridge, United Kingdom and New York, NY, USA, 91 pp.
- Cockburn, J.M.H., Lamoureux, S.F., 2007. Century-scale variability in late-summer rainfall events recorded over seven centuries in sub annually laminated lacustrine sediments, White Pass, British Columbia. *Quaternary Research* 67, 193-203.
- Corella, J.P., Benito, G., Rodríguez-Lloveras, X., Brauer, A., Valero-Garcés, B.L., 2014. Annually-resolved lake record of extreme hydro-meteorological events since AD 1347 in NE Iberian Peninsula. *Quaternary Science Reviews* 93, 77-90.
- Czymzik, M., Brauer, A., Dulski, P., Plessen, B., Naumann, R., von Grafenstein, U., Scheffler, R., 2013. Orbital and solar forcing of shifts in Mid-to Late Holocene flood intensity from varved sediments of pre-alpine Lake Ammersee (southern Germany). *Quaternary Science Reviews* 61, 96-110.
- Czymzik, M., Dulski, P., Plessen, B., von Grafenstein, U., Naumann, R., Brauer, A., 2010. A 450-year record of spring-summer flood layers in annually laminated sediments from Lake Ammersee (Southern Germany). *Water Resources Research* 46, W11528.
- Debret, M., Sebag, D., Desmet, M., Balsam, W., Copard, Y., Mourier, B., Susperrigui, A.-S., Arnaud, F., Bentaleb, I., Chapron, E., Lallier-Vergès, E., Winiarski, T., 2011. Spectrocolorimetric interpretation of sedimentary dynamics: The new “Q7/4 diagram”. *Earth-Science Reviews* 109, 1-19.

- Debret, M., Chapron, E., Desmet, M., Rolland-Revel, M., Magand, O., Trentesaux, A., Bout-Roumazeille, V., Nomade, J., Arnaud, F., 2010. North western Alps Holocene paleohydrology recorded by flooding activity in Lake Le Bourget, France. *Quaternary Science Reviews* 29, 2185-2200.
- Dobrovolný, P., Brázdil, R., Trnka, M., Kotyza, O., Valášek, H., 2014. Precipitation reconstruction for the Czech Lands, AD 1501–2010. *International Journal of Climatology*. doi: 10.1002/joc.3957.
- Giguet-Covex, C., Arnaud, F., Enters, D., Poulencard, J., Millet, L., Francus, P., David, F., Rey, P.-J., Wilhelm, B., Delannoy, J.-J., 2012. Frequency and intensity of high-altitude floods over the last 3.5 ka in northwestern French Alps (Lake Anterne). *Quaternary Research* 77, 12-22.
- Gilli, A., Anselmetti, F.S., Glur, L., Wirth, S.B., 2013. Lake sediments as archives of recurrence rates and intensities of past flood events. In: Schneuwly- Bollschweiler, M., Stoffel, M., Rudolf-Miklau, F. (Eds.), *Dating Torrential Processes on Fans and Cones – Methods and Their Application for Hazard and Risk Assessment*. *Advances in Global Change Research*, 47. Springer Netherlands, pp 225-242.
- Glur, L., Wirth, S.B., Büntgen, U., Gilli, A., Haug, G.H., Schär, C., Beer, J., Anselmetti, F.S., 2013. Frequent floods in the European Alps coincide with cooler periods of the past 2500 years. *Scientific Reports* 3, 2770-2774.
- Greve, P., Orlowsky, B., Mueller, B., Sheffield, J., Reichstein, M., Seneviratne, S.I., 2014. Global assessment of trends in wetting and drying over land. *Nature Geoscience*, Advance Online Publication (14 September 2014).
- Heiri, O., Lotter, A.F., Lemcke, G., 2001. Loss on ignition as a method for estimating organic and carbonate content in sediments: reproducibility and comparability of results. *Journal of Paleolimnology* 25, 101-110.
- Held, I.M., Soden, B.J., 2006. Robust Responses of the Hydrological Cycle to Global Warming. *Journal of Climate* 19, 5686-5699.
- Hodder, K.R., Gilbert, R., Desloges, J.R., 2007. Glaciolacustrine varved sediment as an alpine hydroclimatic proxy. *Journal of Paleolimnology* 38, 365-394.
- Holzhauser, H., Magny, M., Zumbühl, H.J., 2005. Glacier and lake-level variations in west-central Europe over the last 3500 years. *The Holocene* 15, 789-801.
- Huntington, T.G., 2006. Evidence for intensification of the global water cycle: Review and synthesis. *Journal of Hydrology* 319, 83-95.
- IPCC, 2013: Summary for Policymakers. In: *Climate Change 2013: The Physical Science Basis*. Contribution of Working Group I to the Fifth Assessment Report of the Intergovernmental Panel on Climate Change [Stocker, T.F., Qin, D., Plattner, G.-K., Tignor, M., Allen, S.K., Boschung, J., Nauels, A., Xia, Y., Bex, V., Midgley, P.M. (eds.)]. Cambridge University Press, Cambridge, United Kingdom and New York, NY, USA, 29 pp.
- IPCC, 2012. *Managing the Risks of Extreme Events and Disasters to Advance Climate Change Adaptation*. A Special Report of Working Groups I and II of the Intergovernmental Panel on Climate Change [Field, C.B., Barros, V., Stocker, T.F., Qin, D., Dokken, D.J., Ebi, K.L., Mastrandrea, M.D., Mach, K.J., Plattner, G.-K., Allen, S.K., Tignor, M., Midgley, P.M. (eds.)]. Cambridge University Press, Cambridge, UK, and New York, NY, USA, 582 pp.
- Jacobeit, J., Wanner, H., Luterbacher, J., Beck, C., Phillip, A., Sturm, K., 2003. Atmospheric circulation variability in the North-Atlantic-European area since the mid-seventeenth century. *Climate Dynamics* 20, 341-352.
- Jenny, J.-P., Wilhelm, B., Arnaud, F., Sabatier, P., Giguet-Covex, C., Mélo, A., Fanget, B., Malet, E., Ployon, E., Perga, M.E., 2014. A 4D sedimentological approach to reconstructing the flood frequency and intensity of the Rhône River (Lake Bourget, NW European Alps). *Journal of Paleolimnology* 51, 469-483.
- Jones, P., Harris, I., 2013. CRU TS3.21: Climatic Research Unit (CRU) Time-Series (TS) Version 3.21 of High Resolution Gridded Data of Month-by-month Variation in Climate

- (Jan.1901 - Dec.2012), [Internet]. University of East Anglia Climatic Research Unit (CRU). NCAS British Atmospheric Data Centre.
- Jönsson, K., Nilsson, C., 2009. Scots Pine (*pinussylvestris* L.) on Shingle Fields: A Dendrochronologic Reconstruction of Early Summer Precipitation in Mideast Sweden. *Journal of Climate* 22, 4710-4722.
- Kaufman, C.A., Lamoureux, S.F., Kaufman, D.S., 2011. Long-term river discharge and multidecadal climate variability inferred from varved sediments, southwest Alaska. *Quaternary Research* 76, 1-9.
- Knudsen, M.F., Seidenkrantz, M-S., Jacobsen, B.H., Kuijpers, A. 2011. Tracking the Atlantic Multidecadal Oscillation through the last 8,000 years. *Nature Communications* 2, 178.
- Köplin, N., Schädler, B., Viviroli, D., Weingartner, R., 2014. Seasonality and magnitude of floods in Switzerland under future climate change. *Hydrological Processes* 28, 2567-2578.
- Küttel, M., Luterbacher, J., Wanner, H., 2011. Multidecadal changes in winter circulation-climate relationship in Europe: frequency variations, within-type modifications, and long-term trends. *Climate Dynamics* 36, 957-972.
- Lamoureux, S.F., 2001. Varve chronology techniques. In: Last, W.M., Smol, J.P. (eds). *Tracking environmental change using lake sediments: basin analysis, coring, and chronological techniques*. Kluwer, Dordrecht, pp 247–260.
- Linderholm, H.W., Chen, D., 2005. Central Scandinavian winter precipitation variability during the past five centuries reconstructed from *Pinussylvestris* tree rings. *Boreas* 34, 43-52.
- Luterbacher, J., Rickli, R., Xoplaki, E., Tinguely, C., Beck, C., Pfister, C., Wanner, H., 2001. The Late Maunder Minimum (1675-1715) – A key period for studying decadal scale climatic change in Europe. *Climatic Change* 49, 441-462.
- Masson-Delmotte, V., Schulz, M., Abe-Ouchi, A., Beer, J., Ganopolski, A., González Rouco, J.F., Jansen, E., Lambeck, K., Luterbacher, J., Naish, T., Osborn, T., Otto-Bliesner, B., Quinn, T., Ramesh, R., Rojas, M., Shao, X., Timmermann, A., 2013. Information from Paleoclimate Archives. In: *Climate Change 2013: The Physical Science Basis. Contribution of Working Group I to the Fifth Assessment Report of the Intergovernmental Panel on Climate Change* [Stocker, T.F., Qin, D., Plattner, G.-K., Tignor, M., Allen, S.K., Boschung, J., Nauels, A., Xia, Y., Bex, V., Midgley, P.M. (eds.)]. Cambridge University Press, Cambridge, United Kingdom and New York, NY, USA.
- Meyer, M.C., Faber, R., Spotl, C., 2006. The wingeol lamination tool: new software for rapid, semi-automated analysis of laminated climate archives. *Holocene* 16, 753-761.
- Niklaus, M., 1967. Geomorphologische und limnologische Untersuchungen am Öschinensee. PhD thesis. Kümmerly und Frey, Bern.
- Nissen, K.M, Ulbrich, U., Leckebusch, G.C., 2014. Vb cyclones and associated rainfall extremes over Central Europe under present day and climate change conditions. *Meteorologische Zeitschrift* 22, 649-660.
- Nussbaumer, S.U., Steinhilber, F., Trachsel, M., Breitenmoser, P., Beer, J., Blass, A., Grosjean, M., Hafner, A., Holzhauser, H., Wanner, H., Zumbühl, H.J., 2011. Alpine climate during the Holocene: a comparison between records of glaciers, lake sediments and solar activity. *Journal of Quaternary Science* 26, 703-713.
- O’Gorman, P.A., Muller, C.J., 2010. How closely do changes in surface and column water vapor follow Clausius-Clapeyron scaling in climate-change simulations? *Environmental Research Letters* 5, 025207.
- Ojala, A.E.K., Francus, P., Zolitschka, B., Besonen, M., Lamoureux, S.F., 2012. Characteristics of sedimentary varve chronologies – a review. *Quaternary Science Reviews* 43, 45-60.
- PAGES 2 k Consortium, 2013. Continental-scale temperature variability during the last two millennia. *Nature Geoscience* 6, 339-346.
- Pfister, C., 1999. *Wetternachhersage: 500 Jahre Klimavariationen und Naturkatastrophen (1496-1995)*. Verlag Paul Haupt, Bern.

- Reimer, P., Bard, E., Bayliss, A., Beck, J., Blackwell, P., Bronk Ramsey, C., Buck, C., Cheng, H., Edwards, R., Friedrich, M., Grootes, P., Guilderson, T., Hafliðason, H., Hajdas, I., Hatté, C., Heaton, T., Hoffmann, D., Hogg, A., Hughen, K., Kaiser, K., Kromer, B., Manning, S., Niu, M., Reimer, R., Richards, D., Scott, E., Southon, J., Staff, R., Turney, C., van der Plicht, J., 2013. Intcal13 and Marine13 radiocarbon age calibration curves 0–50,000 yearscal BP. *Radiocarbon* 55, 1869-1887.
- Romero-Viana, L., Julià, R., Schimmel, M., Camacho, A., Vicente, E., Miracle, M.R., 2011. Reconstruction of annual winter rainfall since A.D.1579 in central-eastern Spain based on calcite laminated sediment from Lake La Cruz. *Climatic Change*, 343-361.
- Schmocker-Fackel, P., Naef, F., 2010. More frequent flooding? Changes in flood frequency in Switzerland since 1850. *Journal of Hydrology* 381, 1-8.
- Smith, K., 2013. Environmental hazards: Assessing risk and reducing disaster. Routledge, Taylor and Francis Group (eds.). New York, NY, USA, 478 pp.
- Sodemann, H., Zubler, E., 2010. Seasonal and inter-annual variability of the moisture sources for Alpine precipitation during 1995–2002. *International Journal of Climatology* 30, 947-961.
- Steiner, D., Pauling, A., Nussbaumer, S.U., Nesje, A., Luterbacher, J., Wanner, H., Zumbühl, H.J., 2008. Sensitivity of European glaciers to precipitation and temperature – two case studies. *Climatic Change* 90/4, 413-441.
- Stewart, M.M., Grosjean, M., Kuglitsch, F.G., Nussbaumer, S.U., von Gunten, L., 2011. Reconstructions of late Holocene paleofloods and glacier length changes in the Upper Engadine, Switzerland (ca. 1450 BC–AD 420). *Palaeogeography, Palaeoclimatology, Palaeoecology* 311, 215-223.
- Suchy, V., Frey, M., Wolf, M., 1997. Vitrinite reflectance and shear-induced graphitization in orogenic belts: a case study from the Kandersteg area, Helvetic Alps, Switzerland. *International Journal of Coal Geology* 34, 1-20.
- Swierczynski, T., Lauterbach, S., Dulski, P., Delgado, J., Merz, B., Brauer, A., 2013. Mid- to late Holocene flood frequency changes in the northeastern Alps as recorded in varved sediments of Lake Mondsee (Upper Austria). *Quaternary Science Reviews* 80, 78-90.
- Swierczynski, T., Brauer, A., Lauterbach, S., Martín-Puertas, C., Dulski, P., von Grafenstein, U., Rohr, C., 2012. A 1600 yr seasonally resolved record of decadal-scale flood variability from the Austrian Pre-Alps. *Geology* 40, 1047-1050.
- Szidat, S., Salazar, G.A., Vogel, E., Battaglia, M., Wacker, L., Sinal, H.-A., Türlér, A., 2014. ¹⁴C analysis and sample preparation at the new Bern Laboratory for the Analysis of Radiocarbon with AMS (LARA). *Radiocarbon* 56, 561-566.
- Trachsel, M., Eggenberger, U., Grosjean, M., Blass, A., Sturm, M., 2008. Mineralogy-based quantitative precipitation and temperature reconstructions from annually laminated lake sediments (Swiss Alps) since AD 1580. *Geophysical Research Letters* 35, L13707.
- Trenberth, K.E., Shea, D.J., 2005. Relationships between precipitation and surface temperature. *Geophysical Research Letters* 32, L14703.
- Wanner, H., Rickli, R., Salvisberg, E., Schmutz, C., Schüepp, M., 1997. Global climate change and variability and its influence on Alpine climate – concepts and observations. *Theoretical and Applied Climatology* 58, 221-243.
- Wilhelm, B., Arnaud, F., Sabatier, P., Magand, O., Chapron, E., Courp, T., Tachikawa, K., Fanget, B., Malet, E., Pignol, C., Bard, E., Delannoy, J.J., 2013. Palaeoflood activity and climate change over the last 1400 years recorded by lake sediments in the north-west European Alps. *Journal of Quaternary Science* 28, 189-199.

Wilhelm, B., Arnaud, F., Sabatier, P., Crouzet, C., Brisset, E., Chaumillon, E., Disnar, J.-R., Guiter, F., Malet, E., Reyss, J.-L., Tachikawa, K., Bard, E., Delannoy, J.-J., 2012a. 1400 years of extreme precipitation patterns over the Mediterranean French Alps and possible forcing mechanisms. *Quaternary Research* 78, 1-12.

Wilhelm, B., Arnaud, F., Enters, D., Allignol, F., Legaz, A., Magand, O., Revillon, S., Giguët-Covex, C., Malet, E., 2012b. Does global warming favour the occurrence of extreme floods in European Alps? First evidences from a NW Alps proglacial lake sediment record. *Climatic Change* 113, 563-581.

Wilson, R., Miles, D., Loader, N.J., Melvin, T., Cunningham, L., Cooper, R., Briffa, K., 2013. A millennial long March–July precipitation reconstruction for southern-central England. *Climate Dynamics* 40, 997-1017.

Wilson, R.J.S., Luckman, B.H., Esper, J., 2005. A 500 year dendroclimatic reconstruction of spring-summer precipitation from the lower Bavarian Forest region, Germany. *International Journal of Climatology* 25, 611-630.

Wirth, S.B., Gilli, A., Simonneau, A., Ariztegui, D., Vannièrè, B., Glur, L., Chapron, E., Magny, M., Anselmetti, F.S., 2013a. A 2000-year long seasonal record of floods in the southern European Alps. *Geophysical Research Letters* 40, 4025-4029.

Wirth, S.B., Glur, L., Gilli, A., Anselmetti, F.S., 2013b. Holocene flood frequency across the Central Alps e solar forcing and evidence for variations in North Atlantic atmospheric circulation. *Quaternary Science Reviews* 80, 112-128.

Zolitschka, B., 2007. Varved lake sediments. In: Elias SA (ed) *Encyclopedia of quaternary science*. Elsevier, Amsterdam, pp 3105-3114.

Supplementary material S1

The fresh sediment cores were scanned for Visible Reflectance Spectroscopy (VIS-RS) using a portable Gretag-Spectrolino (GretagMcBeth, Switzerland). This instrument provides reflectance spectra in the visible range (380 – 730 nm) with a spatial resolution of 2 mm (Trachsel et al. 2010). We calibrated the VIS-RS reflectance properties of 44 individual samples with known proportions of calcite/siliciclastics as derived from LOI. We used a simple linear model ($r^2 = 0.932$) between the mean value of each first-derivative spectrum (overall spectral slope) and conventional LOI₉₅₀ measurements and the residuals, respectively (Fig. S1). The first-derivative spectrum enables eliminating the influence of water content in the sediments (Debret et al. 2011). The principle is the following: the higher the calcite_(bright)/siliciclastics_(dark) ratio is, the brighter is the sample and the higher is the mean reflectance spectrum and its 1st derivative. This allows us to rapidly infer the sediment composition (mainly calcite/siliciclastics) of the entire core section at a very high (2 mm) resolution.

References (supplementary material S1)

Debret, M., Sebag, D., Desmet, M., Balsam, W., Copard, Y., Mourier, B., Susperrigui, A.-S., Arnaud, F., Bentaleb, I., Chapron, E., Lallier-Vergès, E., Winiarski, T., 2011. Spectrocolorimetric interpretation of sedimentary dynamics: The new “Q7/4 diagram”. *Earth-Science Reviews* 109, 1-19.

Trachsel, M., Grosjean, M., Schnyder, D., Kamenik, C., Rein, B., 2010. Scanning reflectance spectroscopy (380-730 nm): a novel method for quantitative high-resolution climate reconstructions from minerogenic lake sediments. *Journal of Paleolimnology* 44, 979-994.

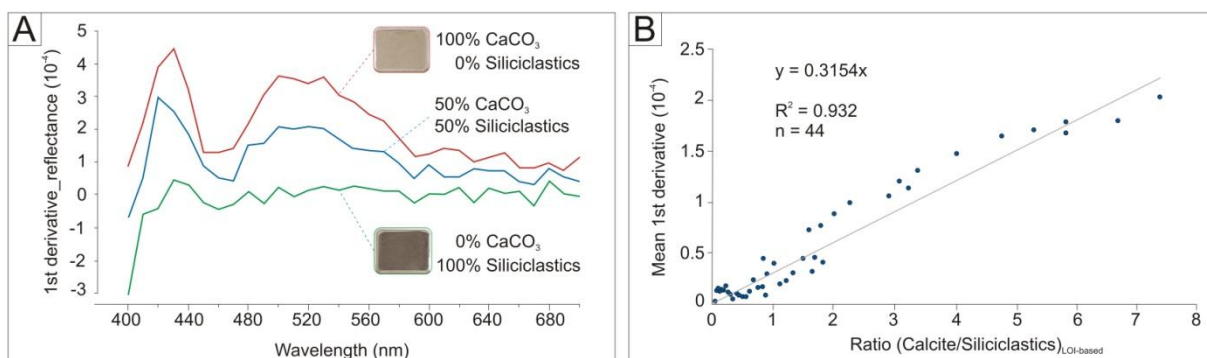


Fig. S1 Visible Reflectance Spectroscopy (VIS-RS) properties with a) the first derivative spectra characteristic of three samples with different calcite/siliciclastics ratios [typical end-members], and b) the proxy-proxy calibration model between the mean first derivative and LOI-based calcite/siliciclastics ratios

Supplementary material S2

Our data show that the relation between precipitation and temperature (PP-TT) in the NW Alps is not stationary over the past millennium (Fig. S2a). On multidecadal time scales, phases with strong positive correlations (up to $r = 0.5$) alternate with phases of strong negative correlations (up to $r = -0.6$). A Continuous Wavelet Transform (CWT) analysis was performed on this 31-year running correlation time series to detect possible periodicities along the record (Fig. S2b). Highest squared correlation strength (power) can be detected for periods >60 years, while noise remains principally for lower periods. Then, we tested in a REDFIT spectral analysis (Schulz and Mudelsee 2002) whether non-AR1

components can be identified in the time series (Fig. S2c).

Results show that spectral peaks with periods of [58 – 73] years exceed the false-alarm levels (χ^2 95% and 99%). This suggests that the 31-yr running correlations between warm-season precipitation and temperature oscillated with a highly significant periodicity between 58 – 73 years throughout the last millennium.

References (supplementary material S2)

Schulz, M., Mudelsee, M., 2002. REDFIT: estimating red-noise spectra directly from unevenly spaced paleoclimatic time series. *Computers and Geosciences* 28, 421-426.

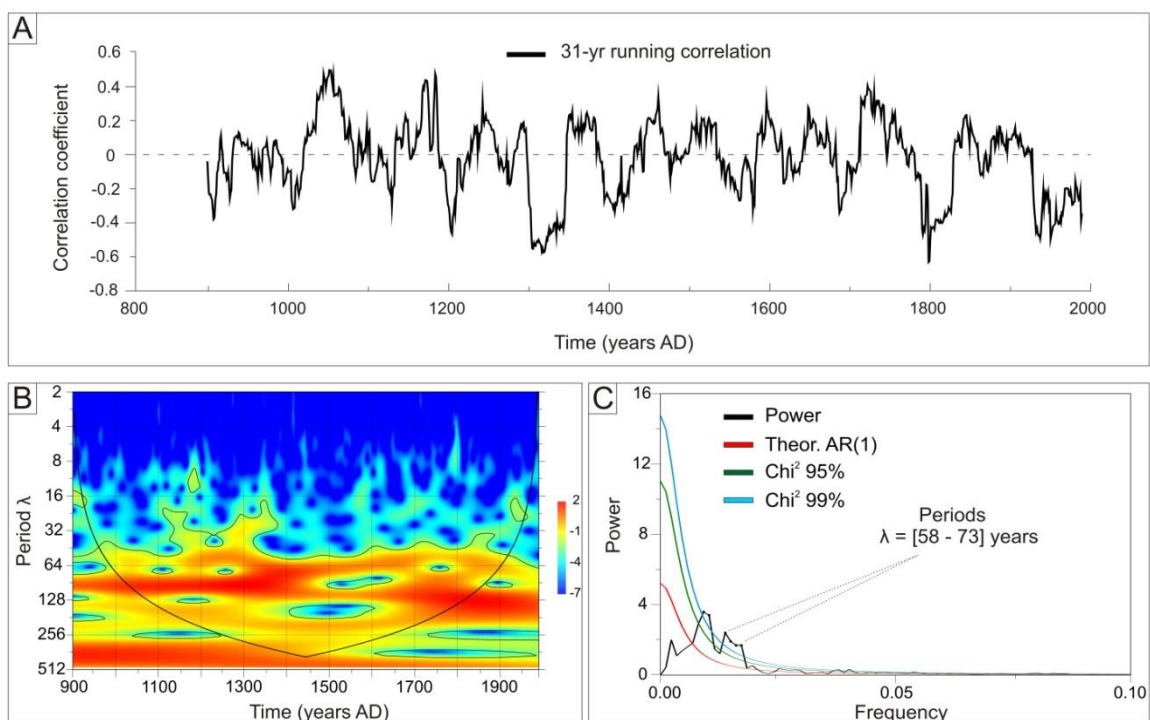


Fig. S2 Properties of the relation between warm season precipitation (this study) and summer European Alps temperature (Büntgen et al. 2006) with a) the 31-year running correlations plotted with time, b) the continuous wavelet transform analysis of this running correlation (Morlet wavelet) with contour lines representing the 95 % significance level, and c) the corresponding power spectrum of the time series (REFFIT; Welch method) (black line), theoretical red-noise spectrum (red line) and false-alarm levels at 95% and 99% (green and blue lines respectively). Spectral peaks at periods of [58 - 73] years are inconsistent with AR(1) origin.

Chapter 5



5. Lake Żabińskie: biochemical varves

5.1. Site selection and description

In recent comprehensive surveys in northeast Poland and the Great Masurian Lake District, Tylmann et al. (2006; 2013a) uncovered the presence of several postglacial lakes that contain undisturbed continuous sequences of annually laminated sediments with biochemical varves. These varves have been investigated for highly precise and accurate chronologies (Kinder et al. 2013; Tylmann et al. 2013b).

In September 2011, three of these lakes with biochemical varves were investigated for this project. Eleven sediment sections were retrieved from Lake Żabińskie, Lake Głęboka Kuta and Lake Jaczno (Fig. 5.1). Criteria for the site selection were: (i) a sequence continuously laminated to develop a precise varve chorology; (ii) no major disturbances in the core structure; (iii) reasonable sedimentation rates enabling varve-by-varve sub-sampling (preferably $\geq 2 \text{ mm.yr}^{-1}$); and (iv) a time range that encompasses 1000 years. Lake Żabińskie fulfilled all criteria and was selected for a high-quality, millennial-long, quantitative climate (temperature) reconstruction from north-eastern Poland.

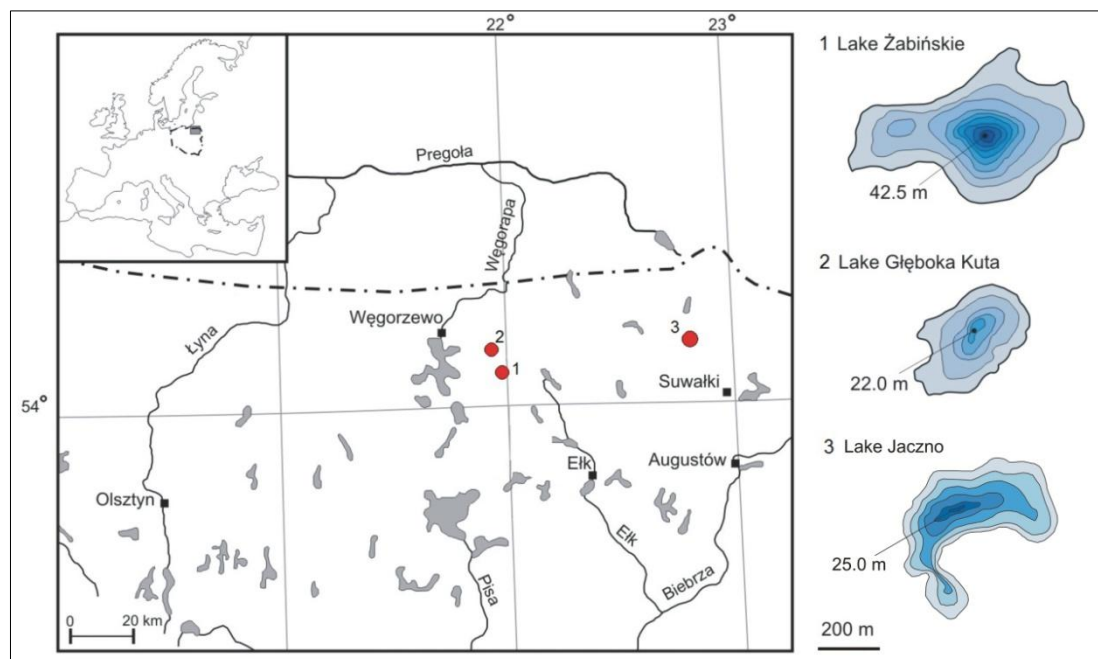


Fig. 5.1 Location and bathymetric maps of the three lakes investigated for a millennial-long paleoclimate reconstruction from northeast Poland. Lake Żabińskie (1) is the lake selected for this purpose

5. Lake Żabińskie: biochemical varves

Lake Żabińskie (54°07'N, 21°59'E) is a low elevation (120 m a.s.l.) glacial lake located in the Masurian Lake District that has formed after the deglaciation of the Fennoscandian Ice Field around 15 kyr BP (Kaufmann et al. 2000; Szumański 2000). The catchment area of Lake Żabińskie is rather small (2.3 km²), but it is incorporated in a much larger catchment (24 km²) that also comprises the catchments of Lake Łękuk (13.2 km²) and Lake Purwin (8.5 km²) (Fig. 5.2a).

Bedrock of the entire area consists mainly of Quaternary glacial till interrupted by several widespread moraines (Fig. 5.2b). The river valleys are composed of fluvial sediments, while lacustrine deposits occupy the westernmost part of the catchment (Bonk et al. submitted).

Lake Żabińskie is exorheic, receiving water mainly from Lake Purwin, and discharges westward (Fig. 5.2c). A mixed forest composes the major part of the northern catchment, while peatlands have developed in waterlogged areas. Arable lands and meadows evidence human occupation in the lake surroundings. The village of Żabinka was established < 1 km southeast of Lake Żabińskie in AD 1713 and has about 100 inhabitants living in today. Buildings were constructed directly at the northern lake shore between AD 1910 and AD 1920. A holiday resort was also established in the 1950s and enlarged in the 1970s and mid-1980s. It should also be noted that the use of artificial fertilizers for agriculture increased considerably in this region after AD 1965-1975.

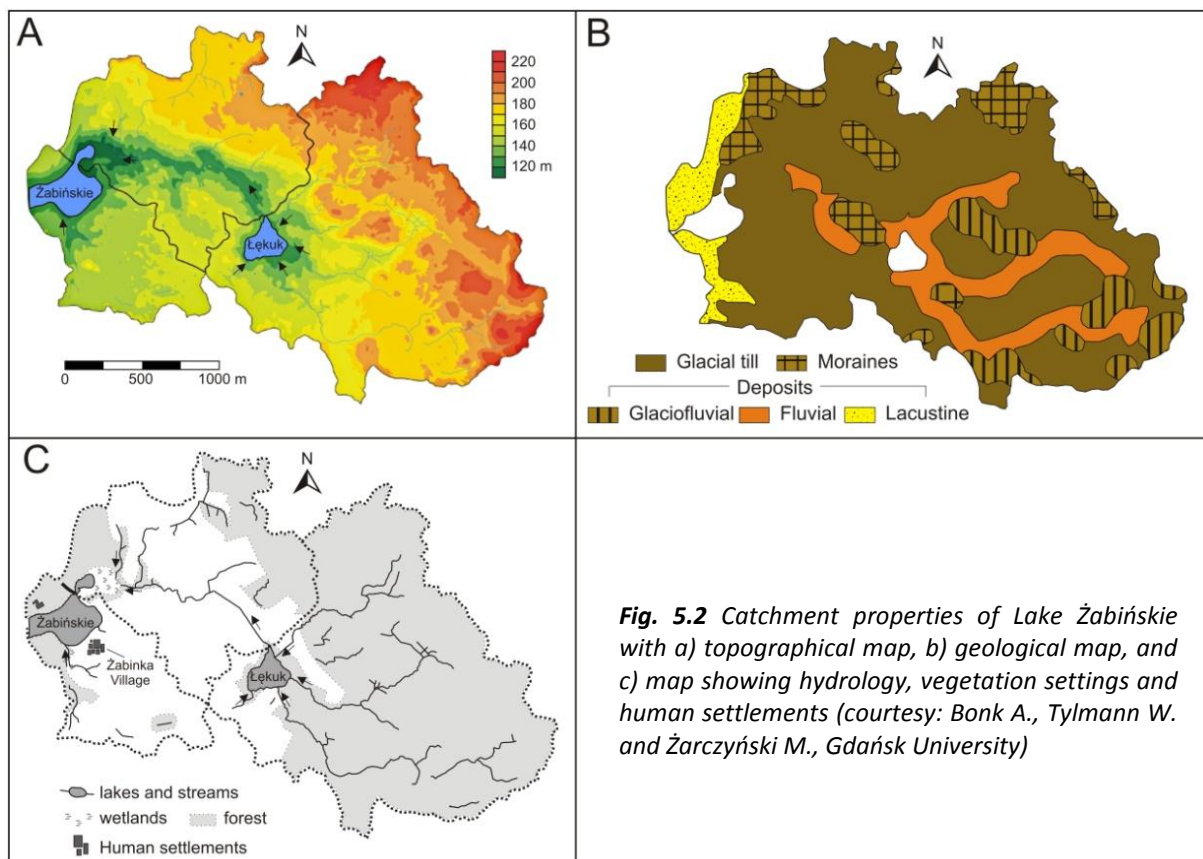


Fig. 5.2 Catchment properties of Lake Żabińskie with a) topographical map, b) geological map, and c) map showing hydrology, vegetation settings and human settlements (courtesy: Bonk A., Tylmann W. and Żarczyński M., Gdańsk University)

5.2. Climate

Climate of northeast Poland

Poland lies in Central Europe with influences from a continental climate from Eastern Europe and maritime climate from Western Europe. Its climate belongs to the humid continental warm summer type (Dwb) according to the Köppen classification.

Luterbacher et al. (2010) showed that the climate in Poland represents a good estimate of climate in Europe as a whole. They demonstrated that atmospheric circulation is the main factor influencing climate variations in Poland. Moreover, as the country is relatively flat (1% above 1000 m a.s.l.), local fluctuations in temperature are relatively small.

However, this study was focused on the winter season. Thus, maps for annual means and March-to-May temperature (target of the study on Lake Żabińskie) were created to explore whether this feature from winter could also be observed for other time windows. Figs. 5.3a, b show that global and European annual mean temperatures (CRU TS 3.21 data set) are relatively homogenous and remain in the same range for a large part of Central, Western and Eastern Europe. A similar pattern is also reflected for mean March-to-May temperature (Fig. 5.3c).

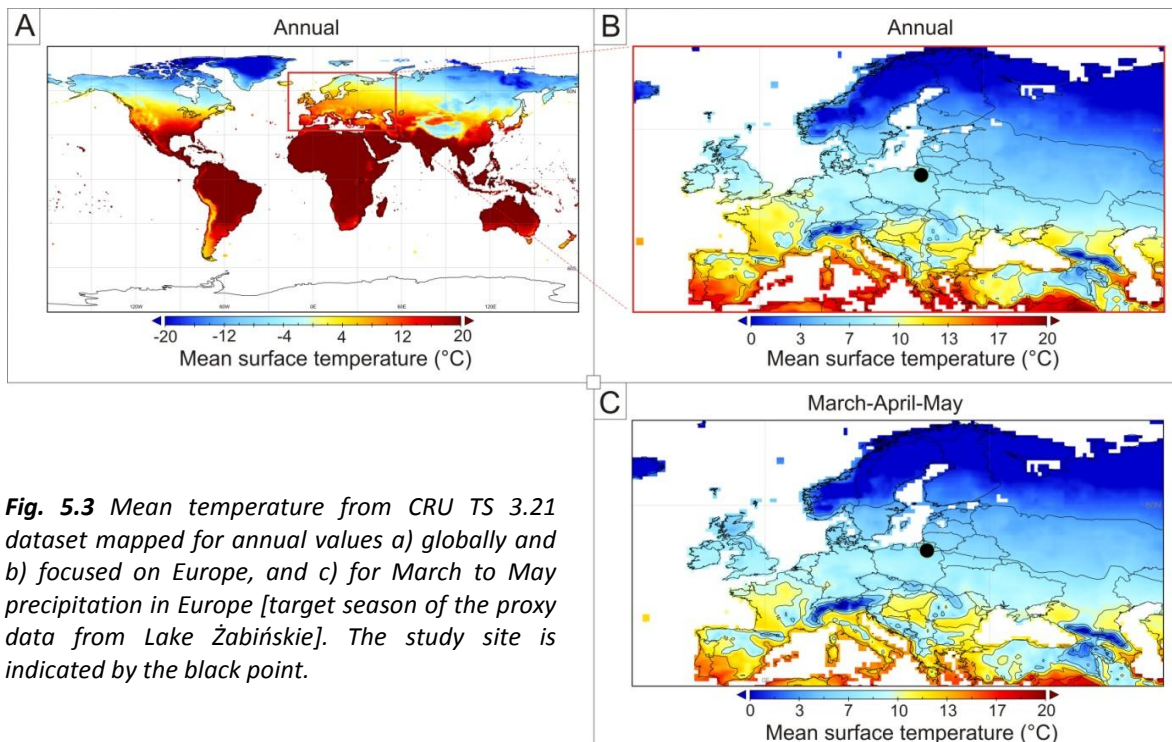


Fig. 5.3 Mean temperature from CRU TS 3.21 dataset mapped for annual values a) globally and b) focused on Europe, and c) for March to May precipitation in Europe [target season of the proxy data from Lake Żabińskie]. The study site is indicated by the black point.

Correlation field analysis for our study site and Europe (CRU TS 3.21 data) shows that spring temperature from our study site is highly representative (correlation > 0.7) for a large part of Europe (Fig. 5.4). This covers all Scandinavian countries and spreads westward to northeast France, and eastward to westernmost parts of Russia.

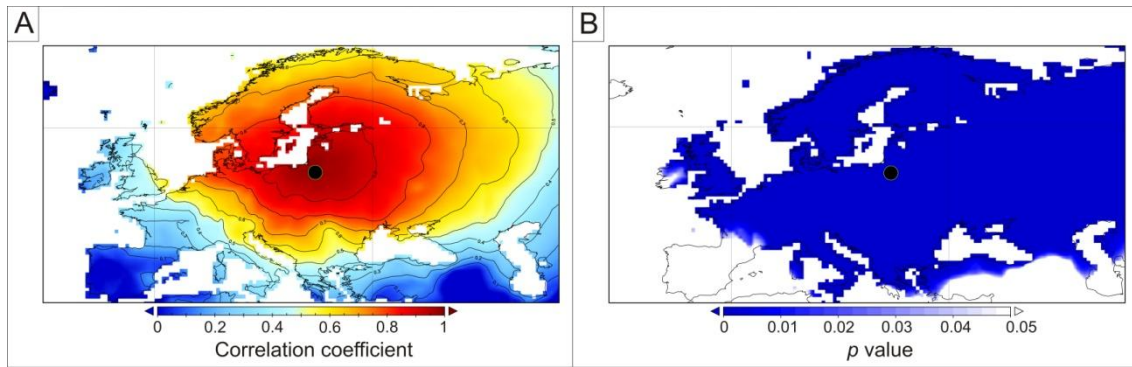


Fig. 5.4 a) Correlation map between March-to-May temperature for our study site (Lake Żabińskie) and Europe and b) corresponding p values where the blue zone delimitates highly significant correlations. The study site is indicated by the black point.

Besides the high spatial representativeness of Polish climate, the history of climate in Poland is rich with long homogenous temperature series. The longest data series extend back to AD 1779 and AD 1792 from Warsaw and Cracow, respectively (Przybylak et al. 2005). Furthermore, Poland has a large amount of documentary data, which have been kept since the 15th century (Przybylak et al. 2010).

Despite this potential, to our knowledge, no quantitative high-resolution and well-calibrated lacustrine sediment record exists from Poland. The majority of research on sediments is restricted to low-resolution paleoenvironmental studies, generally with a focus on human impact rather than climate changes. This is the reason why none of the comprehensive European or hemispherical climate reconstructions that cover the last 1000 years included Polish data (e.g. MILLENNIUM 2011; Mann et al. 2008; PAGES 2k Consortium 2013). Thus, data from Poland are of first-order significance for paleoclimate studies.

Instrumental data for Lake Żabińskie

Climate series were constructed from ten nearby meteorological stations and downscaled to the lake site. Calculations followed Alexandersson and Moberg (1997):

$$T_s = \frac{\sum_{i=1}^n T_i e^{-0.001L_i}}{\sum_i e^{-0.001L_i}} \quad P_s = \frac{\sum_{i=1}^n P_i e^{-0.005L_i}}{\sum_i e^{-0.005L_i}}$$

Whereby, T_s (P_s) is the air temperature (precipitation) at the site location, T_i (P_i) is the air temperature (precipitation) recorded at the i -station, and L_i is the distance (km) separating the i -station and the study site (Larocque-Tobler et al. submitted).

Meteorological data were tested for homogeneity (Standard Normal Homogeneity Test) and spatial geo-interpolation was performed using the Ordinary Kriging method for temperature (AD 1885-2010) and the Thiessen polygon method for precipitation (AD 1891-2010; Larocque-Tobler et al. submitted).

5.3. Sedimentation processes and varve formation

Water column analysis

Limnological monitoring of the water column of Lake Żabińskie was operated on a monthly basis during a two-year period from October 2011 to December 2013 (Bonk et al. submitted). Water profiles of temperature, oxygen and chlorophyll-*a* (Chl-*a*) are shown in Fig. 5.5. Results show that Lake Żabińskie presents features of a dimictic lake (spring and autumn overturn is usually complete); however, this seems to be dependent on the timing of the ice-cover development and its melting (Bonk et al. submitted). For instance, the long and severe winter in 2012/2013 (Dec. 2012-Apr. 2013) led to incomplete fall 2012 mixing, while summer 2013 stratification developed almost immediately after ice break-up and prevented spring 2013 mixing. Results also show the lake is stratified from May to late October generally, with anoxic conditions in the hypolimnion (10 m to the bottom) that develop throughout the entire stratification period.

Chl-*a* concentrations show maxima in the epilimnion in May, following the ice break-up (158 $\mu\text{g}\cdot\text{g}^{-1}$ in 2012, 84.2 $\mu\text{g}\cdot\text{g}^{-1}$ in 2013; Fig. 5.5). Interestingly, the high Chl-*a* concentrations are restricted to spring and nearly disappear in June for the rest of the growing season. According to Kufel (2001), this is a typical feature of Great Masurian Lakes with a seasonal succession from green-algae (rich in Chl-*a*) and a diatom-rich environment in spring, towards blooms of blue-green algae (poorer in Chl-*a*) in summer.

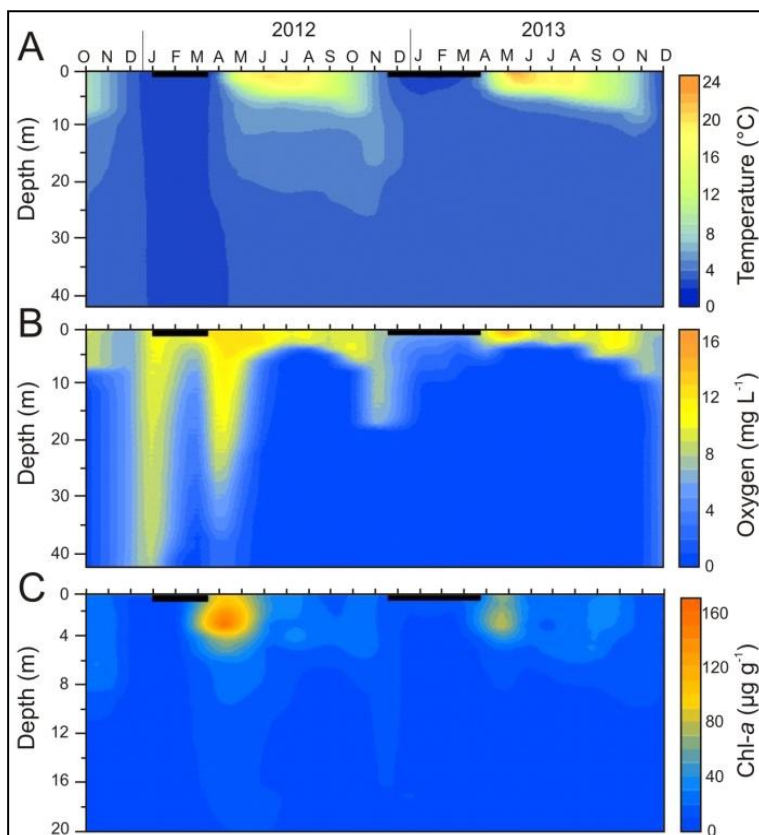


Fig. 5.5
*Limnological measurements of Lake Żabińskie showing temperature, oxygen concentration and Chl-*a* concentration of the water column between October 2011 and December 2013 (courtesy: Bonk A., Tylmann W., Gdańsk University)*

Sediment trap analysis

Fig. 5.6 shows the monthly data obtained from sediment trapped near the lake bottom (data from Bonk et al. submitted). The sediment composition presents the following seasonal characteristics: in spring, a bloom of green algae develops and diatoms grow. Immediately after, the mass accumulation rate (MAR, purple bars Fig. 5.6) increases rapidly mainly through the deposition of calcite (CaCO_3 , red bars Fig. 5.6) and the sedimentation of diatoms in May and June (BSi, blue bars Fig. 5.6). This suggests that development of phytoplankton and photosynthetic activity, together with rapidly increasing temperatures in the epilimnion, affect the carbonate saturation point by decreasing CO_2 (aq), increasing pH, and favouring CaCO_3 precipitation (Bonk et al. submitted). In summer, the chlorophyte community is replaced by blue-green algae, which are more shade tolerant (Kufel 2001; Downing et al. 2001; Scheffer and Van Ness 2007). Minimum values in total sediment flux are recorded during this time. In winter, ice-cover develops and strong anoxic conditions take place, leading to high burial rates of total sulphur (TS, yellow bars Fig. 5.6) and higher deposition of organic-rich detritus (two thirds of winter accumulation rates).

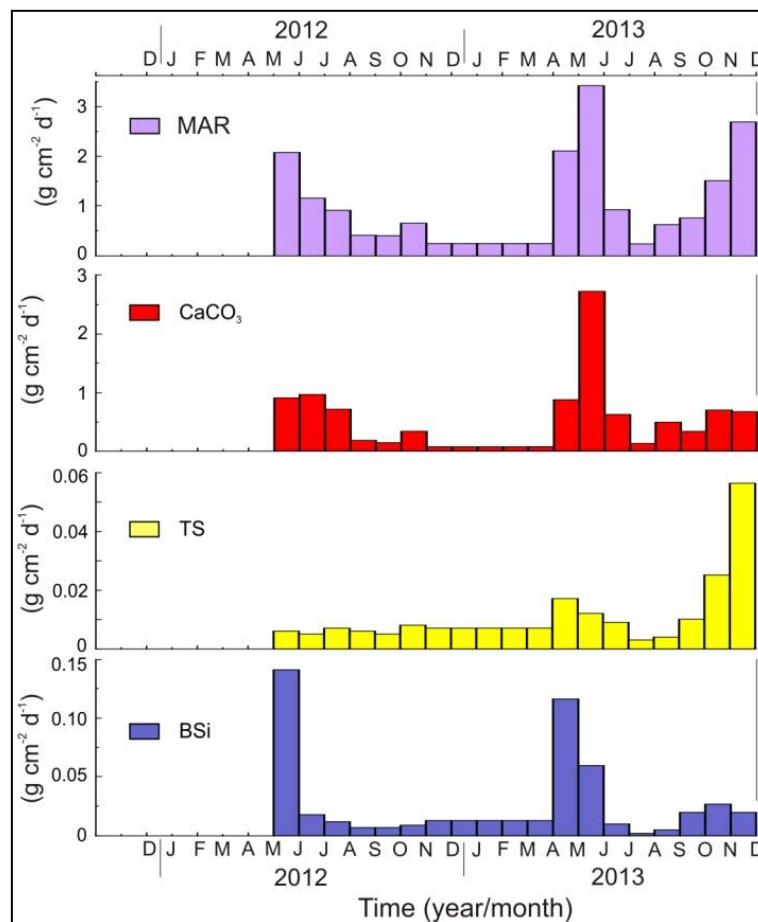


Fig. 5.6 Monthly mass fluxes (in $\text{g cm}^{-2} \text{d}^{-1}$) from sediment traps for mass accumulation rate (MAR), calcite (CaCO_3), total sulphur (TS) and biogenic silica (BSi) for the period 2012-2013 (data from Bonk et al. submitted)

Sediment analysis

The seasonal succession interpreted in the previous section is also reflected in the microscopic image and μ -XRF data of a single varve (Fig. 5.7; data from Bonk et al. submitted). The within-year succession shows: (i) a peak of silica in spring as an indicator of diatom productivity (blue curve Fig. 5.7); (ii) a high content of calcium as an indicator of CaCO_3 precipitation due to a change in the carbonate saturation point through photosynthetic activity and high temperature in summer (red curve Fig. 5.7); (iii) a peak in TS indicating enhanced anoxic conditions at the end of summer-autumn (yellow curve Fig. 5.7), and (iv) a peak in potassium (K), an indicator of clay minerals that are deposited by settling through the water column under ice-cover conditions (green curve Fig. 5.7).

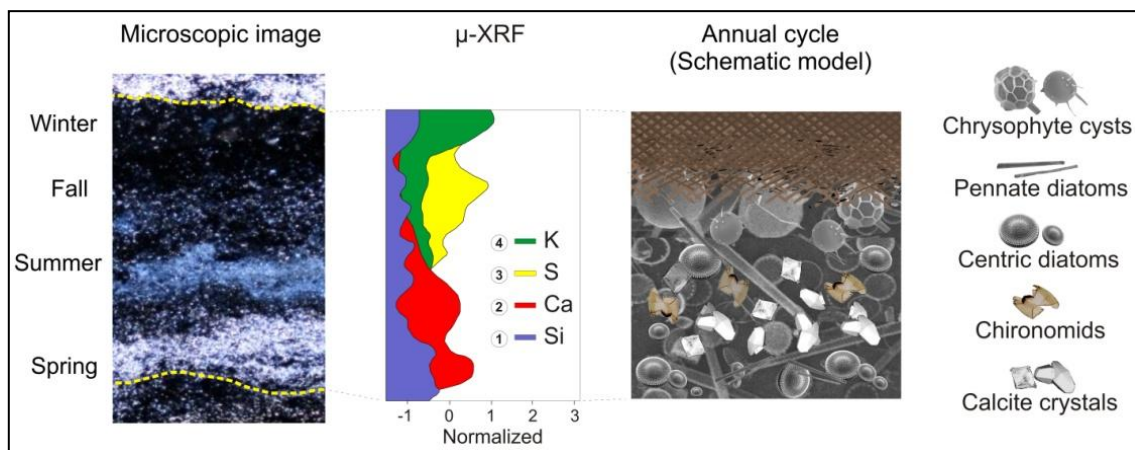


Fig. 5.7 Microscopic image of a thin section, μ -XRF data, and a schematic model of an annual sediment deposition in Lake Żabińskie

After the climate of the study area, the properties of the lake catchment and of the biochemical varves from Lake Żabińskie were introduced in details, we present a set of sedimentary pigments and other biogeochemical data from a short sediment core. It will be shown that the biogeochemical dataset can be used to infer a spring temperature signal and a history of human eutrophication. This study is presented in the following section (study published in *Global and Planetary Change*).

References (Chapter 5.1 – 5.3)

- Alexandersson, H., Moberg, A., 1997. Homogenization of Swedish temperature data .1. Homogeneity test for linear trends. *International Journal of Climatology* 17, 25-34
- Bonk, A., Tylmann, W., Amann, B., Enters, D., Grosjean, M., submitted. Modern limnology, sediment accumulation and varve formation processes in Lake Żabińskie, northeastern Poland: comprehensive process studies as a key for understanding sediment record. *Journal of Limnology*
- Downing, J.A., Watson, S.B., McCauley, E., 2001. Predicting Cyanobacteria dominance in lakes. *Canadian Journal of Fisheries and Aquatic Sciences* 58, 1905-1908
- Kaufmann, G., Wu, P., Li, G., 2000. Glacial isostatic adjustment in Fennoscandia for a laterally heterogeneous earth. *Geophysical Journal International* 143, 262-273
- Kinder, M., Tylmann, W., Enters, D., Piotrowska, N., Poręba, G., Zolitschka, B., 2013. Construction and validation of calendar-year time scale for annually laminated sediments - an example from Lake Szurpiły (NE Poland). *Journal of the Geological Society of Sweden GFF* 135, 248-257
- Kufel, L., 2001. Uncoupling of chlorophyll and nutrients in lakes – possible reasons, expected consequences. *Hydrobiology* 443, 59-67
- Larocque-Tobler, I., Filipiak, J., Grosjean, M., Bonk, A., Tylmann, W., submitted. Comparison between chironomid-inferred mean-August temperature from varved Lake Żabińskie (Poland) and instrumental data since 1896 AD
- Luterbacher, J., Xoplaki, E., Küttel, M., Zorita, E., González-Rouco, J.F., Jones, P.D., Stössel, M., Rutishauser, T., Wanner, H., Wibig, J., Przybylak, R., 2010. Climate Change in Poland in the Past Centuries and its Relationship to European Climate: Evidence from Reconstructions and Coupled Climate Models. In: R. Przybylak et al. (eds.), *The Polish Climate in the European Context: An Historical Overview*. [R. Przybylak et al. (eds.)], Springer, Berlin, pp 3-39, chapter 1
- Mann, M.E., Zhang, Z., Hughes, M.K., Bradley, R.S., Miller S.K., Rutherford, S., Ni, F., 2008. Proxy-based reconstructions of hemispheric and global surface temperature variations over the past two millennia. *Proceedings of the National Academy of Sciences* 105, 13252-13257
- MILLENNIUM 2011. EU FP6 IP_ <http://www.ncdc.noaa.gov/paleo/pubs/millennium/millennium.html>
- PAGES 2k Consortium, 2013. Continental-scale temperature variability during the last two millennia. *Nature Geoscience* 6, 339-346
- Przybylak, R., Majorowicz, J., Wojcik, G., Zielski, A., Chorazyczewski, W., Marciniak, K., Nowosad, W., Oliński, P., Syta, K., 2005. Temperature changes in Poland from the 16th to the 20th centuries. *International Journal of Climatology* 25, 773-791
- Przybylak, R., Oliński, P., Chorazyczewski, W., Nowosad, W., Syta, K., 2010. Documentary evidence. In R. Przybylak et al. (eds.), *The Polish Climate in the European Context: An Historical Overview*. Chapter 6, 167-190
- Scheffer, M., van Nes, E.H., 2007. Shallow lakes theory revisited: various alternative regimes driven by climate, nutrients, depth and lake size. *Hydrobiology* 584, 455-466

Szumański, A., 2000. *Objaśnienia do Szczegółowej Mapy Geologicznej Polski, Arkusz Giżycko (104)*, Państwowy Instytut Geologiczny, Warszawa, 1-33

Tylmann, W., Woźniak, P.P., Czarnecka, K., Jaźwiecka, M., 2006. New sites with laminated lake sediments in north-eastern Poland: preliminary results of field survey. *Limnological Review* 6, 283-288

Tylmann, W., Zolitschka, B., Enters, D., Ohlendorf, C., 2013a. Laminated lake sediments in northeast Poland: distribution, preconditions for formation and potential for paleoenvironmental investigation. *Journal of Paleolimnology* 50, 487-503

Tylmann, W., Enters, D., Kinder, M., Moska, P., Ohlendorf, C., Poręba, G., Zolitschka, B., 2013b. Multiple dating of varved sediments from Lake Łazduny, northern Poland: Toward an improved chronology for the last 150 years. *Quaternary Geochronology* 15, 98-107

5.4. Spring temperature variability and eutrophication history inferred from sedimentary pigments in the varved sediments of Lake Żabińskie, NE Poland AD 1907-2008

Study accepted in the journal *Global and Planetary Change*

Spring temperature variability and eutrophication history inferred from sedimentary pigments in the varved sediments of Lake Żabińskie, north-eastern Poland, 1907 – 2008 AD

Amann Benjamin¹, Lobsiger Simon², Fischer Daniela¹, Tylmann Wojciech³, Bonk Alicja³, Filipiak Janusz³, Grosjean Martin¹

¹ Oeschger Centre for Climate Change Research and Institute of Geography, University of Bern, Switzerland

² Department of Chemistry, University of Virginia, Charlottesville VA, USA

³ Institute of Geography, University of Gdańsk, Poland

Benjamin Amann

benjamin.amann@giub.unibe.ch

Simon Lobsiger: simon.lobsiger@gmx.ch

Daniela Fisher: daniela.fischer@giub.unibe.ch

Wojciech Tylmann: geowt@univ.gda.pl

Alicja Bonk: a.bonk@ug.edu.pl

Janusz Filipiak: filipiak@univ.gda.pl

Martin Grosjean: martin.grosjean@oeschger.unibe.ch

DOI: 10.1016/j.gloplacha.2014.10.008

Abstract

Varved lake sediments are excellent natural archives providing quantitative insights into climatic and environmental changes at very high resolution and chronological accuracy. However, due to the multitude of responses within lake ecosystems it is often difficult to understand how climate variability interacts with other environmental pressures such as eutrophication, and to attribute observed changes to specific causes. This is particularly challenging during the past 100 years when multiple strong trends are superposed.

Here we present a high-resolution multi-proxy record of sedimentary pigments and other biogeochemical data from the varved sediments of Lake Żabińskie (Masurian Lake District, north-eastern Poland, 54°N-22°E, 120m a.s.l.) spanning AD 1907 to 2008. Lake Żabińskie exhibits biogeochemical varves with highly organic late summer and winter layers separated by white layers of endogenous calcite precipitated in early summer.

The aim of our study is to investigate whether climate-driven changes and anthropogenic changes can be separated in a multi-proxy sediment data set, and to explore which sediment proxies are potentially suitable for long quantitative climate reconstructions. We also test if convoluted analytical techniques (e.g. HPLC) can be substituted by rapid scanning techniques (Visible Reflectance Spectroscopy VIS-RS; 380-730 nm).

We used Principal Component Analysis and Cluster Analysis to show that the recent eutrophication of Lake Żabińskie can be discriminated from climate-driven changes for the period 1907-2008 AD. The eutrophication signal (PC1 = 46.4%; TOC, TN, TS, Phe-*b*, high TC/CD ratios Total Carotenoids/Chlorophyll-*a* Derivatives) is mainly expressed as increasing aquatic primary production, increasing hypolimnetic anoxia and a change in the algal community from green algae to blue-green algae. The proxies diagnostic for eutrophication

show a smooth positive trend between 1907 and ca 1980 followed by a very rapid increase from ca. 1980 ± 2 onwards. We demonstrate that PC2 (24.4%, Chl-*a*-related pigments) is not affected by the eutrophication signal, but instead is sensitive to spring (MAM) temperature ($r = 0.63$, $p_{\text{corr}} < 0.05$, RMSEP = 0.56°C; 5-yr filtered). Limnological monitoring data (2011 – 2013) support this finding.

We also demonstrate that scanning visible reflectance spectroscopy (VIS-RS) data can be calibrated to HPLC-measured chloropigment data and be used to infer concentrations of sedimentary Chl-*a* derivatives {pheophytin *a* + pyropheophytin *a*}. This offers the possibility for very high-resolution (multi)millennial-long paleoenvironmental reconstructions.

Keywords: Climate change - trophic status - Anthropocene - limnology - HPLC - Europe

Highlights:

- PCA discriminates two environmental signals: eutrophication and climate
- Chl-*a*-related pigments are sensitive to spring March-May temperatures
- Scanning VIS-RS data can be calibrated to HPLC-Chlorophyll-*a* derivatives {Phe-*a* + PyrPhea}
- The lake is suitable for quantitative high-resolution paleoclimatic reconstructions

1. Introduction

High-resolution quantitative climate reconstructions across the world are required to place recent changes from local to planetary scales into a long-term perspective, to evaluate the causes (detection and attribution) and to anticipate the challenges of future climate change (PAGES 2k Consortium, 2013; Masson-Delmotte et al. 2013).

Lake sediments are valuable natural archives recording physical, chemical and biological changes of natural and anthropogenic origin in the recent and more distant history of the Earth. Varved lake sediments, in particular, hold great potential due to their annual resolution and high chronological precision and accuracy (Zolitschka 2007). Varved lake sediments have been successfully investigated using a wide range of sedimentological, biogeochemical and biological proxies to assess environmental (trophic state, land use, acidification, pollution) and climatic changes (O'Sullivan 1983; Pienitz and Lotter 2009; Ojala et al. 2012).

Due to the multitude of impacts and responses within lake ecosystems, one of the key issues is to understand how climate variability interacts with other environmental pressures such as eutrophication or land use changes (Kienel et al. 2005, 2013). This is particularly challenging during the 20th and early-21st centuries when strong simultaneous covariant trends in the atmosphere-catchment-lake system (climate, land use, nutrient cycles, and aquatic food web) are superposed. Thus discriminating climatic from anthropogenic effects is relevant with regard to climate research (Adrian et al. 2009) as well as ecosystem management (Smith et al. 2006; Hobaek et al. 2012).

Sedimentary pigments provide valuable information about environmental and climate changes. In general, changes in the pigment composition and stratigraphy reflect variations in the phytoplankton structure and abundance

(Leavitt and Hodgson 2001), which in turn reflects changes in light availability, temperature, nutrients, lake stratification, food web and some other factors (Wetzel 2001). Several studies across the world have demonstrated that sedimentary pigments can be used to infer past climate changes in Scandinavia and Central Europe (Lami et al. 2000), Antarctica (Hodgson et al. 2005; Chen et al. 2013), Mongolia (Nara et al. 2005), Chile (von Gunten et al. 2009a) and Nepal (Lami et al. 2010) or to document changes in the trophic levels of lakes in Florida (Waters et al. 2005), Chile (von Gunten et al. 2009b), Sweden (Reuss et al. 2010), Hungary (Korponai et al. 2011) and Estonia (Leeben et al. 2013) among others.

Since pigment measurements are quite convoluted and expensive (Reuss et al. 2010), long and high-resolution reconstructions are difficult to obtain. Recent advances in reflectance spectroscopic techniques in the visible-near-infrared range 400 – 1000 nm (VIS-RS) have shown that, although the pigment measurements are less specific, reflectance spectra can be used to approximate sedimentary chlorophyll *a*, Chl-*a* derivatives (chlorins) and carotenoids (Rein and Sirocko 2002; Das et al. 2005; Wolfe et al. 2006; Michelutti et al. 2010; Chen et al. 2013). In specific cases, changes in the stratigraphy and abundance of these pigments may reflect climate variability (Rein et al. 2005; von Gunten et al. 2009a; Saunders et al. 2013). Scanning VIS-RS techniques, in particular, hold great potential for high-resolution environmental reconstructions, but these methods are still in their infancy.

A recent comprehensive survey by Tylmann et al. (2013a) in north-eastern Poland, uncovered the presence of several postglacial lakes that contain undisturbed continuous sequences of annually laminated sediments with biochemical varves. These varves provide highly precise and accurate chronologies (Kinder et al. 2013; Tylmann et al. 2013b). These lakes show mostly anoxic conditions in the hypolimnion and the sediments are highly organic and anoxic thus

providing best conditions for the preservation of sedimentary pigments (Leavitt 1993; Reuss et al. 2005). Moreover, Poland is a very interesting area because, situated in the centre of Europe, its climate reflects approximately average European conditions (Luterbacher et al. 2010). Therefore, the varved lake sediments in NE Poland provide unique opportunities for paleoclimate research.

Here we present a multi-proxy data set with sedimentary pigments and other biogeochemical data from the varved sediments of eutrophic Lake Żabińskie (Masurian Lake District) for the recent past (1907 – 2008 AD). The aims of our study are (i) to investigate which proxies are diagnostic to differentiate climate-driven changes from changes induced by eutrophication and anthropogenic activities and (ii) to explore whether rapid reflectance spectroscopic techniques are able to approximate expensive but specific pigment measurements (HPLC). In more general terms, both aims target the question whether the sediments of Lake Żabińskie are a suitable archive for millennial-long quantitative high-resolution paleoclimatic reconstructions. Which are the best proxies for that purpose, and which are the most suitable techniques to acquire the data? We will show that, in this particular lake, (i) Chl-*a* derivatives (pheophytin *a* and pyropheophytin *a*) can be used to reconstruct spring (March – May) temperatures and (ii) scanning visible reflectance spectroscopy (VIS-RS) data can be calibrated to HPLC data and be used to infer concentrations of Chl-*a* derivatives in these lake sediments.

2. Study site

Lake Żabińskie (54°07'54" N; 21°59'01" E; 120 m a.s.l.) is a postglacial lake located in the Masurian Lake District, north-eastern Poland (Fig. 1a). The lake has formed after the deglaciation of the Fennoscandian Ice Field around 15 kyr BP (Kaufmann et al. 2000). The geology of the area consists mainly of

Quaternary glacial and fluvio-glacial deposits composed of morainic till as well as fluvio-glacial and fluvial sands and gravels (Szumański 2000).

The climate of the Masurian Lake District belongs to the humid continental warm summer type (Dwb) according to the Köppen classification. Monthly mean temperatures downscaled for Lake Żabińskie range from -3°C in January to 18°C in July (Fig. 1b). Total annual precipitation is 610 mm. Snow accounts for approximately two thirds of winter precipitation (December-March). Correlation field analysis of spring March-May MAM temperature (the target of our study; CRU TS 3.0 data; Mitchell and Jones 2005) shows that the study site is a good predictor ($r > 0.7$, $p < 0.001$) for spring temperature in most areas of Western, Central and Eastern Europe, and southern Scandinavia (Fig. 1b).

The catchment of the lake has experienced important human impacts during the 20th century with the construction of buildings between 1910 and 1920 AD at the northern lake shore directly (Fig. 1a). A holiday resort was also established between 1950 AD and 1960 AD and enlarged in the 1970s and mid-1980s. The resort centre is today privately owned and connected to the sewage treatment system only since 1998 AD only. The use of artificial fertilizers for agriculture increased considerably in this region after 1965-1975 AD.

Lake Żabińskie is an exorheic lake. It receives water from the forested north-eastern part of its catchment mainly (Lake Purwin; Fig. 1a) and from two southern streams supplying water from cultivated fields. The lake discharges westward into the larger Lake Gołdopiwo. The lake is dimictic (spring and fall overturn usually complete except in warm winters like 2012/2013) and experiences summer stratification between May and October (Fig. 2). The thermocline is at around 5-10 m and anoxic conditions establish in the hypolimnion during summer. The water surface is covered by ice during winter months (generally January to early March).

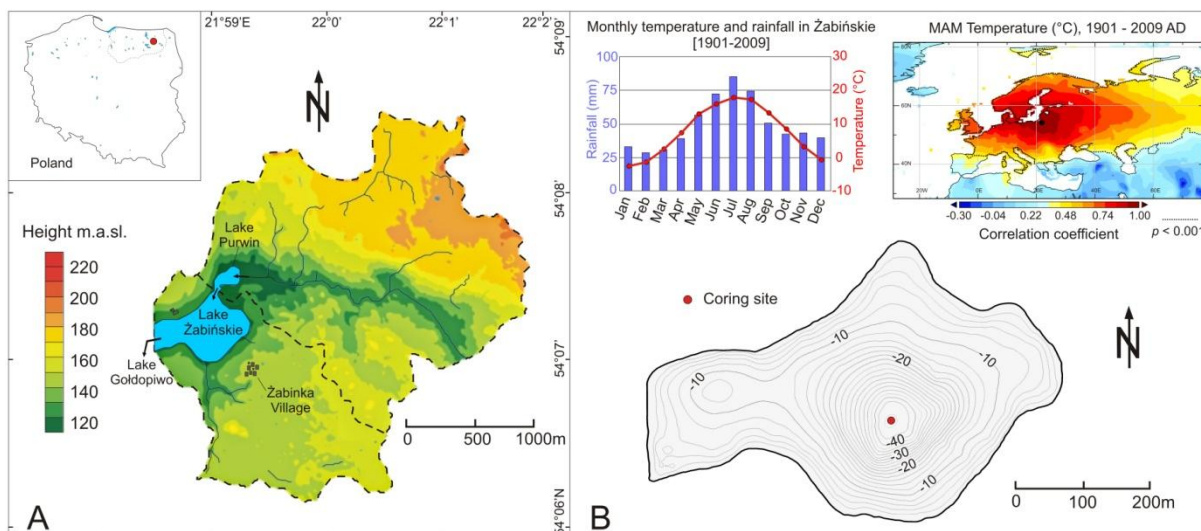


Fig. 1. Characteristics of Lake Żabińskie: a location in the Masurian Lake District of north-eastern Poland, topographic and hydrological settings of the catchment area; b bathymetric map of the lake basin, temperature and precipitation regime at the lake for the last century, and spatial correlation map for spring (MAM) season temperature

Today, Lake Żabińskie is eutrophic. Distinct algal blooms are observed during the growing season and are typically associated with very low water transparency (Secchi disk visibility <math>< 1.2</math> m). Chl-*a* concentrations in the epilimnion are high in spring and early summer following the ice break-up with a maximum in May (158 $\mu\text{g}\cdot\text{L}^{-1}$ in 2012, 84.2 $\mu\text{g}\cdot\text{L}^{-1}$ in 2013; Fig. 2). According to Kufel (2001), light becomes limiting in early summer and blue-green algal blooms develop during the rest of the summer season, which is typical for Masurian lakes. The Electric Conductivity through the water column varies in the range of 350-450 $\mu\text{S}\cdot\text{cm}^{-1}$ and pH fluctuates between 6.9 and 9.4.

Lake Żabińskie forms biogeochemical varves with a spring-to-fall layer composed of endogenous calcite grains, diatoms and chrysophytes and a winter layer rich in amorphous organic matter (Tylmann et al. 2013a).

3. Material and methods

3.1 Sediment coring and sampling

A 51-cm long sediment core was retrieved at the deepest point of Lake Żabińskie (Fig. 1b) using a

gravity corer (UWITEC, Φ 6 cm) in August 2011. The core was sealed, kept dark after collection and stored under cool (4°C) conditions in the laboratory.

The core was split lengthwise in two halves. Laminae identification and varve chronology were generated from core half A with high-resolution digital images of the fresh core surface and resin-embedded polished sediment slabs. We applied the same criteria for varve distinction and counting as established by Tylmann et al. (2013a).

Core half B was sectioned in continuous 1-cm intervals for the analysis of sedimentary pigments and other biogeochemical data.

3.2 Biogeochemical analysis

The relative proportions of organic matter and endogenous calcite were measured by loss-on-ignition (LOI) at 550°C and 950°C respectively (Heiri et al. 2001). Biogenic silica (BSi), a proxy for diatom abundance and productivity (Conley and Schelske 2001), was determined by the alkaline leaching method and ICP-OES measurements (corrected for lithogenic Si; Ohlendorf and Sturm 2008). Total organic carbon (TOC), nitrogen (TN) and sulphur (TS)

were measured with a CNS elemental analyser (vario EL cube, Elementar) on 12 mg homogenized and freeze-dried samples after removal of inorganic carbon with HCl. We calculated C/N atomic ratios to distinguish the source of the sedimentary organic matter (terrestrial versus aquatic). Lacustrine algae generally have C/N ratios ranging from 6 to 12, whereas vascular terrestrial plants produce organic matter with C/N ratios higher than 20 (Meyers and Ishiwatari 1993). Total sulphur TS was used in this study as a qualitative indicator of redox conditions and productivity. Enhanced productivity and anoxic conditions in the hypolimnion and in the sediments lead to greater net sulphur burial rates (Holmer and Storkholm 2001).

Sedimentary pigments were measured with three different techniques in order to test the applicability of rapid scanning techniques: (i) High Performance Liquid Chromatography (HPLC) is a compound-specific established technique but expensive, (ii) Ultraviolet-Visible photospectrometry (UV-VIS) is less specific, faster and cost efficient, and (iii) scanning Reflectance Spectroscopy in the visible range (VIS-RS) allows for direct measurements on the fresh sediment core at very high resolution (2 mm). The three methods are outlined hereafter:

For the HPLC analysis, all steps from sample sectioning to pigment extraction and measurements were done with minimal light, oxygen and heat exposure to prevent pigments from degrading. Pigments were extracted from 0.2 g freeze-dried sediment using 3 mL pure acetone and filtered (0.2 µm Nylon filter) until a colourless filtrate was obtained. The solvent was then evaporated under a N₂ stream and the dry pigment extracts were stored at -18°C prior to analysis (Reuss et al. 2005). We used the reversed-phase HPLC procedure following a modified method from Airs et al. (2001) in which the dried pigment extracts were eluted in a mixture of methanol, acetonitrile and 0.5 M ammonium acetate (80:15:5). The mixture was then injected into a Beckmann Coulter HPLC

system equipped with a Waters Spherisorb ODS2 5 µm column (250 mm x 4.6 mm). Pigments were detected using a diode array (Beckmann model 168) and a fluorescence detector (RF-20A Shimadzu at 438 nm and 470 nm). Finally, pigment concentrations were calculated using calibrated dilution series of standard stock-solutions (Sigma-Aldrich and crude spinach extract).

UV-VIS absorption spectra of pigment extracts (in 2.0 mL acetone) were measured with a Shimadzu UV-VIS spectrometer (UV-1800 CE 230V; 300-800 nm) at 0.2 nm step size. Chl-*a*, and total carotenoid (TC) concentrations are expressed in µg g⁻¹ sediment sample following the calculations by Lichtenhaler and Buschmann (2001) and Guilizzoni et al. 2011:

$$\text{Chl-}a \text{ (}\mu\text{g}\cdot\text{mL}^{-1}\text{)} = 11.24\cdot A_{661.6} - 2.04\cdot A_{644.8}$$

$$\text{TC (}\mu\text{g}\cdot\text{mL}^{-1}\text{)} = (A_{450} - 0.8\cdot A_{665}) / A^{1\text{cm}}$$

$$\text{Concentration (}\mu\text{g}\cdot\text{g}^{-1}\text{)} = \text{Concentration (}\mu\text{g}\cdot\text{mL}^{-1}\text{)} \cdot V \cdot D / m_{\text{pigment}}$$

whereby A_y is the absorbance at the wavelength y , $A^{1\text{cm}}$ is the average absorbance of carotenoids extract from 1 cm container (2,250), V the total volume of solution (2 mL), D the dilution factor (20) and m_{pigment} the mass of pigment (~0.2 g).

VIS reflectance spectroscopy (VIS-RS) scans on the fresh sediment cores were obtained with a portable Gretag-Spectrolino (GretagMcBeth, Switzerland). This instrument provides calibrated reflectance spectra in the visible range (380-730 nm) with a spectral resolution of 10 nm and a spatial resolution of 2 mm (Trachsel et al. 2010). Following Rein and Sirocko (2002) and Rein et al. (2005), we calculated two spectral indices, (i) the Relative Absorption Band Depth (RABD_{660;670}) indicative of total chlorins (diagenetic products of Chl-*a*) and (ii) the ratio R_{660}/R_{670} indicative of chlorophyll diagenesis.

Based on standard solutions available, we detected the following pigments in the sediment of Lake Żabińskie and interpreted their distribution following the schemes by Swain

(1985), Lami et al. (2000), Leavitt and Hodgson (2001):

- Chl-*a* and diagenetic products phaeophytin *a* (Phe-*a*) and pyropheophytin *a* (PyrPhe-*a*) are interpreted as proxies for the abundance of phototrophic green algae.
- The presence of phaeophorbide *a* can be used as an indicator of the food web intensity (grazing) and oxidation.
- Chlorophyll *b* (Chl-*b*) and phaeophytin *b* (Phe-*b*) indicate terrestrial plant debris and littoral inputs.
- β -carotene is an indicator for total algal biomass while lutein is specific for chlorophytes (green-algae). Blue-green algae are rich in β -carotene (30 to 60 % of the total amount of carotenoids) but do not contain lutein (Goodwin 1957). Thus changes in the lutein/ β -carotene ratio imply alteration in the relative importance of blue-green algae to green algae.
- We also use the ratio between total carotenoids (TC) and total chlorophyll derivatives (CD; sum of phaeophytins, pyro-phaeophytins and their isomers; Guilizzoni et al. 2011) as a proxy for algal composition (TC/CD). Because blue-green algae tend to dominate in nutrient-rich lakes and produce more carotenoids than green algae, carotenoid concentrations are expected to be higher in the sediments of eutrophic lakes. Accordingly, high TC/CD is typical for high primary productivity, low oxygen profundal water and the dominance of blue-green algae (Swain 1985; Lami et al. 2000; Mikomägi and Punning 2007).

3.3 Statistical analyses

In order to support the interpretation of the multi-proxy data matrix, principal component analysis (PCA) and stratigraphically constrained cluster analysis (CONISS, Grimm 1987) were performed on the log-transformed multi-proxy data set. This allows us to attribute individual lake sediment proxies or groups of proxies to different processes and cause (climate versus eutrophication) and to define stratigraphic phases in the sediment core.

Following the procedure by von Gunten et al. (2012), the proxy data (1 cm sampling intervals corresponding to 1-2 varve years) were regularized with linear interpolation to annual values according to the varve chronology. Prior to the proxy-climate calibration, both time series (the proxies and the meteorological data) were 3-yr and 5-yr triangular filtered to account for errors in sampling, regularization and varve counting uncertainties.

Meteorological data were spatially averaged and downscaled from stations close to the lake (Larocque-Tobler et al. submitted). Each proxy was correlated in a matrix with individual monthly and 2–12 months means of temperature. Statistical calibrations were performed using ordinary least squares regression (inverse regression) and probability values (*p*) were corrected for serial autocorrelation (Bayley and Hammersley 1946). We used the split-period approach for validation and the objective criteria (Reduction of Error RE, Coefficient of Efficiency CE and Root Mean Square Error of Prediction RMSEP) to evaluate the quality of the calibration model (von Gunten et al. 2012).

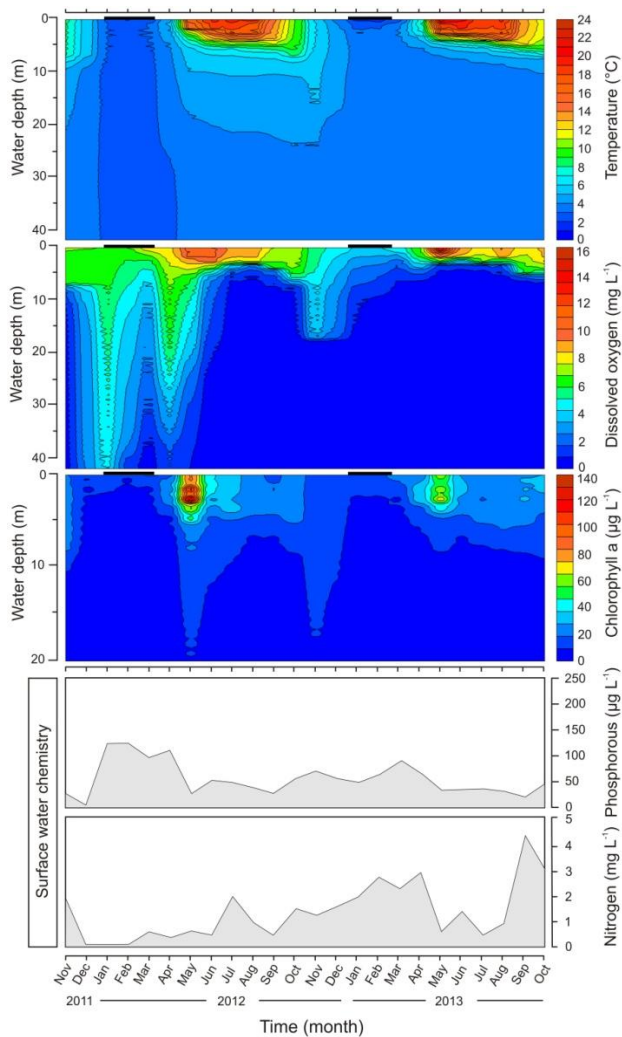


Fig. 2. Monthly limnological measurements of the water column and hydrochemical data (TP, TN) from the surface water over the period October 2011 – October 2013 in Lake Żabińskie

4. Results and interpretation

4.1 Pigment stratigraphy and other biogeochemical proxies

The comparison of the three different techniques to measure photopigments (HPLC, UV-VIS and VIS-RS) is reported in Table 1 and Fig. 3. The results show that

- (i) UV-VIS Chl-*a* measurements correspond to the overall sum of Chl-*a* and diagenetic products {Chl-*a* + Phe-*a* + PyrPhe-*a*} as measured by HPLC ($r^2 = 0.951$; data on the 1:1 line).

- (ii) The spectral index $RABD_{660;670}$ calculated from scanning VIS-RS on the fresh sediment core is significantly correlated with HPLC-inferred concentrations of total chlorins {Phe-*a* + PyrPhe-*a*} in dry sediments ($r = 0.75$, $p < 0.001$). The indices for the degree of diagenesis R_{660}/R_{670} and the total chlorin concentration $RABD_{660;670}$ are highly correlated ($r = 0.90$, $p = 5.3 \cdot 10^{-39}$).

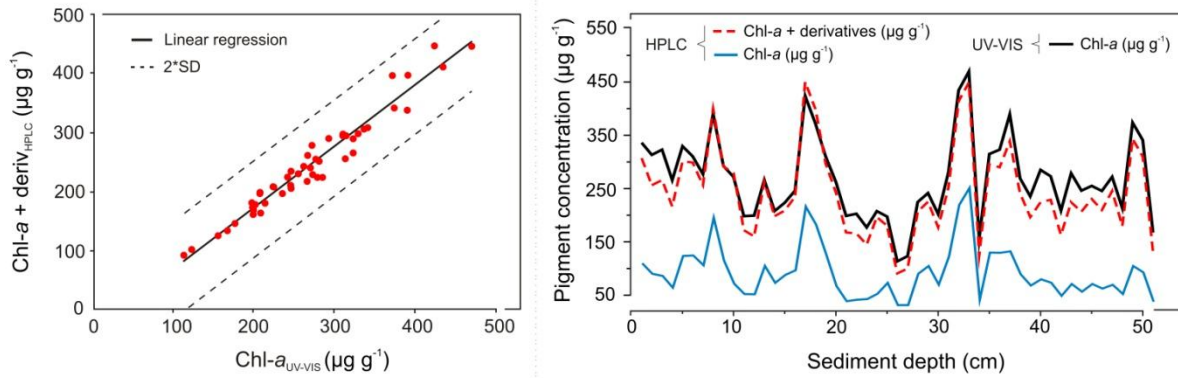
We used stratigraphically constrained cluster analysis to identify major changes in HPLC-measured sedimentary pigments (Fig. 4a) and biogeochemical data (Fig. 4b). According to the CONISS analysis, the core stratigraphy can be divided into three distinct ($p < 0.05$; ANOSIM test) zones:

Zone I (51-36 cm; AD 1907-1939) indicates particularly high amounts of Chl-*a*, Phe-*a* and PyrPhe-*a* (mean sum $> 300 \mu\text{g}\cdot\text{g}^{-1}$) which contrast with low values for β -carotene ($29.2 \mu\text{g}\cdot\text{g}^{-1}$) and TC/CD (mean 1.34). Maximum BSi concentrations are also observed in this zone peaking at $100 \text{ mg}\cdot\text{g}^{-1}$. C/N atomic ratios stay fairly stable with a mean value of 7.8. Lowest concentrations of TN (mean 1.12%), TOC (mean 10.1%) and TS (mean 1.85%) are found in this zone.

These results suggest aquatic sources of organic matter predominate, most likely produced by diatoms and green algae. These two types of phytoplankton dominate over blue-green algae in this zone.

Zone II (35-12 cm; AD 1940-1979) highlights a section with higher variability of most proxies and with first major changes in the core stratigraphy. Highest concentrations of Chl-*a* and Phe-*a* are detected in this section ($248 \mu\text{g}\cdot\text{g}^{-1}$ and $211 \mu\text{g}\cdot\text{g}^{-1}$ respectively) while β -carotene and TC/CD remain relatively low. Phe-*b* slightly increases along with TN, TOC and TS (average increase +20%). BSi gradually decreases to a mean value of $48.7 \text{ mg}\cdot\text{g}^{-1}$.

A UV-VIS and HPLC



B VIS-RS and HPLC

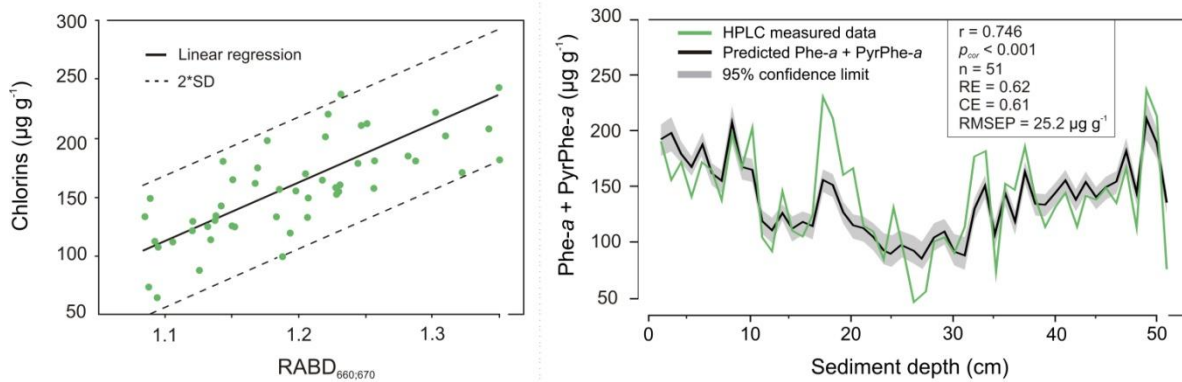


Fig. 3. Proxy-proxy calibration models with associated scatterplots and downcore comparison: a between compound-specific HPLC pigments and UV-VIS measurements; b between HPLC sedimentary pigments and VIS-RS logging

		HPLC		
		Chl-a _{HPLC}	Chl-a+deriv. _{HPLC}	Chlorins _{HPLC}
UV-VIS	Chl-a _{UV-VIS}	0.89*	0.97*	0.90*
	RABD _{660;670}	0.36	0.58*	0.75*
VIS-RS	R ₆₆₀ /R ₆₇₀	0.36*	0.57	0.73*

* $p < 0.01$

Table 1

Pearson correlation coefficients between compound-specific HPLC data and pigment information derived from UV-VIS and VIS-RS techniques. The best correlation is highlighted in bold

We interpret the results from this zone as a slight increase of anoxia with continuing dominance of green algae. C/N values significantly increase to a mean of 9 which may indicate a slightly growing influence of littoral organic matter inputs.

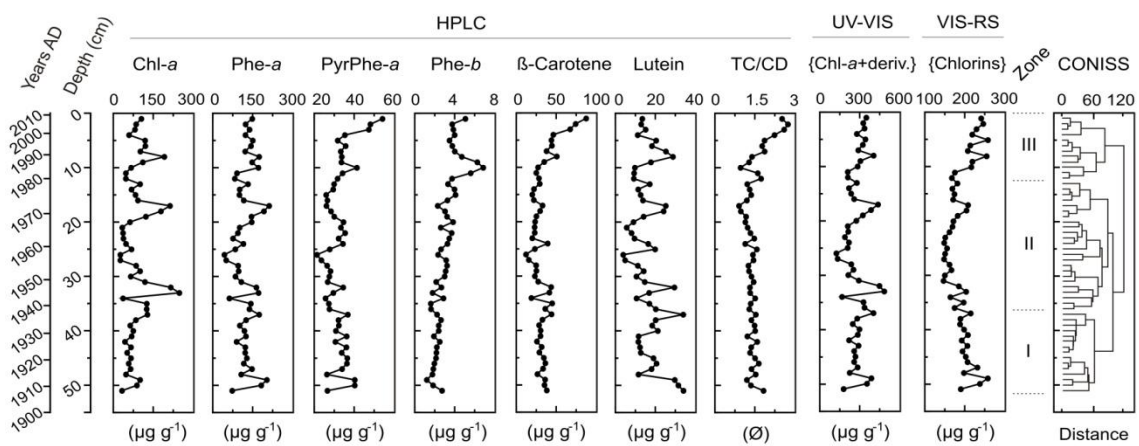
Zone III (12-1 cm; AD 1980-2008) characterizes a sequence with the most pronounced changes throughout the pigment stratigraphy and biogeochemical data. In particular, an increase in β -carotene (max $87.4 \mu\text{g}\cdot\text{g}^{-1}$) and TC/CD (max 2.62) can be noticed while no positive trends are observed for Chl-*a*, Phe-*a* and lutein concentrations. Increased concentrations of endogenous CaCO_3 (max 34.6 %) and TS (average increase +30%) are also found during this period. In contrast, BSi concentrations decrease to a minimum value of $9.4 \text{ mg}\cdot\text{g}^{-1}$. C/N ratios remain at a mean value of 9.15.

This sequence marks a change in the structure of the phototrophic community. We interpret these changes as increasing abundance of blue-green algae associated with the development of more anoxic conditions in the last three decades.

4.2 Factor attribution and proxy-climate calibration

We used the combination of PCA and cluster analysis to identify the most important causes that affect the pigments distribution and biogeochemical data (Fig. 5). Two principal components were discriminated capturing 71 % of the total variance (PC1 46 % and PC2 25 % respectively) and contrasting significantly from random testing (PCA-Scoreplot; Fig. 5a).

A Sedimentary pigments



B Biogeochemical data

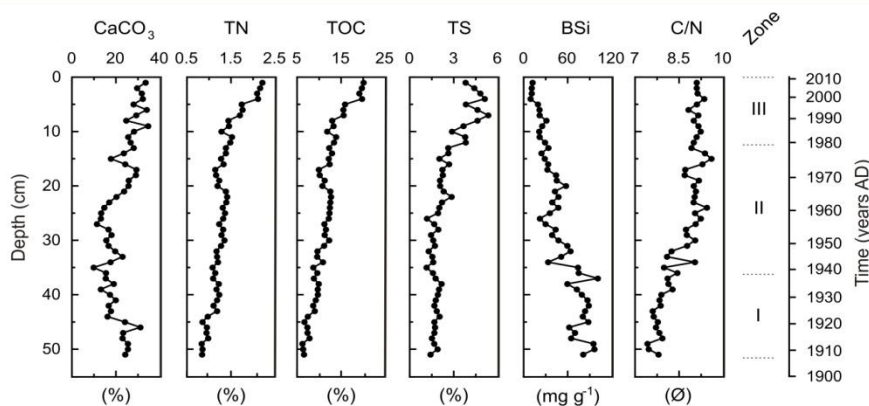


Fig. 4. Depth- and TS of sediment proxy data: a for sedimentary pigments; b for biogeochemical data

4.2.1 PC1: Eutrophication

Most of the proxies of our data set are positioned along the first principal component axis (PC1; Fig. 5a): CaCO_3 , the ratio TC/CD, TS, TN, TOC and Phe-*b* (correlation loadings of PC1 $>|0.5|$; and correlation loadings of PC2 $<|0.5|$). All of these proxies are indicative of nutrients, overall lake productivity and anoxia. BSi is negatively correlated with TOC ($r = -0.85$, $p < 0.01$) and positioned along negative values of the first PC axis.

The factor scores of PC1 reveal a significant increase in the top 12 cm sediment depth which correspond to the years AD 1980 ± 2 onwards (PC1-Scores; Fig. 5b). This section encompasses the zone III in Fig. 4 and shows that these uppermost 12 cm of the core are clearly distinguishable from the lower part. Eutrophication is the dominant process in Lake Żabińskie after AD 1980.

4.2.2 PC2: Climate variability

The second PC axis separates Chl-*a*, Phe-*a* and lutein from the other proxies (PC2; Fig. 5a). PyrPhe-*a* and β -carotene have loadings greater than 0.5 for PC1 and PC2 indicating that both proxies vary along axis 1 (eutrophication) and axis 2.

In contrast to PC1, no positive trend can be detected for the scores of PC2 in the uppermost part of the sediment core (PC2-Scores; Fig. 5b). Chl-*a* and Phe-*a* (PC2) do not follow the eutrophication signal (PC1) and show much larger downcore variability.

Therefore, we compare PC2-related proxies with temperature data (individual monthly and 2–12 months means). Pearson correlation matrix reveals that the factor scores of PC2 correlates best ($p_c < 0.05$) with spring temperature variability (MAM and May; Table 2).

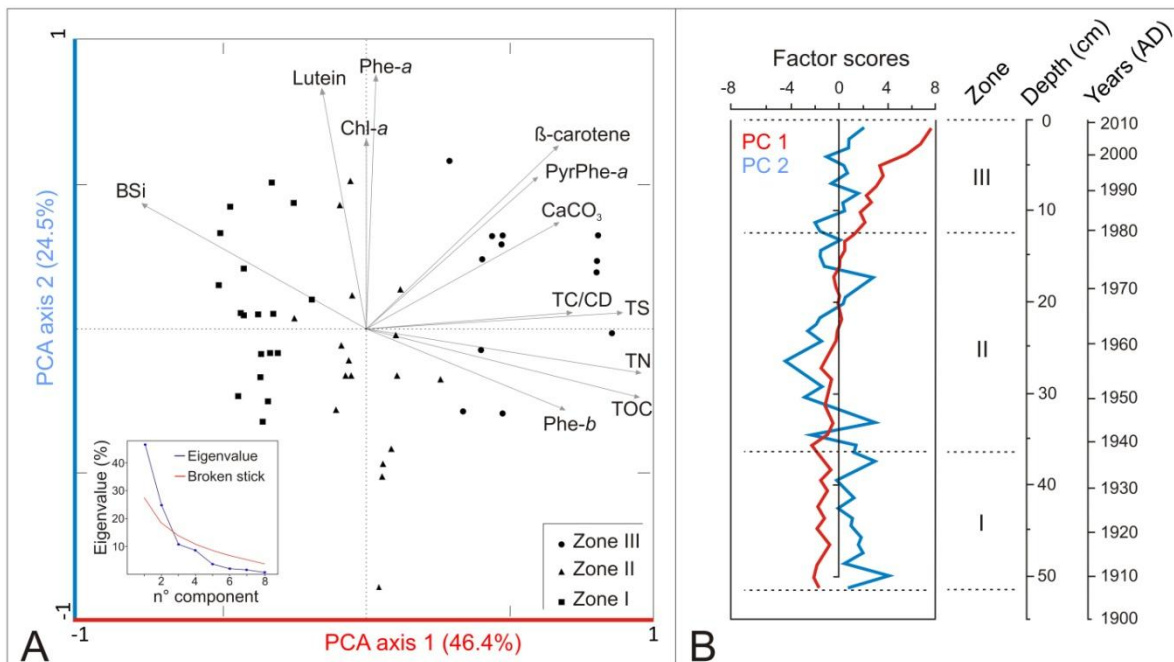


Fig. 5. PCA and cluster analysis. The dark-red lines highlight the characteristics of PC1, the light-blue lines PC2

This is true for annual, 3-yr and 5-yr filtered data. Table 2 also reveals that the VIS-RS spectral index $RABD_{660,670}$ (indicative of chlorins) shows the best proxy-climate relationship ($r = 0.63$, $p_c < 0.05$) to predict spring season MAM temperature. In contrast, no significant summer temperature signal (JJA, $p_c > 0.05$) can be reported.

Fig. 6a shows the calibration of 5-yr filtered $RABD_{660,670}$ data to MAM temperature. The calibration statistics yield a RMSEP = 0.56 °C for MAM that accounts for 17.7 % of its peak-to-peak amplitude and 9.0 % of its mean. Filtering the data from 3 to 5 years significantly improves the model, reducing the RMSEP by 31 %. The objective criteria for model performance assessment and model validation are low but positive (RE = CE = 0.1). Interestingly, (multi-)decadal trends are very well preserved while sub-decadal variability shows very small amplitudes.

5. Discussion

5.1 Pigment preservation and measurement techniques

Preservation of pigments in sediments is a major concern and may affect the interpretation. Ideal conditions for pigment preservation are high productivity, anoxia in the hypolimnion and the sediments, and low water transparency (Leavitt 1993; Reuss et al. 2005). Such conditions prevail in Lake Żabińskie. Several lines of evidence suggest that pigments are well preserved throughout the sediments considered here. Chemically unstable (labile) Chl-*a* and total carotenoids are abundant and there are no systematic downcore diagenetic effects such as decreasing ratios between Chl-*a* and its diagenetic products (Phe-*a*, PyrPhe-*a*) through the past 100 years. This is confirmed by all of the three independent analytical techniques HPLC, UV-VIS (Fig. 3a) and VIS-RS (Fig. 3b). Moreover, the high correlation in the VIS-RS data between the degree of diagenesis R_{660}/R_{670} and the total

chlorin concentration $RABD_{660,670}$ ($r = 0.90$, $p = 5.3 \cdot 10^{-39}$) also suggests minimal diagenetic effects. Finally, pheophorbide-*a* could hardly be detected with HPLC and UV-VIS suggesting that grazing activity is deficient.

The comparison of the three different methods HPLC (substance specific but expensive), UV-VIS (less specific and less expensive) and VIS-RS (relatively unspecific, very rapid and cost efficient) shows that (i) the VIS-RS spectral index $RABD_{660,670}$ can be used in Lake Żabińskie to approximate sedimentary chlorins {Phe-*a* + PyrPhe-*a*} and (ii) UV-VIS provides very good estimates for {Chl-*a* + derivatives}. Our calibration of VIS-RS inferred chloropigments with HPLC data is consistent with earlier studies (Das et al. 2005, Rein et al. 2005, Wolfe et al. 2006; Michelutti et al. 2010; Chen et al. 2013). This suggests that the VIS-RS technique yields good results in different lake environments. Nevertheless, the calibration between VIS-RS and HPLC data still leaves room for improvements. The difficulty is that scanning VIS-RS takes data from the fresh sediment core while HPLC reports pigment concentrations relative to dry sediment samples. Thus we suggest two lines for improvements; (i) implement correction factors for sediment porosity, specific sediment density and water content, and (ii) improve the geo-referencing for the VIS-RS measurements and the sediment subsampling in order to get a better spatial match between samples analysed with both methods. This second point is critically important in varved sediments where the sediment composition changes drastically at very fine mm-scales.

5.2 PC1 – Eutrophication signal

There are multiple lines of evidence for gradual slow eutrophication throughout the 20th century with a strong trophic state change and increasing anoxia in Lake Żabińskie after ca. AD 1980 (Zone III). TOC and TN increase simultaneously and C/N ratios remain constant

suggesting higher aquatic primary production. This in turn leads to hypolimnetic oxygen depletion under stratified conditions. Increased anoxia is manifested by higher TS embedding in sediments as a result of enhanced bacterial sulphur reduction (Holmer and Storkholm 2001). Increased anoxia from 1985 onwards was also concluded from anoxic chironomid taxa in the same lake (Larocque-Tobler et al. submitted).

Also TC/CD appears to be helpful in the interpretation of trophic and redox state changes. Swain (1985) established low TC/CD values (= 1.39) for oligotrophic and mesotrophic lakes and high TC/CD values (= 2.22) for eutrophic lakes. Lake Żabińskie experienced TC/CD values ranging between 1.3 – 1.5 in the bottom sections (Zone I and II, Fig. 4) but rapidly increasing values (TC/CD ranging between 2 – 3) in its topmost section (zone III, Fig. 4). A similar stratigraphic transition has also been documented in Estonian lakes (Mikomägi and Punning 2007).

The eutrophication of the last three decades in Lake Żabińskie is also reflected by a shift in the algal community from green algae (Chl-*a* rich) and a diatom-rich environment (high BSi values) to a dominance of blue-green algae (β -carotene rich, high TC/CD). Such a community change is also a plausible explanation for the decreasing trend of sedimentary diatom opal in the sediments. Kufel (2001) reported the seasonal phytoplankton succession in a series of Masurian lakes. He showed that blue-green algae outcompete green algae at the beginning of the summer when turbidity in the epilimnion increases and light becomes limiting. This succession is also found in the limnological monitoring data of Lake of Żabińskie (2011-2013, Fig. 2) showing that the presence of Chl-*a* is restricted to spring and disappears in June for the rest of the growing season.

Preliminary results of non-pollen palynomorphs in Lake Żabińskie confirm this observation with a clear decrease of green algae genus (*Coelastrum*, *Botryococcus* and *Pediastrum*) shifting towards blue-green algae

genus (*Planktothrix rubescens* - *Oscillatoriales*) in the 1980s (Weisbrodt D., personal communication 2013).

In high turbidity conditions, as observed in Lake Żabińskie (secchi disk < 1.2 m), blue-green algae are known to have a competitive advantage (Scheffer and van Ness 2007). When they dominate over green algae, they may establish phytoplankton communities that are completely devoid of diatoms (Conley and Schelske 2001) and cause eutrophication of lakes. A shift towards dominance of blue-green algae is also one of the most consistent eutrophication effects of lakes in the temperate zones (Downing et al. 2001; Smith et al. 2006).

Several studies have documented anthropogenic eutrophication of European lakes in the 20th century in Sweden (Renberg et al. 2001), Norway (Hobaek et al. 2012), Estonia (Leeben et al. 2013), Germany (Kienel et al. 2013), Switzerland (Blass et al. 2007; Naeher et al. 2012) and elsewhere. However, in all of the European studies cited here, the start of the eutrophication process was found after 1950-early 1960s while the eutrophication in our study site from north-eastern Poland is delayed and started ca. 1980 \pm 2 yrs (Fig. 5). This coincides with the enlargement of the holiday resort on the shore of Lake Żabińskie (late 1970s-early 1980s) and with the intensification of fertilizer use in the region after 1975. This timing documents the delayed economic growth in peripheral areas of north-eastern Poland as compared to densely populated areas in Europe.

5.3 PC2 – Climate signal

We have shown that Chl-*a* and Phe-*a* (PC2) are independent from the eutrophication signal (PC1) and instead respond to spring temperature variability. Chiefly, chlorins are statistically significantly related to spring MAM temperature variability during the calibration period AD 1907-2008 (Fig. 5; Table 2). This result is reproducible with all the three measurement techniques used in this study. VIS-RS inferred chlorin

Table 2 Pearson correlation coefficient tests between monthly to seasonal temperature variables and sediment proxy data. PC2 represents the factor scores of the second component from the PCA, RABD_{660;670} is derived from high-resolution VIS-RS data logging while chlorins and {Chl-*a*+derivatives} are measured by HPLC. The best correlation is highlighted in bold.

Proxies	MAM T°C			May T°C			JJA T°C		
	Unfilt.	3-yr filt.	5-yr filt.	Unfilt.	3-yr filt.	5-yr filt.	Unfilt.	3-yr filt.	5-yr filt.
PC 2	0.36 *	0.50 *	0.59 *	0.32 *	0.47 *	0.52 *	0.14	0.24	0.28
RABD _{660;670}	0.36 *	0.52 *	0.63 *	0.26 *	0.41 *	0.46	0.13	0.22	0.23
Chlorins _{HPLC}	0.37 *	0.52 *	0.59 *	0.30 *	0.46 *	0.48 *	0.15	0.24	0.26
Chl- <i>a</i> +deriv. _{HPLC}	0.31 *	0.43 *	0.48	0.32 *	0.49 *	0.51 *	0.16	0.25	0.29

* $p_c < 0.05$

concentration (RABD_{660;670}) was found to be the best predictor for MAM temperature in Lake Żabińskie ($r = 0.63$, $p_c < 0.05$; Fig. 6a). This proxy-climate model confirms findings from recent studies in other eutrophic lakes. The same proxy (VIS-RS inferred chlorin concentration RABD_{660;670}) showed to be sensitive to summer temperature (von Gunten et al. 2009a) and annual temperature (Saunders et al. 2013) and was used for Millennial-long high resolution temperature reconstructions.

Our result is surprising in two aspects: (i) why do chlorin concentrations in eutrophic Lake Żabińskie record a temperature signal and (ii) why are chlorin concentrations sensitive to spring temperature and not to temperatures during the entire growing season?

In this lake, the chlorin-climate correlations are consistent with the limnological monitoring data (Fig. 2) showing that Chl-*a* production in the epilimnion develops during spring mixing and ends with the beginning of the summer stratification. Green algae blooms in Masurian lakes are observed in spring following the ice-out typically but they develop rarely during summer stratification as they are replaced by blue-green algae (Kufel 2001). Blue-green algae are known to be more shade tolerant and competitive in turbid nutrient-rich lakes (Downing et al. 2001; Scheffer and van Ness 2007). This particular window of opportunity for the green algae in spring would explain why chlorin concentrations are sensitive

to March-May temperatures but not to temperatures of the entire summer (Table 2).

Several studies have stressed the importance of light in regulating aquatic productivity (McGowan 2005; Reuss et al. 2010). Similarly to our results, von Gunten et al. (2009a) found a strong eutrophication signal in Laguna Aculeo (Chile) through increasing TOC and decreasing BSi, while chlorin concentrations in the sediments were not affected. It can be argued that, with increasing nutrient loads, primary productivity increases along with turbidity, which in turn limits Chl-*a* production. This process results in higher TOC in the sediments, a shift from Chl-*a* production to carotenoid production and, in consequence high TC/CD ratios (Swain 1985). Under such conditions, Chl-*a* production is suggested to be sensitive to light availability, and to temperature indirectly. Although these processes need to be experimentally tested, it is suggested that, in certain lakes Chl-*a* concentrations in sediments do contain a climate (temperature) signal.

A major caveat in the proxy-climate calibration model (Fig. 6a) and possible temperature reconstruction is that the seasonal cycle of pigment production depends highly on phenology. The causal relationship between spring temperature and chlorin concentration is indirect and modulated by several parameters such as the duration of the ice-cover, the start, length and stability of water stratification, alkalinity, turbidity and nutrient availability as a function of mixing (Battarbee 2000; Bohrer and

Schultze 2008; Reuss et al. 2010). All of these effects give reason for the remaining 59% of unexplained variance in the calibration model. As the ‘phenological clock’ does not follow the ‘calendar clock’ of the climate data, a temporal mismatch between the proxy (phenology) and the climate-calendar is likely in particularly warm or cold springs.

The calibrated quantitative season-specific temperature signal of chlorins in Lake Żabińskie through the 20th and early 21st centuries offers nonetheless the possibility for climate reconstructions back in time and for several applications such as data-data comparisons (Trachsel et al. 2012), data-model comparisons or proxy-data assimilation in climate models simulations (Goosse et al. 2012). In this context our chlorin proxy for MAM temperature is interesting since information about spring temperature is very rare in natural paleoclimate archives.

At the same time, it is increasingly recognized that the temporal structure of climate variability differs substantially among the four seasons of the year (Luterbacher et al. 2004; Xoplaki et al. 2005, de Jong et al. 2013). These findings support the critical need for seasonally explicit climate proxies and seasonally explicit climate reconstructions. The relevance of seasonal temperature variability and the great potential of lake sediments as paleoclimate archive are highlighted in Fig. 6a and 6b. The figure shows the comparison of chlorin-inferred March-May temperatures (this study) with chironomid-inferred August temperatures (Larocque-Tobler et al. submitted) from the same lake (Lake Żabińskie) in the calibration period. Both time series are poorly correlated at sub-decadal scale ($r_{(MAM;Aug)} = 0.21, p = 0.025$) and they differ substantially in the decadal and multi-decadal variability bands. This demonstrates that both proxies contain unique information and care should be taken if both data series are merged to a multi-proxy series.

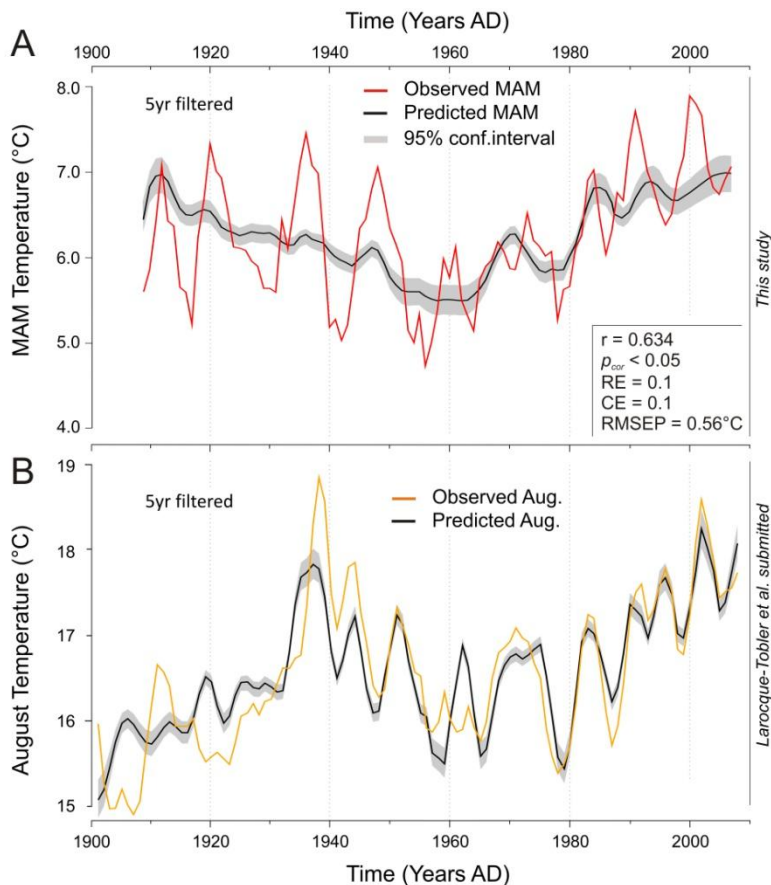


Fig. 6.

Proxy-climate calibration models: a from this study with MAM temperature data (red lines) and predicted temperature from RABD660;670= Chlorin concentrations (black line represents the mean; grey area the 95 % confidence envelop); b From Larocque et al. (submitted), with August temperature (orange lines) and predicted values from chironomids (black lines)

6. Conclusions

We investigated the composition of sedimentary pigments and other biogeochemical data in the varves of Lake Żabińskie with the aims (i) to differentiate the proxies that are diagnostic for climate-driven changes from those affected by eutrophication and anthropogenic activities, (ii) to explore whether rapid reflectance spectroscopic techniques are able to approximate expensive but specific pigment measurements (HPLC) and (iii) to test whether any of the lake sediment proxies can be used for millennial-long quantitative high-resolution paleoclimatic reconstructions.

We demonstrated that PCA and stratigraphically constrained cluster analysis performed on our multi-proxy data set is a suitable tool to quantitatively separate eutrophication-related processes (PC1) from processes governed by climate variability (PC2).

Eutrophication as reflected by increasing TOC and TN concentrations in the sediments and progressive summer anoxia (PC1 proxies) is detected as a smooth positive trend throughout the 20th century followed by a very rapid increase from ca. 1980 ± 2 onwards. Progressive eutrophication has also resulted in a shift in the algal community from green algae (rich in Chl-*a*) and diatoms (high BSi concentrations) to more blue-green algae (rich in β-carotene, TC/CD > 2). Blue-green algae are more shade tolerant which is thought to be a competitive advantage in an increasingly turbid aquatic environment resulting from eutrophication. As it is observed today during the annual cycle, light is an important limiting factor for Chl-*a* production during most of the year. Chl-*a* concentrations in the water column are high only during spring mixing, i.e. after the ice out and before summer stratification.

In this particular lake we found that Chl-*a*-related pigment concentrations (PC2 proxies) respond to spring temperature variability for the period AD 1907-2008 but not to eutrophication. Chlorin concentrations best contain the best

climate signal explaining approximately 40 % of the variance of spring MAM temperature ($r = 0.63$, $p_c < 0.05$). The proxy-climate calibration model shows that the multi-decadal temperature trend is well captured, while the interannual signal is strongly smoothed.

We also demonstrated that scanning visible reflectance spectroscopy (VIS-RS) data can be calibrated to HPLC-measured chloropigment data and be used to infer concentrations of sedimentary Chl-*a* derivatives {pheophytin *a* + pyropheophytin *a*}. This offers the possibility for a very high-resolution (multi)millennial-long temperature reconstruction.

This study highlights the importance in discriminating the climate signal from eutrophication, and providing season-specific climate assessments and reconstructions from natural paleoclimatic archives. This study also addresses the advantages of a multi-proxy approach. It allows a more complete understanding of the processes, the causes and the diverse responses of the lake ecosystem to environmental changes.

Acknowledgements

We thank the CLIMPOL project members for active and fruitful discussions, in particular Małgorzata Kinder (Gdańsk University). Thanks go also to Paraskevi Giannakaki (UniBern) for help with gridded meteorological data and correlation field analysis, Mathias Trachsel (University of Bergen) for statistical expertise and Krystyna Saunders, Rixt de Jong and Iván Hernandez-Almeida (UniBern) for support and comments on this manuscript. This research was supported by a grant from Switzerland through Swiss Contribution to the enlarged European Union (CLIMPOL PSPB-086/2010) and the Swiss National Science Foundation grant 200020-134945/1.

References

- Adrian, R., O'Reilly, C.M., Zagarese, H., Baines, S.B., Hessen, D.O., Keller, W., Livingstone, D.M., Sommaruga, R., Straile, D., Van Donk, E., Weyhenmeyer, G.A., Winder M., 2009. Lakes as sentinels of climate change. *Limnology and Oceanography* 54: 2283-2297
- Airs, R.L., Atkinson, J.A., Keely, B.J., 2001. Development and application of a high resolution liquid chromatographic method for the analysis of complex pigment distributions. *Journal of Chromatography* 917: 167-177
- Battarbee, R., 2000. Palaeolimnological approaches to climate change, with special regard to the biological record. *Quaternary Science Reviews* 19: 107-124
- Bayley, G.V., Hammersley, J.M., 1946. The "effective" number of independent observations in an autocorrelated time series. *Supplement to the Journal of the Royal Statistical Society* 8: 184-197
- Blass, A., Bigler, C., Grosjean, M., Sturm, M., 2007. Decadal-scale autumn temperature reconstruction back to A.D. 1580 inferred from varved sediments of Lake Silvaplana (south-eastern Swiss Alps). *Quaternary Research* 68: 184-195
- Boehrer, B., Schultz, M., 2008. Stratification of lakes. *Reviews of Geophysics* 46: 1-27
- Chen, Q., Liu, X., Nie, Y., Sun, L., 2013. Using visible reflectance spectroscopy to reconstruct historical changes in chlorophyll a concentration in East Antarctic ponds. *Polar Research* 32: 199-212
- Conley, D.J., Schelske, C.L., 2001. Biogenic silica. In: Smol JP, Birks HJB, Last WM (eds) *Tracking environmental change using lake sediments*. Vol 3: terrestrial, algal and siliceous indicators. Kluwer, Dordrecht, pp 281-293
- Das, B., Vinebrooke, R.D., Sanchez-Azofeifa, A., Rivard, B., Wolfe, A.P., 2005. Inferring sedimentary chlorophyll concentrations with reflectance spectroscopy: a novel approach to reconstructing historical changes in the trophic status of mountain lakes. *Canadian Journal of Fisheries and Aquatic Sciences* 62: 1067-1078
- De Jong, R., von Gunten, L., Grosjean, M., 2013. Cold-season temperatures in the European Alps during the past millennium: variability, seasonality and recent trends. *Quaternary Science Reviews* 82: 1-12
- Downing, J.A., Watson, S.B., McCauley, E., 2001. Predicting Cyanobacteria dominance in lakes. *Canadian Journal of Fisheries and Aquatic Sciences* 58: 1905-1908
- Goodwin, T.W., 1957. The Nature and Distribution of Carotenoids in some Blue-Green Algae. *Journal of general Microbiology* 17: 467-473
- Goosse, H., Guiot, J., Mann, M.E., Dubinkina, S., Sallaz-Damaz, Y., 2012. The medieval climate anomaly in Europe: comparison of the summer and annual mean signals in two reconstructions and in simulations with data assimilation. *Global and Planetary Change* 84-85: 35-47
- Grimm, E.C., 1987. CONISS: a FORTRAN 77 program for stratigraphically constrained cluster analysis by the method of incremental sum of squares. *Computer & Geosciences* 13: 13-35
- Heiri, O., Lotter, A.F., Lemcke, G., 2001. Loss on ignition as a method for estimating organic and carbonate content in sediments: reproducibility and comparability of results. *Journal of Paleolimnology* 25: 101-110
- Hodgson, D.A., Verleyen, E., Sabbe, K., Squier, A.H., Keely, B.J., Leng, M.J., Saunders, K.M, Vyverman, W., 2005. Late Quaternary climate-driven environmental change in the Larsemann Hills, East Antarctica, multi-proxy evidence from a lake sediment core. *Quaternary Research* 64: 83-99
- Hobæk, A., Løvik, J., Rohrlack, T., Moe, S.J., Grung, M., Bennion, H., Clarke, G., Piliposyan, G.T., 2012. Eutrophication, recovery and temperature in Lake Mjøsa: detecting trends with monitoring data and sediment records. *Freshwater Biology* 57: 1998-2014
- Holmer, M., Storkholm, P., 2001. Sulphate reduction and sulphur cycling in lake sediments: a review. *Freshwater Biology* 46: 431-451
- Kaufmann, G., Wu, P., Li, G., 2000. Glacial isostatic adjustment in Fennoscandia for a laterally heterogeneous earth. *Geophysical Journal International* 143: 262-273

- Kienel, U., Schwab, M., Schettler, G., 2005. Distinguishing climatic from direct anthropogenic influences during the past 400 years in varved sediments from Lake Holzmaar (Eifel, Germany). *Journal of Paleolimnology* 33: 327-347
- Kienel, U., Vos, H., Dulski, P., Lücke, A., Moschen, R., Nowaczyk, N., Schwab, M.J., 2013. Modification of climate signals by human activities recorded in varved sediments (AD 1608–1942) of Lake Holzmaar (Germany). *Journal of Paleolimnology* 50: 561-575
- Kinder, M., Tylmann, W., Enters, D., Piotrowska, N., Poręba, G., Zolitschka, B., 2013. Construction and validation of calendar-year time scale for annually laminated sediments - an example from Lake Szurpiły (NE Poland). *Journal of the Geological Society of Sweden GFF* 135: 248-257
- Korponai, J., Varga, K.A., Lengré, T., Papp, I., Tóth, A., Braun, M., 2011. Paleolimnological reconstruction of the trophic state in Lake Balaton (Hungary) using Cladocera remains. *Hydrobiologia* 676: 237-248
- Kufel, L., 2001. Uncoupling of chlorophyll and nutrients in lakes – possible reasons, expected consequences. *Hydrobiologia* 443: 59-67
- Lami, A., Guilizzoni, P., Marchetto, A., 2000. High resolution analysis of fossil pigments, carbon, nitrogen and sulphur in the sediment of eight European Alpine lakes: the MOLAR project. *Journal of Limnology* 59: 15-28
- Lami, A., Marchetto, A., Musazzi, S., Salerno, F., Tartari, G., Guilizzoni, P., Rogora, M., Tartari, G.A., 2010. Chemical and biological response of two small lakes in the Khumbu Valley, Himalayas (Nepal) to short-term variability and climatic change as detected by long-term monitoring and paleolimnological methods. *Hydrobiologia* 648: 189-205
- Larocque-Tobler, I., Filipiak, J., Tylmann, W., Bonk, A., Grosjean, M., submitted. Chironomid-inferred mean-August temperature since 1883 AD in varved Lake Zabinskie, Poland: local and regional patterns. *Quaternary Science Reviews*
- Leavitt, P.R., 1993. A review of factors that regulate carotenoid and chlorophyll deposition and fossil pigment abundance. *Journal of Paleolimnology*, 9: 109-127
- Leavitt, P.R., Hodgson, D.A., 2001. Sedimentary pigments. In: Smol JP, Birks HJB, Last WM (eds) *Tracking environmental change using lake sediments*. Vol 3: terrestrial, algal and siliceous indicators. Kluwer, Dordrecht, pp 295-325
- Leeben, A., Freiberg, R., Tonno, I., Koiv, T., Alliksaar, T., Heinsalu, A., 2013. A comparison of the palaeolimnology of Peipsi and Vortsjärvi: connected shallow lakes in north-eastern Europe for the twentieth century, especially in relation to eutrophication progression and water-level fluctuations. *Hydrobiologia* 710: 227-240
- Lichtenthaler, H.K., Buschmann, C., 2001. Chlorophylls and Carotenoids: Measurement and Characterization by UV-VIS Spectroscopy. *Current Protocols in Food Analytical Chemistry* F4.3
- Luterbacher, J., Xoplaki, E., Küttel, M., Zorita, E., González-Rouco, J.F., Jones, P.D., Stössel, M., Rutishauser, T., Wanner, H., Wibig, J., Przybylak, R., 2010. Climate Change in Poland in the Past Centuries and its Relationship to European Climate: Evidence from Reconstructions and Coupled Climate Models. In: R. Przybylak et al. (eds.), *The Polish Climate in the European Context: An Historical Overview*. [R. Przybylak et al. (eds.)], Springer, Berlin, pp 3-39, chapter 1
- Luterbacher, J., Dietrich, D., Xoplaki, E., Grosjean, M., Wanner, H., 2004. European Seasonal and Annual Temperature Variability, Trends, and Extremes Since 1500. *Science* 303: 1499-1503
- Masson-Delmotte, V., Schulz, M., Abe-Ouchi, A., Beer, J., Ganopolski, A., González Rouco, J.F., Jansen, E., Lambeck, K., Luterbacher, J., Naish, T., Osborn, T., Otto-Bliesner, B., Quinn, T., Ramesh, R., Rojas, M., Shao, X., Timmermann, A., 2013. Information from Paleoclimate Archives. In: *Climate Change 2013: The Physical Science Basis. Contribution of Working Group I to the Fifth Assessment Report of the Intergovernmental Panel on Climate Change* [Stocker, T.F., D. Qin, G.-K. Plattner, M. Tignor, S.K. Allen, J. Boschung, A. Nauels, Y. Xia, V. Bex and P.M. Midgley (eds.)]. Cambridge University Press, Cambridge, United Kingdom and New York, NY, USA.
- McGowan, S., Leavitt, P.R., Hall, R.I., Anderson, N.J., Jeppesen, E., Odgaard, B.V., 2005. Controls of algal abundance and community composition

- during ecosystem state change. *Ecology* 86: 2200-2211
- Meyers, P., Ishiwatari, R., 1993. Lacustrine organic geochemistry: an overview of indicators of organic matter sources and diagenesis in lake sediments. *Organic Geochemistry* 20: 867-900
- Michelutti, N., Blais, J. M., Cumming, B.F., Paterson, A.M., Rühland, K., Wolfe, A.P., Smol, J.P., 2010. Do spectrally inferred determinations of chlorophyll a reflect trends in lake trophic status? *Journal of Paleolimnology* 43: 205-217
- Mikomägi, A., Punning, J.-M., 2007. Fossil pigments in surface sediments of some Estonian lakes. *Proceedings of the Estonian Academy of Sciences, Biology and Ecology* 56: 239-250
- Mitchell, T.D., Jones, P.D., 2005. An improved method of constructing a database of monthly climate observations and associated high-resolution grids. *International Journal of Climatology* 25: 693-712
- Naeher, S., Smittenberg, R.H., Gilli, A., Kirilova, E.P., Lotter, A., Schubert, C.J., 2012. Impact of recent lake eutrophication on microbial community changes as revealed by high resolution lipid biomarkers in Rotsee (Switzerland). *Organic Geochemistry* 49: 86-95
- Nara, F., Tani, Y., Soma, M., Naraoka, H., Watanabe, T., Horiuchi, K., Kawai, T., Oda, T., Nakamura, T., 2005. Response of phytoplankton productivity to climate change recorded by sedimentary photosynthetic pigments in Lake Hovsgol (Mongolia) for the last 23,000 years. *Quaternary International* 136: 71-81
- Ohlendorf, C., Sturm, M., 2008. A modified method for biogenic silica determination. *Journal of Paleolimnology* 39: 137-142
- Ojala, A.E.K., Francus, P., Zolitschka, B., Besonen, M., Lamoureux, S.F., 2012. Characteristics of sedimentary varve chronologies— a review. *Quaternary Science Reviews* 43: 45-60
- O'Sullivan, P.E., 1983. Annually-laminated lake sediments and the study of Quaternary environmental changes - a review. *Quaternary Science Reviews* 1: 245-313
- PAGES 2 k Consortium, 2013. Continental-scale temperature variability during the last two millennia. *Natural Geoscience* 6: 339-346
- Pienitz, R., Lotter, A., 2009. Editorial: advances in paleolimnology. In: Pienitz R, Lotter A, Newman L, Kiefer T (eds) *Advances in paleolimnology. PAGES News* 17, 3: 89-136
- Rein, B., Sirocko, F., 2002. In-situ reflectance spectroscopy – analysing techniques for high-resolution pigment logging in sediment cores. *International Journal of Earth Sciences* 91: 950-954
- Rein, B., Lückge, A., Reinhardt, L., Sirocko, F., Wolf, A., Dullo, W.-C., 2005. El Niño variability off Peru during the last 20,000 years. *Paleoceanography* 20: 1-17
- Renberg, I., Bindler, R., Bradshaw, E., Emteryd, O., McGowan, S., 2001. Sediment evidence of early eutrophication and heavy metal pollution of Lake Mälaren, Central Sweden. *Ambio* 30: 496-502
- Reuss, N., Conley, D.J., Bianchi, T.S., 2005. Preservation conditions and the use of sediment pigments as a tool for recent ecological reconstruction in four Northern European estuaries. *Marine Chemistry* 95: 283-302
- Reuss, N., Leavitt, P.R., Hall, R.I., Bigler, C., Hammarlund, D., 2010. Development and application of sedimentary pigments for assessing effects of climatic and environmental changes on subarctic lakes in northern Sweden. *Journal of Paleolimnology* 43: 149-169
- Saunders, K.M., Grosjean, M., Hodgson, D.A., 2013. A 950-year temperature reconstruction from Duckhole Lake, southern Tasmania, Australia. *The Holocene* 23: 771 - 783
- Scheffer, M., van Nes, E.H., 2007. Shallow lakes theory revisited: various alternative regimes driven by climate, nutrients, depth and lake size. *Hydrobiologia* 584: 455-466
- Smith, V.H., Joye, S.B., Howart, R.W., 2006. Eutrophication of freshwater and marine ecosystems. *Limnology and Oceanography* 51: 351-355
- Swain, E.B., 1985. Measurement and interpretation of sedimentary pigments. *Freshwater Biology* 15: 53-75
- Szumański, A., 2000. *Objaśnienia do Szczegółowej Mapy Geologicznej Polski*, Arkusz Giżycko (104), Państwowy Instytut Geologiczny, Warszawa, 1-33

- Trachsel, M., Grosjean, M., Schnyder, D., Kamenik, C., Rein, B., 2010. Scanning reflectance spectroscopy (380-730 nm): a novel method for quantitative high-resolution climate reconstructions from minerogenic lake sediments. *Journal of Paleolimnology* 44: 979-994
- Trachsel, M., Kamenik, C., Grosjean, M., McCarroll, D., Moberg, A., Brázdil, R., Büntgen, U., Dobrovolský, P., Esper, J., Frank, D.C., Friedrich, M., Glaser, R., Larocque-Tobler, I., Nicolussi, K., Riemann, D., 2012. Multi-archive summer temperature reconstruction for the European Alps, AD 1053–1996. *Quaternary Science Reviews* 46: 66-79
- Tylmann, W., Zolitschka, B., Enters, D., Ohlendorf, C., 2013a. Laminated lake sediments in northeast Poland: distribution, preconditions for formation and potential for paleoenvironmental investigation. *Journal of Paleolimnology* 50: 487-503
- Tylmann, W., Enters, D., Kinder, M., Moska, P., Ohlendorf, C., Poręba, G., Zolitschka, B., 2013b. Multiple dating of varved sediments from Lake Łazduny, northern Poland: Toward an improved chronology for the last 150 years, *Quaternary Geochronology*, 15: 98-107
- von Gunten, L., Grosjean, M., Rein, B., Urrutia, R., Appleby, P., 2009a. A quantitative high-resolution summer temperature reconstruction based on sedimentary pigments from Laguna Aculeo, central Chile, back to AD 850. *The Holocene* 19: 873-881
- von Gunten, L., Grosjean, M., Eggenberger, U., Grob, P., Urrutia, R., Morales, A., 2009b. Pollution and eutrophication history AD 1800–2005 as recorded in sediments from five lakes in Central Chile. *Global and Planetary Change* 68: 198-208
- von Gunten, L., Grosjean, M., Kamenik, C., Fujak, M., Urrutia, R., 2012. Calibrating biogeochemical and physical climate proxies from non-varved lake sediments with meteorological data: methods and case studies. *Journal of Paleolimnology* 47: 583-600
- Wetzel, R.G., 2001. *Limnology: Lake and River Ecosystems*. 3rd edition. Academic Press, San Diego, CA.
- Waters, M.N., Schelske, C.L., Kenney, W.F., Chapman, A.D., 2005. The use of sedimentary algal pigments to infer historic algal communities in Lake Apopka, Florida. *Journal of Paleolimnology* 33: 53-71
- Wolfe, A.P., Vinebrooke, R.D., Michelutti, N., Rivard, B., Das, B., 2006. Experimental calibration of lake-sediment spectral reflectance to chlorophyll a concentrations: methodology and paleolimnological validation. *Journal of Paleolimnology* 36: 91-100
- Xoplaki, E., Luterbacher, J., Paeth, H., Dietrich, D., Steiner, N., Grosjean, M., Wanner, H., 2005. European spring and autumn temperature variability and change of extremes over the last half millennium. *Geophysical Research Letters* 32: L15713
- Zolitschka, B., 2007. Varved lake sediments. In: Elias SA (ed) *Encyclopedia of Quaternary Science*. Elsevier, Amsterdam, pp 3105-311

Chapter 6



6. Summary and conclusions

Sound knowledge of past climate and its variability is required to improve our understanding of the operational mode of the Earth system, to assess the sensitivity of the Earth climate to natural and anthropogenic forcings and, to reduce uncertainty in future climate projections. However, further advances in this field of research are limited by the scarcity of well calibrated and quantified, annually resolved time series of reconstructed variables from natural paleoclimate archives that cover the last Millennium.

Among climate variables, not only long seasonal temperature series are important, but also time series of precipitation and long records of extreme events, such as flood events. To date, it remains poorly understood how changes in temperature, precipitation and regional synoptic-scale weather patterns interacted with each other over the past 1000 years and how they influenced the properties and statistics of flood events.

This is the reason why this project was initiated with the main goal to produce high-quality temperature and precipitation reconstructions, as well as a flood history for Europe. We used one of the unique natural archives that provide insight into each of these three variables: varved lake sediments.

Specifically, we investigated two lake sites for their potential as paleoclimate archives:

- Proglacial **Lake Oeschinen** in the Northern Swiss Alps that contains clastic varves
- Glacial **Lake Żabińskie** in northeast Poland that contains biochemical varves

Varve lake sediments are a well-known natural paleoclimatic archive that provide high-resolution records of past climatic changes. However, producing such high-quality datasets is very difficult due to the fact that most of the analytical techniques are destructive, time consuming and often expensive. This is the reason why recent developments of rapid scanning techniques are so important.

The following three research questions were addressed through this PhD thesis:

(i) Can we use rapid reflectance scanning spectroscopy in the visible (VIS-RS) as a quantitative proxy for the composition of biochemical and clastic sediments?

(ii) Can we calibrate sediment proxy data and VIS-RS data with climate variables during the instrumental period?

(iii) Can we produce a 1000-year long quantitative climate reconstruction from sedimentological proxies and VIS-RS data?

A first study consisted in understanding the sedimentation processes and varve formation in each of the two lakes. This study comprised a careful analysis of the catchment, >2 years monitoring of the water column, and the analysis of recent deposition from sediment traps. This was used as a pre-requisite to improve system understanding, and in turn, to improve the reliability of climate reconstructions derived from lake sediments.

Sediment cores were recovered in each lake, dated, and analysed at high temporal resolution. The best proxy from the most suitable technique was selected for the calibration to meteorological time series (for Żabińskie and Oeschinen), and for a 1000-year reconstruction (for Oeschinen).

Through this thesis project, important milestones were achieved:

(i) We explored scanning VIS-RS methodology on the biochemical varves of Lake Żabińskie and on the clastic varves of Lake Oeschinen. Our results showed VIS-RS technique can be used to detect amount and composition of specific constituents from both types of varves, answering research question (i).

For Lake Żabińskie, six VIS-RS indices related to chloropigments were calculated following standard literature and compared with specific sedimentary pigment compounds as measured by High Performance Liquid Chromatography (HPLC). The absorption trough centred at 660-670nm (RABD_{660,670}) presented the best correlations and could be calibrated to total concentration of chlorins (chlorophyll-*a* degradation products = {Pheophytin-*a* + Porphopheophytin-*a*}; $r = 0.75$, $p < 0.01$). Further, chlorins-inferred VIS-RS have shown statistical skills to reconstruct spring temperature in northeast Poland.

A specific methodology was developed for the clastic varves of Lake Oeschinen based on the hypothesis that proportions of calcite (bright) and siliciclastic material (dark) could be distinguished using VIS-RS data. A series of 'synthetic sediments' with known mixing ratios in calcite and siliciclastics contents (as determined by loss on ignition at 950°C) were prepared and then analysed with VIS-RS scans. The mean 1st derivative VIS-RS spectra were used to infer the relative proportions of calcite/siliciclastics in the sediments ($r = 0.96$, $p < 0.01$).

These two case studies showed VIS-RS technique can successfully be applied to infer composition and concentrations of specific biochemical and mineroclastic compounds from lake sediments. However, results from this technique are specific to each individual lake and require systematic testing for different environments.

(ii) Based on an accurate, precise and reproducible varve chronology from Lake Oeschinen, we demonstrated that varve thickness could be used as a quantitative predictor for cumulative alpine warm-season precipitation ($r_{MJ} = 0.71$, $r_{MJJA} = 0.60$, $p_c < 0.01$). This calibration model from varve thickness and climate data during the instrumental period (AD 1901-2008) was used as a basis for the reconstruction of precipitation and flood frequency back to AD 884.

Beyond answering research question (ii) and (iii), this millennial-long record from Lake Oeschinen enabled to assess whether a relation existed between flood frequency, precipitation and already-established temperature over the past 1000 years. Results revealed no persistent relationship between warm-season precipitation and temperature, which was not in line with the 'dry gets drier, wet gets wetter' scheme. In contrast, this relationship has oscillated with a 60-70-year periodicity over the last Millennium. Although this required more advanced investigation, possible explanations for this multidecadal variability were changes in the weather-type statistics or the within-weather-type variability.

Sediment properties of Lake Oeschinen also provided the unique opportunity to investigate the long-term relationship between flood frequency and the amount of precipitation from the same location and the same natural archive. Results suggested flood frequency increased under cool and humid climates. This was true for 7 out of 8 cases over the past Millennium, while the 13th century revealed a period of high flood frequency along with very warm and moderately dry conditions. Although these are important findings, they leave room for different scenarios of the relation floods-precipitation-temperature.

(iii) Based on multivariate statistical analysis of a high-resolution multi-proxy data set from the biochemical varves of Lake Żabińskie, we were able to quantitatively discriminate the recent lake eutrophication from climate-driven changes for the period AD 1907-2008. We demonstrated that sedimentary pigments related to chlorophyll-*a* (primary material and degradation products) were not affected by the eutrophication processes.

In contrast, these pigments could be used as a quantitative predictor for spring temperature. Best correlations were found between chlorins-inferred VIS-RS and March-to-May temperature ($r = 0.63$, $p_c < 0.05$). This suggested that sediment proxy data from Lake Żabińskie and, particularly, VIS-RS data could be calibrated to spring temperature and be used for a climate reconstruction.

Acknowledgments

First of all, many thanks go to Prof. Dr. Martin Grosjean. Martin, you have been a supervisor with great support. You have accompanied me with your incredible experience and expertise at each step of my research project from fieldworks, to lab analyses, and data management and interpretation. Particularly, I am very grateful for the time you devoted to improve my skills in writing and editing scientific English, as well as speaking English with me, even though you can speak French. I really appreciated that.

Particular thanks also go to Prof. Dr. Scott Lamoureux, who has kindly accepted to read and evaluate the present thesis and Prof. Dr. Flavio Ansellmetti for his enthusiasm in being the chair of my forthcoming PhD defence.

I would also like to thank, in this first stage, Daniela Fischer and Samuel Hagnauer. You have been two of the most important persons who have made this work possible. You always found the time to answer my questions related to laboratory work, data analysis and interpretation; I have learnt a lot from both of you.

I want to show gratitude to Rixt de Jong, Krystyna Saunders (my official English proof-reader), Isabelle Larocque-Tobler, Julie Elbert, Paty, Iván Hernández-Almeida, Christoph Butz and Tobias Schneider. All, you have been more than just colleagues throughout these three years. This is not simply a matter of coffee breaks and lunches!

A short but specific sentence for Bruno Wilhelm, for our fruitful discussions, for your great expertise and novel ideas related to paleoflood research and for giving me one of the few French moments I had in Bern. Thank you.

External help was provided by several persons: special thanks to Adrian Gilli for providing the additional sediment cores from Lake Oeschinen needed for a good quality record and a millennial-long chronology. Resin embedded blocks and thin sections were prepared by Willy Tschudin from GEOPREP, Basel. Plant macrofossils for ^{14}C dating were identified by Petra Kaltenrieder at the Institute of Plant Sciences, Bern.

During numerous travels to Poland for coring and monitoring surveys, and for CLIMPOL group workshops, I had the opportunity to make good friends and acquaintances. Among others, thank you Gosia K., Alicja B. and Wojciech T. for support in field trips, for sharing data and for the time spent together. 'Into the wild' with you were fantastic (nicely rocked by Eddie Vedder, Hendrix, or David Gilmour *live in Gdańsk*).

Administrative assistance was appreciated from Isabella Geissbuhler and Marlis Rothlisberg of the Institute of Geography and by Margaret Mohl and Monika Wälti at the Oeschger Centre for Climate Change Research.

For all wonderful moments experienced in Bern, thanks to you Federico and Stéphane, Reni, Oli, Rocio, Ari, Erin, Juliette, Adrien, Chrigu, Nicolas, Iván, Martín 'le Merveilleux', Silvia, Cristina, Valeria, Livio, Miguel and Ghislain.

Finally, I cannot finish without saying 'Merci' Maman, Papa, Quentin & MC, Cécile and all my family in France for the support, for keeping track of me and for your numerous visits and shared moments in this beautiful country, which is geographically so close from home, but relatively far from our daily life.

Appendix



Varve Chronology– Lake Oeschinen

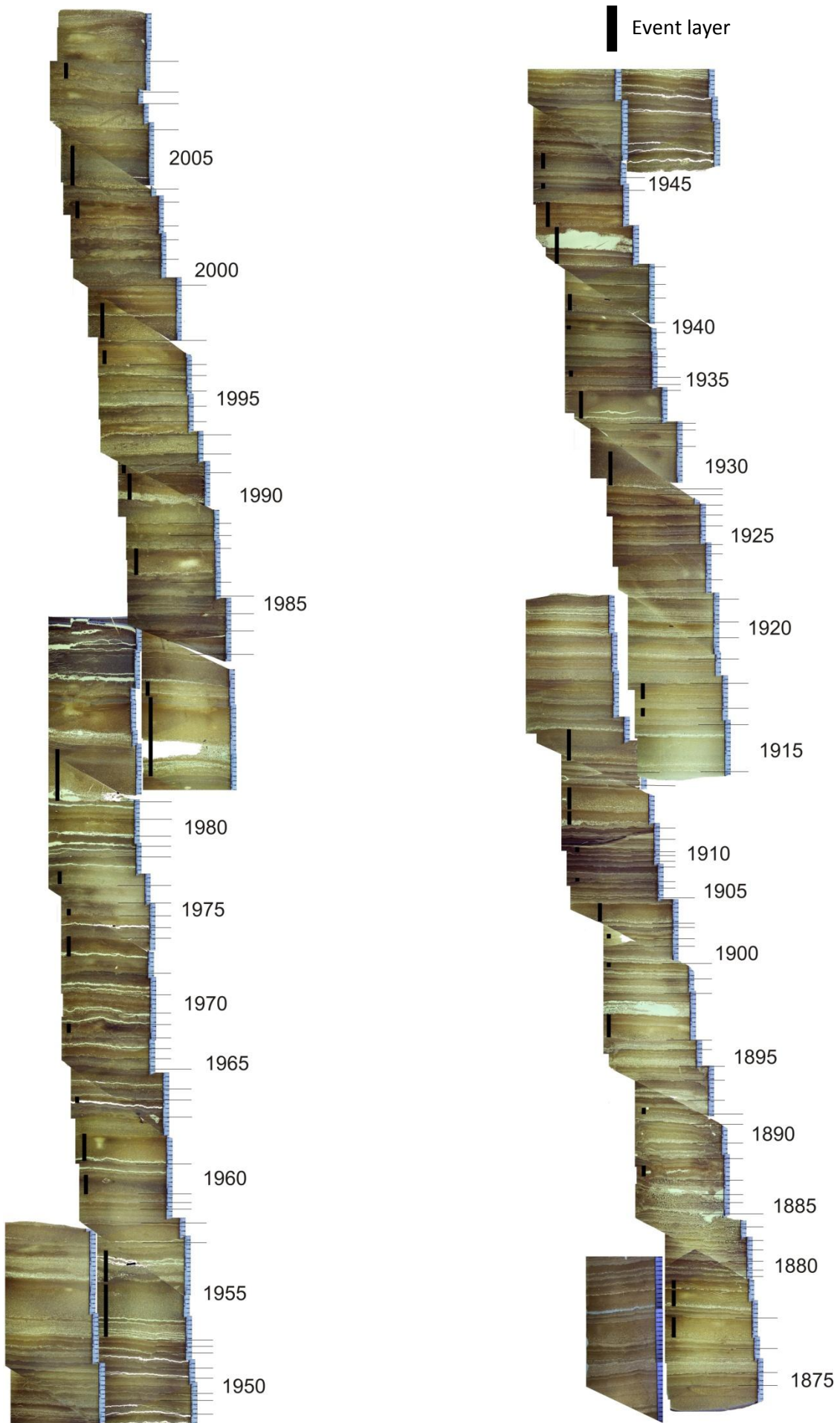


Fig. A1.1 Varve chronology from Lake Oeschinen (instrumental period used in Chapter 6)

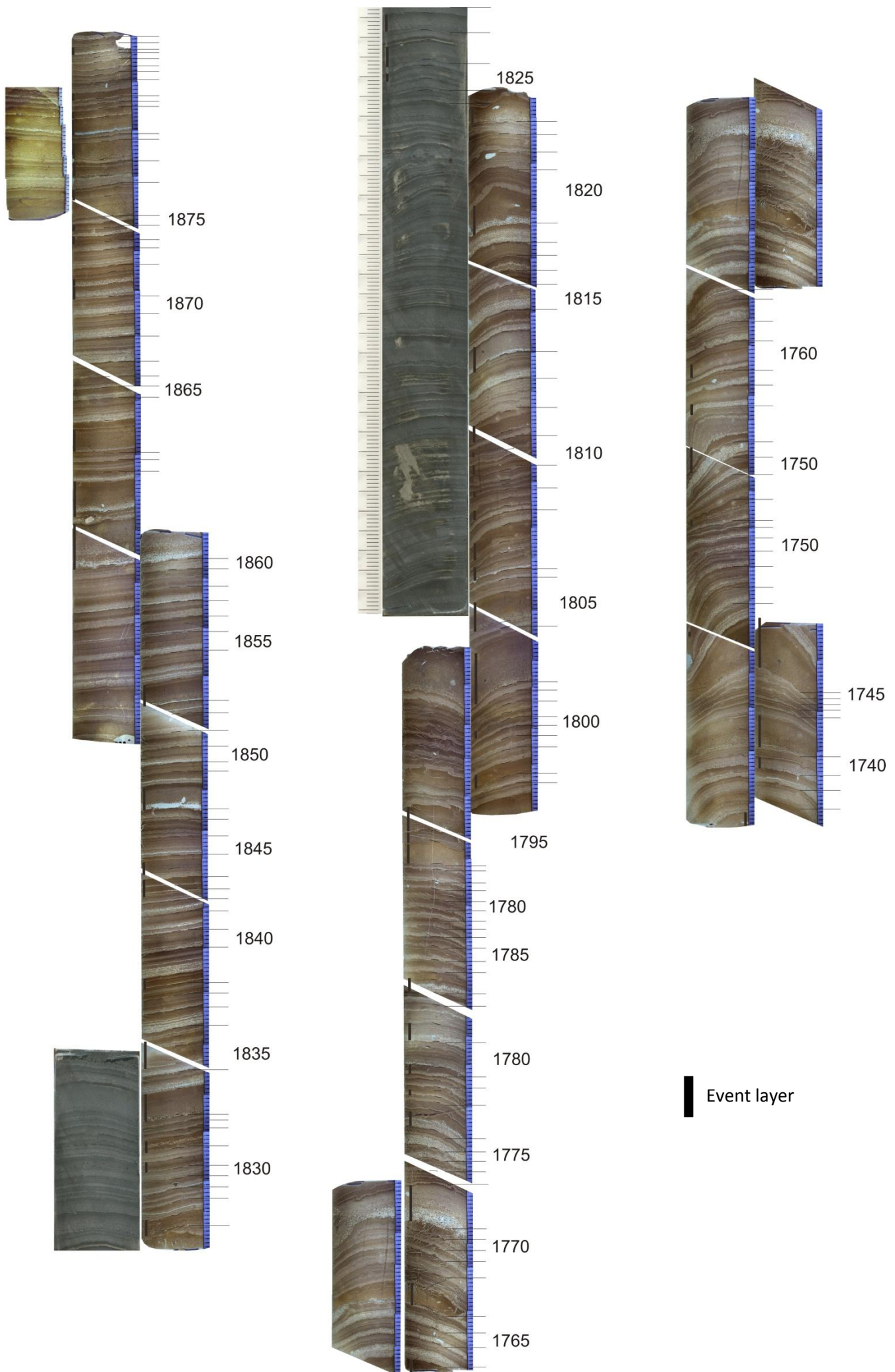


Fig. A1.2 Varve chronology from Lake Oeschinen (part2)

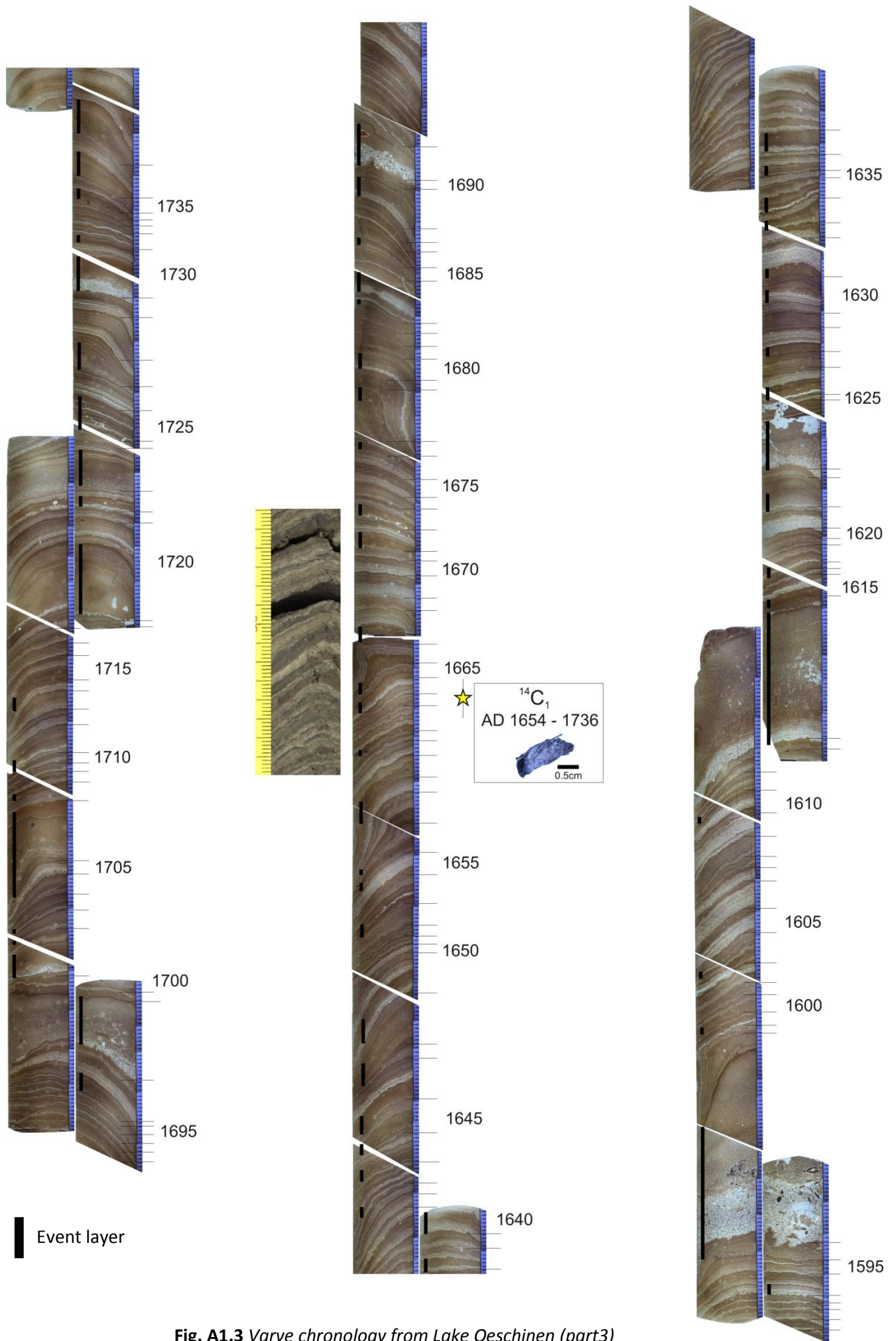
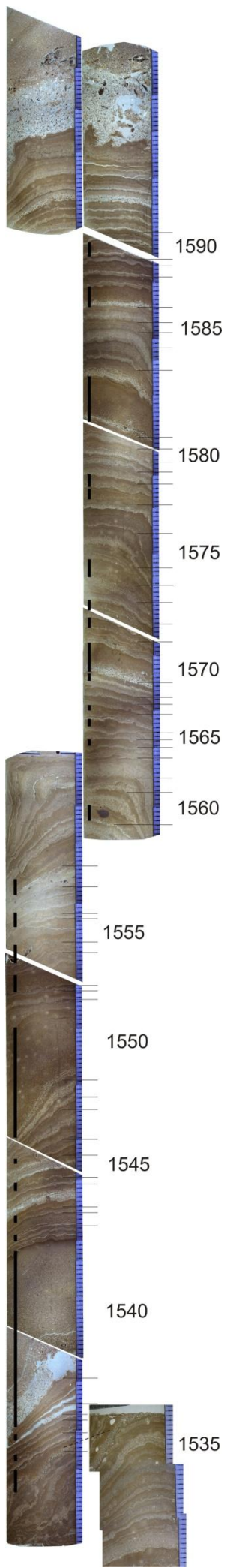


Fig. A1.3 Varve chronology from Lake Oeschinen (part3)



Event layer

Fig. A1.4 Varve chronology from Lake Oeschinen (part4)

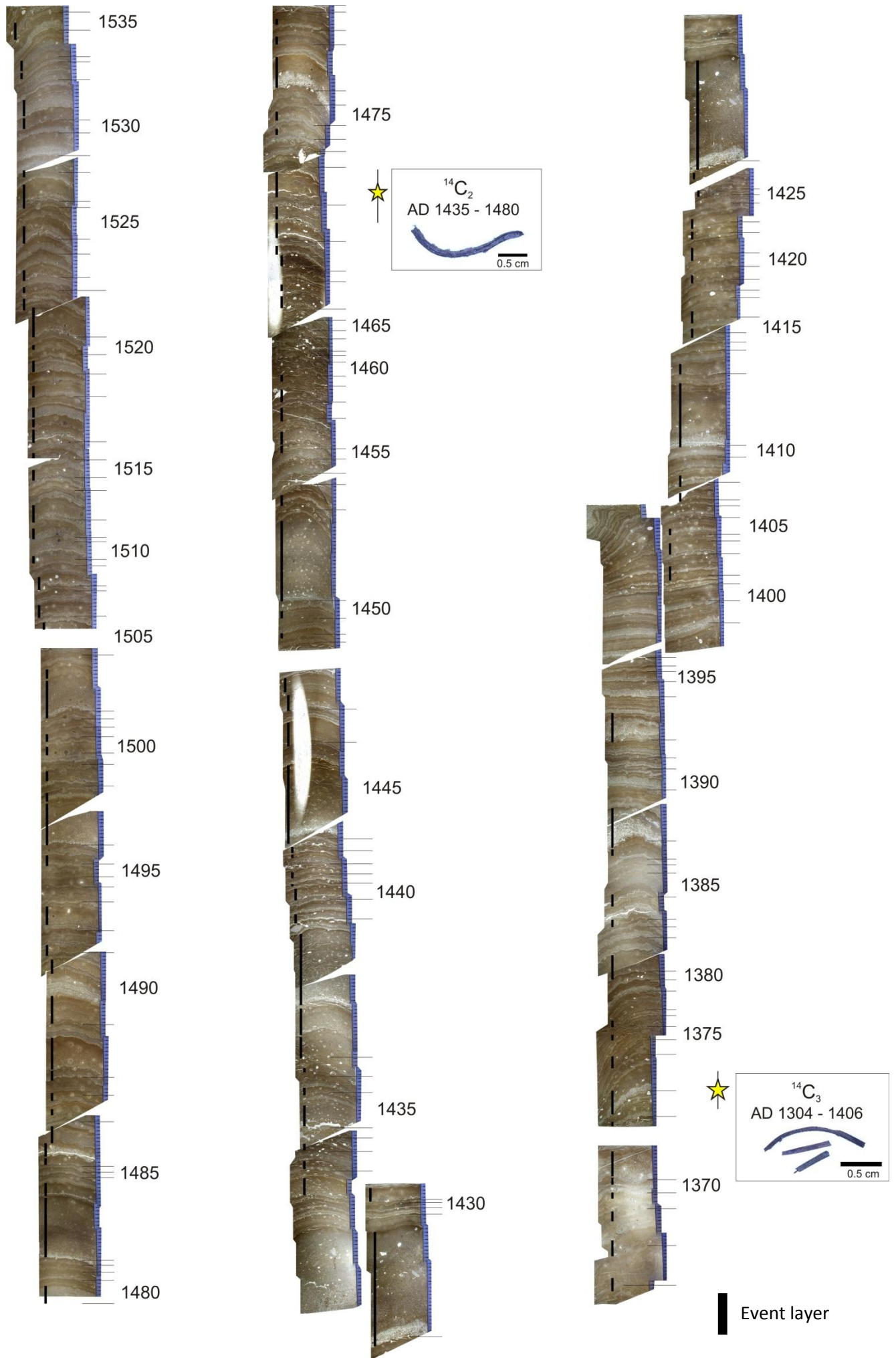


Fig. A1.5 Varve chronology from Lake Oeschinen (part5)

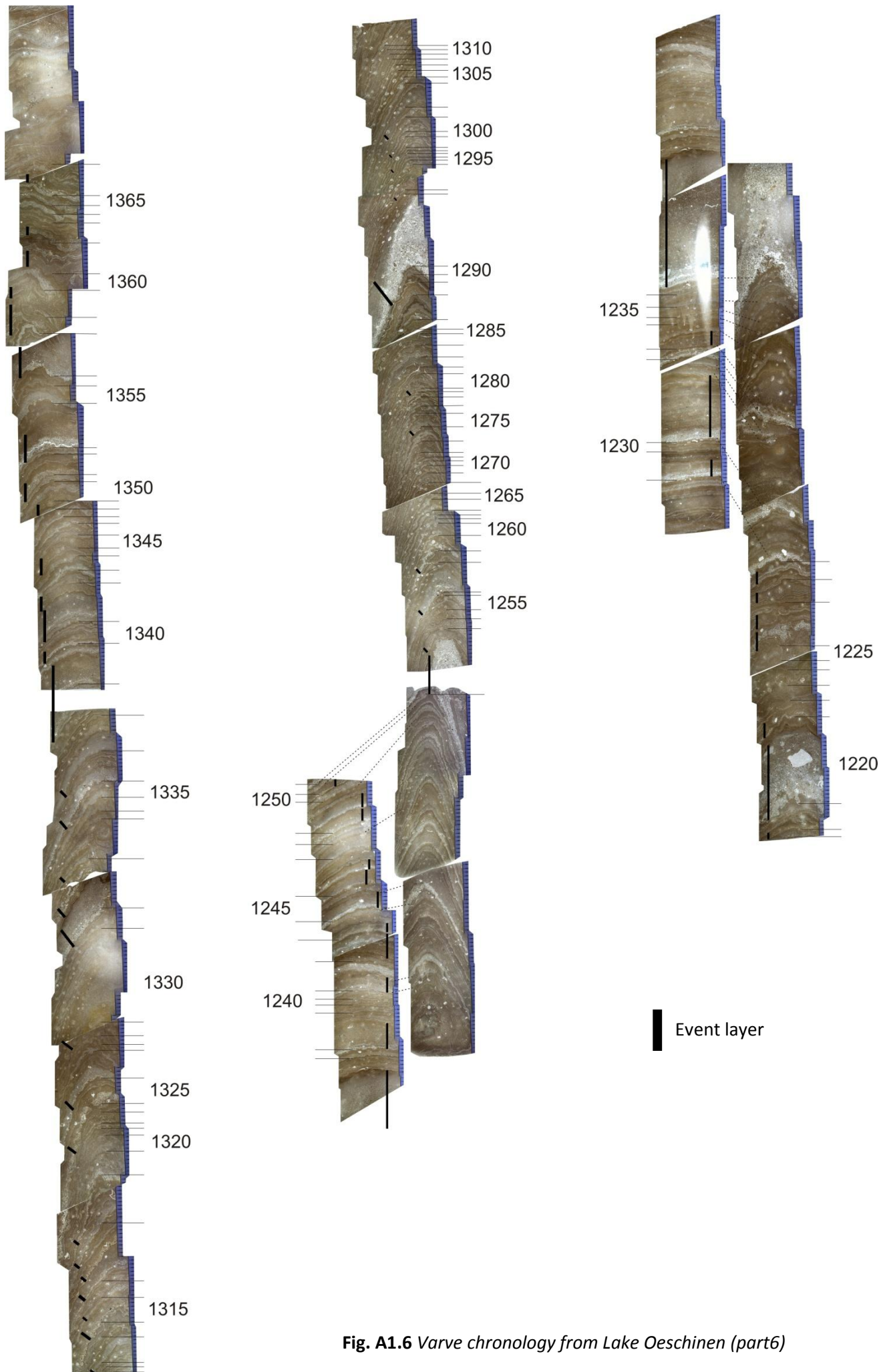


Fig. A1.6 Varve chronology from Lake Oeschinen (part6)

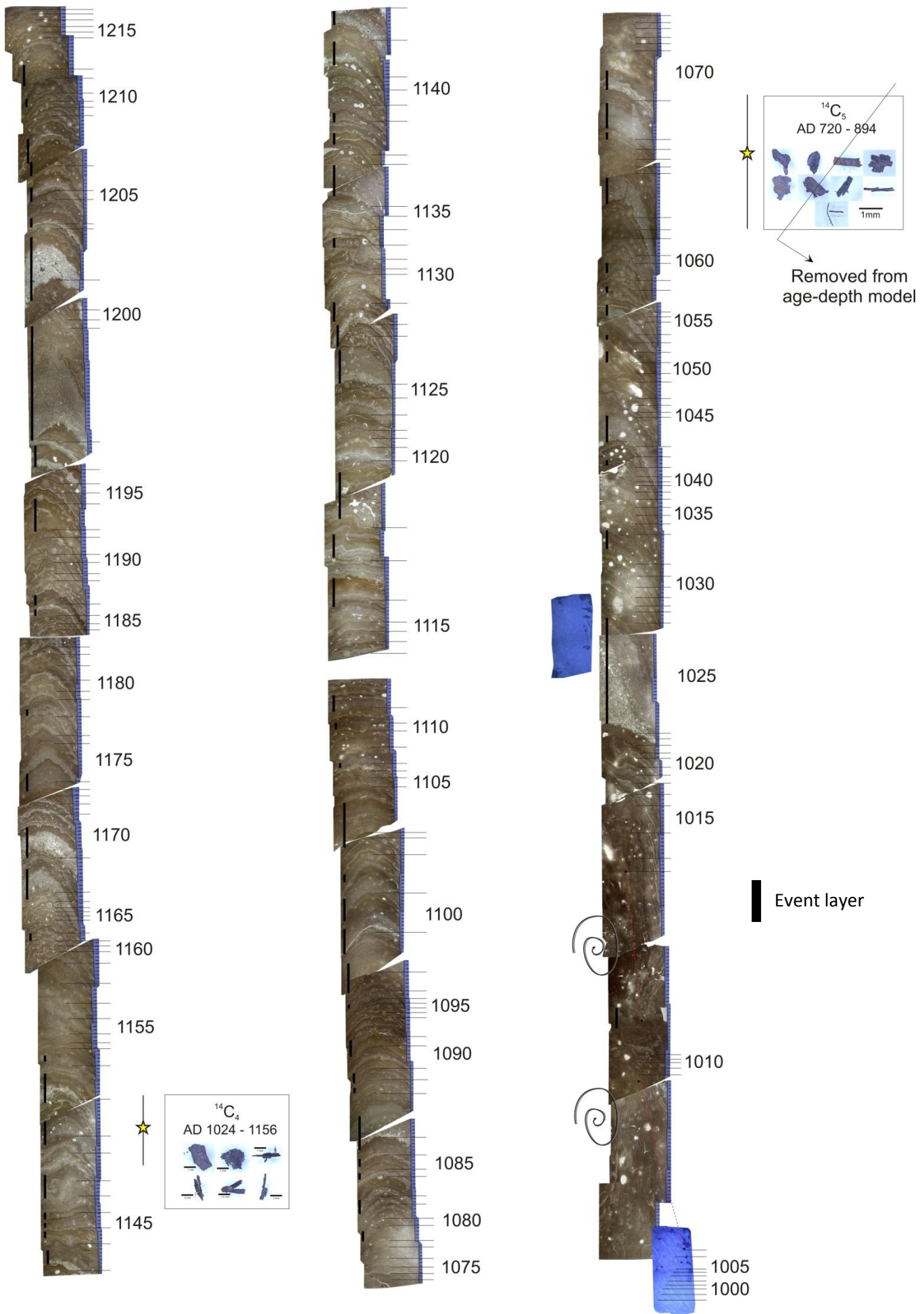


Fig. A1.7 Varve chronology from Lake Oeschinen (part7)

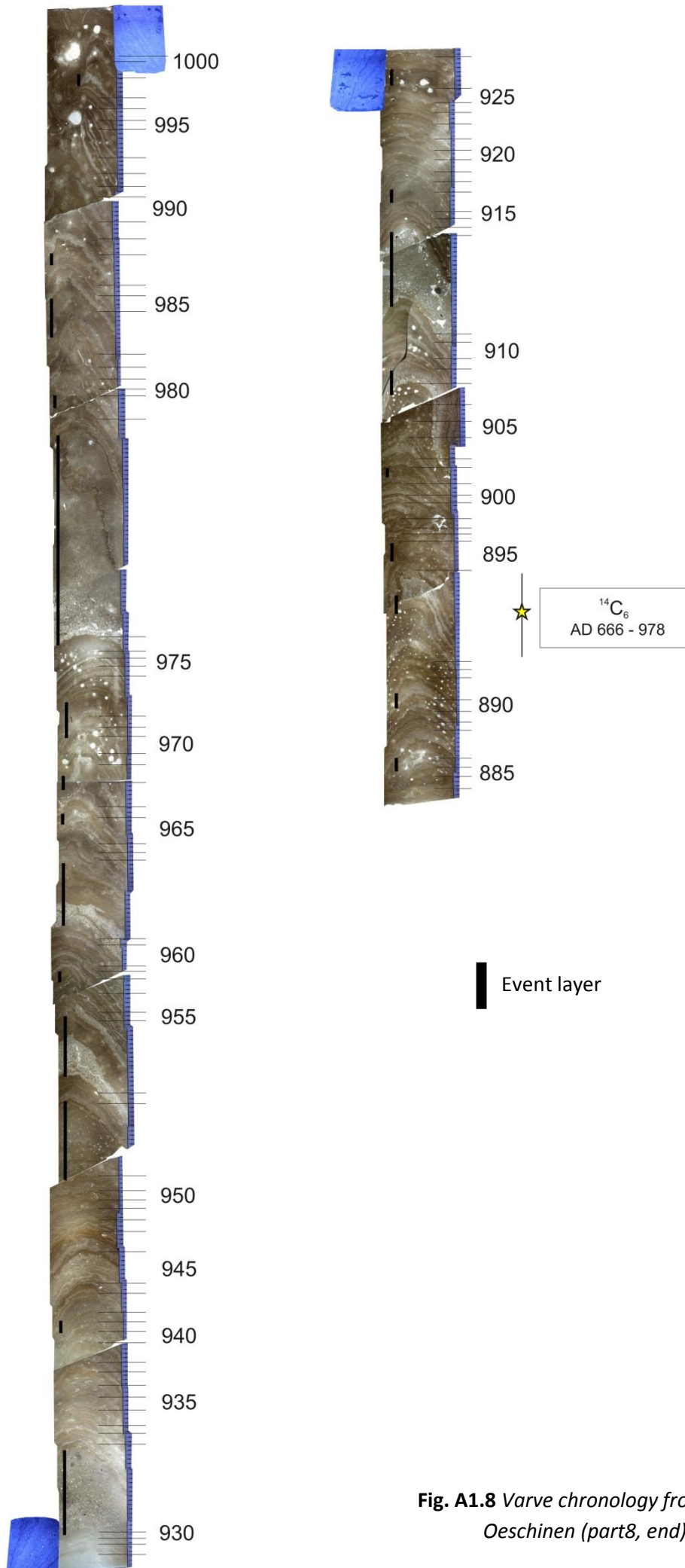


Fig. A1.8 Varve chronology from Lake Oeschinen (part8, end)

Varve Chronology– Lake Žabińskie

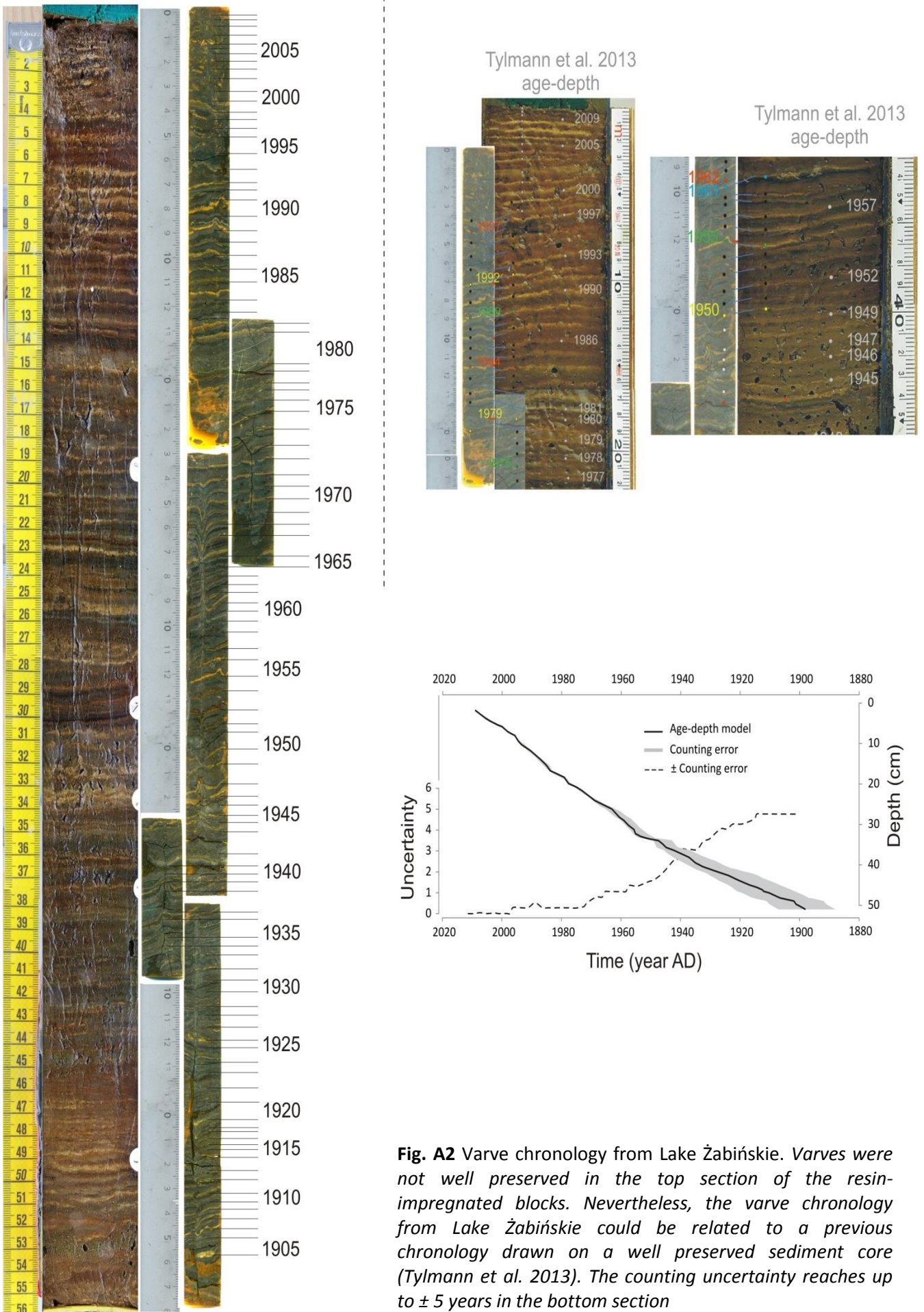


Fig. A2 Varve chronology from Lake Žabińskie. Varves were not well preserved in the top section of the resin-impregnated blocks. Nevertheless, the varve chronology from Lake Žabińskie could be related to a previous chronology drawn on a well preserved sediment core (Tylmann et al. 2013). The counting uncertainty reaches up to ± 5 years in the bottom section

Table A1 Record of varve thickness and turbidite thickness from Lake Oeschinen

Time	Varve (mm)	Time	Varve (mm)	Time	Turbidite (mm)	Time	Turbidite (mm)
2008	2.606	1959	1.411	2008		1959	
2007	5.382	1958	3.57	2007		1958	
2006	3.587	1957	3.704	2006		1957	
2005	2.816	1956	2.026	2005	10.204	1956	
2004	5.253	1955	2.6395	2004		1955	16.9765
2003	2.155	1954	1.827	2003		1954	
2002	4.858	1953	3.15	2002		1953	
2001	6.136	1952	1.823	2001		1952	
2000	2.502	1951	3.383	2000	1.555	1951	
1999	2.259	1950	1.202	1999	7.443	1950	
1998	3.758	1949	2.82	1998		1949	
1997	2.257	1948	2.72	1997		1948	
1996	3.418	1947	1.711	1996		1947	3.165
1995	3.763	1946	1.376	1995		1946	1.801
1994	3.366	1945	2.868	1994		1945	
1993	2.602	1944	0.975	1993		1944	10.44
1992	2.039	1943	2.374	1992	2.473	1943	
1991	2.089	1942	3.952	1991		1942	
1990	2.139	1941	2.98	1990		1941	
1989	3.588	1940	3.377	1989	7.7	1940	
1988	1.794	1939	4.021	1988	3.675	1939	
1987	4.634	1938	3.76	1987	3.474	1938	
1986	3.818	1937	1.792	1986		1937	
1985	4.278	1936	2.081	1985		1936	
1984	3.711	1935	2.428	1984		1935	
1983	4.683	1934	2.833	1983		1934	
1982	6.52	1933	2.2335	1982	30.343	1933	4.7885
1981	3.901	1932	1.853	1981		1932	
1980	4.622	1931	3.581	1980		1931	
1979	6.124	1930	3.54	1979		1930	8.791
1978	6.906	1929	2.318	1978		1929	
1977	2.403	1928	2.45	1977		1928	
1976	2.38	1927	4.509	1976		1927	
1975	4.146	1926	7.334	1975		1926	
1974	3.306	1925	3.929	1974		1925	
1973	4.715	1924	5.223	1973		1924	
1972	1.502	1923	3.468	1972		1923	
1971	2.635	1922	4.737	1971		1922	
1970	2.582	1921	2.8	1970		1921	2.509
1969	3.159	1920	2.97	1969		1920	2.209
1968	2.234	1919	3.665	1968		1919	
1967	2.134	1918	2.139	1967		1918	
1966	2.126	1917	1.827	1966		1917	7.338
1965	6.562	1916	2.892	1965		1916	
1964	2.286	1915	2.5335	1964		1915	7.5265
1963	5.798	1914	1.943	1963		1914	
1962	2.402	1913	2.011	1962	6.13	1913	
1961	4.591	1912	1.543	1961		1912	
1960	1.795	1911	1.402	1960		1911	

Time	Varve (mm)	Time	Varve (mm)	Time	Turbidite (mm)	Time	Turbidite (mm)
1910	1.214	1860	4.176	1910		1860	
1909	3.42	1859	4.026	1909		1859	
1908	1.411	1858	4.125	1908		1858	
1907	2.149	1857	2.371	1907		1857	1.66
1906	1.294	1856	3.876	1906		1856	
1905	3.804	1855	6.972	1905	1.436	1855	
1904	1.615	1854	2.767	1904		1854	5.261
1903	1.109	1853	4.468	1903		1853	
1902	1.496	1852	3.488	1902		1852	
1901	3.804	1851	4.027	1901		1851	
1900	2.936	1850	2.112	1900		1850	
1899	3.128	1849	2.897	1899		1849	
1898	4.524	1848	1.571	1898		1848	7.759
1897	2.214	1847	3.633	1897	4.813	1847	
1896	3.225	1846	4.403	1896		1846	
1895	2.936	1845	2.505	1895		1845	3.241
1894	3.56	1844	1.671	1894		1844	3.781
1893	2.743	1843	4.419	1893		1843	2.996
1892	2.503	1842	4.812	1892	1.925	1842	
1891	2.551	1841	3.857	1891	2.12	1841	2.141
1890	2.743	1840	2.259	1890		1840	4
1889	2.888	1839	2.493	1889	1.974	1839	
1888	1.639	1838	1.871	1888		1838	2.549
1887	1.22	1837	2.16	1887	1.636	1837	8.985
1886	1.286	1836	3.977	1886		1836	
1885	1.827	1835	1.424	1885		1835	6.663
1884	1.366	1834	1.768	1884		1834	
1883	1.688	1833	1.427	1883		1833	
1882	2.33	1832	2.904	1882		1832	2.839
1881	1.348	1831	2.732	1881	1.499	1831	1.936
1880	1.492	1830	2.357	1880		1830	
1879	1.444	1829	3.438	1879	4.621	1829	
1878	1.732	1828	3.142	1878	4.139	1828	
1877	2.84	1827	2.602	1877	1.974	1827	4.174
1876	1.636	1826	1.228	1876	7.364	1826	4.665
1875	1.829	1825	3.143	1875	1.348	1825	3.045
1874	1.822	1824	1.572	1874	1.682	1824	4.223
1873	4.075	1823	2.259	1873		1823	2.816
1872	1.389	1822	3.262	1872	3.002	1822	
1871	3.244	1821	1.773	1871		1821	3.263
1870	5.206	1820	4.017	1870		1820	9.477
1869	6.172	1819	3.628	1869		1819	
1868	3.584	1818	3.339	1868		1818	
1867	2.602	1817	3.977	1867		1817	
1866	3.192	1816	2.737	1866		1816	2.959
1865	5.008	1815	2.099	1865		1815	2.959
1864	1.642	1814	3.329	1864	8.163	1814	5.843
1863	2.111	1813	7.365	1863		1813	
1862	2.848	1812	3.535	1862		1812	3.535
1861	1.942	1811	4.223	1861	14.08	1811	

Time	Varve (mm)	Time	Varve (mm)	Time	Turbidite (mm)	Time	Turbidite (mm)
1810	1.094	1760	5.01	1810	3.242	1760	3.977
1809	1.572	1759	2.406	1809	2.406	1759	
1808	3.241	1758	3.584	1808		1758	4.566
1807	2.16	1757	3.836	1807	4.367	1757	
1806	2.803	1756	3.021	1806		1756	
1805	3.427	1755	0.96	1805	7.525	1755	2.043
1804	2.553	1754	2.308	1804	12.226	1754	3.388
1803	1.87	1753	1.866	1803		1753	
1802	1.929	1752	2.553	1802		1752	
1801	2.132	1751	3.535	1801	1.275	1751	
1800	2.206	1750	3.439	1800		1750	
1799	2.597	1749	4.026	1799		1749	
1798	2.787	1748	4.162	1798		1748	1.56
1797	2.072	1747	3.427	1797	3.596	1747	
1796	2.706	1746	1.625	1796		1746	13.308
1795	1.817	1745	1.768	1795	7.186	1745	
1794	2.603	1744	2.013	1794		1744	
1793	2.048	1743	1.915	1793		1743	
1792	2.506	1742	2.308	1792		1742	
1791	2.21	1741	2.013	1791		1741	8.103
1790	2.553	1740	2.897	1790		1740	2.553
1789	2.112	1739	3.781	1789		1739	
1788	2.259	1738	2.314	1788		1738	2.681
1787	2.406	1737	4.922	1787		1737	5.598
1786	3.388	1736	3.192	1786		1736	5.636
1785	2.946	1735	1.768	1785		1735	2.946
1784	2.357	1734	2.16	1784		1734	
1783	2.637	1733	2.308	1783	2.848	1733	
1782	2.602	1732	2.16	1782	2.505	1732	
1781	2.112	1731	2.161	1781	4.321	1731	3.633
1780	1.032	1730	4.519	1780	3.732	1730	8.79
1779	1.424	1729	6.039	1779		1729	
1778	1.574	1728	2.701	1778	1.263	1728	
1777	1.956	1727	5.843	1777	4.603	1727	6.776
1776	2.75	1726	3.767	1776	2.32	1726	
1775	3.079	1725	2.602	1775		1725	5.008
1774	3.585	1724	3.19	1774		1724	
1773	9.476	1723	2.29	1773		1723	9.28
1772	2.259	1722	2.451	1772		1722	2.772
1771	2.308	1721	1.883	1771		1721	4.251
1770	2.652	1720	2.111	1770		1720	16.743
1769	3.634	1719	2.848	1769		1719	
1768	4.567	1718	3.339	1768		1718	
1767	3.584	1717	3.242	1767	5.058	1717	
1766	4.027	1716	3.093	1766		1716	
1765	5.763	1715	2.406	1765		1715	3.356
1764	2.406	1714	4.763	1764	3.781	1714	
1763	5.156	1713	4.08	1763		1713	
1762	3.786	1712	2.799	1762	3.122	1712	
1761	1.669	1711	1.031	1761	3.241	1711	3.095

Time	Varve (mm)	Time	Varve (mm)	Time	Turbidite (mm)	Time	Turbidite (mm)
1710	2.357	1660	4.203	1710		1660	
1709	2.406	1659	3.781	1709		1659	4.616
1708	2.946	1658	4.335	1708		1658	
1707	2.739	1657	3.589	1707	1.583	1657	3.826
1706	1.848	1656	4.367	1706	17.298	1656	3.343
1705	4.131	1655	2.357	1705		1655	2.259
1704	2.357	1654	5.156	1704		1654	3.88
1703	4.175	1653	3.279	1703	1.866	1653	
1702	3.781	1652	1.915	1702		1652	
1701	1.178	1651	1.964	1701	7.71	1651	
1700	2.406	1650	4.763	1700		1650	
1699	1.866	1649	3.328	1699		1649	4.939
1698	4.8	1648	3.29	1698	12.812	1648	10.315
1697	0.983	1647	5.99	1697	3.192	1647	
1696	1.719	1646	3.242	1696		1646	4.518
1695	1.228	1645	3.98	1695		1645	5.857
1694	1.522	1644	1.51	1694		1644	2.413
1693	1.473	1643	2.379	1693		1643	
1692	2.946	1642	2.051	1692		1642	2.716
1691	2.3	1641	3.307	1691	9.806	1641	
1690	2.341	1640	2.023	1690	5.369	1640	2.59
1689	2.736	1639	2.956	1689		1639	
1688	2.75	1638	2.365	1688	5.012	1638	
1687	3.079	1637	3.619	1687	3.144	1637	4.615
1686	1.523	1636	2.406	1686	4.321	1636	1.966
1685	3.149	1635	2.456	1685		1635	
1684	3.486	1634	1.935	1684		1634	3.614
1683	3.192	1633	2.848	1683		1633	3.111
1682	2.308	1632	6.187	1682		1632	
1681	1.425	1631	1.817	1681	3.732	1631	2.504
1680	1.621	1630	2.614	1680		1630	5.049
1679	1.916	1629	4.851	1679		1629	3.547
1678	2.89	1628	1.768	1678	2.391	1628	2.517
1677	3.242	1627	3.474	1677	2.849	1627	
1676	2.622	1626	2.31	1676	1.85	1626	3.291
1675	3.391	1625	2.848	1675		1625	
1674	2.656	1624	2.469	1674		1624	12.247
1673	2.376	1623	3.307	1673	3.68	1623	
1672	2.21	1622	1.768	1672	4.128	1622	4.388
1671	4.272	1621	1.237	1671		1621	4.379
1670	5.99	1620	1.901	1670		1620	1.647
1669	0.884	1619	1.669	1669	1.965	1619	
1668	4.223	1618	1.719	1668		1618	2.91
1667	2.456	1617	1.216	1667	4.35	1617	
1666	1.817	1616	3.046	1666	3.536	1616	
1665	1.79	1615	2.161	1665	1.72	1615	2.652
1664	2.69	1614	2.259	1664		1614	32.588
1663	4.102	1613	3.83	1663		1613	
1662	2.552	1612	2.651	1662		1612	
1661	2.188	1611	6.614	1661	2.028	1611	4.42

Time	Varve (mm)	Time	Varve (mm)	Time	Turbidite (mm)	Time	Turbidite (mm)
1610	5.107	1560	3.299	1610		1560	3.111
1609	2.457	1559	3.977	1609		1559	6.117
1608	3.977	1558	2.455	1608		1558	
1607	6.874	1557	1.08	1607		1557	2.603
1606	6.138	1556	2.652	1606		1556	
1605	4.419	1555	3.051	1605		1555	1.982
1604	3.103	1554	2.312	1604	3.079	1554	
1603	3.516	1553	1.432	1603		1553	4.677
1602	2.454	1552	1.915	1602		1552	
1601	1.787	1551	1.916	1601		1551	
1600	0.871	1550	2.975	1600	1.647	1550	17.187
1599	1.693	1549	5.239	1599	1.74	1549	
1598	4.751	1548	2.259	1598		1548	
1597	5.108	1547	2.16	1597	45.929	1547	
1596	3.977	1546	1.849	1596		1546	2.522
1595	3.339	1545	1.801	1595		1545	1.785
1594	2.129	1544	3.313	1594	2.408	1544	
1593	1.719	1543	1.13	1593		1543	1.572
1592	2.225	1542	2.754	1592		1542	
1591	2.586	1541	2.946	1591		1541	
1590	1.62	1540	2.765	1590	2.848	1540	30.986
1589	2.996	1539	1.978	1589		1539	2.386
1588	2.211	1538	1.289	1588		1538	
1587	3.186	1537	1.542	1587	4.566	1537	
1586	1.887	1536	1.859	1586		1536	1.262
1585	2.634	1535	2.75	1585		1535	
1584	2.187	1534	4.808	1584		1534	
1583	1.916	1533	2.576	1583	12.491	1533	
1582	2.603	1532	1.908	1582		1532	5.832
1581	2.145	1531	1.849	1581		1531	4.592
1580	2.75	1530	2.087	1580		1530	
1579	2.554	1529	3.518	1579		1529	4.294
1578	2.308	1528	6.384	1578	2.111	1528	
1577	3.585	1527	3.28	1577		1527	
1576	4.126	1526	2.207	1576		1526	1.85
1575	3.291	1525	1.789	1575		1525	6.661
1574	1.849	1524	3.697	1574	4.188	1524	
1573	3.142	1523	2.386	1573		1523	5.005
1572	2.259	1522	3.877	1572	1.915	1522	2.333
1571	3.095	1521	2.411	1571	2.013	1521	3.282
1570	2.799	1520	2.165	1570	6.678	1520	4.709
1569	2.081	1519	2.095	1569		1519	7.738
1568	2.112	1518	2.641	1568		1518	3.225
1567	2.997	1517	2.991	1567		1517	3.586
1566	1.278	1516	2.516	1566	2.8	1516	4.355
1565	2.21	1515	2.388	1565		1515	7.644
1564	2.063	1514	2.091	1564		1514	2.207
1563	4.37	1513	1.908	1563		1513	3.282
1562	2.504	1512	2.445	1562		1512	2.507
1561	3.859	1511	1.671	1561		1511	5.511

Time	Varve (mm)	Time	Varve (mm)	Time	Turbidite (mm)	Time	Turbidite (mm)
1510	2.147	1460	1.971	1510	2.505	1460	1.377
1509	3.88	1459	1.79	1509		1459	2.088
1508	2.326	1458	1.55	1508	3.759	1458	2.37
1507	1.789	1457	3.897	1507	3.803	1457	6.394
1506	4.037	1456	3.34	1506		1456	
1505	1.968	1455	3.519	1505	3.757	1455	
1504	2.695	1454	1.968	1504	2.398	1454	
1503	2.564	1453	1.194	1503	16.306	1453	3.042
1502	2.088	1452	2.624	1502		1452	
1501	2.206	1451	2.267	1501	2.505	1451	25.965
1500	2.15	1450	3.044	1500	3.4	1450	3.204
1499	3.995	1449	2.041	1499	2.326	1449	2.329
1498	2.207	1448	2.277	1498	2.266	1448	
1497	2.571	1447	3.339	1497	13.656	1447	5.688
1496	1.845	1446	4.922	1496	2.82	1446	7.258
1495	2.505	1445	1.968	1495	2.747	1445	22.057
1494	3.459	1444	2.383	1494		1444	2.448
1493	2.028	1443	2.202	1493	5.069	1443	
1492	3.441	1442	2.267	1492		1442	2.752
1491	1.849	1441	1.79	1491	3.936	1441	3.101
1490	2.565	1440	2.907	1490	9.346	1440	
1489	2.267	1439	2.338	1489	8.946	1439	2.749
1488	2.386	1438	2.611	1488	3.995	1438	22.111
1487	1.61	1437	2.808	1487	5.487	1437	3.536
1486	1.79	1436	2.624	1486		1436	2.406
1485	2.743	1435	2.445	1485		1435	8.603
1484	1.674	1434	1.909	1484	18.409	1434	
1483	1.85	1433	2.564	1483		1433	2.627
1482	2.206	1432	1.969	1482	2.565	1432	2.683
1481	2.296	1431	1.372	1481	4.532	1431	5.725
1480	1.73	1430	2.206	1480	2.316	1430	
1479	1.479	1429	2.147	1479	3.355	1429	
1478	1.431	1428	3.638	1478	1.968	1428	
1477	2.923	1427	2.507	1477	8.949	1427	34.096
1476	3.103	1426	1.62	1476		1426	2.088
1475	2.53	1425	1.73	1475	2.641	1425	
1474	2.516	1424	2.567	1474	2.868	1424	
1473	3.565	1423	1.55	1473		1423	3.578
1472	2.565	1422	1.312	1472		1422	1.908
1471	2.743	1421	2.266	1471		1421	4.95
1470	2.266	1420	2.027	1470	8.81	1420	2.923
1469	2.924	1419	2.624	1469	4.592	1419	
1468	2.865	1418	2.505	1468	3.757	1418	
1467	1.777	1417	2.206	1467		1417	
1466	3.529	1416	2.683	1466	3.728	1416	3.522
1465	2.68	1415	2.027	1465		1415	3.399
1464	2.712	1414	2.266	1464		1414	
1463	1.641	1413	2.445	1463		1413	
1462	2.054	1412	2.743	1462		1412	5.012
1461	2.471	1411	3.101	1461		1411	19.037

Time	Varve (mm)	Time	Varve (mm)	Time	Turbidite (mm)	Time	Turbidite (mm)
1410	2.348	1360	2.451	1410	2.385	1360	
1409	1.79	1359	2.211	1409	2.027	1359	
1408	2.148	1358	3.34	1408		1358	5.482
1407	2.07	1357	3.208	1407	2.448	1357	2.603
1406	1.927	1356	1.971	1406	2.849	1356	10.553
1405	2.505	1355	2.04	1405		1355	2.737
1404	2.147	1354	3.359	1404	2.147	1354	2.68
1403	1.789	1353	1.923	1403	2.923	1353	9.988
1402	2.446	1352	2.627	1402		1352	
1401	2.386	1351	1.755	1401	4.294	1351	3.344
1400	5.746	1350	1.627	1400		1350	1.834
1399	7.019	1349	1.462	1399		1349	3.568
1398	6.142	1348	2.829	1398		1348	
1397	3.996	1347	3.006	1397		1347	
1396	3.702	1346	1.982	1396		1346	
1395	4.353	1345	2.62	1395		1345	4.469
1394	5.111	1344	2.762	1394		1344	
1393	2.148	1343	2.633	1393	8.895	1343	
1392	3.143	1342	2.448	1392	2.43	1342	8.89
1391	3.041	1341	2.505	1391		1341	3.938
1390	4.991	1340	2.616	1390	4.175	1340	8.541
1389	2.436	1339	2.291	1389	9.789	1339	
1388	1.969	1338	2.138	1388	3.816	1338	3.378
1387	2.267	1337	2.101	1387		1337	5.775
1386	3.638	1336	3.28	1386		1336	2.684
1385	4.477	1335	2.744	1385	4.532	1335	
1384	1.971	1334	2.106	1384	2.743	1334	
1383	3.58	1333	2.048	1383		1333	3.712
1382	3.342	1332	2.316	1382		1332	7.136
1381	2.386	1331	5.772	1381	6.968	1331	
1380	4.178	1330	3.222	1380		1330	8.562
1379	2.326	1329	4.55	1379	1.771	1329	
1378	2.031	1328	3.406	1378	2.056	1328	
1377	3.051	1327	2.834	1377		1327	
1376	2.118	1326	2.581	1376		1326	3.883
1375	3.373	1325	2.345	1375	2.108	1325	5.275
1374	1.674	1324	2.825	1374	2.167	1324	
1373	3.759	1323	2.439	1373	9.128	1323	
1372	3.816	1322	2.358	1372	4.876	1322	
1371	2.147	1321	3.689	1371	2.803	1321	
1370	3.992	1320	2.884	1370	2.445	1320	
1369	2.223	1319	3.581	1369	5.194	1319	5.227
1368	3.354	1318	4.678	1368		1318	4.955
1367	2.61	1317	1.798	1367	6.542	1317	6.391
1366	2.627	1316	2.304	1366		1316	2.987
1365	2.707	1315	4.008	1365	2.803	1315	3.278
1364	2.684	1314	3.952	1364		1314	
1363	2.865	1313	3.121	1363		1313	3.972
1362	2.743	1312	2.624	1362	2.148	1312	
1361	2.923	1311	0.931	1361	6.065	1311	1.001

Time	Varve (mm)	Time	Varve (mm)	Time	Turbidite (mm)	Time	Turbidite (mm)
1310	0.894	1260	1.674	1310		1260	
1309	1.224	1259	2.984	1309		1259	3.761
1308	0.634	1258	2.872	1308		1258	
1307	1.308	1257	0.827	1307	0.886	1257	15.45
1306	0.992	1256	2.145	1306	1.637	1256	1.923
1305	2.085	1255	2.108	1305		1255	
1304	1.34	1254	1.886	1304		1254	3.899
1303	1.28	1253	1.591	1303	2.775	1253	2.893
1302	1.793	1252	1.417	1302	1.496	1252	1.779
1301	0.956	1251	2.539	1301	2.507	1251	
1300	1.789	1250	2.387	1300	1.436	1250	3.191
1299	1.491	1249	3.188	1299		1249	4.985
1298	1.716	1248	2.932	1298		1248	
1297	1.377	1247	2.868	1297		1247	3.041
1296	1.73	1246	2.805	1296		1246	
1295	1.626	1245	1.849	1295		1245	4.177
1294	1.704	1244	2.803	1294		1244	
1293	1.372	1243	2.505	1293		1243	
1292	2.005	1242	2.505	1292		1242	
1291	2.07	1241	2.386	1291	9.116	1241	7.767
1290	3.044	1240	3.787	1290		1240	
1289	2.176	1239	2.565	1289		1239	38.93
1288	2.507	1238	2.15	1288		1238	
1287	3.756	1237	1.793	1287	1.857	1237	
1286	1.971	1236	2.088	1286		1236	1.73
1285	2.031	1235	2.505	1285		1235	
1284	1.923	1234	2.451	1284	1.793	1234	4.115
1283	1.614	1233	2.386	1283		1233	
1282	1.258	1232	2.924	1282	1.873	1232	
1281	2.049	1231	2.805	1281		1231	18.655
1280	1.674	1230	4.538	1280	2.24	1230	2.923
1279	2.279	1229	2.624	1279		1229	
1278	2.868	1228	3.22	1278		1228	
1277	1.561	1227	2.683	1277	1.793	1227	4.595
1276	3.354	1226	3.207	1276		1226	4.353
1275	1.407	1225	2.81	1275		1225	2.857
1274	1.308	1224	2.296	1274		1224	
1273	1.456	1223	2.041	1273		1223	
1272	1.629	1222	2.104	1272		1222	2.115
1271	1.333	1221	2.273	1271		1221	1.976
1270	1.888	1220	3.997	1270		1220	23.185
1269	1.463	1219	2.235	1269		1219	2.404
1268	1.362	1218	1.794	1268		1218	
1267	1.518	1217	1.971	1267		1217	
1266	1.935	1216	2.028	1266	2.282	1216	
1265	2.648	1215	2.095	1265	1.496	1215	
1264	2.417	1214	1.909	1264		1214	
1263	1.966	1213	3.234	1263		1213	7.648
1262	1.731	1212	1.579	1262		1212	3.199
1261	1.569	1211	1.691	1261	6.399	1211	

Time	Varve (mm)	Time	Varve (mm)	Time	Turbidite (mm)	Time	Turbidite (mm)
1210	1.687	1160	4.817	1210		1160	
1209	2.226	1159	4.518	1209		1159	
1208	2.226	1158	4.247	1208		1158	
1207	3.345	1157	3.627	1207	6.983	1157	
1206	3.203	1156	2.516	1206	5.072	1156	
1205	2.803	1155	3.115	1205		1155	5.072
1204	1.548	1154	3.018	1204	3.878	1154	9.052
1203	2.155	1153	3.415	1203		1153	7.51
1202	1.185	1152	3.07	1202	12.766	1152	
1201	1.021	1151	3.996	1201		1151	7.676
1200	1.787	1150	3.221	1200	1.531	1150	
1199	2.803	1149	3.757	1199	24.014	1149	
1198	3.699	1148	2.505	1198	6.619	1148	
1197	3.051	1147	2.626	1197		1147	
1196	2.908	1146	5.032	1196		1146	5.465
1195	4.118	1145	4.066	1195	4.238	1145	5.163
1194	2.984	1144	3.824	1194		1144	
1193	3.52	1143	5.092	1193		1143	
1192	2.627	1142	3.206	1192		1142	
1191	3.52	1141	2.82	1191		1141	
1190	3.103	1140	1.982	1190		1140	2.271
1189	3.106	1139	2.517	1189		1139	1.696
1188	2.525	1138	3.616	1188	3.103	1138	10.179
1187	1.849	1137	3.572	1187		1137	
1186	1.79	1136	1.811	1186		1136	
1185	2.091	1135	2.131	1185		1135	
1184	2.407	1134	3.199	1184		1134	
1183	2.077	1133	3.147	1183		1133	
1182	1.95	1132	1.383	1182		1132	1.569
1181	1.95	1131	4.295	1181		1131	1.628
1180	2.39	1130	2.53	1180	2.772	1130	2.966
1179	2.608	1129	1.746	1179		1129	2.694
1178	2.266	1128	3.596	1178	3.578	1128	
1177	2.636	1127	3.285	1177	2.323	1127	
1176	3.924	1126	3.11	1176		1126	10.559
1175	1.962	1125	2.549	1175	4.723	1125	3.645
1174	2.199	1124	2.826	1174		1124	
1173	2.451	1123	3.502	1173		1123	
1172	2.885	1122	2.868	1172		1122	
1171	4.071	1121	4.355	1171		1121	
1170	2.984	1120	3.161	1170	8.076	1120	
1169	2.702	1119	4.598	1169	4.593	1119	15.578
1168	2.991	1118	4.474	1168		1118	8.128
1167	2.041	1117	5.964	1167		1117	7.698
1166	1.923	1116	3.106	1166		1116	
1165	1.194	1115	3.783	1165		1115	
1164	2.207	1114	4.808	1164		1114	
1163	2.445	1113	1.733	1163	2.805	1113	
1162	2.06	1112	1.808	1162		1112	4.397
1161	4.036	1111	1.491	1161		1111	4.72

Time	Varve (mm)	Time	Varve (mm)	Time	Turbidite (mm)	Time	Turbidite (mm)
1110	3.34	1060	1.851	1110		1060	
1109	1.969	1059	2.641	1109	3.877	1059	
1108	2.388	1058	1.857	1108		1058	
1107	3.225	1057	1.765	1107		1057	2.218
1106	4.066	1056	1.58	1106		1056	
1105	2.463	1055	0.895	1105	9.81	1055	
1104	2.581	1054	1.496	1104		1054	
1103	2.775	1053	2.234	1103	2.056	1053	3.062
1102	4.623	1052	2.135	1102		1052	4.07
1101	3.103	1051	1.611	1101	11.097	1051	
1100	3.042	1050	1.695	1100	9.733	1050	
1099	2.266	1049	1.52	1099	1.361	1049	
1098	2.303	1048	1.857	1098		1048	
1097	1.188	1047	2.094	1097		1047	2.232
1096	1.429	1046	1.728	1096		1046	
1095	2.233	1045	1.95	1095		1045	
1094	3.111	1044	2.257	1094	3.078	1044	
1093	1.824	1043	1.821	1093		1043	5.746
1092	2.235	1042	1.854	1092	2.598	1042	
1091	3.011	1041	2.353	1091		1041	
1090	2.516	1040	2.297	1090		1040	
1089	2.69	1039	3.622	1089		1039	
1088	1.885	1038	2.008	1088		1038	
1087	2.938	1037	1.827	1087	10.598	1037	
1086	2.054	1036	1.502	1086	2.64	1036	
1085	1.822	1035	1.774	1085		1035	
1084	2.627	1034	1.53	1084	5.291	1034	
1083	2.21	1033	1.774	1083		1033	
1082	2.63	1032	2.193	1082	2.344	1032	2.717
1081	3.404	1031	2.7	1081		1031	
1080	2.083	1030	1.689	1080		1030	
1079	1.939	1029	2.004	1079		1029	
1078	2.304	1028	1.481	1078		1028	
1077	2.356	1027	2.32	1077		1027	
1076	2.206	1026	1.999	1076		1026	
1075	2.603	1025	1.776	1075		1025	23.875
1074	1.948	1024	1.457	1074		1024	
1073	1.864	1023	1.882	1073		1023	
1072	3.062	1022	1.693	1072		1022	
1071	2.733	1021	2.404	1071		1021	
1070	2.319	1020	1.103	1070	6.652	1020	
1069	2.546	1019	1.114	1069		1019	
1068	1.592	1018	2.32	1068	6.491	1018	
1067	1.812	1017	1.974	1067		1017	
1066	2.454	1016	1.567	1066		1016	
1065	2.72	1015	1.788	1065		1015	
1064	2.326	1014	2.008	1064		1014	
1063	1.54	1013	1.845	1063	9.246	1013	
1062	1.784	1012	1.93	1062		1012	9.912
1061	1.622	1011	2.061	1061		1011	

Time	Varve (mm)	Time	Varve (mm)	Time	Turbidite (mm)	Time	Turbidite (mm)
1010	1.245	960	1.708	1010		960	
1009	1.573	959	1.931	1009		959	1.982
1008	2.119	958	1.872	1008		958	
1007	2.508	957	1.695	1007		957	
1006	2.38	956	2.086	1006		956	
1005	1.941	955	2.337	1005		955	
1004	2.203	954	2.205	1004		954	
1003	2.466	953	2.228	1003		953	12.095
1002	1.752	952	3.661	1002		952	
1001	3.096	951	3.578	1001		951	18.612
1000	2.02	950	2.147	1000	4.1	950	
999	1.54	949	2.445	999		949	
998	1.55	948	3.28	998		948	
997	1.754	947	2.744	997		947	
996	1.633	946	3.769	996		946	
995	1.669	945	7.3	995		945	
994	1.156	944	2.422	994		944	
993	1.049	943	1.699	993		943	
992	1.678	942	3.044	992		942	4.017
991	2.094	941	3.471	991	2.704	941	
990	2.616	940	2.267	990		940	2.753
989	2.851	939	2.326	989		939	
988	3.094	938	3.459	988		938	
987	2.387	937	2.449	987	2.882	937	
986	2.07	936	2.982	986		936	
985	1.978	935	2.922	985	4.61	935	
984	1.979	934	2.932	984		934	
983	1.265	933	1.773	983		933	
982	1.649	932	2.488	982		932	
981	1.898	931	2.235	981		931	18.914
980	1.628	930	2.049	980	2.254	930	
979	2.784	929	2.991	979	36.726	929	
978	4.488	928	2.813	978		928	4.476
977	1.76	927	1.526	977		927	3.734
976	1.701	926	2.525	976		926	
975	2.23	925	3.029	975		925	
974	2.705	924	3.353	974		924	
973	2.229	923	2.893	973	4.807	923	
972	1.936	922	1.857	972		922	
971	2.054	921	2.219	971		921	
970	1.803	920	2.279	970		920	
969	2.323	919	1.872	969		919	
968	2.428	918	2.333	968		918	
967	2.877	917	1.986	967		917	1.773
966	2.972	916	1.184	966		916	
965	1.789	915	1.313	965	3.665	915	
964	2.301	914	1.313	964		914	
963	1.975	913	2.07	963		913	14.188
962	2.565	912	3.196	962		912	
961	2.116	911	1.841	961	13.373	911	

Time	Varve (mm)
910	1.81
909	2.397
908	2.517
907	2.924
906	2.412
905	2.505
904	2.803
903	1.976
902	1.85
901	1.502
900	2.567
899	3.177
898	2.188
897	2.041
896	2.52
895	3.137
894	2.567
893	1.789
892	3.041
891	3.818
890	3.578
889	2.388
888	2.565
887	2.686
886	2.088
885	2.863
884	3.101

Time	Turbidite (mm)
910	
909	6.284
908	
907	
906	
905	
904	
903	2.404
902	
901	
900	
899	
898	
897	
896	
895	3.348
894	10.054
893	
892	
891	
890	
889	
888	
887	
886	5.256
885	
884	

Appendix A.3 High performance Liquid Chromatography (HPLC) technique: extraction, identification and quantification of sedimentary pigment compounds

All steps that comprise sample sectioning, pigment standard preparation, pigment extraction, and measurements were done with minimal light, oxygen and heat exposure in order to prevent pigments from degrading.

Sedimentary pigments were extracted from 0.2 g of freeze-dried sediment using 3 mL pure acetone. Extracts were filtered using a syringe equipped with a 0.2 μm Nylon filter until a colourless filtrate was obtained. After solvent evaporation under an N_2 stream the dried pigment extracts were stored at $-18\text{ }^\circ\text{C}$ prior analysis.

The reversed-phase HPLC procedure was a modified method of Airs et al. (2001). Dried pigment extracts were eluted in a mixture of methanol, acetonitrile and 0.5 M ammonium acetate (80:15:5) and injected into a Beckmann Coulter HPLC system with a Waters Spherisorb ODS2 5 μm column (250 mm x 4.6 mm). The pigments were separated using a mobile phase gradient with a ternary solvent system given in the table below at a flow rate of 1 mL min^{-1} .

Time	A / % ^{a)}	B / % ^{b)}	C / % ^{c)}
0	100	0	0
5	100	0	0
60	36.8	63.2	0
61	0	100	0
66	0	0	100
71	0	0	100
76	100	0	0
88	100	0	0

a) solvent A (methanol, acetonitrile, 0.5 M ammonium acetate; 80:15:5), b) solvent B (methanol, acetonitrile, ethyl acetate; 20:15:65), c) solvent C (methanol, acetonitrile, ethyl acetate; 1:1:98)

Pigments were detected using a diode array (Beckmann model 168) and a fluorescence detector (RF-20A Shimadzu at 438 nm and 470 nm). The absorption was measured at 438 nm and 470 nm. In addition, a complete absorption spectrum from 300 to 600 nm was recorded at a 1 Hz repetition rate. Fluorescence spectra were recorded at 440 nm excitation and 660 nm detection wavelengths. Pigments were identified based on their retention time and absorption/emission properties and quantified using the peak area of the chromatogram (Fig. A3, next page).

Pigment concentrations were derived from calibrated dilution series of standard stock-solutions. Chlorophyll a, lutein and β -carotene were obtained from Sigma-Aldrich dissolved in acetone. Phaeophytin *a* and *b* were prepared from a crude spinach extract dissolved in 10 mL of acetone and treated with 5-10 mL of 0.1 M hydrochloric acid. The mixture was extracted with 2-5 mL of petroleum ether. The ether phase was washed three times with 1-2 mL of brine and dried over sodium sulphate. The phaeophytin extracts were applied onto a preparative TLC plate (glass, 2 mm silica gel layer). Petroleum ether (60 %), cyclohexane (16 %), acetone (10 %), ethyl acetate (10 %) and methanol (4 %) were used as mobile phase. HPLC pigment concentrations were expressed in $\mu\text{g g}^{-1}$ dry sample mass.

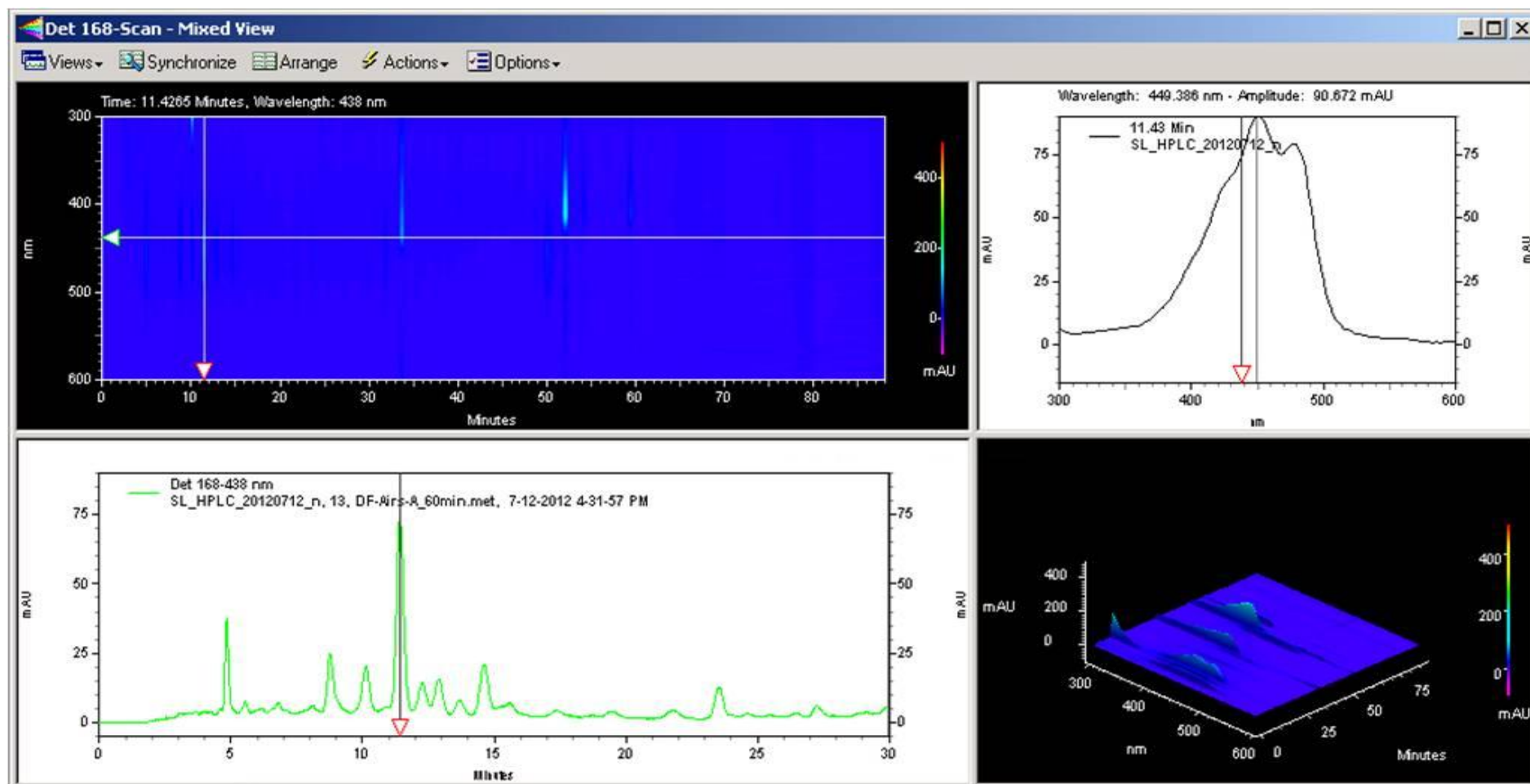


Fig. A.3 Example of a mixed view during HPLC measurements. Sedimentary pigment identification was based on retention time from the HPLC chromatogram (lower left panel) and cross-validated with known spectral characteristics of each pigment in the visible range (upper right panel). The peak targeted here is for lutein.

Erklärung

gemäss Art. 28 Abs. 2 RSL 05

Name/Vorname:

Matrikelnummer:

Studiengang:

Bachelor Master Dissertation

Titel der Arbeit:

.....

.....

LeiterIn der Arbeit:

.....

Ich erkläre hiermit, dass ich diese Arbeit selbständig verfasst und keine anderen als die angegebenen Quellen benutzt habe. Alle Stellen, die wörtlich oder sinngemäss aus Quellen entnommen wurden, habe ich als solche gekennzeichnet. Mir ist bekannt, dass andernfalls der Senat gemäss Artikel 36 Absatz 1 Buchstabe r des Gesetzes vom 5. September 1996 über die Universität zum Entzug des auf Grund dieser Arbeit verliehenen Titels berechtigt ist.

Ich gewähre hiermit Einsicht in diese Arbeit.

.....

Ort/Datum

.....

Unterschrift

Curriculum vitæ

Name: Amann Benjamin, Jean-François
Date of birth: 08 January 1988
Place of birth: Belfort, France

EDUCATION

- 2011 - 2014 **Doctoral studies in Climate Sciences**
Oeschger Centre for Climate Change Research & Institute of Geography,
University of Bern - Switzerland
Dissertation title: 'Varved lake sediments as archives for high-resolution millennial-long
climate reconstructions: from sedimentation processes to paleoclimatology'
Supervisor: Prof.Dr. Martin Grosjean (University of Bern, Switzerland)
External referee: Prof. Dr. Scott Lamoureux (Queen's University, Ontario Canada)
Chair of the PhD defense: Prof. Dr. Flavio Anselmetti (University of Bern, Switzerland)
- 2009 - 2011 **M.Sc. à finalité Recherche - Hydrology, Hydrochemistry, Soil, Environment**
Université Paul Sabatier II, Toulouse - France
Dissertation title: 'Tracing early atmospheric metal pollution from mining in central
Sweden: multi-element analysis of a peat record from Borrnessen'
Supervisor1: Prof. Dr. Richard Bindler (Umeå University, Sweden)
Supervisor2: Dr. François de Vleeschouwer (EcoLab Toulouse, France)
- 2006 - 2009 **Bachelor degree in Physics-Chemistry**
Université des Sciences et Techniques, Besançon - France

PUBLICATIONS

Amann B., Mauchle F., Grosjean M., 2014. Quantitative high-resolution warm season rainfall recorded in varved sediments of Lake Oeschinen, northern Swiss Alps: calibration and validation AD 1901-2008. *Journal of Paleolimnology*

Amann B., Lobsiger S., Fischer D., Tylmann W., Bonk A., Filipiak J., Grosjean M., 2014. Spring temperature variability and eutrophication history inferred from sedimentary pigments in the varved sediments of Lake Żabioskie, north-eastern Poland, AD 1907 – 2008. *Global and Planetary Change*

Amann B., Szidat S., Grosjean M., (in review). A millennial-long record of warm season precipitation and flood frequency for the North-western Alps inferred from varved lake sediments: implications for the future

Grosjean M., **Amann B.**, Butz C., Rein B., Tylmann W., 2014. Hyperspectral imaging: a novel, nondestructive method for investigating subannual sediment structures and composition. In *PAGES News, Annual recorders of the past*, eds. Zolitschka B., Pike J., von Gunten L., Kiefer T., 22: 10-11

Bonk A., Tylmann W., **Amann B.**, Enters D., Grosjean M., (in review). Meteorological and limnological conditions of modern sedimentation and varve formation processes in Lake Żabińskie, northeastern Poland